Regulation of plant stress responses by clade I TGA transcription factors and interacting CC-type glutaredoxins

Dissertation

for the award of the degree

"Doctor rerum naturalium"
of the Georg-August-University Göttingen

within the doctoral program "IRTG2172 – PRoTECT"
of the Georg-August University School of Science (GAUSS)

submitted by
Anja Maren Pelizaeus
from Gütersloh, Germany

Göttingen, 16 February 2023

Thesis Advisory Committee

Prof. Dr. Christiane Gatz, Department of Plant Molecular Biology and Physiology, Albrecht-von-Haller-Institut for Plant Sciences, Georg-August-Universität Göttingen

Prof. Dr. Marcel Wiermer, Department of Biochemistry of Plant-Microbe Interactions, Institute for Biology, Freie Universität Berlin

Prof. Dr. Yuelin Zhang, Department of Botany, University of British Columbia

Members of the Examination Board

First Reviewer
Prof. Dr. Christiane Gatz, Department of Plant Molecular Biology and Physiology, Albrecht-von-Haller-Institut for Plant Sciences, Georg-August-Universität Göttingen

Second Reviewer
Prof. Dr. Marcel Wiermer, Department of Biochemistry of Plant-Microbe Interactions, Institute for Biology, Freie Universität Berlin

Further Members of the Examination Board

Prof. Dr. Yuelin Zhang, Department of Botany, University of British Columbia

Prof. Dr. Andrea Polle, Department of Forest Botany and Tree Physiology, Georg-August-Universität Göttingen

Prof. Dr. Ivo Feußner, Department for Plant Biochemistry, Albrecht-von-Haller-Institut for Plant Sciences, Georg-August-Universität Göttingen

Prof. Dr. Kai Heimel, Department of Microbial Cell Biology, Institute for Microbiology and Genetics, Georg-August-Universität Göttingen

Date of oral examination: 30 March 2023

Content

Summary

TGACG-BINDING (TGA) transcription factors are important regulators in numerous processes such as pathogen defense, development and detoxification. To control some of these responses, plant specific CC-type glutaredoxins (ROXYs) interact with and repress TGA factors. The *Arabidopsis thaliana* genome encodes 21 ROXYs, which can be further divided according to their C terminus. 17 members encode an ALWL motif whereas four ROXYs do not contain this motif. ROXYs can recruit the transcriptional co-repressor TOPLESS (TPL) through the ALWL motif. TPL-mediated repression represents most likely one of the mechanisms of how ROXYs control the activity of TGAs. ROXY6, 7, 8 and 9 are the only ROXYs without an ALWL motif. Analysis of plants ectopically expressing ROXY8 or ROXY9 has shown that they repress the activity of clade I TGAs (TGA1, TGA4), but not the activity of clade II TGAs (TGA2, TGA5, TGA6).

In this thesis, we wanted to analyze how gene expression is regulated by ROXY6, 7, 8, 9. Previous studies showed that the expression of *ROXY6*, *ROXY8* and *ROXY9* is induced in the shoots upon nitrogen (N) starvation. Subsequently, the ROXYs travel to the roots, where they activate expression of genes for e.g. nitrate uptake. As TGA1 and 4 are also involved in N starvation responses, ROXY6, 7, 8, 9 and TGA1, 4 might regulate the expression together. Using transcriptome analysis, we identified 350 genes that are activated by ROXY6, 7, 8, 9 under N limiting conditions as well as 212 repressed genes. We found that TGA1, 4 can function as a repressor of those genes that are induced upon N starvation and that ROXY6, 7, 8, 9 serve to interfere with this repression. Proximity labeling experiments identified TPL as an indirect interaction partner. Since ROXY9 interacts with proteins of the JASMONATE ZIM DOMAIN (JAZ) family and since JAZs interact with TPL through the adaptor protein NOVEL INTERACTOR OF JAZ (NINJA), analysis of the corresponding loss-of-function mutants was performed. These studies suggest that the repressive capacity of ROXY6, 7, 8, 9 is dampened by the JAZ/NINJA/TPL complex. As JA signaling leads to the degradation of JAZ, enhanced JA levels might further promote activation of gene expression.

To further determine the mechanism of ROXY9-mediated gene expression, the importance of the CCLC active site motif was analyzed. The active center of a glutaredoxin is required for oxidoreductase activities or binding of iron sulfur (Fe-S) clusters. Surprisingly, the first and second cysteine of the active site motif are dispensable, indicating that oxidoreductase activity or Fe-S cluster binding is not involved in the regulation.

Besides their function in the regulation of N starvation responses, TGA1, 4 are involved in activation of gene expression to induce systemic acquired resistance (SAR). SAR is established in uninfected leaves upon local pathogen infection. When a SAR leaf is attacked by a pathogen, it mounts a much more effective defense response compared to the naïve leaf. For the establishment of SAR, the plant hormones salicylic acid (SA) and N-hydroxypipecolic acid (NHP) are synthesized. Inductionof SA and NHP synthesis genes requires basal SA levels, while other SAR genes, like *PR1*, require pathogen-induced SA levels for maximum induction. In this study, we wanted to analyze in how far the response to *Psm*-infected SAR leaves depends on the two different TGA clades at basal SA levels. For this, we performed transcriptome analysis with the respective mutants in the *sid2* background in *Psm*-infected SAR leaves. 4184 induced genes were identified of which most are regulated to some extent by one or both TGA clades. WRKY51 and its closest homologue WRKY50 are activated only by TGA1, 4 in SAR conditions. Together with TGA2, 5, 6, WRKY50, 51 might regulate the expression of SAR-induced genes.

No transcription factor was highly induced by only clade II TGAs, suggesting that most TGA2, 5, 6-induced factors are also activated by clade I TGAs. For example, *WRKY75* and *WRKY31* are highly upregulated in SAR by both TGA clades. They could amplify the response and activate even promoters without TGA binding sites.

1. Introduction

1.1. TGA transcription factors

TGA factors are a family of basic leucine zipper (bZIP) transcription factors which is conserved in land plants. A region of basic amino acids enables binding to DNA and the leucine zipper domain mediates dimerization (Jakoby *et al.,* 2002). As dimers, TGAs are able to bind to the TGACG motif in promoter regions (Figure 1a; Izawa *et al.,* 1993). Besides the bZIP domain, all TGAs contain two glutamine rich domains (Q1 and Q2), which might be involved in transcriptional activation (Katagiri *et al.,* 1989) as this has been shown for other transcription factors (Courey *et al.,* 1989; Johannessen *et al.,* 2004; Gemayel *et al.,* 2015).

Ten TGAs are encoded in the *Arabidopsis thaliana* genome, which are further grouped into five clades according to sequence homologies (Jakoby *et al.,* 2002; Gatz, 2013). The TGA factors in clade I to III were initially described as being involved in pathogen defense processes (Zhang *et al.,* 2003; Kesarwani *et al.,* 2007; Zander *et al.,* 2010) whereas clade IV and V TGA factors play a role in flower development (Figure 1b; Chuang *et al.,* 1999; Hepworth *et al.,* 2005; Murmu *et al.,* 2010). However, recent publications indicate that TGAs are also involved in other processes like activation of the detoxification response (Mueller *et al.,* 2008; Fode *et al.,* 2008), responses to nitrate (Alvarez *et al.,* 2014) or establishment of organ boundaries (Wang *et al.,* 2019). All TGA factors can interact with CC-type glutaredoxins (Xing *et al.,* 2005; Ndamukong *et al.,* 2007; Li *et al.,* 2009; Zander *et al.,* 2012; Uhrig *et al.,* 2017; Li *et al.,* 2019).

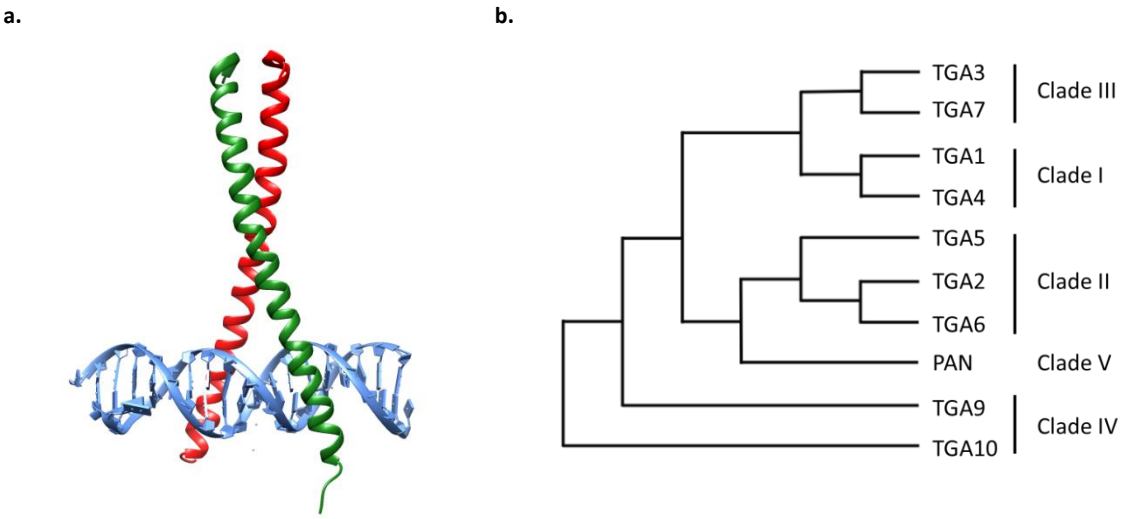

Figure 1: **TGACG-BINDING factors (TGAs) are plant specific basic leucine zipper (bZIP) transcription factors. a.** Structure of the bZIP domain from *Saccharomyces cerevisiae* GCN4, bound as dimer (red, green) to DNA (blue) (1YSA, Ellenberger *et al.,* 1992). **b.** Cladogram of *A. thaliana* TGA factors. The TGA transcription factor family consists out of 10 members which are grouped into five clades: TGA1 and TGA4 are in clade I; TGA2, TGA5, TGA6 in clade II, TGA3 and TGA7 in clade III; TGA9 and TGA10 in clade IV and PERIANTHIA (PAN) in clade V (adapted from Gutsche & Zachgo, 2016)

1.1.1. TGA factors in plant innate immunity

Clade I, II and III TGA factors are important regulators of plant innate immunity (Figure 2). In response to attack by biotrophic pathogens, the expression of *SYSTEMIC ACQUIRED RESISTANCE 1* (*SARD1*) and its closest homologue *CALMODULIN-BINDING PROTEIN 60g* (*CBP60g*) is induced by clade I TGA factors in a NONREPRESSPR OF PATHOGENESIS-RELATED GENES 1 (NPR1)-dependent manner (Sun *et al.,* 2018; Budimir *et al.,* 2021). SARD1 and CBP60g are transcription factors which activate the expression of several target genes including *ICS1 (ISOCHORISMATE SYNTHASE 1)*, *ENHANCED DISEASE SUSCEPTIBILITY 5* (*EDS5*) and *AVRPPHB SUSCEPTIBLE 3* (*PBS3*; Zhang *et al.,* 2010; Sun *et al.,* 2015). ICS1, EDS5 and PBS3 are part of the major salicylic acid (SA) synthesis pathway after pathogen attack. In the chloroplasts, ICS1 converts chorismate to isochorismate (Wildermuth *et al.,* 2001; Garcion *et al.,* 2008). After export to the cytosol via EDS5, PBS3 catalyzes isochorismate to isochorismate-9-glutamate, which is converted into SA either spontaneously or by ENHANCED PSEUDOMONAS SUSCEPTIBILITY 1 (EPS1; Torrens-Spence *et al.,* 2019; Rekhter *et al.,* 2019). NPR1 binds SA (Wu *et al.,* 2012) and interacts with TGAs to activate the expression of several pathogenesis-related (PR) genes (Dong, 2004; Ding *et al.,* 2018). This leads to enhanced resistance in the plant (Zhang *et al.,* 2003). Among others, the expression of *SARD1* is amplified, resulting in enhanced SA synthesis. After activation of gene expression, NPR1 is degraded (Spoel *et al.,* 2009). To replenish the nuclear NPR1 pool, cytosolic NPR1 oligomers are monomerized by reduction of critical cysteines and the NPR1 monomer is transported into the nucleus (Mou *et al.,* 2003).

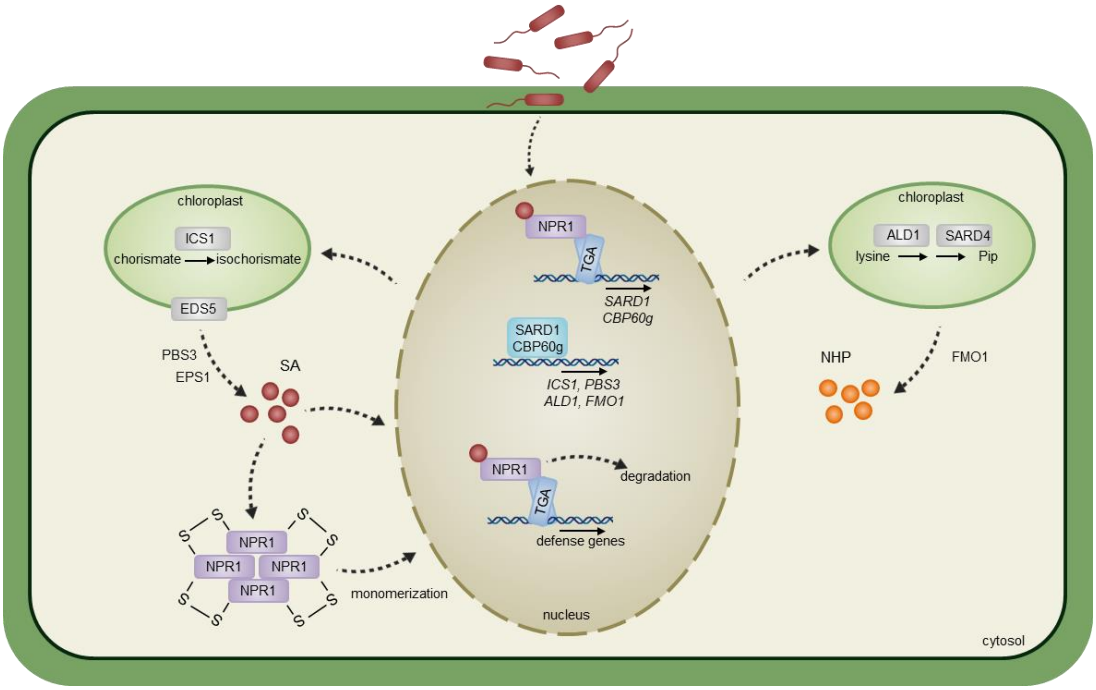

Figure 2: **Schematic representation of plant innate immunity.** After pathogen attack, TGA factors and NONREPRESSPR OF PATHOGENESIS-RELATED GENES 1 (NPR1) activate the expression of *SYSTEMIC ACQUIRED RESISTANCE 1* (*SARD1*) and *CALMODULIN-BINDING PROTEIN 60g* (*CBP60g*). SARD1 and CBP60g induce the expression of *ICS1 (ISOCHORISMATE SYNTHASE 1)*, *ENHANCED DISEASE SUSCEPTIBILITY 5* (*EDS5*) and *AVRPPHB SUSCEPTIBLE 3* (*PBS3*). ICS1 catalyzes chorismate to isochorismate in the chloroplasts. EDS5 transports isochorismate to the cytosol, where PBS3 converts it to isochorismate-9-glutamate. Isochorismate-9-glutamate either spontaneously desintegrates to salicylic acid (SA) or ENHANCED PSEUDOMONAS SUSCEPTIBILITY 1 (EPS1) mediates this reaction. SA binds to NPR1 which activates the expression of defense genes together with TGAs. As NPR1 is degraded after the activation of gene expression, additional NPR1 is transported into the nucleus after monomerization of NPR1 oligomers in the cytosol. SARD1 and CBP60g also activate the expression of *AGD2-LIKE DEFENSE RESPONSE PROTEIN 1* (*ALD1*), *SARD4* and *FLAVIN-DEPENDENT MONOOXYGENASE 1* (*FMO1*), leading to the production of N-hydroxy pipecolic acid (NHP) from lysine via pipecolic acid (Pip).

In addition to SA biosynthesis genes, SARD1 and CBP60g activate the expression of *AGD2-LIKE DEFENSE RESPONSE PROTEIN 1* (*ALD1*), *SARD4* and *FLAVIN-DEPENDENT MONOOXYGENASE 1* (*FMO1*; Sun *et al.,* 2015; 2018). ALD1 and SARD4 are involved in the synthesis of pipecolic acid (Pip) from lysine (Návarová *et al.,* 2012; Ding *et al.,* 2016; Hartmann *et al.,* 2017) and FMO1 catalyzes the h ydroxylation of Pip to N-hydroxy pipecolic acid (NHP; Hartmann *et al.,* 2018). To combat further pathogen attacks, NHP is transported to uninfected parts of the plant (Mohnike *et al.,* 2021), in which biosynthesis of SA and NHP is activated. Subsequently, the increased SA levels in the systemic leaves activate TGA-dependent expression of genes. Both SA and NHP are crucial for the priming of the uninfected parts of the plant, leading to a hyperactivated immune response upon pathogen attack. This immune response is called systemic acquired resistance (SAR).

1.1.2. Clade I TGA factors

Clade I TGAs 1 and 4 were first described as positive regulators of basal pathogen defense responses and SAR (Kesarwani *et al.,* 2007; Shearer *et al.,* 2012; Nair *et al.,* 2021). TGA1, 4 directly bind to the promoter of *SARD1* and activate its expression. Consequently, the *tga1 tga4* loss-of-function mutant produces less SA and is more susceptible to the hemi-biotrophic pathogen *Pseudomonas syringae* after local infection and in SAR conditions (Sun *et al.,* 2018). TGA1, 4 contain four conserved cysteines of which Cys260 and Cys266 of TGA1 can form an intramolecular disulfide bridge (Figure 3; Després *et al.,* 2003). An additional disulfide bridge between Cys172 and Cys287 has been shown (Lindermayr *et al.,* 2010). The disulfide bridge between Cys260 and Cys266 becomes reduced *in planta* upon SA treatment. This allows TGA1 to interact with NPR1 (Després *et al.,* 2003). The importance of the redox modulation of TGA1, 4 are unclear since Budimir *et al.,* 2021, showed that the conserved cysteines of TGA1 are not required for regulation of gene expression after *Psm* infection or SA spray.

However, mutating the critical cysteines reduces the binding capability of TGA1, 4 to the NPR1-like proteins BLADE-ON-PETIOLE 1 and 2 (BOP1, 2), at least in the yeast two-hybrid system (Wang *et al.,* 2019). BOP1, 2 are important regulators in plant development and morphogenesis (Hepworth *et al.,* 2005). TGA1, 4 and BOP1, 2 colocalize to the promoter region of *ATH1* (*ARABIDOPSIS THALIANA HOMEOBOX GENE1*) and activate its expression (Wang *et al.,* 2019). ATH1 is a transcription factor involved in photomorphogenesis (Quaedvlieg *et al.,* 1995) and development of organ boundaries (Gómez-Mena & Sablowski, 2008; Khan *et al.,* 2015).

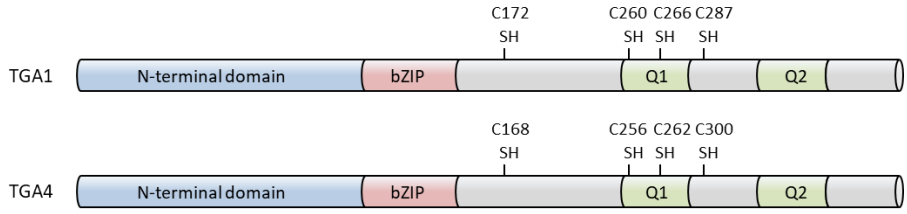

Figure 3: **Schematic representation of TGA1, 4 with conserved cysteine residues.** TGA1, 4 harbor an N-terminal domain (blue), a bZIP domain (red) and two glutamine-rich regions (Q1, Q2, green). All cysteines are indicated. Figure adapted from Gatz, 2013.

Recently, a crosstalk between defense responses and brassinosteroid (BR) signaling was proposed. BR is essential for plant growth and development (Ye *et al.,* 2010; Domagalska *et al.,* 2010; Jiang *et al.,* 2013; Nolan *et al.,* 2020), but can also induce *PR1* expression (Divi *et al.,* 2010). In unchallenged plants, the kinase BR-INSENSITIVE 2 (BIN2) interacts with and phosphorylates TGA1, 4. The phosphorylated TGA4 is destabilized and the interaction with NPR1 is impaired. Upon pathogen infection, BIN2 is inhibited by BR, TGA4 is stabilized and gene expression is activated (Kim *et al.,* 2022).

Besides, TGA1, 4 have been shown to regulate hyponastic growth (Li *et al.,* 2019). Hyponastic growth, or hyponasty, is the upwards movement of leaves in order to escape unfavorable environmental conditions such as low light (LL) stress (Vandenbussche *et al.,* 2003; Millenaar *et al.,* 2009), submergence (Cox *et al.,* 2003; Pierik *et al.,* 2005) or elevated temperatures (Koini *et al.,* 2009; van Zanten *et al.,* 2009). This movement is managed by cell elongation in the petioles and is induced by the plant hormone auxin (Cox *et al.,* 2003; Polko *et al.,* 2012; Pantazopoulou *et al.,* 2017; Michaud *et al.,* 2017). In LL conditions, the *tga1 tga4* mutant fails to initiate hyponasty and is impaired in the activation of LL-induced *INDOLE-ACETIC-3-ACID INDUCIBLE 19 (IAA19)* and *XYLOGLUCAN ENDOTRANS-GLUCOSYLASE/HYDROLASE8 (XTH8*; Li *et al.,* 2019). These genes are involved in auxin signaling (Tatematsu *et al.,* 2004) and cell wall loosening (Fry *et al.,* 1992) and thus might contribute to the cell elongation at the lower part of the petiole.

Interestingly, recent western blot analysis in our department revealed that at least TGA1 is much higher expressed in the roots than in the shoots (Budimir, 2019). Transcriptome analysis showed that 97 % of the genes differentially expressed in roots of the *tga1 tga4* mutant are nitrate responsive. Moreover, TGA1, 4 directly bind to the promoters of two of those genes, *NRT2.1* and *NRT2.2*, which encode for nitrate transporters (Alvarez *et al.,* 2014).

1.1.3. Clade II TGA factors

TGA2, TGA5 and TGA6 are in clade II and crucial regulators for SA-mediated defense responses. For this, TGA2, 5, 6 interact with NPR1 (Zhang *et al.,* 1999; 2003). The *tga2 tga5 tga6* mutant is impaired in *PR1* expression upon treatment with the SA analog 2,6-dichloroisonicotinic acid (INA) and is compromised in the establishment of SAR (Zhang *et al.,* 2003). However, in the uninduced state, TGA2, 5, 6 fulfill different functions. While TGA6 activates basal *PR1* expression, TGA2 functions as repressor (Kesarwani *et al.,* 2007).

Besides, TGA2, 5, 6 are involved in the crosstalk of SA and jasmonic acid (JA)/ethylene (ET) signaling. While the SA pathway is initiated to combat attacks from biotrophic pathogens, the JA/ET pathway mediates defense responses against necrotrophs (Glazebrook, 2005). The crosstalk is important to launch the appropriate immune response to the respective pathogen with minimal costs (Huot *et al.,* 2014). For this, both pathways can negatively regulate each other (Spoel *et al.,* 2003; Zheng *et al.,* 2012). The major regulator in JA/ET signaling is OCTADECANOID-RESPONSIVE ARABIDOPSIS APETALA2/ETHYLENE RESPONSE FACTOR DOMAIN PROTEIN 59 (ORA59; Pré *et al.,* 2008). Treatment with the ethylene precursor 1-aminocyclopropane-1-carboxylic acid (ACC) leads to the activation of *ORA59* expression, mediated by TGA2, 5, 6 (Zander *et al.,* 2014). Upon infection with *Botrytis cinerea* or treatment with ACC, TGA2, 5, 6 induce the expression of the defense gene *PLANT DEFENSIN 1.2 (PDF1.2)*. However, upon JA treatment, activation of *PDF1.2* is independent of the TGAs. Both JA- and ET-induced *PDF1.2* expression can be repressed by SA. In both cases, TGA2, 5, 6 are required for this negative effect of SA on the JA/ET pathway (Zander *et al.,* 2010).

Apart from the importance in pathogen defense, TGA2, 5, 6 regulate the detoxification response against toxic chemicals (Fode *et al.,* 2008; Mueller *et al.,* 2008; Huang *et al.,* 2016). Microarray analysis revealed that 60 % of A_1-phytoprostanes (PPA_1)-induced and 56 % of herbicide safener-induced genes are activated by TGA2, 5, 6 (Mueller *et al.,* 2008; Behringer *et al.,* 2011). As 42 % of the PPA_1-induced genes contain a TGACG motif in the promoter region (Mueller *et al.,* 2008), TGA2, 5, 6 most likely directly activates gene expression upon xenobiotic stress. TGA2 can interact with transcriptional co-activator SCARECROW-LIKE 14 (SCL14). In response to SA and the auxin mimic 2,4-Dichloro-phenoxyacetic acid (2,4-D), TGA2 and SCL14 activate the expression of *CYTOCHROM P450 FAMILY*

PROTEIN 81D11 (*CYP81D11*), *MEDICAGO TRUNCATULA NODULIN 19* (*MtN19)-like* and *GLUTATHIONE S-TRANSFERASE 7* (*GSTU7*; Fode *et al.,* 2008). After 2,3,5-triiodobenzoic acid (TIBA) treatment, TGA2, 5, 6 and SCL14 induce *CYP81D11* and *NAC DOMAIN CONTAINING PROTEIN 32* (*NAC032*; Fode *et al.,* 2008; Huang *et al.,* 2016). However, it is not known how the plant senses the toxic chemical and how this leads to activation of gene expression.

In response to UV-B light, TGA2, 5, 6 activate the expression of *GSTU7, GSTU8* and *GSTU25*. *GSTU*s encode for peroxide-scavenging enzymes confer tolerance to UV-B stress. Consistently, the *tga2 tga5 tga6* mutant is more susceptible to UV-B treatment (Herrera-Vásquez *et al.,* 2021).

1.1.4. Clade III, IV and V TGA factors

Clade III consists out of TGA3 and TGA7. Like clade I and clade II TGAs, TGA3 is involved in basal immunity and can interact with NPR1 (Després *et al.,* 2000; Shearer *et al.,* 2009). Similar to TGA2, 5, 6, TGA3 mediates resistance and activates *PR1* expression (Kesarwani *et al.,* 2007). Like TGA1, 4, TGA3 can be phosphorylated by BIN2 in response to SA. This phosphorylation is both required and sufficient for the activation of *PR1* expression. Apparently, this is due to enhanced TGA3 DNA binding ability and NPR1-TGA3 complex formation. Strikingly, the phosphorylated mimic of TGA3 constitutively activates defense even in the absence of NPR1 (Han *et al.,* 2022). Moreover, TGA3 interacts with ARABIDOPSIS TYPE-B RESPONSE REGULATOR2 (ARR2). This interaction mediates the enhanced defense response that is observed in the presence of cytokinin (Choi *et al.,* 2010).

In contrast to the other clades, clade IV and V TGAs have been described as regulators of flower development. TGA9, 10 belong to clade IV and are required for anther development. The *tga9 tga10* mutant is male sterile (Murmu *et al.,* 2010). PERANTHIA (PAN) is the single member of clade V TGAs and negatively regulates petal development (Chuang *et al.,* 1999). For this, PAN interacts with BOP1, 2 (Hepworth *et al.,* 2005).

1.2. Glutaredoxins

Glutaredoxins (GRX) belong to the thioredoxin superfamily and were first described as small enzymes which are able to modify the redox state of target proteins (Laurent *et al.,* 1964). All GRX share characteristic structural similarities: the thioredoxin fold, the active site motif CxxC or CxxS and a glutathione (GSH) binding site. The thioredoxin fold consists out of four stranded β-sheets which are flanked by three α-helices (Martin, 1995), depicted in Figure 4.

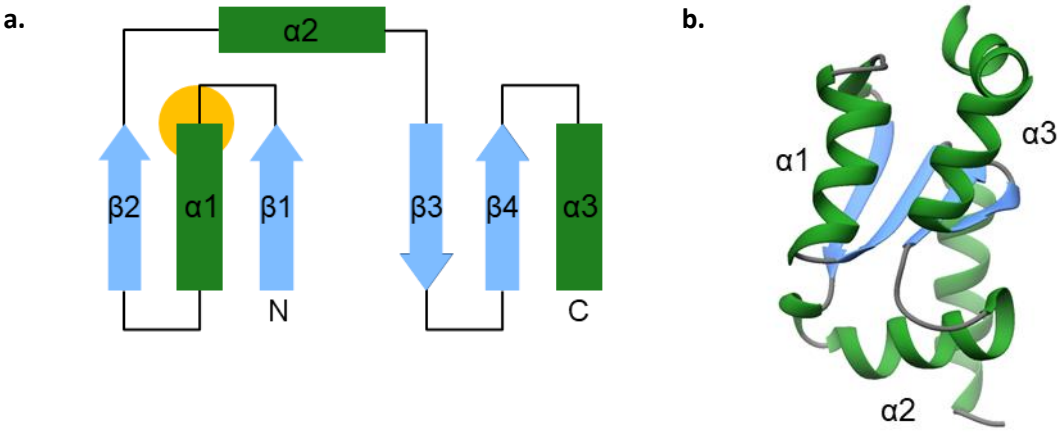

Figure 4: **Schematic representation of the core thioredoxin fold. a.** The thioredoxin fold consists out of three α-helices (green) and four stranded β-sheets (blue). The active site is marked with yellow background N: N-terminus. C: C-terminus. adapted from (Martin, 1995). **b.** Structure of *Saccharomyces cerevisiae* GRX1 (3C1R; Yu *et al.,* 2008). The four stranded β-sheets (blue) are surrounded by three α-helices (green).

The active site motif is located at the N-terminus of the first α-helix and is important for binding of GSH as well as for the enzymatic activity of the GRX (Lillig *et al.,* 2008; Deponte, 2013). Depending on the number of cysteines involved, the mono- or dithiol mechanism is used for the reduction of disulfide bridges or GSH-mixed disulfides in target proteins (Rouhier *et al.,* 2008; Deponte, 2013; Ukuwela *et al.,* 2018). Both mechanisms start with the reduction of the substrate and the oxidization of the GRX (Figure 5).

In the monothiol mechanism, the N-terminal cysteine of the active site attacks the GSH-mixed disulfide or the protein disulfide. In case of a GSH-mixed disulfide, the first cysteine of the active site of the GRX forms a disulfide with the thiol group of the GSH, resulting in a covalent link between the GRX and the GSH and a free thiol group in the target protein. If a protein disulfide is used as a substrate, the GRX forms an intermolecular disulfide bridge with the substrate to resolve the disulfide. Subsequently, the intermolecular disulfide is reduced by GSH which leads to glutathionylated GRX and a reduced thiol group in the target protein. The reduced state of the GRX is re-established by another GSH molecule, which attacks the disulfide bridge between the GSH and the GRX. This leads to the formation of a glutathione disulfide (GSSG). NADPH can convert GSSG into two GSH molecules (Lillig *et al.,* 2008; Rouhier *et al.,* 2008; Deponte, 2013; Ukuwela *et al.,* 2018).

In contrast to the monothiol mechanism, which only requires one cysteine, a second cysteine is involved in the dithiol mechanism. This can be located within or outside the active site motif. As in the monothiol mechanism, the GRX is first glutathionylated after reduction of the glutathionylated substrate. This can be resolved by another cysteine of the GRX resulting in an intramolecular disulfide bond within the GRX and free GSH. When the substrate is a protein disulfide, the intermolecular disulfide link between the target and the GRX can also directly be resolved by creating an intramolecular disulfide within the GRX. The oxidized GRX is reduced by either two GSH molecules or

a ferredoxin thioredoxin reductase (Zaffagnini *et al.,* 2008; Lillig *et al.,* 2008; Rouhier *et al.,* 2008; Deponte, 2013; Ukuwela *et al.,* 2018).

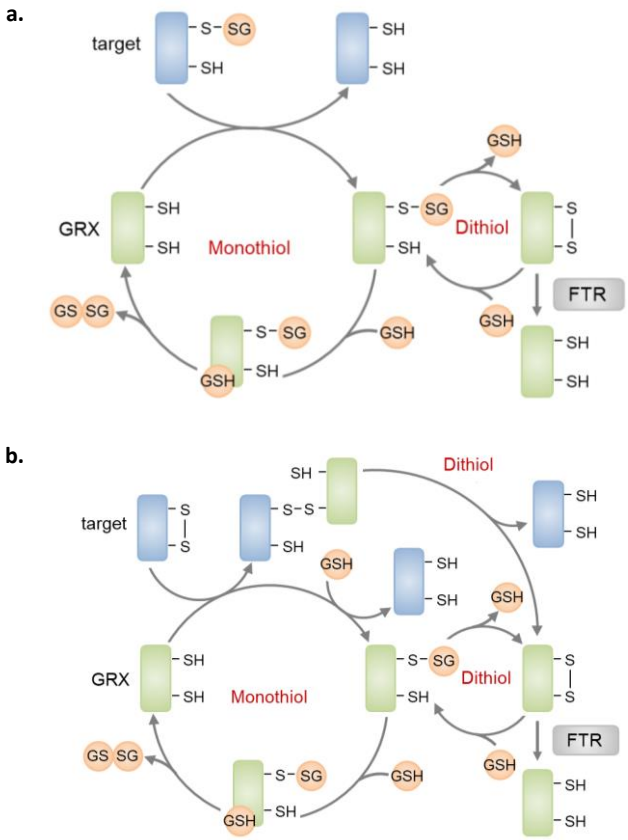

Figure 5: **Mono- and dithiol mechanism used by glutaredoxins. a. Mechanism used for glutathionylated protein as substrate**. To reduce the target protein, the GRX takes over the glutathione (GSH). In the monothiol mechanism, the GRX is reduced by an additional GSH, leading to the formation glutathione disulfide (GSSG). In the dithiol mechanism, an intermolecular disulfide bridge can be formed in the GRX. This can be resolved by ferredoxin thioredoxin reductase (FTR) or two molecules of GSH. **b. Mechanism used for protein disulfide as substrate**. To resolve the disulfide bridge within the target protein, the thiol group of the GRX can form intermolecular disulfide bridge with the substrate protein. In the monothiol mechanism, the substrate can be fully reduced by glutathionylation of the GRX. In the dithiol mechanism, the GRX forms an intramolecular disulfide bridge and thus releases the thiol group of the target protein. Figure adapted from Treffon, 2019.

GRX can be subdivided into three classes, which are named and classified according to conserved amino acids at the active site. The CPYC (Class I)- and CGFS (Class II)-types are found in most of the so far characterized organisms. In contrast, the CC-type is specific for land plants (Ziemann *et al.,* 2009). The amount of CPYC- and CGFS-type GRX remained nearly constant during the evolution of land plants, whereas the number of CC-type GRX has drastically increased through multiple gene duplication events (Lemaire, 2004; Ziemann *et al.,* 2009). In general, the CPYC class is involved in the reduction of disulfide bridges and oxidation of thiol groups (Holmgren, 1976) and the (de)glutathionylation of target proteins (Gravina & Mieyal, 1993; Couturier *et al.,* 2011). Members of the CGFS-type GRX bind iron sulfur (Fe-S) clusters as dimers. The Fe-S cluster is bound by the active site cysteines and the thiols of the glutathione (Picciocchi *et al.,* 2007; Iwema *et al.,* 2009) and can be transferred to target proteins (Rodríguez-Manzaneque *et al.,* 2002; Bandyopadhyay *et al.,* 2008). There are at least 31 GRX in *A. thaliana*. Six and four belong to class I and II, whereas class III is the largest subgroup with 21 members (Rouhier *et al.,* 2004).

1.2.1. CPYC-type glutaredoxins

The six members of the class I GRX in *A. thaliana* have a C[G/P/S]Y[C/S] consensus sequence and can be subdivided into three groups, each containing two members and distinct localization. GRXC1, 2 are located in the cytosol and nucleus (Müller-Schüssele *et al.,* 2021). They are essential for the plant as the loss-of-function mutant is lethal (Riondet *et al.,* 2012). GRXC2 can glutathionylate BR- INSENSITIVE 1-ASSOCIATED RECEPTOR-LIKE KINASE 1 (BAK1), which is involved in BR signaling as well as recognition of pathogens (Bender *et al.,* 2015). GRXC3, 4 contain an N-terminal extension, which might be a signal peptide for secretion or might function as anchor to the membrane (Zaffagnini *et al.,* 2019). GRXC5, S12 are localized in the plastids (Couturier *et al.,* 2011).

Oxidoreductase activity has been shown for GRXC1, 2, 5, S12, whereby at least GRXC5 uses a monothiol mechanism despite having two cysteines in the active site (Couturier *et al.,* 2011; Riondet *et al.,* 2012). The enzymatic activity of GRXC3, 4 has not been analyzed so far. In addition, GRXC1 and GRXC5 with CGYC and CSYC active site motif, respectively, are able to bind a 2Fe-2S-cluster (Riondet *et al.,* 2012). However, in contrast to clusters bound by CFGS-type GRX, this cluster is less likely transferred to target proteins. Instead, it could function as a sensor upon oxidative stress, since it dissociates under oxidative conditions thus releasing oxidoreductase activity (Lillig *et al.,* 2008; Rouhier *et al.,* 2010).

1.2.2. CGFS-type glutaredoxins

The active site of the type II GRX is a highly conserved CGFS motif. There are four members in *A. thaliana* of which GRXS17 is a multidomain protein containing three GRX regions. While GRXS14, 16 are localized in plastids and GRXS17 in the cytosol, GRXS16 is the only described GRX located in mitochondria. All CGFS-type GRX can bind 2Fe-2S clusters as dimers with the help of GSH (Bandyopadhyay *et al.,* 2008; Liu *et al.,* 2013) and have weak oxidoreductase activity (Rodríguez-Manzaneque *et al.,* 2002; Bandyopadhyay *et al.,* 2008).

Moreover, some distinct functions have been described. GRXS14 protects the plant proteins from oxidative damage (Cheng *et al.,* 2006) and is involved in the maintenance of the chlorophyll content (Rey *et al.,* 2017). Being the only mitochondrial GRX in *A. thaliana*, GRXS15 is essential for the plant (Moseler *et al.,* 2015). GRXS15 can transfer the Fe-S cluster onto aconitase (Moseler *et al.,* 2015) and the membrane carrier proteins IRON SULFUR CLUSTER ASSEMBLY (ISCA) 1a, 1b, 2 (Azam *et al.,* 2020). Besides, GRXS15 protects the root from oxidative stress (Cheng, 2008) and arsenic treatment (Ströher *et al.,* 2016). In addition to the typical thioredoxin fold, GRXS16 harbors a catalytically active N-terminal endonuclease domain. Upon oxidative stress, the endonuclease activity is reduced by the formation of an intramolecular disulphide bridge (Liu *et al.,* 2013). GRXS16 is the only described *A. thaliana* GRX that can accept Fe-S clusters from carrier proteins (Gao *et al.,* 2013). Whether this is of physiological relevance remains unclear. In contrast to all other GRX of *A. thaliana*, GRXS17 contains three GRX domains with CGFS active site motifs. GRXS17 confers thermotolerance through oligomerization (Cheng *et al.,* 2011; Martins *et al.,* 2020) and is involved in plant development in long light periods (Knuesting *et al.,* 2015).

1.2.3. CC-type glutaredoxins

The 21 CC-type GRX of *A. thaliana* share a CC[M/L][C/S/G] active site motif (Rouhier *et al.,* 2004). After the first member, ROXY1, was characterized, this class was named ROXY-type GRX (Xing *et al.,* 2005). In general, ROXYs seem to repress the activity of TGA transcription factors, whereby the repressive mechanism is only partially understood. ROXYs can be further divided into proteins encoding a C-terminal A[L/I]W[L/I/V/A] motif and ROXYs that do not have the motif (Figure 6). The ALWL motif

enables the interaction with transcriptional co-repressor TOPLESS (TPL; Uhrig *et al.,* 2017). The recruitment of TPL represents most likely one of the mechanisms how ROXY-mediated repression can work. ROXY16 contains a AIWI motif and fails to interact with TPL (Uhrig *et al.,* 2017). The ALWL motif is needed for the biological function of at least ROXY1 and ROXY19 (Li *et al.,* 2009; Zander *et al.,* 2012). ROXY6, 7, 8, 9 are the only members of the ROXYs without the ALWL motif. Still, ROXY8, 9 can repress the function of TGA1, 4 (Li *et al.,* 2019) and it is unclear how this repression is mediated. The subcellular localization has been determined for ROXY1, 6, 8, 18 and 20, which are all located in the cytoplasm and the nucleus (Li *et al.,* 2009; Couturier *et al.,* 2011; Ohkubo *et al.,* 2017; Ota *et al.,* 2020).

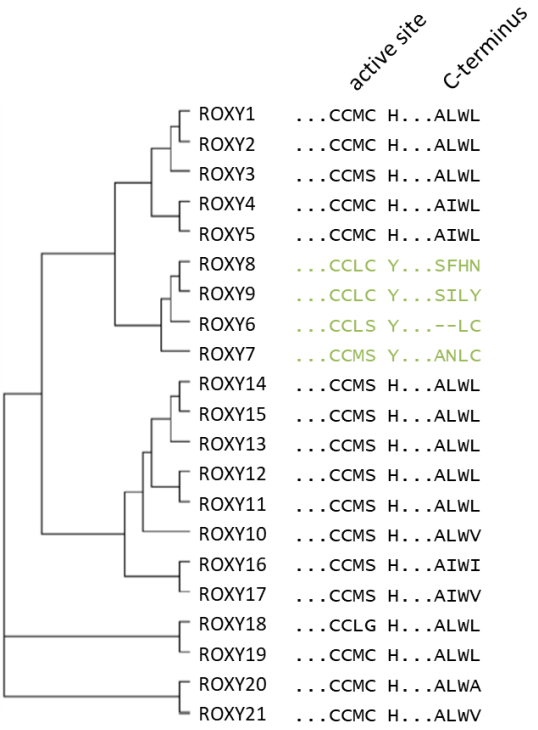

Figure 6: **Phylogenetic tree of *A. thaliana* CC-type glutaredoxins (ROXYs) according to the active site motif.** There are 21 ROXYs described in *A. thaliana* which either contain an ALWL motif (black) or not (green). Figure adapted from Li *et al.,* 2019.

1.2.3.1. ALWL-containing CC-type glutaredoxins

The first characterized CC-type GRX in *A. thaliana*, ROXY1, is a regulator of flower development as it controls the number of petals (Xing *et al.,* 2005). For this, ROXY1 interacts with and represses the function of the TGA factor PAN in the nucleus (Li *et al.,* 2009). Together with its closest homologue ROXY2, ROXY1 represses TGA9, 10 to maintain normal anther development (Murmu *et al.,* 2010). Additionally, ROXY1 co-localizes with RNA Polymerase II during transcription. Upon H_2O_2 treatment, this co-localization decreases (Maß *et al.,* 2020).

Several pieces of evidence suggest that ROXY19 might regulate crosstalk between SA and JA signaling. Upon SA treatment, the expression of *ROXY19* is induced by TGA2, 5, 6, and NPR1. The ectopically expressed ROXY19 interferes with TGA2, 5, 6 to repress the expression of the *B. cinerea*-inducible and SA-repressed *PDF1.2* (Ndamukong *et al.,* 2007). ORA59 is crucial for the expression of *PDF1.*2 (Pré *et al.,* 2008). As ectopically expressed ROXY19 interferes with the expression of *ORA59*, this is most likely the reason why *PDF1.2* expression is repressed. The C-terminal ALWL motif of ROXY19 is essential for this repressive effect. In a transient assay, ALWL-containing ROXY1, 2, 3, 4, 5, 10, 12, 17, 18 were also shown to repress *ORA59* (Zander *et al.,* 2012). Additionally, the *35S:*HA-ROXY18 and *35S:*HA-ROXY19

overexpressor lines are more susceptible to xenobiotic stress and at least *ROXY19* expression is induced in response to treatment with TIBA. The ectopically expressed ROXY19 represses the TGA2, 5, 6-activated expression of *CYP81D11* and *NAC032* after TIBA treatment (Huang *et al.,* 2016). So far, studies with ROXY19 have only been performed with ectopically expressed protein. The *roxy19* knock-out mutant shows no phenotype in regard to detoxification against harmful chemicals and SA-JA/ET crosstalk (Huang *et al.,* 2016), most likely due to the high similarity to other ALWL-containing ROXYs.

1.2.3.2. ALWL-free CC-type glutaredoxins

There are only four ROXYs without an ALWL motif, namely ROXY6, 7, 8, and 9. Studies with ectopically expressed ROXY9 revealed that these GRXs interact and represses TGA1, 4 under low light (LL) conditions in order to interfere with hyponastic growth. Moreover, expression of LL-induced and TGA, 4-activated *IAA19* and *XTH8* in the petioles are repressed by ROXY9 (Li *et al.,* 2019). IAA19 is involved in auxin-mediated signaling (Tatematsu *et al.,* 2004) and XTH8 is an enzyme that most likely contributes to cell wall loosening (Fry *et al.,* 1992). Thus, ROXY9 might interfere with auxin-mediated cell-elongation which mediates hyponastic growth.

Studies in our group showed that the *35S:HA-ROXY9* overexpression line is more susceptible to *P. syringae* infection and impaired in *FMO1* expression in SAR leaves (Jung, 2016; Nair, unpublished). As TGA1, 4 are important regulators of the immune response against *P. syringae* and for the expression of *FMO1*, ROXY9 might generally interfere with the function of TGA1, 4.

Besides, the ALWL-free ROXYs have been linked to nitrogen (N) starvation responses. Under N limiting conditions, members of the C-TERMINALLY ENCODED PEPTIDE (CEP) family are produced in the stele of the lateral roots (Figure 7). The CEPs are subsequently transported to the shoot through the xylem (Tabata *et al.,* 2014). In the shoot, CEP1 spreads within the vascular tissue and reaches the phloem (Ohkubo *et al.,* 2017) where it interacts with leucine rich receptor kinases CEP RECEPTOR (CEPR) 1 and 2 (Tabata *et al.,* 2014). This leads to the activation of the expression of *ROXY6*, *ROXY8* and *ROXY9* (Ohkubo *et al.,* 2017; Ota *et al.,* 2020). ROXY6, 8, 9 travel through the phloem to the roots and initiate the expression of e.g. *NRT2.1* and *CEPH* (Ohkubo *et al.,* 2017; Ota *et al.,* 2020; Ohkubo *et al.,* 2021). *NRT2.1* encodes for a high-affinity nitrate transporter which is activated through dephosphorylation by CEPH (Ohkubo *et al.,* 2021). As TGA1 binds to the promoter region of *NRT2.1* (Alvarez *et al.,* 2014), ROXY6, 7, 8, 9 and TGA1, 4 might regulate gene expression upon N starvation together.

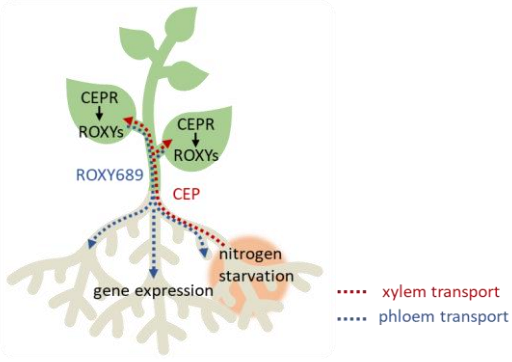

Figure 7: ROXY6, 8, 9 are produced in response to nitrogen starvation and initiate gene expression in the roots. In response to nitrogen starvation, C-TERMINALLY ENCODED PEPTIDE (CEP) is produced in the roots and travels through the xylem to the shoots. CEP binds to the CEP RECEPTOR (CEPR) 1, 2 which activates the expression of *ROXY6, 8, 9*. ROXY6, 8, 9 are subsequently transported through the phloem to the roots where gene expression is activated.

1.3. Aim of this study

The aim of this study was to unravel how TGA1, 4 and ROXY6, 7, 8, 9 regulate gene expression. Previous studies on the ROXYs without ALWL motif were performed with ectopically expressed ROXY9. These revealed that ROXY9 represses the function of TGA1, 4 with regard to hyponastic growth and defense processes against *P. syringae*. In this study, the quadruple loss-of-function mutant *roxy6 roxy7 roxy8 roxy9* (*roxy6789*) was analyzed. The first aim was to determine whether the function of these ROXYs as inferred from the *35S*:HA-ROXY9 overexpressor line was confirmed in the *roxy6789* mutant. Moreover, additional phenotypes were characterized. Both TGA1, 4 and ROXY6, 7, 8, 9 have been shown to regulate gene expression upon nitrogen starvation. Thus, we investigated in this study whether ROXY6, 7, 8, 9 and TGA1, 4 function in one pathway to regulate N starvation responses. For this, transcriptome analysis was performed to identify suitable target genes.

After identifying suitable target genes upon biotic and abiotic stresses, the second aim was to approach the mechanism of action of ROXY9. To this aim, potential redox modulation of TGA1, 4 by ROXY6, 7, 8, 9 was addressed. Moreover, we tried to identify new interaction partners of ROXY9 by using proximity labeling by TurboID and subsequent mass spectrometry analysis.

As an additional project, distinct roles of clade I and clade II TGA factors in the establishment of SAR were analyzed. Special attention was laid on the processes that occur in the absence of pathogen-induced SA. After performing transcriptome analysis of suitable mutants to identify differentially regulated genes encoding for transcription factors, mutants were generated and their influence in SAR was investigated.

2. Material

2.1. Organisms

2.1.1. Bacteria and yeasts

Table 1: List of bacteria and yeast strains.

Organism	Description	Reference
Agrobacterium tumefaciens GV3101	pMP90RK *Rif*^{r}, *Gent*^{r}	Koncz & Schell, 1984
*Escherichia coli DH5*α	F– Φ80*lac*ZΔM15 Δ(*lac*ZYA-*arg*F) U169 *rec*A1 *end*A1 *hsd*R17 (rK–,mK+) *pho*A *sup*E44 λ– *thi*-1 *gyr*A96 *rel*A1	Hanahan, 1983
Pseudomonas syringae pv. maculicola ES4326	*Rif*^{r}	Whalen *et al.,* 1991
Pseudomonas syringae pv. tomatoe DC3000 *luxCDABE*	*Rif*^{r}, P_{kan}*:luxCDABE*	Matsumoto *et al.,* 2022

2.1.2. Plants

Table 2: List of *Arabidopsis thaliana* genotypes.

Genotype	Description	Reference
Col-0	Ecotype Columbia-0, wild type	NASC stock number N1092
tga1 tga4	Contains T-DNA insertions in the coding regions of *TGA1* and *TGA4* in Col-0 background	Kesarwani *et al.,* 2007
tga2 tga5 tga6 (tga256)	Contains a 9.7 kb deletion on chromosome 5 resulting in the loss of *TGA2* and *TGA5* and a 2.7 kb deletion on chromosome 3 resulting in the loss of *TGA6* in Col-0 background	Zhang *et al.,* 2003
tga1 tga2 tga4 tga5 tga6 (tga12456)	Obtained by crossing *tga1 tga4* with *tga2 tga5 tga6,* contains T-DNA insertions in the coding regions of *TGA1* and *TGA4*, 9.7 kb deletion on chromosome 5 resulting in the loss of *TGA2* and *TGA5* and a 2.7 kb deletion on chromosome 3 resulting in the loss of *TGA6* in Col-0 background	Gatz group, 2013
tga3 tga7 (tga37)	Contains T-DNA insertions in the coding regions of *TGA3* and *TGA7* in Col-0 background	Gatz group, 2010
tga2 tga3 tga5 tga6 (tga2356)	Obtained by crossing *tga2 tga5 tga6* with *tga3*, contains a 9.7 kb deletion on chromosome 5 resulting in the loss of *TGA2* and *TGA5*, a 2.7 kb deletion on chromosome 3 resulting in the loss of *TGA6* and a T-DNA insertion in the coding region of *TGA3*	Gatz group, 2014

Genotype	Description	Reference
roxy6 roxy7 roxy8 roxy9 (roxy6789)	CRISPR-Cas9 generated mutant line in Col-0 background with 1 bp insertion in the coding region for *ROXY6* and deletions in the coding regions for *ROXY7* (1 bp), *ROXY8* (16 bp) and *ROXY9* (7 bp) all resulting in frameshifts and premature stop codons	Budimir, 2019
roxy6 roxy8 roxy9 (roxy689)	CRISPR-Cas9 generated mutant line in Col-0 background with 1 bp insertion in the coding region for and deletions in the coding regions for *ROXY8* (16 bp) and *ROXY9* (7 bp) all resulting in frameshifts and premature stop codons	Gatz group, 2019
roxy6 roxy7 roxy9 (roxy679)	CRISPR-Cas9 generated mutant line in Col-0 background with 1 bp insertion in the coding region for *ROXY6* and deletions in the coding regions for *ROXY7* (1 bp) and *ROXY9* (7 bp) all resulting in frameshifts and premature stop codons	Budimir, 2019
roxy7 roxy9 (roxy79)	CRISPR-Cas9 generated mutant line in Col-0 background with deletions in the coding regions for *ROXY7* (1 bp) and *ROXY9* (7 bp) all resulting in frameshifts and premature stop codons	Gatz group, 2019
roxy10 roxy11-15 (roxy10-15)	CRISPR-Cas9 generated mutant line in Col-0 background with 78 bp deletion in coding region for *ROXY10* and 11.5 kb deletion on chromosome 4 resulting in the loss of *ROXY14*, *ROXY13*, *ROXY12* and creating a chimeric product of *ROXY15* and *ROXY11* with a premature stop codon	Gatz group, 2019
cepr1-3	Contains T-DNA insertion in the coding region of *CEPR1* in Col-0 background	Chapman *et al.,* 2019
tga1 tga4 with *TGA1:HA-3'UTR*	*tga1 tga4* mutant expressing the 3'UTR of *TGA1* with a N-terminal 1x HA-tag under control of the native promoter	Budimir *et al.,* 2021
tga1 tga4 with *TGA1:HA-gTGA1* (TGA1ox)	*tga1 tga4* mutant expressing genomic *TGA1* with N-terminal 1x HA-tag under control of the native promoter	Budimir *et al.,* 2021
tga1 tga4 with *TGA1:HA-gTGA1R* (TGA1red)	*tga1 tga4* mutant expressing *TGA1* with 4 mutated cysteines (C172N, C260N, C266S, C287S) and N-terminal 1x HA-tag under control of the native promoter	Budimir *et al.,* 2021
jaz decuple (jazD)	Contains T-DNA insertions in the coding regions of *JAZ3*, *JAZ4*, *JAZ5*, *JAZ7*, *JAZ9*, *JAZ10*, *JAZ13* and transposon insertions in the coding regions of *JAZ1*, *JAZ2* and *JAZ6* in the Col-0 background	Guo *et al.,* 2018
Col-0 with *JAZ10:GUS*	Col-0 wild type expressing *GUS* with under control of the *JAZ10* promoter	Acosta *et al.,* 2013

Genotype	Description	Reference
ninja-1 with *JAZ10:GUS*	Contains a point mutation in the coding region of *NINJA* (C673T) resulting in a premature stop codon, expressing *GUS* with under control of the *JAZ10* promoter	Acosta *et al.,* 2013
myc2-2 myc3 myc4 (*myc234*)	Contains a point mutation in the coding region of *MYC2* (G851A) resulting in a premature stop codon and T-DNA insertions in the coding regions of *MYC3* and *MYC4* in Col-0 background	Lorenzo *et al.,* 2004; Fernández-Calvo *et al.,* 2011
sid2-2	Contains not yet annotated deletions (6748 bp) in the coding region for *ISOCHORISMATE SYNTHASE 1 (ICS1)* in the Col-0 background	Wildermuth *et al.,* 2001
sid2-2 tga1 tga4 (sid2 tga14)	Obtained by crossing *sid2-2* with *tga1 tga4*, contains deletions in the coding region for *ICS1* and T-DNA insertion in *TGA1* and *TGA4* coding region	Muthreich, 2014
sid2-2 tga2 tga5 tga6 (sid2 tga256)	Obtained by crossing *sid2-2* with *tga2 tga5 tga6*, contains deletions in the coding region for *ICS1*, a 9.7 kb deletion on chromosome 5 resulting in the loss of *TGA2* and *TGA5* and a 2.7 kb deletion on chromosome 3 resulting in the loss of *TGA6* in Col-0 background	Rindermann, 2010
sid2-2 npr1-1 (sid2 npr1)	Obtained by crossing *sid2-2* with *npr1-1*, contains deletions in the coding region for *ICS1* and a point mutation in *NPR1* (H334Y) resulting in a *NPR1* loss-of-function mutant	Nair *et al.,* 2021
roxy6789 with *35S:HA*	*roxy6 roxy7 roxy8 roxy9* mutant expressing 3x HA-tag under control of the *35S* promoter	This work
roxy6789 with *35S:HA-L-ROXY9*	*roxy6 roxy7 roxy8 roxy9* mutant expressing *ROXY9* with N-terminal 3x HA-tag and linker under control of the *35S* promoter	This work
roxy6789 with *35S:HA-L-ROXY9 SCLC*	*roxy6 roxy7 roxy8 roxy9* mutant expressing *ROXY9* with altered active site (C21S), N-terminal 3x HA-tag and linker under control of the *35S* promoter	This work
roxy6789 with *35S:HA-L-ROXY9 CSLC*	*roxy6 roxy7 roxy8 roxy9* mutant expressing *ROXY9* with altered active site (C22S), N-terminal 3x HA-tag and linker under control of the *35S* promoter	This work
roxy6789 with *35S:HA-L-ROXY9 CPYC*	*roxy6 roxy7 roxy8 roxy9* mutant expressing *ROXY9* with altered active site (C22P, L23Y), N-terminal 3x HA-tag and linker under control of the *35S* promoter	This work
roxy6789 with *35S:HA-L-ROXY9 CCLCA*	*roxy6 roxy7 roxy8 roxy9* mutant expressing *ROXY9* with an aa exchange (Y25A) and N-terminal 3x HA-tag under control of the *35S* promoter	This work

Genotype	Description	Reference
roxy6789 with *UBQ10:2HA-Turbo*	*roxy6 roxy7 roxy8 roxy9* mutant expressing biotin ligase Turbo with N-terminal 2x HA-tag under control of the *UBQ10* promoter	This work
roxy6789 with *UBQ10:2HA-Turbo-ROXY9*	*roxy6 roxy7 roxy8 roxy9* mutant expressing *ROXY9* with N-terminal biotin ligase Turbo and 2x HA-tag under control of the *UBQ10* promoter	This work
sid2-2 wrky51-1 (*sid2 wrky51*)	Obtained by crossing *sid2-2* with *wrky51-1* contains deletions in the coding region for *ICS1* and a T-DNA insertion in the coding region of *WRKY51*, needs to be sprayed with SA for propagation	This work
sid2-2 wrky50-1 wrky51-1 (*sid2 wrky5051*)	Obtained by crossing *sid2-2* with *wrky50-1 wrky51-1* contains deletions in the coding region for *ICS1* and a T-DNA insertions in the coding regions of *WRKY50* and *WRKY51*	This work

2.2. Culture media

2.2.1. Bacteria

The ingredients for bacterial culture media were mixed and the pH was set (Table 3). For plates, 1.2 % agar was added. After autoclaving, required antibiotics were added and the media was either stored at RT or media containing agar was poured into round agar plates. The plates were stored at 4°C.

Table 3: Ingredients for bacterial culture media.

Medium	Ingredient	Final concentration
Lysogeny Broth (LB)	Tryptone/Peptone from casein	1 %
adapted from Bertani, 1951	Yeast Extract	0.5 %
	NaCl	1 %
	pH = 7.0 (with NaOH)	
double Yeast Tryptone (dYT)	Tryptone/Peptone from casein	1.6 %
	Yeast Extract	1 %
	NaCl	0.5 %
	pH = 7.0 (with NaOH)	
Yeast Extract Broth (YEB)	Meat Extract	1 %
	Tryptone/Peptone from casein	0.5 %
	Yeast Extract	0.2 %
	Sucrose	0.5 %
	pH = 7.0 (with NaOH)	
	Add after autoclaving:	
	$MgSO_4$	2 mM
King's B	Peptone II Bacto™ pepton	10 g
adapted from King *et al.,*	86 % glycerin	5 ml
1954	K_2HPO_4	0.75 g
	pH = 7.0 – 7.2	
	Add after autoclaving:	
	$MgSO_4$	5 mM

2.2.2. Yeast

For plates, 1.2 % agar was added before autoclaving.

Table 4: Ingredients for *S. cerevisiae* culture media.

Medium	Ingredient	Amount for 1 l
Synthetic-Defined (SD)	Yeast nitrogen base w/o amino acids	0.67 %
	Glucose	2 %
	Aminoacid dropout mixture	0.061 %
	pH = 5.6	
SD-Ura	Yeast nitrogen base w/o amino acids	0.67 %
(SD-Medium deficient of	Glucose	2 %
uracil)	CSM Aminoacid dropout mixture	0.062 %
	–Leu/ –Trp/ –Ura	
	Leucine	100 mg
	Tryptophan	50 mg
	pH = 5.6	
Transformation media	Yeast nitrogen base w/o amino acids	0.67 %
(SD-Medium deficient of	Glucose	2 %
leucine, tryptophan and	CSM Aminoacid dropout mixture	0.062 %
uracil)	–Leu/ –Trp/ –Ura	
	pH = 5.6	
Interaction media	Yeast nitrogen base w/o amino acids	0.67 %
(SD-Medium deficient of	Glucose	2 %
adenine, histidine, leucine,	CSM Aminoacid dropout mixture	0.059 %
tryptophan and uracil)	–Ade/ –His/–Leu/ –Trp/ –Ura	
	pH = 5.6	
Yeast Extract Peptone	BD Bacto Yeast Extract	10 g
Adenine Dextrose (YPAD)	BD Bacto Peptone	20 g
	Glucose	20 g
	Adenine	100 mg
	pH = 6.0 with HCl	

2.2.3. Plants

For the cultivation of plants on plates, FN, LN or MS media was used. The ingredients were mixed, pH was set and 0.68 % agar plant was added (Table 5). The media was autoclaved and poured into square agar plates.

Table 5: Ingredients for *A. thaliana* culture media.

Medium	Ingredient	Final concentration
Full nutrition (FN)	Glutamine	1 mM
adapted from	KNO_3	2 mM
Scheible *et al.,* 2004	NH_4NO_3	1 mM
	Sucrose	0.5 %
	$CaCl_2$	4 mM
	K_2SO_4	2 mM
	Potassium phosphate buffer pH 5.8	3 mM
	MES pH 5.8 (with KOH)	3 mM
	$Na_2FeEDTA$	40 µM
	H_3BO_3	60 µM
	$MnSO_4 \cdot H_2O$	14 µM
	$ZnSO_4 \cdot 7\ H_2O$	1 µM
	$CuSO_4$	0.6 µM
	$NiCl_2 \cdot 6\ H_2O$	0.4 µM
	$Na_2MoO_4 \cdot 2\ H_2O$	0.3 µM
	$CoCl_2 \cdot 6\ H_2O$	20 nM
	Add after autoclaving:	
	$MgSO_4 \cdot 7\ H_2O$	1 mM
Low nitrogen (LN)	KCl	3 mM
adapted from	KNO_3	0.1 mM
Scheible *et al.,* 2004	NH_4NO_3	0.05 mM
	Sucrose	0.5 %
	$CaCl_2$	4 mM
	$MgSO_4 \cdot 7\ H_2O$	1 mM
	K_2SO_4	2 mM
	Potassium phosphate buffer pH 5.8	3 mM
	MES pH 5.8 (with KOH)	3 mM
	$Na_2FeEDTA$	40 µM
	H_3BO_3	60 µM
	$MnSO_4 \cdot H_2O$	14 µM
	$ZnSO_4 \cdot 7\ H_2O$	1 µM
	$CuSO_4$	0.6 µM
	$NiCl_2 \cdot 6\ H_2O$	0.4 µM
	$Na_2MoO_4 \cdot 2\ H_2O$	0.3 µM
	$CoCl_2 \cdot 6\ H_2O$	20 nM
	Add after autoclaving:	
	$MgSO_4 \cdot 7\ H_2O$	1 mM

Medium	Ingredient	Final concentration
No nitrogen (NN) (FN medium without nitrogen)	Sucrose	0.5 %
	$CaCl_2$	4 mM
	$MgSO_4 \cdot 7\ H_2O$	1 mM
	K_2SO_4	2 mM
	Potassium phosphate buffer pH 5.8	3 mM
	MES pH 5.8 (with KOH)	3 mM
	$Na_2FeEDTA$	40 µM
	H_3BO_3	60 µM
	$MnSO_4 \cdot H_2O$	14 µM
	$ZnSO_4 \cdot 7\ H_2O$	1 µM
	$CuSO_4$	0.6 µM
	$NiCl_2 \cdot 6\ H_2O$	0.4 µM
	$Na_2MoO_4 \cdot 2\ H_2O$	0.3 µM
	$CoCl_2 \cdot 6\ H_2O$	20 nM
	Add after autoclaving:	
	$MgSO_4 \cdot 7\ H_2O$	1 mM
2 Murashige and Skoog (MS) + PPT	Murashige and Skoog Basal Salt Mixture	0.44 %
	Sucrose	2 %
	pH = 5.7 with KOH	
	Add after autoclaving:	
	12 µg/ml PPT	

2.3. Antibiotics, herbicides and peptides

Table 6: List of used antibiotics with concentrations.

Antibiotic	Final concentration	Manufacturer
Ampicillin	100 µg/ml	Carl Roth, Germany
Gentamicin	25 µg/ml	Duchefa Biochemie, Germany
Kanamycin	100 µg/ml	Carl Roth, Germany
Rifampicin	50 µg/ml	Duchefa Biochemie, Germany
Spectinomycin	100 µg/ml	Duchefa Biochemie, Germany

Table 7: List of used herbicides with concentrations.

Herbicide	Final concentration	Manufacturer
Basta®	200 mM	Bayer, Germany
Phosphinotricin (PPT)	12 µg/ml	Duchefa Biochemie, Germany

Table 8: List of used peptide with concentration.

Peptide	Final concentration	Manufacturer
C-TERMINALLY ENDODED PEPTIDE 1 (CEP1)	1 µM	GenScript, USA

2.4. Plasmids

Table 9: List of plasmids.

Plasmid	Description	Reference
pDONR207-L-ROXY9	Donor vector for Gateway™ technology, contains coding region for ROXY9 with N-terminal linker, flanked by *attL* sites, introduces gentamycin resistance	Mrozek, unpublished
pDONR207-L-ROXY9SCLC	Donor vector for Gateway™ technology, contains coding region for ROXY9 with altered active site (C20S) and N-terminal linker, flanked by *attL* sites, introduces gentamycin resistance	This work
pDONR207-L-ROXY9CSLC	Donor vector for Gateway™ technology, contains coding region for ROXY9 with altered active site (C21S) and N-terminal linker, flanked by *attL* sites, introduces gentamycin resistance	This work
pDONR207-L-ROXY9CPYC	Donor vector for Gateway™ technology, contains coding region for ROXY9 with altered active site (C22P, L23Y) and N-terminal linker, flanked by *attL* sites, introduces gentamycin resistance	This work
pDONR207-L-ROXY9CCLCA	Donor vector for Gateway™ technology, contains altered coding region for ROXY9 (Y25A) with N-terminal linker, flanked by *attL* sites, introduces gentamycin resistance	This work
pB2HAGW7	Destination vector for Gateway™ technology, contains *35S* promoter, coding region for 3x HA-tag, Gateway™	Li *et al.,* 2019

Plasmid	Description	Reference
	cassette, consisting out of coding region for chloramphenicol resistance and toxin CcdB, flanked by *attR* sites, and *35S* terminator, flanked by left and right border for *Agrobacterium tumefaciens* mediated transformation introduces spectinomycin and basta resistance	
pB2HA	Contains coding region for 3x HA-tag under control of *35S* promoter and *35S* terminator, flanked by left and right border for *Agrobacterium tumefaciens* mediated transformation introduces spectinomycin and basta resistance	Gatz group, 2014
pB2HA-L-ROXY9	Recombination of pB2GW7 and pDONR207-L-ROXY9 by LR reaction, contains coding region for HA-L-ROXY9 under control of the *35S* promoter, flanked by left and right border for *Agrobacterium tumefaciens* mediated transformation, introduces spectinomycin and basta resistance	Mrozek, unpublished
pB2HA-L-ROXY9SCLC	Recombination of pB2GW7 and pDONR207-L-ROXY9SCLC by LR reaction, contains coding region for HA-L-ROXY9 with altered active site (C20S) under control of the *35S* promoter, flanked by left and right border for *Agrobacterium tumefaciens* mediated transformation, introduces spectinomycin and basta resistance	This work
pB2HA-L-ROXY9CSLC	Recombination of pB2GW7 and pDONR207-L-ROXY9CSLC by LR reaction, contains coding region for HA-L-ROXY9 with altered active site (C21S) under control of the *35S* promoter, flanked by left and right border for *Agrobacterium tumefaciens* mediated transformation, introduces spectinomycin and basta resistance	This work
pB2HA-L-ROXY9CPYC	Recombination of pB2GW7 and pDONR207-L-ROXY9CPYC by LR reaction, contains coding region for HA-L-ROXY9 with altered active site (C22P, L23Y) under control of the *35S* promoter, flanked by left and right border for *Agrobacterium tumefaciens* mediated transformation, introduces spectinomycin and basta resistance	This work
pB2HA-L-ROXY9CCLCA	Recombination of pB2GW7 and pDONR207-L-ROXY9CCLCA by LR reaction, contains coding region for HA-L-ROXY9 with altered active site (Y25A) under control of the *35S* promoter, flanked by left and right border for *Agrobacterium tumefaciens* mediated transformation, introduces spectinomycin and basta resistance	This work
pB35S-2HA-Turbo	Contains coding region for 2x HA-tagged biotin ligase Turbo under control of the *35S* promoter and E9 terminator, introduces kanamycin and basta resistance	Tian *et al.,* 2021
pB35S-2HA-Turbo-ROXY19E9	Contains coding region for Turbo-ROXY19 fusion protein under control of the *35S* promoter and E9 terminator, introduces kanamycin and basta resistance	Goyal, unpublished

Plasmid	Description	Reference
pUBQ10-2HA-Turbo	Created by classical cloning, contains coding region for HA-Turbo under control of *UBQ10* promoter, flanked by left and right border for *Agrobacterium tumefaciens* mediated transformation, introduces spectinomycin and basta resistance	This work
pUBQ10-2HA-Turbo-ROXY9	Created by classical cloning, contains coding region for HA-Turbo-ROXY9 fusion protein under control of *UBQ10* promoter, flanked by left and right border for *Agrobacterium tumefaciens* mediated transformation, introduces spectinomycin and basta resistance	This work

2.5. Oligonucleotides

Table 10: List of primers used for qRT-PCR.

Primer	Sequence	Reference
AIR1	GTGGACCTAACATTGGGAAAC ACGCTGAGATTGATAGGAAGG	This work
ALD1	Quantitect QT00751387	Qiagen, Netherlands
AMT1-5	GCGAGGAATGGATTTAGCAGGTCAT GGCTGGAGGGTTAGGCGCACGAGGT	Yuan *et al.,* 2007
CEPH	TTGGGCTCTGTCTCTTCTTTA AACGCTCCTTCTTCTGTTCC	Thurow, unpublished
CLE3	CCTGCTTCTAGTACTCGAATTGAC ATTTCCAAGGATCGTCTCTTCGCC	Araya *et al.,* 2014
DLO1	AATATCGGCGACCAAATGC CGCTCGTTCTCGGTGTTTAC	Zeilmaker *et al.,* 2015
EDS1	GCTCAATGACCTTGGAGTGAGC TCTTCCTCTAATGCAGCTTGAACG	Nair *et al.,* 2021
endogenous ROXY9	TTCACCTTAGTGGCTCTCTTGTC CTAGCTCACACTCTAGCTGTAACTGTG	This work
FMO1	GTCTAAAACCAAACCATTCTTTCG ATCATCCCTTTATCCGCTTCC	Thurow, unpublished
IAA19	TGACGTCGTCGGGTAGTAATAGTG AGCGTCACCACCAGATGAAACG	Li *et al.,* 2019
NLP3	TGTTTGGAGATTCGATGCTG CGCTTTGCGATCTCTCTTCT	Konishi & Yanagisawa, 2013
NRT2.1	CCATGGGAGTTGAGTTGAGCACTG GTGGAGCTTCAAGTGAAACCTGTC	Li, unpublished
NRT2.2	GCAGCAGATTGGCATGCATTT AAGCATTGTTGGTTGCGTTCC	Ruffel *et al.,* 2021
NRT2.4	GAACAAGGGCTGACATGGAT GCTTCTCGGTCTCTGTCCAC	Ruffel *et al.,* 2021
PAD4	AGATACGCGAGCACAACGCAAG TTCTCGCCTCATCCAACCACTC	Vogelmann *et al.,* 2012
PBS3	Quantitect QT00828471	Qiagen, Netherlands
PER10	CTCTCTAAGCTAAAGGACACGTG GTTCGCGTAGTAAGCATTGTCAAAC	Thurow, unpublished
PER71	AGCATTAGCCGCTCGTGACACAG GGACGACGAGATCACGAGTATTGAGT	Shigeto *et al.,* 2015
PR1	CTGACTTTCTCCAAACAACTTG GCGAGAAGGCTAACTACAACTAC	Budimir *et al.,* 2021
RL3	GCGTTATCCACATCCCAATTACC GAACCATGTCCACTTCAGTAGAGC	Thurow, unpublished
ROXY6	Quantitect QT00852516	Qiagen, Netherlands
ROXY7	Quantitect QT00760144	Qiagen, Netherlands

Primer	Sequence	Reference
ROXY8	AGAAGGCCTTAGTTCGTCTTGGC	Muthreich, 2014
	AACCCACGAGCTTGCCACTTAC	
ROXY10	AGCCAACGAGGTCATGAGTCTAC	Muthreich, 2014
	AGCCCGCTTAAGCATGGGAATC	
ROXY11	GCGTGAACCCGACGATCTATGAAC	Muthreich, 2014
	CCTATGAACACCACTGGCACTGTC	
ROXY12	ACTTTGGCGTGAACCCGACTATC	Muthreich, 2014
	CCAATGCTTGCTCTATCTCCCTTC	
ROXY13	TCCATCTCAATCGCTCTCTGGTTC	Muthreich, 2014
	ATCAAAGCCATAGTGCTCCAACCC	
ROXY14	TTCATAGGAGGGCAGCTTGTCG	Muthreich, 2014
	AGCATTGGAATGAGAGAACGGTTG	
ROXY15	TTGGCGTGAACCCGACAATC	Muthreich, 2014
	GCCAAGCTGAGCCAATGCATAC	
SARD1	TCAAGGCGTTGTGGTTTGTG	Sun *et al.,* 2018
	CGTCAACGACGGATAGTTTC	
SWEET11	GCCAATCTCAGTGGTTCGTCAAG	Rouina *et al.,* 2021
	GAAGAGGACTGCTTGCCATGT	
TFL1	GCACAACAGATGCTACGTTTG	Chen *et al.,* 2021
	GTTGAAGTGATCTCTCGAAGG	
TGA1	ACGAACCTGTCCATCAATTCGG	Li *et al.,* 2019
	CCATGGGAAGTATCCTCTGACACG	
TGA4	AAAGTCGTTTGCGCAAGAAAGC	Li *et al.,* 2019
	AGCATTGGTATCTACTCCGTTCCC	
transgenic ROXY9	CCTTAGTGGCTCTCTTGTCCCATTG	This work
	GATTTTTGCGGACTCTAGCATGGC	
UBQ5	GACGCTTCATCTCGTCC	Kesarwani *et al.,* 2007
	GTAAACGTAGGTGAGTCCA	
UMAMIT35	Quantitect QT00883463	Qiagen, Netherlands
WRKY33	CTCGTGGTAGCGGTTACGCC	Liu *et al.,* 2017b
	CCTTTGCTCTAGAGAATCCACC	
WRKY50	Quantitect QT00838831	Qiagen, Netherlands
WRKY51	TGATGTGATGGATGATGGTTTTAAATG	Thurow, unpublished
	CAACCTTCACTTGAGCATTTGTAG	
XTH8	TCTATCGCAGCAACACCGACAC	Li *et al.,* 2019
	TGCTTTGTCTGAAATCCACATCCG	

Table 11: List of primers used for PCR or sequencing. Guide RNAs used in the CRISPR-Cas9 system are underlined. Primers were designed by various members of the Gatz department.

Primer	Sequence
35S-Prom	ATTGATGTGATATCTCCACTGAC
BAR-fwd	GGTCTGCACCATCGTCAACCAC
BAR-rev	CAGCTGCCAGAAACCCACGTC
cepr1-3 RP	AATTGGGAGAATTAAAACCGG
cepr1-3 LP	TGGCTTACCTTCACCATGATC
LBb1 (SALK)	GCGTGGACCGCTTGCTGCAACT
pB2GW7 fwd	CACAATCCCACTATCCTTCGCA
pB2GW7 rev	CATGAGCGAAACCCTATAAGAACC
ROXY6 fwd	TTTCTTGTTGCATAGTTTGGGTCAC
ROXY6 rev	TAAATATGGCTTCACTAGGGGAACG
ROXY7 fwd	ACCCTCTTTTCTTCAAACAGGAACC
ROXY7 rev	AGACAAGAAGACAAATCGTTGCCTG
ROXY8 downstream fwd	GCCGCTTTAATTCTTCGGAGGGAATCTG
ROXY8 downstream rev	CATCAGTACATCCACCGATTAGTTAAGCTGG
ROXY9genom-71 fwd	GCAAGAAAAAAACACACTCGAAAGACTC
ROXY9genom568 rev	GTTGATTAACTAAACTGAAACACGAGAGAAGC
roxy9A28fwd	GCTCATGTTGTCTCTGCTACGCATC
sid2-2 fwd1	TTCTTCATGCAGGGGAGGAG
sid2-2 fwd2	CAACCACCTGGTGCACCAGC
sid2-2 rev	AAGCAAAATGTTTGAGTCAGCA
tga1 SALK_028210 RP	CGTGTCCCCTCTGGTTTCTTTC
tga1 SALK_028210 LP	AACCTGGATTCATGGTTTCCG
tga4 SALK_127923 RP	GACACATTTTGTTCCACCGAG
tga4 SALK_127923 LP	GGTCTAAATCCGCCTATCCAC
TurboNcoI rev	GAGCAGCCATGGTACCCTTTTCGGCAGACC
wrky50-1 SALK045803-LP	GGTGATGTTTTTGGTTTGTGG
wrky50-1 SALK045803-RP	CTATAAGAATGCGTGATCTTCCC
wrky51-1 SALK022198-LP	CACTTGCTCTAGTTCTTGGATGC
wrky51-1 SALK022198-RP	TTGCTTTCAAACCATGCTTTG
XhoI2xHA fwd	GAGACGCTCGAGAACAATGTACCCATACGATGTTCCTGAC

2.6. Enzymes

Table 12: List of used enzymes.

Name	Manufacturer
50X Advantage Polymerase ® 2 Polymerase Mix	TaKaRa, Japan
BIOTAQ™ DNA Polymerase (5 u/µl)	Bio-Line, UK
Calf Intestinal Alkaline Phosphatase (1 U/µl)	Thermo Fisher Scientific, USA
DNase I, RNase-free (1 U/µl)	Thermo Fisher Scientific, USA
Gateway™ LR Clonase™ II enzyme mix	Thermo Fisher Scientific, USA
RevertAid H Minus Reverse Transcriptase (200 U/µl)	Thermo Fisher Scientific, USA
Phusion DNA Polymerase (2 U/µl)	Thermo Fisher Scientific, USA
Ribonuclease A (90 U/mg)	Carl Roth, Germany
T4 DNA Ligase (5 U/µl)	Thermo Fisher Scientific, USA
Trypsin Sequencing grade, modified from porcine pancreas	Serva, Germany

Table 13: List of used restriction enzymes for cloning.

Name	Manufacturer
*Bsp*1407I / *Bsr*GI (10 u/µl)	Thermo Fisher Scientific, USA
*Bsu*36I / *Eco*81I (10 u/µl)	Thermo Fisher Scientific, USA
*Eco*31I / *Bsa*I (10 u/µl)	Thermo Fisher Scientific, USA
*Nco*I (10 u/µl)	Thermo Fisher Scientific, USA
*Sac*I (10 u/µl)	Thermo Fisher Scientific, USA
*Ssp*I (10 u/µl)	Thermo Fisher Scientific, USA
*Xho*I (50 u/µl)	Thermo Fisher Scientific, USA

2.7. Antibodies

Table 14: List of used antibodies.

Antibody	Source		Manufacturer
α-TGA1	rabbit	AS16 3208	Agrisera, Sweden
α-TGA2,5	rabbit	SA4364 SAB	Eurogentec, Beldium
α-HA ChIP Grade	rabbit	ab9110	abcam, United Kingdom
α-PEPC	rabbit	100-4163	Biomol GmbH, Germany
α-flag	rabbit	F7425	Sigma-Aldrich
α-rabbit IgG Peroxidase-linked	goat	AS09 602	Agrisera, Sweden
Streptavidin Peroxidase-linked	*Streptomyces avidinii*	ab7403	abcam, United Kingdom

2.8. Buffers and solutions

Table 15: List of used buffers and solutions.

Buffer	Ingredient	Final concentration
TRIZOL buffer	Guanidine Thiocyanate	0.8 M
	Ammonium Thiocyanate	0.4 M
	Glycerin	5 %
	Na-acetate pH 5.2 (adjusted with CH_3COOH)	0.1 M
	Phenol with 0.1 M citrate buffer	38 %
DNA Extraction buffer	Tris pH 7.5	200 mM
	NaCl	250 mM
	EDTA	25 mM
	SDS	0.5 %
TAE buffer	Tris	40 mM
	Acetic acid	0.115 %
	EDTA	1 mM
SDS running buffer	Tris	25 mM
	Glycine	192 mM
	SDS	0.1 %
	pH = 8	
Transfer buffer	Tris	25 mM
	Glycine	192 mM
	SDS	0.04 %
	Methanol	20 %
	pH = 9	
Tris-buffered saline (TBS)	Tris	20 mM
	NaCl	136 mM
	pH = 7.6 with NaCl	
TBS + Tween (TBST	Tris	20 mM
	NaCl	136 mM
	Tween	0.1 %
	pH = 7.6 with NaCl	
Coomassie Solution	Coomassie Brillant Blue G-250	100 mg
	Acetic acid	10 %
Immunoprecipitation (IP) Extraction Buffer	Tris HCl pH 8	25 mM
	EDTA pH 8	1 mM
	NaCl	150 mM
	NP-40	0.1 %
	Glycerol	5 %
	PMSF	1 mM
Desalting Buffer	Tris HCl pH 7.5	50 mM
	NaF	50 mM
	Sucrose	300 mM
	Triton-X	1 %
Wash Buffer	Tris pH 7.5	50 mM

Buffer	Ingredient	Final concentration
	NaF	50 mM
	NaCl	100 mM
	Triton-X	0.1 %
4x SDS PAGE Loading Buffer	Tris HCl pH 6.8	200 mM
	DTT	400 mM
	Bromphenol blue	0.4 %
	glycerol	40 %
Urea Buffer	Urea	4 M
	Gylcerin	16.7 %
	SDS	5 %
	Bromophenol blue	0.05 %
	Add before usage:	
	β-mercaptoethanol	5 %
Stripping Solution	Tris-HCl	62.5 mM
	SDS	2 %
	Add before usage:	
	β-mercaptoethanol	0.72 %

2.9. Chemicals

Table 16: List of used devises.

Chemical	Molecular formula / Abbreviation	Manufacturer
1,4-Dithiotreit	DTT	Carl Roth, Germany
2-(N-morpholino)ethanesulfonic acid	MES	Carl Roth, Germany
β-mercaptoethanol	β-ME	Carl Roth, Germany
Acetic acid	CH_3COOH	Carl Roth, Germany
Acrylamide-Bisacrylamide 30 %		Carl Roth, Germany
Agar-Agar Kobe I		Carl Roth, Germany
Agar-Agar Plant		Carl Roth, Germany
Agarose		Sigma-Aldrich, USA
Ammonium nitrate	NH_4NO_3	Carl Roth, Germany
Ammonium thiocyanate	NH_4SCN	Merck, Germany
Bromphenol blue		Carl Roth, Germany
Boric acid	H_3BO_3	Carl Roth, Germany
Bovine serum albumin	BSA	AppliChem, Germany
Calcium nitrate	$Ca(NO_3)_2 \cdot 4\ H_2O$	Carl Roth, Germany
Chloroform	$ChCl_3$	Carl Roth, Germany
Cobalt chloride	$CoCl_2 \cdot 6\ H_2O$	Carl Roth, Germany
Coomassie Brilliant Blue	CBB	Merck, Germany
Copper sulfate	$CuSO_4$	Carl Roth, Germany
D(+)-sucrose	$C_{12}H_{22}O_{11}$	Carl Roth, Germany
Dipotassium phosphate	K_2HPO_4	Carl Roth, Germany
Ethanol	C_2H_6O, EtOH	W. Krannich, Germany
Ethidium bromide	EtBr	Carl Roth, Germany
Ethylenediaminetetraacetic acid	EDTA	Carl Roth, Germany
Ethylenediaminetetraacetic acid ferric sodium salt	$Na_2FeEDTA$	Sigma-Aldrich, USA
Glycerine 86 %	$C_3H_8O_3$	Carl Roth, Germany
Glycine	$C_2H_5NO_2$	Carl Roth, Germany
Guanine thiocyanate	$C_2H_6N_4S$	Carl Roth, Germany
Hydrochloric acid	HCl	Carl Roth, Germany
Isopropanol	C_3H_8O	CHEMSOLUTE®, Germany
L-Glutamine	$C_5H_{10}N_2O_3$	Carl Roth, Germany
Magnesium chloride	$MgCl_2$	Carl Roth, Germany
Magnesium sulphate	$MgSO_4 \cdot 7\ H_2O$	Carl Roth, Germany

Chemical	Molecular formula / Abbreviation	Manufacturer
Manganese sulphate	$MnSO_4 \cdot H_2O$	Merck, Germany
Meat Extract		Carl Roth, Germany
Methanol	MeOH	Merck, Germany
Murashige & Skoog Basal Salt Mixture	MS	Duchefa Biochemie, Germany
N-hydroxy pipecolic acid	NHP	MedChem Express, USA
Nonident P-40	NP-40	Fluka® Analytical, USA
Nickel chloride	$NiCl_2 \cdot 6\ H_2O$	Carl Roth, Germany
Nitrogen, liquid	N_2	Liquid Air, Germany
Peptone II Bacto™ pepton		Difco, Germany
Phenol with 0.1 M citrate buffer		Carl Roth, Germany
Phenylmethansulfonylfluoride	PMSF	Amresco, United Stated
Potassium chloride	KCl	Carl Roth, Germany
Potassium dihydrogen phosphate	KH_2PO_4	Carl Roth, Germany
Potassium hydroxide	KOH	Carl Roth, Germany
Potassium nitrate	KNO_3	Carl Roth, Germany
Potassium sulphate	K_2SO_4	Carl Roth, Germany
Protease Inhibitor Cocktail	PI	Sigma-Aldrich, USA
Silwet L77		Kurt Obermeier
Skimmed milk powder		SUCOFIN, Germany
Sodium lauryl sulphate	SDS	Carl Roth, Germany
Sodium acetate	NaOAc	Carl Roth, Germany
Sodium chloride	NaCl	Carl Roth, Germany
Sodium fluoride	NaF	Fluka® Analytical, USA
Sodium hypochlorite, 12 % Cl	NaOCl	Carl Roth, Germany
Sodium molybate	$Na_2MoO_4 \cdot 2\ H_2O$	Sigma-Aldrich, USA
Sodium metasilicate	$NaSiO_3 \cdot 9\ H_2O$	
Sodium salicylate	SA	Sigma-Aldrich, USA
TEMED		Carl Roth, Germany
Tris(hydroxymethyl)aminomethane	Tris	Carl Roth, Germany
Tryptone/Peptone from casein		Carl Roth, Germany
Tween-20		Carl Roth, Germany
Urea	CH_4N_2O	Carl Roth, Germany
WUXAL ® Super		Hauert MANNA, Germany
Yeast Extract		Carl Roth, Germany

Chemical	Molecular formula / Abbreviation	Manufacturer
Zinc sulphate	$ZnSO_4 \cdot 7\ H_2O$	Honeywell, USA

2.10. Consumables

Table 17: List of used consumables.

Consumable	Model	Manufacturer
Blotting Paper	MN 218 B	Macherey-Nagel, Germany
Cutting mat	2 x 3 in	GE Healthcare, USA
Desalting column	PD10	GE Healthcare, USA
Dynabeads™	M-280 Streptavidin	Thermo Fisher Scientific, USA
Low-bind tube	Protein LoBind Tube	Eppendorf, Germany
Membrane	PVDF 0.45 µm	Carl Roth, Germany
Metal beads	Stainless steel, ⌀ 5 mm	Kugel-Rollen UG, Germany
Microtiter plate	96-well, round base 96-well, flat base 96-well LUMITRAC™ 200 384-well LUMITRAC™ 200	Sarstedt, Germany Sarstedt, Germany Greiner AG, Austria Greiner AG, Austria
Plant pots	6.0 cm	
Polyester-viscose-fleece	Leukopor®, 2.5 cm x 9 m	BSN medical, Germany
Punch	3.0 mm 4.0 mm	Harris Uni-Core™ Harris Uni-Core™
Scalpel blades	No. 11 and 21	C. Bruno Bayha, Germany
Screw cap	ND10, 7 mm centre hole, 1.3 mm, 45° shore A	LABSOLUTE®, Germany
Screw neck vials	ND10, 1.5 ml, 32 x 11.6 mm	LABSOLUTE®, Germany
Soil	Spezial substrat, fruhstorfer erde	HAWITA, Germany
Sterile filter	Minisart® 0.2 mm	Sartorius Stedim Biotech, Germany
Syringe	Omnican® U-40 Insulin without cannula	B. Braun, Germany
Vial insert	250 µl, glass with polymer feet, Insert size: 5.6 x 30 mm	Agilent, USA

2.11. Devices

Table 18: List of used devises.

Device	Model	Manufacturer
Analytical scale	A 120 S ED1245	Sartorius Stedim Biotech, Germany Sartorius Stedim Biotech, Germany
Autoclave	VX-95 VX-150	Systec, Germany Systec, Germany
Binocular microscope with fluorescence equipment	SteREO Discovery.V8	Carl Zeiss AG, Germany
Blot apparatus		Workshop Albrecht-von-Haller Institute
Camera	PowerShot G11	Canon, Japan
Centrifuge	Rotina 38R Hereaus Fresco 17 Hereaus Pico 17 Sorvall RC6+	Hettich Zentrifugen, Germany Thermo Fisher Scientific, USA Thermo Fisher Scientific, USA Thermo Fisher Scientific, USA
Climate Chamber	Climate Chamber	Johnson Controls International plc, Ireland
Color Mixing Unit		
Desiccator		Glaswerkstatt Wertheim, Germany
Electrophoresis Power Supply	EV231 EV243 E323	Consort, Belgium Consort, Belgium Consort, Belgium
Electroporation cuvette	Polystyrene 10 × 4 × 45 mm	Sarstedt, Germany
Electroporation device	Capacitance Extender Plus Gene Pulser® II Pulse Controller Plus	Bio-Rad Laboratories, USA Bio-Rad Laboratories, USA Bio-Rad Laboratories, USA
Fluorescence Microscope	SteREO Discovery.V8	Carl Zeiss AG, Germany
Gel documentation camera		Intas Science Imaging Instruments GmbH, Germany
Gel documentation station	FLX20M	Vilber Lourmat
Gel electrophoresis apparature		Workshop Albrecht-von-Haller Institute
Grinding machine	Mixer Mill MM301	Retsch, Germany
Growth Cabinet	Intellus Control system AR-66L	Percival Scientific, Germany
Incubator	UNE 600	Memmert, Germany
Luminescence imager	ChemoCam	INTAS Science Imaging Instruments, Germany
Luminometer	Centro XS3 LB 960 Microplate	Berthold Technologies, Germany
NanoDrop	NanoDrop One	Thermo Fisher Scientific, USA
pH Meter	pH 211 Microprocessor	Hanna Instruments, Germany

Device	Model	Manufacturer
Plate reader	Synergy™ HT	BioTek, USA
Photometer	Libra S11	Biochrom, Germany
Pulse counter	HPX 120 C	Kübler, Germany
qRT- PCR Detection System	CFX Connect	Bio-Rad Laboratories, USA
Refrigerated Vapor Trap	RV1100	Savant
Scale	Kern PFB Kern 572 SPO 51	Kern & Sohn GmbH, Germany Kern & Sohn GmbH, Germany Scaltec Instruments, Germany
Shaking incubator	Certomat® BS-1	Sartorius Stedim Biotech, Germany
Thermal cycler	MyCylcerTM	Bio-Rad Laboratories, USA
Ultrasonic bath	Transsonic TP690	ultrasonics, Germany
Vacuum pump	Diaphragm Vacuum Pump MD1C	Vacuubrand GMbH & Co KG, Germany
Vacuum pump	AEPF71BL	Atma Antriebstechnik, Germany
Water Purification System	arium® pro DI	Sartorius Stedim Biotech, Germany

3. Methods

3.1. Standard molecular techniques

3.1.1. Isolation of genomic DNA (gDNA)

To analyze genomic DNA (gDNA), *A. thaliana* leaf material was harvested into a 1.5 ml reaction tube and frozen in liquid nitrogen. For the gDNA extraction, 400 µl DNA extraction buffer was added and the material was ground with a plastic pestle. The samples were incubated for 5 min and centrifuged (13,000 rpm, 15 min). 300 µl supernatant was transferred into a new reaction tube containing 300 µl isopropanol. After centrifugation (13,000 rpm, 15 min), the supernatant was discarded and the DNA pellet was washed with 500 µl 70 % absolute ethanol (13,000 rpm, 5 min). The supernatant was discarded and the pellet was dried with open lid. The DNA was eluted with 50 µl H_2O, incubated at 65°C for 10 min and stored at -20°C.

3.1.2. Polymerase chain reaction (PCR)

Polymerase chain reactions (PCRs) were used to amplify specific regions from a plasmid or gDNA. For this, various primers (Table 11) and the proofreading Phusion High-Fidelity DNA polymerase were used. The pipetting scheme per reaction can be found in Table 19, the cycler program is displayed in Table 20. The annealing temperature and the elongation time depend on the primers and the length of the amplified fragment.

Table 19: Pipetting scheme for Polymerase Chain Reactions.

Ingredient	Amount
5 x Phusion HF Buffer	10 µl
10 mM dNTPs	1 µl
Forward Primer (10 µM)	2.5 µl
Reverse Primer (10 µM)	2.5 µl
Template DNA	10 ng
Phusion High-Fidelity DNA Polymerase (2 U/µl)	0.5 µl
H_2O	Ad 50 µl

Table 20: Cycler program for Polymerase Chain Reaction.

Step	Temperature [°C]	Time [min]	Repeats
Initial denaturation	98	0:30	
Denaturation	98	0:10	35x
Annealing	65	0:30	
Elongation	72	1:00	
Final elongation	72	10:00	
Final hold	4	∞	

3.1.3. Classical molecular cloning with restriction and ligation

Classical molecular cloning was used for the construction of new plasmids. The plasmid DNA was cut by various restriction enzymes (Table 13), using formula (1) to calculate the appropriate enzyme amount:

$$\text{Units}_{\text{enzyme}} = \frac{\lambda\ \text{DNA [bp]} * \text{plasmid DNA [µg]} * \text{restriction sites plasmid DNA} * \lambda\ \text{activity [\%]}}{\text{plasmid DNA [bp]} * \text{restriction sites}\ \lambda\ \text{DNA} * \text{time [h]} * \text{enzyme activity [\%]}} \quad \textbf{(1)}$$

The phage λ DNA consists out of 48,500 bp, 1 µg plasmid DNA was used and the λ activity is 100. The enzyme activity represents the activity of the enzyme in the used buffer. The enzymatic fragmentation was planned with the software Clone Manager Professional Version 9.

In a total volume of 10 µl, plasmid DNA, the restriction enzymes and the respective buffer were mixed and incubated at 37°C for several hours. For blunt end fragments, 0.4 µl CIAP (Calf Intestine Alkaline Phosphatase) was added. The mixture was incubated at 37°C for 30 min. The phosphatase was inactivated at 85°C for 10 min, the mixture was run on an agarose gel (see section 3.1.8) and the DNA fragments were extracted from the gel (see section 3.1.9).

For the ligation, 1 µl ligase, 2 µl ligase buffer and the different fragments for ligation were mixed in a total volume of 20 µl. After incubation at RT for several hours, 10 µl were transformed into *E. coli* DH5α.

3.1.4. Gateway™ cloning

The Gateway™ Technology (Thermo Fisher Scientific, USA; Katzen, 2007) is derived from phage λ which is able to integrate parts of its genome into bacteria (Campbell, 1961). For this technology, the coding region of a gene-of-interest is flanked by *attL* sites on the donor vector. By recombination with *attR* sites (LR reaction) on a destination vector, the expression vector and a by-product is created (Figure 8). This reaction is mediated by the LR clonase.

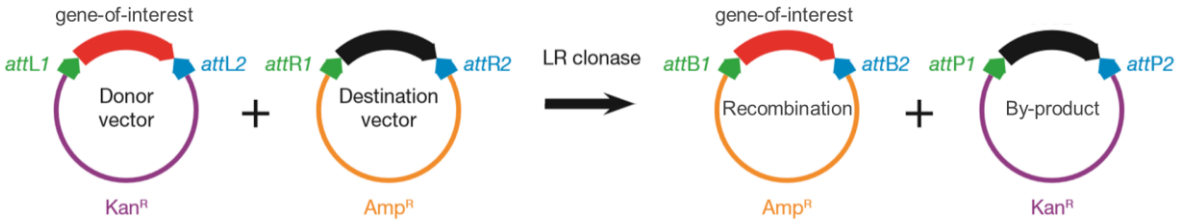

Figure 8*:* Schematic representation of the LR reaction with Gateway™ Cloning Technology. By recombination of *attL* sites on the donor vector with *attR* sites on the destination vector, the expression vector and a by-product is created. This is mediated by the LR clonase. Kan$^{R:}$ kanamycin resistance, Amp^{R}: ampicillin resistance (Katzen, 2007; modified).

The donor vectors used in this study were constructed by classical molecular cloning with restriction and ligation (Table 9). The destination vectors were provided from the department. To create the expression vectors, 1 µl of the provided LR Clonase™ mix (Thermo Fisher Scientific, USA) was mixed with 100 ng of both the destination vector and the donor vector in a total volume of 5 µl. After incubation at RT for 1 h, the plasmids were transformed into *E. coli* DH5α for amplification. After plasmid isolation, the right assembly was verified by enzymatic fragmentation and sequencing.

3.1.5. Plasmid isolation and purification

The NucleoSpin® Plasmid (Macherey-Nagel, Germany) was used for purification of plasmids from both *E. coli* and *A. tumefaciens*. For plasmids purified from *E. coli*, the manufacturer's instructions were followed apart from the elution, in which 50 µl dH_2O was used. For purification of plasmids from *A. tumefaciens*, the pellet was resuspended in 500 µl buffer A1 and 5 µl RNase (100 mg/ml). 500 µl buffer A2 was added, the samples were mixed by inverting, incubated for 5 min and 600 µl buffer A3 was added. After mixing by inverting, the samples were centrifuged (13,000 rpm, 20 min). From now on, the manufacturer's instructions were followed. The elution was performed in 30 µl dH_2O and the plasmid concentration was measured with the NanoDrop.

3.1.6. Enzymatic fragmentation

Correct assembly of the plasmids was verified by enzymatic fragmentation. To calculate the appropriate amount of enzyme, formula (1) was used. The enzymatic fragmentation was planned with the software Clone Manager Professional Version 9.

In a total volume of 10 µl, plasmid DNA, restriction enzymes and the respective buffer were mixed and incubated at 37°C for several hours. To analyze the DNA fragments, an agarose gel electrophoresis was performed.

3.1.7. Genotyping

To genotype *A. thaliana*, PCRs were performed with the Advantage polymerase and various primers (Table 11). The pipetting scheme per reaction can be found in Table 19, the cycler program is displayed in Table 20.

Table 21: Pipetting scheme for Polymerase Chain Reactions.

Ingredient	Amount
H_2O	6.6 µl
10 x Advantage 2PCR Buffer	1 µl
10 mM dNTPs	0.2 µl
Primer 1 (10 µM)	0.5 µl
Primer 2 (10 µM)	0.5 µl
Primer 3 (10 µM)	0.5 µl
Template DNA	0.5 µl
50 x Advantage 2 Mix Polymerase	0.5 µl

Table 22: Cycler program for Polymerase Chain Reaction.

Step	Temperature [°C]	Time [min]	Repeats
Initial denaturation	95	0:30	
Denaturation	95	0:30	35x
Annealing	68	0:30	
Elongation	68	1:00	
Final elongation	68	7:00	
Final hold	4	∞	

3.1.8. Agarose gel electrophoresis

As preparation for agarose gel electrophoresis, 1 % agarose was dissolved in TAE buffer by heating in the microwave and stored at 65°C. Gels were poured 20 min before usage. For analysis, the restricted plasmids or PCR products were supplemented with Orange G loading dye (1:6) and loaded onto the agarose gel, which was run at 130 V for 45 min. The GeneRuler™ DNA Ladder Mix (Thermo Fisher Scientific, USA) was used as a marker. The gel was stained in a 0.0001 % ethidium bromide solution for 15 min. Ethidium bromide intercalates in DNA and was visualized by excitation with UV light. For DNA extraction from agarose gels, the fragments were visualized with UV light. By using a scalpel, the respective fragments were cut from the gel and transferred into a reaction tube. Pictures of the gels were taken at a gel documentation station at 260 nm UV light.

3.1.9. DNA extraction from agarose gels

The NucleoSpin® Gel and PCR Clean-up kit (Macherey-Nagel, Germany) was used for DNA extraction from agarose gels. The manual was followed until the elution step, which took place in 30 µl H_2O. The DNA concentration was determined with the NanoDrop.

3.1.10. Sequencing

To verify the correct assembly of the plasmids in addition to enzymatic fragmentation, the plasmids were sent for sequencing to Seqlab (Microsynth Seqlab, Germany) according to their requirements. The sequencing results were assembled and analyzed with the Software Geneious Pro 5.3.6.

3.1.11. Protein extraction

For the extraction of proteins, *A. thaliana* leaf or root material was harvested and frozen in liquid nitrogen. The samples were ground with metal beads in the grinding machine (30s, frequency 20 s^{-1}). 200 µl Urea Buffer with β-ME per 100 mg sample was added. The samples were mixed by vortexing and incubated at 65°C for 10 min. After centrifugation (13,000 rpm, 15 min), the supernatant was transferred to a new reaction tube. The proteins were stored at -20°C.

3.1.12. Determination of protein concentrations

Protein concentrations were determined by using the Pierce 660 nm Protein Assay (Thermo Fisher Scientific, USA). Ionic Detergent Compatibility Reagent (IDCR) was mixed with the Pierce Reagent (50 mg/ml). In the first row of a 96-well microtiter plate, a protein standard was pipetted consisting out of 0, 1, 3, 6 and 9 µg BSA in 9 µl H_2O. In the other wells, 9 µl H_2O and 1 µl protein sample was added. 150 µl IDCR in Pierce Reagent was added to each well and mixed by pipetting up and down. After short incubation, the absorption at 660 nm was measured in a plate reader. A standard curve was assembled and the protein concentrations were determined. For Western Blot analysis, the proteins were diluted to the same concentration.

3.1.13. SDS-PAGE and Western Blot

The prepared protein samples were heated for 10 min at 65°C. 30 µl were run on a 4 % SDS stacking gel and 12 % or 15 % SDS resolving gel in SDS running buffer at 160 V for 2.5 h. The ingredients of the gels are described in Table 23. PageRuler™ Prestained Protein Ladder #SM0671 (Thermo Fisher Scientific, USA) was used as a size standard.

Table 23: Ingredients for SDS-gels.

	Ingredient	Amount for 1 gel
15 % Separating gel	H_2O	4.6 ml
	1.5 M Tris HCl pH 8.8	5 ml
	30 % Acrylamide	10 ml
	10 % SDS	200 µl
	10 % APS	200 µl
	TEMED	20 µl
12 % Separating gel	H_2O	6.6 ml
	1.5 M Tris HCl pH 8.8	5 ml
	30 % Acrylamide	8 ml
	10 % SDS	200 µl
	10 % APS	200 µl
	TEMED	20 µl
4 % Stacking gel	H_2O	7.2 ml
	1 M Tris HCl pH 6.8	1.25 ml
	30 % Acrylamide	1.34 ml
	10 % SDS	100 µl
	10 % APS	100 µl
	TEMED	10 µl

The gel was washed in transfer buffer before the proteins were transferred to the methanol activated PVDF membrane by electroblotting at 125 mA for 1 h. After blotting, the membrane was blocked with 5 % BSA or skimmed milk powder in TBS for 2 h while shaking. The primary antibody was diluted in 5 % BSA or skimmed milk powder in TBST and applied overnight at 4°C. The membrane was washed three times with TBST for 10 min before the secondary antibody fused horseradish peroxidase (HRP) was applied for 2 h. The secondary antibody was diluted in TBST with 5 % BSA or skimmed milk powder. After washing 5 times with TBS for 5 min, the Luminata™ Forte Western HRP Substrate (Thermo Fisher Scientific, USA) was applied. For the chemiluminescence detection, the luminescence imager and the software ChemoStarProfessional was used.

To use another primary antibody, the membrane was stripped with stripping solution for 1 h at 50°C. After washing twice with TBS for 5 min, the blocking solution was applied and the already described protocol was repeated.

3.2. Growth conditions and treatment of organisms

3.2.1. Cultivation and transformation of *Escherichia coli*

Escherichia coli strain DH5α was grown on LB plates or in liquid dYT medium containing the respective antibiotic. Bacterial cells were grown at 37°C, liquid cultures were shaken at 220 rpm. For the transformation, the provided chemically competent *E. coli* cells were defrosted on ice for 30 minutes. The respective plasmids were added and incubated for 30 minutes on ice. During a 90-second heat shock at 42°C, the bacteria are supposed to take up the plasmids. After 3 minutes incubation on ice, dYT was added and the bacteria were incubated for 45 minutes at 37°C. The cells were harvested by centrifugation (13,000 rpm, 1 min), resuspended in the backflow and plated on LB agar plates containing the respective antibiotic. After incubation overnight, single colonies were and inoculated in a liquid culture. After growth overnight, the bacteria were harvested by centrifugation (13,000 rpm, 1 min) and the plasmids extracted.

3.2.2. Cultivation and transformation of *Agrobacterium tumefaciens*

Agrobacterium tumefaciens strain GV3101 was grown at 29°C on YEB plates or liquid YEB containing the respective antibiotics. Liquid cultures were shaken at 220 rpm.

The constructed plasmids were transformed into *A. tumefaciens* by electroporation. For this, provided electro competent cells were defrosted on ice for 30 min. 100 ng of the respective plasmids were added to the cells. After incubation on ice for 30 min, the bacterial cells were transferred into an electroporation cuvette. A single electroshock (2.5 kV, 200 Ω, 25 µF) mediates the transformation. 1 ml YEB was added and the bacteria were transferred into a reaction tube. After growth for 2 h at 29°C, the cells were plated on YEB plates containing gentamycin, spectinomycin and rifampicin for two days.

3.2.3. Cultivation of *Arabidopsis thaliana*

For the cultivation of *A. thaliana,* seeds were surface sterilized with chlorine gas. For this, 50 ml sodium hypochlorite was filled into a jar and placed into the desiccator. Seeds were transferred into a reaction tube and placed with open lid in the desiccator. 2.5 ml 32 % hydrochloride acid was added and 0.2 bar vacuum was applied for 2 h. The steamed soil was fertilized with 0.2 % Wuxal® Super and transferred into round pots. After sterilization, seeds were put out on soil and incubated at 4°C for two days for stratification.

The surface sterilization of *A. thaliana* seeds for growth on agar plates varies slightly from the protocol used for soil. The seeds were sterilized with 100 ml sodium hypochlorite and 5 ml 32 % hydrochloride acid for 4 h.

If not otherwise stated, plants were grown under 12/12 h light regime, 100-120 µmol photons $m^{-2} s^{-1}$, 22°C and 60 % relative humidity.

3.3. Phenotypic characterization

3.3.1. Growth phenotype

For the determination of the fresh weight from different genotypes, plants were grown on soil either under short day (SD), 12/12 h or long day (LD) conditions. In SD, there is an 8 h light period (100-120 µmol photons m^{-2} s^{-1}) and the temperature is 22°C. In LD conditions, there is a 16-hour light period (100-120 µmol photons m^{-2} s^{-1}) with 22°C whereas the temperature during the night was 18°C. The relative humidity was constantly at 60 %. The shoot of 4-week old plants was separated from the roots with a scalpel and the fresh weight of the rosette was measured with an analytical scale.

In addition, the leaf and petiole length were measured. For this, all leaves from 4-week old plants were placed on a sheet of paper and pictures were taken. The length of the total leaf and the petiole was measured with the software Image J and the leaf-to-petiole ratio was calculated.

3.3.2. Hyponastic growth

The hyponastic growth experiments were performed according to the method described in Li *et al.,* 2019. Plants were grown for 4 weeks under normal light (NL) conditions (12/12 h light regime*)*. 1.5 hours after the onset of light, plants were either left in NL conditions or transferred to low light (LL) conditions (15-20 µmol photons m^{-2} s^{-1}). For backshift experiments, plants were transferred back from LL to NL on the next day directly after the onset of light. After 4 h, the plants were positioned so that the 8th leaf points to the right and pictures of the plants were taken. By using the software ImageJ, the leaf angle of the 8th leaf was measured. For transcript analysis, all petioles of four plants were collected 4, 5 or 7.5 h after the onset of light and frozen in liquid nitrogen.

3.4. Pathogen assays

3.4.1. Plant growth conditions

4-week-old *A. thaliana* plants grown were used for local pathogen infection. For SAR experiments, plants were used after 4.5 weeks. To facilitate the opening of the stomata, plants were watered one hour before *Psm* infection.

3.4.2. Cultivation of *Pseudomonas syringae*

P. syringae pv. *maculicola* ES4326 (*Psm*) were grown at 29°C on King's B plates or in liquid King's B medium containing rifampicin. Liquid cultures were shaken at 220 rpm. For the pathogen assays, an overnight culture was harvested by centrifugation (4,000 rpm, 5 min) and washed twice with 10 mM $MgCl_2$ (4,000 rpm, 5 min). Depending on the experiment, different bacterial concentrations were used. To analyze basal resistance after 8 h or 24 h and for bacterial growth assays, *Psm* was diluted to an OD_{600} of 0.001 in 10 mM $MgCl_2$. An OD_{600} of 0.005 was used for used for SAR experiments.

3.4.3. Basal resistance

To analyze basal resistance, three leaves per plant were either left untreated, infiltrated with 10 mM $MgCl_2$ (mock treatment) or infiltrated with *Psm* diluted in 10 mM $MgCl_2$. At 8 or 24 hpi, the three leaves were collected into a 2 ml reaction tube containing a metal bead and frozen in liquid nitrogen. The samples were stored at -70°C.

3.4.4. Systemic acquired resistance

For SAR experiments, three lower leaves per plant were either left untreated, mock treated or infiltrated with *Psm*. 48 h after the first treatment, three upper leaves per plant were infiltrated with *Psm*. After 8 h, the upper infected leaves were collected into a 2 ml reaction tube containing a metal bead, frozen in liquid nitrogen and stored at -70°C.

3.4.5. Bacterial growth assays

To analyze the growth of *Psm* in *A. thaliana*, three leaves per plant were infiltrated with *Psm*. Samples were collected directly after the infiltration (day 0) and after three days (day 3). For the sample collection, three leaf discs (d = 0.3 mm) of the three infected leaves were punched and transferred into a 2 ml tube containing 200 µl 10 mM $MgCl_2$ and two small beads. In a color mixing unit, the bacteria were shaken out of the tissue two times for 2 min. For the day 0 samples, 10 µl of the dilution was plated on King's B plates containing rifampicin. Dilutions ranging from 1:10 to 1:10000 were prepared of the day 3 samples and 10 µl of each dilution was plated. After incubation of the plates for 2 days at 29°C, colonies were counted and the colony forming units (CFUs) per cm^2 were calculated using the following formula:

$$CFU/cm^2 = \frac{n\ (colonies) * dilution\ factor}{V*A} \quad \textbf{(2)}$$

n represents the number of colonies, the plated volume (V) is 0.01 ml and the area of 9 leaf discs (A) is 0.636 cm^2.

3.4.6. Bioluminescence assays

Three leaves per plant were infiltrated with *Pst lux* (Matsumoto *et al.,* 2022). Samples were collected directly after the infiltration (day 0) and after three days (day 3). For the sample collection, leaf discs (d = 0.4 mm) of the infected leaves were punched and transferred into a 96-well plate containing 100 µl sterile water. After incubation for 10 min in the dark, bioluminescence was measured with the luminometer. Untreated or mock treated leaf discs serve as a control for the background luminescence in the leaves. The relative light units per (RLUs) per cm^2 were calculated using the following formula, in which the area (A) of the leaf disc is 0.126 cm^2:

$$RLU/cm^2 = \frac{luminescence\ identities}{A} \quad \textbf{(3)}$$

3.5. Pharmacological treatment

Pharmacological treatment was performed with 4-week-old *A. thaliana* plants. Plants were watered one hour prior to the treatment. For the spray inoculation of salicylic acid (SA), 1 mM sodium salicylate in 10 mM $MgCl_2$ was prepared. The solution was sprayed on each plant 10 times, water was sprayed as a control treatment (mock). After 8 hours, three leaves per plant were harvested and stored at -70°C. For treatment with N-hydroxypipecolic acid (NHP), three leaves were infiltrated with 1 mM NHP in 10 mM $MgCl_2$, infiltration with 10 mM $MgCl_2$ was used as mock treatment. The leaves were harvested after 8 or 48 hours and stored at -70°C.

3.6. Nitrogen starvation assays

To analyze the differential gene expression upon nitrogen sufficient and nitrogen limiting conditions, 13 *A. thaliana* seeds were plated on agar plates containing full nutrition (FN) medium. The plates were sealed with polyester-viscose-fleece (Leukopor®, BSN medical, Germany). After stratification at 4°C overnight, the plates were placed vertically in a growth cabinet under constant light conditions (60-80 µmol photons m^{-2} s^{-1}) with 22°C and 60 % relative humidity. After growth for 7 days, seedlings were transferred to new agar plates containing either FN, low nitrogen (LN) or no nitrogen (NN) medium. To analyze the influence of C-TERMINALLY ENCODED PEPTIDE (CEP) on gene expression, seedlings were transferred to FN plates containing 1 µM CEP1. The plates were sealed with polyester-viscose-fleece and placed vertically in a growth cabinet. Two days later, shoots and roots were harvested separately. All shoots or roots from one plate were pooled into one 2 ml reaction tube containing a metal bead. The samples were immediately frozen in liquid nitrogen and stored at -70°C.

3.7. Transcript analysis

3.7.1. RNA isolation

The frozen samples were ground using metal beads and the grinding machine (30 s, frequency 20 s^{-1}) or ground with mortar and pestle. For the RNA extraction, an adapted TRIZOL protocol was used (Chomczynski & Mackey, 1995). 1400 µl TRIZOL was added to the sample material and mixed by vortexing for 5 min. 250 µl chloroform was added, the samples were vortexed for 10 min and centrifuged (13,000 rpm, 60 min, 4°C). The supernatant was transferred into a new 2 ml tube containing 400 µl HSP buffer (1.2 M $NaCl_2$, 0.8 M sodium citrate) and 400 µl 100 % isopropanol. After inverting, the samples were incubated for 5 min at RT and centrifuged (13,000 rpm, 60-90 min, 4°C). The supernatant was discarded and the pellet was washed with 250 µl 70 % absolute ethanol (13,000 rpm, 5 min, 4°C). 250 µl 70 % absolute ethanol were added. The ethanol and the RNA pellet was transferred into a 1.5 ml tube. After centrifugation (13,000 rpm, 10 min, 4°C), the ethanol was removed and the pellet was dried for 20 min. The RNA was resuspended in 50 µl H_2O at 65°C for 10 min. After vortexing, the samples were centrifuged (13,000 rpm, 5 min, RT) and stored at -20°C.

3.7.2. cDNA synthesis

By using the NanoDrop, the RNA concentration was measured. For the cDNA synthesis, 1 µg of the RNA was diluted in 8 µl H_2O. 1 µl 10x buffer and 1 µl DNase I (10 U/µl) was added to each sample to digest the residual DNA. After 30 min at 37°C in the thermocycler, the DNase I was denaturated by adding 1 µl 25 mM EDTA and incubation at 65°C in the PCR machine. Next, 0.2 µl oligoT primer and 1 µl H_2O were added to each sample. During the incubation at 70°C for 10 min, the primers anneal to the poly(A) tail of the mRNA. For the actual cDNA synthesis, 4 µl RT 5x buffer, 2 µl dNTPs, 1.5 µl H_2O and 0.3 µl reverse transcriptase (200 U/µl) were added. The samples were incubated for 70 min at 42°C and 10 min at 70°C. The cDNA was then diluted by the factor 10 and stored at -20°C until further use.

3.7.3. Quantitative real time PCR

The transcript amount of different genes was analyzed by quantitative real time PCR (qRT-PCR). The samples were pipetted into PCR stripes according to the pipetting schema in Table 24. The primers used for the analysis are described in Table 10, *UBQ5* primers were used as reference. The cycler program is displayed in Table 25.

Table 24: Pipetting schema for qRT-PCR.

Ingredient	Amount
10 x NH4 buffer	2.5 µl
50 mM $MgCl_2$	1 µl
10 mM dNTPs	1 µl
Primer mix (forward, reverse)	2.5 µl
SYBR® Green (1:1000, Molecular Probes, USA)	0.25 µl
Fluorescin (1 µM/1:1000, Bio-Rad Laboratories, USA)	0.25 µl
DNA Polymerase BIOTaq (5 U/µl)	1 µl
Diluted cDNA	1 µl
H_2O	17.2 µl

Table 25: Cycler program for qRT-PCR.

Step	Temperature [°C]	Time [min]	Repeats
Initial denaturation	95	1:30	
Denaturation	95	0:20	39 x
Annealing	55	0:20	
Elongation	72	0:40	
Final Elongation	72	4:00	
Denaturation	95	1:00	
Annealing	55	1:00	
Meltcurve	55 – 95 0.5°C per cycle	0:10	81 x

The results were evaluated using the software Bio-Rad CFX Manager 3.1. After setting the threshold, the fold over reference was calculated using the following formula:

$$\text{fold over reference} = 2^{-[C_T(\text{gene-of-interest})-C_T(\text{reference gene})]} \quad \textbf{(4)}$$

C_T represents the threshold cycle of the analyzed gene and the reference *UBQ5*, respectively.

3.7.4. Transcriptome analysis

The transcriptome analysis was performed by the Next Genome Sequencing Integrative Genomics Core Unit (NIG), University Göttingen. For this, the same experiment was performed four times and RNA was extracted. From each experiment, RNA of four to five replicates was pooled (200 ng/µl) and sent to the NIG. The RNA quality was examined with an AGILENT BIOANALYZER 2100. A library was prepared and 50-bp raw reads were generated with Illumina HiSeq 2000. The sequence images were transformed to BCL files with the Illumina BaseCaller software and demultiplexed with CASAVA (v1.8.2) to FASTQ files. The obtained reads were mapped to the *Arabidopsis thaliana* genome reference sequence TAIR10 with RNA STAR (Galaxy Version 2.5.2b-2, Afgan *et al.,* 2018) and quantified by using htseq-count (Galaxy Version 0.6.1galaxy3, Anders *et al.,* 2015). To determine log2-fold changes and adjusted p-values (Benjamini-Hochberg-corrected), DESeq2 (Galaxy Version 2.11.40.6+galaxy1, Love *et al.,* 2014) was used. For each detected gene, the reads per kilobases (RPK) and the transcript per million (TPM) was calculated using the formulas (5) and (6). Additionally, Principal Component Analysis (PCA) of normalized transcriptome data was performed with this tool to control data distribution.

$$\mathrm{RPK}_{\text{gene of interest}} = \frac{\mathrm{reads}_{\text{gene of interest}}}{\mathrm{length}_{\text{gene of interest}}} * 1000 \quad \textbf{(5)}$$

$$\mathrm{TPM} = \frac{\mathrm{RPK}_{\text{gene of interest}}}{\sum \mathrm{RPK}_{\text{all genes}}} * 1000000 \quad \textbf{(6)}$$

To further analyze the transcriptome datasets, MarVis (Marker Visualization) clustering was performed within the MarVis-Suite application (Version 2.0; Kaever *et al.,* 2009; 2015). Additionally, proportional venn diagrams were generated with the BioVenn web application (Hulsen *et al.,* 2008).

Gene Ontology (GO) enrichment analysis was performed using the Gene Onthology Consortium web site (Ashburner *et al.,* 2000; The Gene Ontology Consortium, 2021) and the PANTHER Classification system version 17.0 (Mi *et al.,* 2013). Differentially expressed genes were sorted according to their biological process into GO groups. By comparison with Arabidopsis genome reference list (GO Ontology database, Carbon & Mungall, 2018) consisting out of 27430 annotated genes, enrichments in a sample set were identified.

Motif enrichment analysis in 1000 bp promoter regions upstream of the predicted transcriptional start sites was performed with Motif Mapper Version 5.2.4.01 (Berendzen *et al.,* 2010). By comparing the promoter regions of an input data set with randomly selected genes from the Arabidopsis reference genome, enrichments were calculated. The reference genome was downloaded from TAIR and contains promotor regions of 33602 genes.

3.8. Transformation of *Arabidopsis thaliana*

3.8.1. Floral dipping method

The floral dipping method is used for *Agrobacterium tumefaciens* mediated transformation of *A. thaliana* egg cells, which results in transgenic embryos after fertilization (Clough & Bent, 1998).

For this, long-day (LD) *A. thaliana* plants were grown on soil. During the 16-hour light period (100-120 µmol photons m^{-2} s^{-1}), there was a temperature of 22°C whereas the temperature during the night was 18°C. The relative humidity was constantly at 60 %. A preculture of *A. tumefaciens* containing the respective plasmids was grown in 20 ml YEB supplemented with the respective antibiotics. After incubation at 29°C and 220 rpm for two days, the main culture was inoculated overnight in 200 ml YEB containing the respective antibiotics. After harvesting (5,000 rpm, 20 min, RT), the cells were resuspended in sugar solution (5 % Sucrose, 0.02 % Silwet) at an OD_{600} = 0.8. Flowering *A. thaliana* plants were dipped into the bacterial sugar solution for 15 s. Overnight, the plants were covered with a hood to promote the transfer of DNA. Fully developed and dehumidified seeds were collected and analyzed.

In this study, the floral dipping method was used to construct complementation lines of *roxy6789* and to generate *A. thaliana* lines expressing ROXY9 fused to the biotin ligase Turbo.

3.8.2. Generation of transgenic lines

To analyze the importance of the ROXY specific active site motif, stable complementation lines were constructed. For this, the coding region for HA-tagged ROXY9 with wild type or altered active site motif under control of the *35S* promoter was introduced into the *roxy6789* mutant by using the floral dipping method. Additionally, *A. thaliana* was stably transformed with ROXY9 fused to the HA-tagged biotin ligase Turbo under control of the *UBQ10* promoter. These plants will be used to identify new interaction partners of ROXY9. In addition to the *ROXY9* transgene, a basta resistance cassette was introduced into the plant which allows distinction between transformed plants and WT plants.

3.8.2.1. Selection of primary transformants

Due to the basta resistance cassette, the primary transformants (T1 generation) was selected by spraying basta solution (200 mM Basta® Herbicide, 0.02 % Silwet) on the seedlings for three times (7-, 11- and 14-day old seedlings). Afterwards, the surviving seedlings were transplanted. To analyze the primary transformants, leaf material was harvested and frozen in liquid nitrogen. Subsequently, the RNA or proteins were isolated and the transgenic *ROXY9* transcript level or the Turbo-ROXY9 protein level was determined. Plants with an intermediate transgenic *ROXY9* level or high Turbo-ROXY9 amount were chosen for further analysis. Seeds of fully developed and dehumidified plants were collected. As only one copy of the construct should be integrated into the genome, the segregation of the seeds of the primary transformants was analyzed on 2MS + PPT plates. Statistically, if only one copy is present, 25 % is homozygous for the wild type allele and thus does not survive on the PPT plates. The other plants are either heterozygous (50 %) or homozygous (25 %) for the transgene that is why they are able to grow in the presence of PPT. To analyze the segregation, 100 seeds were placed on 2MS + PPT plates. The plates were sealed with polyester-viscose-fleece (Leukopor®, BSN medical, Germany). After stratification at 4°C overnight, the plates were placed in a climate chamber under 14/10 h light regime *(*100-120 µmol photons m^{-2} s^{-1}) at 22°C and 60 % relative humidity. After 10 days, the germinated seeds were counted and the survival rate was determined. Transgenic lines with a survival rate of 65 % - 85 % were further cultivated.

3.8.2.2. Selection of secondary transformants

To obtain secondary transformants (T2 generation), seeds from the selected T1 lines were grown on soil. After self-fertilization, homozygous plants can be obtained. Fully developed and dehumidified seeds were collected and analyzed on 2MS + PPT plates as described above for the T1 generation. Plates with a 100 % survival rate indicate homozygous lines with the transgenic *ROXY9* integrated into the genome. The seeds of these lines (T3 generation) were selected and used for all the following experiments.

3.9. TurboID-based proximity labeling

The TurboID method is based on proximity labeling by the biotin ligase Turbo (Branon *et al.,* 2018). Turbo is an altered BioID isolated from *E. coli* with improved the catalytic efficiency. In the presence of biotin, molecules within a 10 nm range of Turbo gets biotinylated (May *et al.,* 2020). By using streptavidin-coated beads, which binds to biotin with a high affinity, the biotinylated proteins can be isolated. The proteins can then either be detected by western blot analysis by using specific antibodies or further analyzed by liquid chromatography coupled with mass spectrometry (LCMS).

3.9.1. Transient transformation and biotin treatment of *N. benthamiana*

To test the functionality of the HA-Turbo-ROXY9 construct, it was transiently co-expressed with flag-TGA2 in *N. benthamiana* leaves. *N. benthamiana* plants were grown for 5 weeks under 16/8 h light regime, 25°C during the day, 22°C at night and 65 % relative humidity. A preculture of *A. tumefaciens* containing the respective plasmids was grown in 10 ml YEB supplemented with the respective antibiotics. After incubation at 29°C and 220 rpm for two days, the cells were harvested (5,000 rpm, 5 min), resuspended in 10 mM $MgCl_2$ to achieve an OD_{600} of 0.5. Subsequently 150 µM acetosyringone was added to enhance the transformation rate. Finally, two leaves per plant were infiltrated with the transgenic *A. tumefaciens* strains.

After two days, the same leaves were infiltrated with 200 µM biotin in 10 mM $MgCl_2$. After incubation for 4-5 hours, the leaves without mid and side rib were harvested in liquid nitrogen. After grinding with mortar and pistil, the samples were stored at -70°C until further use.

3.9.2. Desalting and Immunoprecipitation of *N. benthamiana* material

Immunoprecipitation (IP) extraction buffer with 1:100 protease inhibitor was added to the ground *N. benthamiana* material (double volume of material). The samples were gently rotated for 30 min at 4°C. After centrifugation (13,000 rpm, 10 min, 4°C), the clear supernatant was transferred to a new tube.

To 75 µl of the supernatant, 25 µl 4x SDS was added, boiled at 99°C for 5 min and kept as an input reference. For the rest of the supernatant, the lysate, flag-beads were prepared. 20 µl beads per g tissue were washed with 1 ml IP extraction buffer and centrifuged (6,000 rpm, 1 min, 4°C). The lysate was added to the washed beads, mixed by flipping and gently rotated at 4°C for 2 h. For the elution, 10 µl 4x SDS diluted in IP buffer was added to the samples and it was boiled at 99°C for 5 min. After centrifugation (13,000 rpm, 30 sec), the supernatant was transferred to a new tube. Both the input and the eluate were stored at -20°C until further use. In Western Blot analysis, the primary antibodies α-HA, α-flag and streptavidin were used.

3.9.3. Biotin treatment of *A. thaliana* roots

In order to identify new interaction partners of ROXY9, transgenic *A. thaliana* plants were grown for 4 weeks. The roots were cleaned in water and submerged in 200 µM biotin in 10 mM $MgCl_2$ for 3 h. The material was harvested in liquid nitrogen, ground with mortar and pistil and stored at -70°C.

3.9.4. Desalting and Immunoprecipitation of *A. thaliana* material

For the immunoprecipitation of *A. thaliana* root proteins, an altered IP buffer was used (50 mM Tris pH 7.5, 50 mM NaF, 200 mM sucrose, 1 % triton-X (Kim *et al.,* 2019)). The ground material was resuspended in buffer with 1:00 protease inhibitor in 2.5 times the volume. The samples were rotated at 4°C for 30 min. In the meantime, the PD10 desalting columns and the streptavidin-coated beads were prepared. The end of the PD10 columns was cut off and the column was washed 5 times with 5 ml cold IP buffer. 25 µl beads per g tissue were washed with 1 ml IP buffer. The samples were centrifuged (13,000 rpm, 10 min, 4°C) and the supernatant was transferred into a new reaction tube. This step was repeated at least twice or until the supernatant was clear. The supernatant was transferred onto the PD10 column. After the liquid had completely moved into the column completely, the samples were eluted several times with 1 ml IP buffer. The first eluate was discarded, as it only contains a minor amount of proteins. The second eluate was used in the following steps, it contains the majority of proteins (tested in preliminary experiments). 75 µl of the eluate was mixed with 25 µl 4x SDS, boiled at 99°C for 5 min and kept as an input reference. The residual eluate was added to the prepared streptavidin-coated beads and rotated at 4°C for 3 h. 75 µl of the supernatant were mixed with 25 µl 4x SDS, boiled at 99°C for 5 min and kept as an unbound reference. The remaining supernatant was discarded and the beads were washed with wash buffer 4 times. For this, 1 ml wash buffer was added and the beads were rotated for 5 min at 4°C. The biotinylated proteins were eluted 2 times by adding 45 µl wash buffer and 15 µl 4x SDS and the beads were boiled at 99°C for 5 min. Afterwards everything was stored at -20°C until further use.

3.9.5. In-gel Trypsin Digestion

As preparation for the LCMS analysis, the biotinylated proteins need to be digested with trypsin. For this, the proteins were run on a 4 % SDS stacking gel and 12 % SDS resolving gel in SDS running buffer at 160 V for 1 h. The gel was fixed with 40 % EtOH, 10 % acidic acid and washed twice with H_2O. All proteins smaller than 15 kDa were discarded to avoid contamination of streptavidin. The remaining protein lanes were cut in small pieces and transferred to several Protein LoBind Tubes. The in-gel trypsin digestion was adapted from (Shevchenko *et al.,* 1996) by the LCMS Protein Analytics Service Unit, University Göttingen. 30 µl acetonitrile was added to the gel pieces for dehydration and incubated for 10 min at RT The acetonitrile was removed and 150 µl 10 mM DTT in 100 mM NH_4HCO_3 was added to reduce disulfide bonds. The gel pieces were incubated for 1 h at 56°C. After this, the supernatants were discarded, 150 µl 55 mM iodoacetamide in 100 mM NH_4HCO_3 was added and the samples were incubated for 45 min at RT in the dark. This leads to cysteine alkylation. The iodoacetamide was discarded and the gel pieces were washed twice with 150 µl 100 mM NH_4HCO_3 for 10 min and 150 µl acetonitrile for 10 min. The gel pieces were dried in the speedvac at 50°C for 10 min before 30 µl trypsin (20 µg/ml) in 25 mM NH_4HCO_3 pH 8.0 was added. The samples were incubated on ice for 45 min, the supernatants were discarded, 30 µl 25 mM NH_4HCO_3 was added and incubated over night at 37°C. On the next day, the supernatants were collected to new Protein LoBind Tubes. To extract further peptides, 30 µl 20 mM NH_4HCO_3 were added to the gel pieces and shaken for 10 min at RT. The supernatant with acidic peptides was collected and 30 µl 50 % acetonitrile / 5 % formic acid was added, shaken for 20 min at RT and the basic peptides in the supernatant were collected. Both steps were repeated twice. The pooled supernatants in the fresh tubes were completely dried in the speedvac at 50°C. After several hours, the dried peptide pellets were stored at -20°C.

3.9.6. Stage Tipping

Before performing LCMS analysis, the peptide mixtures need to be cleaned, concentrated and pre-fractionated, for which stop-and-go-extraction tips (StageTips) were used. StageTips are ordinary pipette tips containing very small discs made of beads with a reversed phase, cation-exchange or anion-exchange surfaces embedded in a Teflon mesh. The protocol was provided by the LCMS Protein Analytics Service Unit, University Göttingen and is adapted from (Rappsilber *et al.,* 2003). First, the StageTips were prepared by inserting two layers of the cation exchange C18 material into a 200 µl pipette tip. The tip was then placed with an adaptor in a 2 ml reaction tube without lid. For equilibration, 100 µl HPLC grade methanol with 0.1 % formic acid was added onto the C18 column. The tips in the reaction tube were centrifuged for 2 min at 13,000 rpm. After discarding of the flow through, 100 µl 70 % acetonitrile with 0.1 % formic acid was added, centrifuged and the flow though was discarded. 100 µl H_2O with 0.1 % formic acid was added, the tips were centrifuged and the flow though was discarded. The last step was repeated.

The dried peptide pellets were resuspended in 20 µl fresh sample buffer (98 % H_20, 2 % acetonitrile, 0.1 % formic acid) by pipetting up and down for around 10 times. Additionally, the samples were incubated in an ultrasonic bath for 3 min at maximal power. The samples were loaded onto the StageTip. To ensure that the liquid is in contact with the C18 column, the tip was centrifuged at 1,000 rpm for 5 s. After incubating for 5 min, the samples were centrifuged (4,000 rpm, 5 min). The flow through was reloaded onto the stage tip for better yield, centrifuged again at 4,000 rpm, 5 min and the flow though was discarded. The peptides bound to the C18 material were washed twice with 100 µl of water and 0.1 % formic acid (10,000 rpm, 2 min). The stage tip was transferred to a new 1.5 Protein LoBind Tube. For elution of the peptides, 60 µl 70 % acetonitrile with 0.1 % formic acid was used. The StageTips were discarded and the samples were completely dried in the speed vac at 50°C. The dried peptide pellets were stored at -20°C.

3.9.7. LCMS analysis

To prepare the samples for the LCMS analysis, 20 µl fresh sample buffer (98 % H_20, 2 % acetonitrile, 0.1 % formic acid) was added to the dried peptide pellets. After pipetting up and down for around 10 times, the samples were incubated in an ultrasonic bath for 3 min at maximal power. The samples were then transferred to LCMS vials and delivered to the LCMS Protein Analytics Service Unit, University Göttingen, which performed the actual LCMS analysis.

The LCMS data were mapped to the *A. thaliana* proteome downloaded from TAIR by using the software MaxQuant version 1.6.10.43. With the PerseusGui software version 1.6.0.7, contaminants were excluded, the dataset was filtered for proteins with four valid values in at least one genotype and missing values were randomly replaced. To further analyze the dataset and test for statistical differences, volcano plots were generated.

4. Results Part I – Characterization of the *roxy6789* mutant

To investigate how ROXY6, 7, 8, 9 regulate phenotypes and gene expression in different conditions, the *roxy6 roxy7 roxy8 roxy9* (*roxy6789*) quadruple mutant was characterized. To this aim, the growth phenotype, including biomass measurement, petiole length and hyponasty, was determined and gene expression upon biotic and abiotic stresses was analyzed. The *tga1 tga4* mutant was additionally examined in all experiments, as we were particularly interested in phenotypes that are regulated through the interaction of ROXY6, 7, 8, 9 and TGA1, 4.

4.1. Growth phenotype

4.1.1. *roxy6789* has a reduced biomass under all tested conditions

The rosette fresh weight of 10 plants per genotype was measured after growth for 4 weeks in short day (8/16 h), normal day (12/12 h) or long day (16/8 h) conditions (Figure 9). The fresh weight between Col-0 and *tga1 tga4* did not vary significantly in all tested conditions. The *roxy6789* quadruple mutant has a significantly reduced fresh weight, indicating that ROXY6, 7, 8, 9 regulate growth in different light regimes.

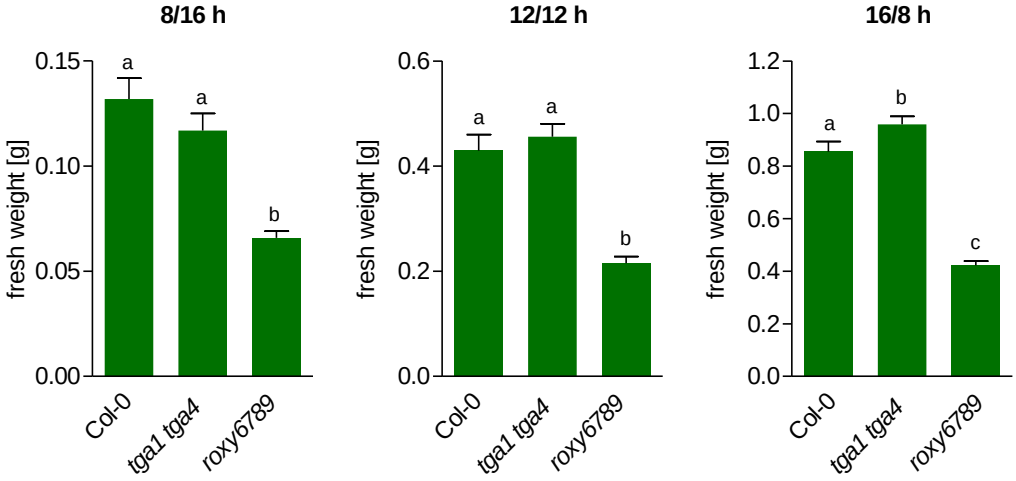

Figure 9: The *roxy6789* mutant has a reduced biomass compared to Col-0 and *tga1 tga4*. *A. thaliana* plants were grown for 4 weeks in different light regimes (8/16 h, 12/12 h, 16/8 h) before the fresh weight of the whole rosette was measured. Mean values of 12-24 biological replicates are shown for each genotype, error bars represent the standard error of the mean. Letters indicate statistically significant differences between the genotypes. Statistical analyses were performed by using one-way analysis of variance (ANOVA) and Tukey's post-test (*p*-value < 0.05).

4.1.2. *roxy6789* has longer petioles than Col-0 and *tga1 tga4*

While analyzing the fresh weight of Col-0, *tga1 tga4* and *roxy6789*, we noticed that the *roxy6789* mutant seems to have longer petioles whereas the *tga1 tga4* mutant has shorter petioles. To further investigate this observation, the leaf and petiole length of all mature leaves from eight plants were measured and the leaf-to-petiole ratio was calculated. In addition to Col-0, *tga1 tga4* and *roxy6789*, the triple mutants *roxy6 roxy8 roxy9* (*roxy689*) and *roxy6 roxy7 roxy9* (*roxy679*) as well as the double mutant *roxy7 roxy9* (*roxy79*) were analyzed.

Figure 10a shows representative leaves for each genotype. The leaf-to-petiole ratio was significantly higher in the *tga1 tga4* mutant and lower in the *roxy6789* mutant compared to the WT (Figure 10b). This suggests that TGA1, 4 negatively regulate the leaf-to-petiole ratio whereas ROXY6, 7, 8, 9 function as a positive regulators. The leaf-to-petiole ratio of *roxy689*, *roxy679* and *roxy79* lies between the values of Col-0 and *roxy6789*, hinting towards an additive function of ROXY6, 7, 8 and 9.

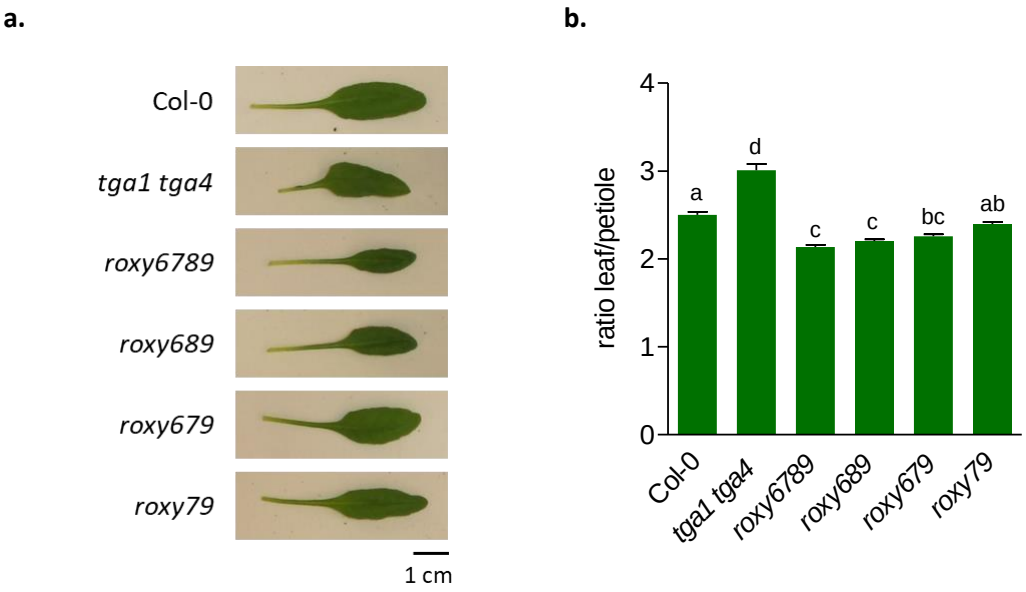

Figure 10: The *roxy6789* mutant has a lower leaf-to-petiole ratio compared to Col-0 and *tga1 tga4*. Leaves of 4-week-old *A. thaliana* plants were analyzed. **a.** Representative leaves of Col-0, *tga1 tga4*, *roxy6789, roxy689*, *roxy689* and *roxy79* are depicted. **b.** Pictures of all leaves of eight plants per line were taken. The length of the leaves and petioles was measures with the ImageJ software and the leaf-to-petiole ratio was calculated. Mean values of around 60 leaf-to-petiole ratios are shown, error bars represent the standard error of the mean. Letters indicate statistically significant differences between the genotypes. Statistical analysis was performed by using one-way ANOVA and Tukey's post-test (*p*-value < 0.05).

4.2. Hyponasty in low light stress

Among others, the petioles are important for hyponastic growth, which occurs in response to unfavorable conditions such as submergence (Cox *et al.,* 2003; Pierik *et al.,* 2005), high temperatures (Koini *et al.,* 2009; van Zanten *et al.,* 2009) or low light (LL) stress (Vandenbussche *et al.,* 2003; Millenaar *et al.,* 2009). To escape these abiotic stresses, plants bend their leaves upwards by elongation of the abaxial epidermal cells of the petioles. To reverse this process, the adaxial cells of the petioles elongate (Polko *et al.,* 2012).

Both the *tga1 tga4* mutant and the *35S:HA-ROXY9* overexpression line are impaired in hyponastic growth in LL stress (Li *et al.,* 2019), indicating that TGA1, 4 activate the leaf movements whereas ROXY9 functions as a repressor. In this study, the hyponasty was analyzed in the loss-of-function mutant *roxy6789*.

4.2.1. Hyponastic growth is preinduced in *roxy6789* and the reversal is impaired

To analyze the hyponastic growth, plants were grown for 4 weeks under normal light (NL) conditions (100-120 µmol photons m^2 s^{-1}). 1.5 h after the onset of light, plants were either left in NL or transferred to LL (15-20 µmol photons m^2 s^{-1}). For backshift experiments (LL ➔ NL), plants were transferred back from LL to NL on the next day directly after the onset of light. Pictures of the plants were taken after 4 h and the leaf angle of the 8th leaf was measured.

In NL conditions, the leaves of *roxy6789* are located in a more upwards position compared to Col-0 and *tga1 tga4*, indicating that hyponasty is pre-induced (Figure 11). When transferred to LL, Col-0 and *roxy6789*, but not *tga1 tga4* tilt their leaves upwards. This result is in line with the published data and confirms that TGA1, 4 activate hyponastic growth and can most likely be repressed by ROXY6, 7, 8, 9. In backshift conditions, the leaves of Col-0 are tilting back down whereas reversal of hyponasty is impaired in the *roxy6789* mutant. In addition, the triple mutants *roxy689* and *roxy679* as well as the double mutant *roxy79* were analyzed. In all LL and LL ➔ NL conditions, the triple mutants behave like

the *roxy6789* quadruple mutant. In NL conditions, the leaf angle is slightly lower, but hyponasty is still preinduced. In contrast, the *roxy79* mutant behaves WT like under NL and LL conditions, but is impaired in the reversal of hyponastic growth in backshift conditions. This shows that ROXY6, 7, 8, 9 function in an additive manner in order to regulate hyponasty in response to LL stress.

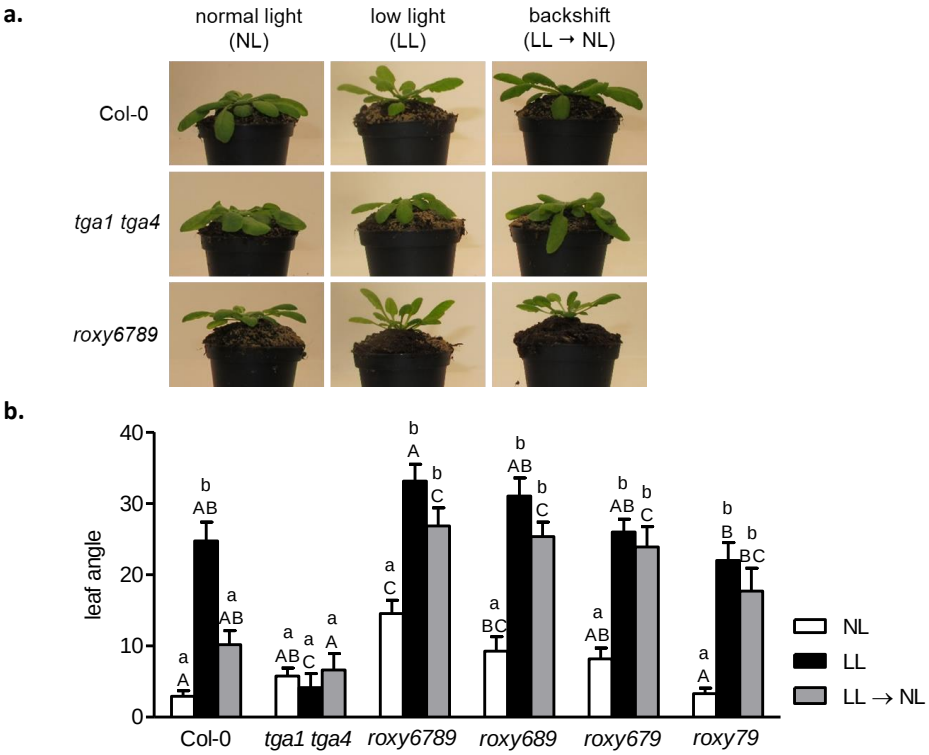

Figure 11: ROXY6, 7, 8, 9 negatively regulate hyponastic growth. Plants were grown in normal light (NL) conditions (100-120 µmol photons m^{-2} s^{-1}) for 4 weeks. 1.5 hours after the onset of light, plants were either left in NL conditions or transferred to low light (LL) conditions (15-20 µmol photons m^{-2} s^{-1}). For backshift experiments (LL → NL), plants were transferred back from LL to NL on the next day directly after the onset of light. Pictures were taken after 4 h. **a.** Representative plants for Col-0, *tga1 tga4* and *roxy6789* in each light condition. **b.** The leaf angle of the 8th leaf was measured by using the ImageJ software. Mean values of ten biological replicates are shown, error bars represent the standard error of the mean. Lowercase letters indicate statistically significant differences within a genotype between different light conditions, uppercase letters indicate significant differences between genotypes subjected to the same light conditions. Statistical analysis was performed by using two-way ANOVA and Bonferroni's post-test (*p*-value < 0.05). The experiment was performed twice and similar results were obtained.

4.2.2. ROXY6, 7, 8, 9 repress *IAA19* expression in petioles

As *roxy6789* has longer petioles, preinduced hyponastic growth and is impaired in its reversal, ROXY6, 7, 8, 9 seem to play an important role in hyponasty. To further analyze their contribution at the level of gene expression, transcript levels of the TGA1, 4-activated, LL-induced genes *INDOLE-ACETIC-3-ACID INDUCIBLE 19 (IAA19, AT3G15540)* and *XYLOGLUCAN ENDOTRANS-GLUCOSYLASE/HYDROLASE8 (XTH8, AT1G11545)* was determined in the petioles of *roxy6789*. For this, plants were grown for 4 weeks in NL conditions (100-120 µmol photons m^2 s^{-1}). To induce LL stress, plants were transferred to reduced light conditions (15-20 µmol photons m^2 s^{-1}) 1.5 h after the onset of light. For backshift experiments (LL ➔ NL), plants were transferred back from LL to NL on the next day directly after the onset of light. All petioles per plant were harvested after 5 h.

The expression of both *IAA19* and *XTH8* is induced in Col-0 petioles upon LL stress (Figure 12). In backshift conditions, the expression of *IAA19* is reduced compared to LL conditions, but there is no statistical difference. In contrast, *XTH8* expression in backshift conditions is similar to the expression in NL. The *roxy6789* mutant shows elevated *IAA19* expression compared to Col-0 under all light

conditions. The *XTH8* expression does not vary significantly between Col-0 and *roxy6789*. These results suggest that ROXY6, 7, 8, 9 negatively regulate *IAA19* expression independent of the light conditions.

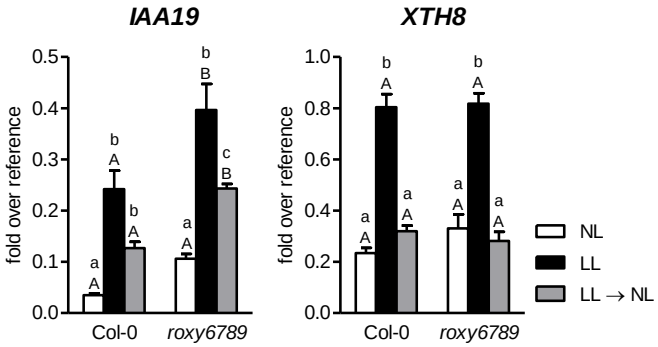

Figure 12: ROXY6, 7, 8, 9 negatively regulate expression of *IAA19*. 4-week-old plants were grown in normal light (NL) conditions (100-120 µmol photons m^{-2} s^{-1}). 1.5 hours after the onset of light, plants were either left in NL conditions or transferred to low light (LL) conditions (15-20 µmol photons m^{-2} s^{-1}). For backshift experiments (LL → NL), plants were transferred back from LL to NL on the next day directly after the onset of light. For each biological replicate, all petioles of four plants were collected after 5 h, RNA was isolated and cDNA synthesized. In qRT-PCR analysis, the expression of *IAA19* and *XTH8* was analyzed and *UBQ5* was used as a reference gene. Mean values of five biological replicates are shown, error bars represent the standard error of the mean. Lowercase letters indicate statistically significant differences within a genotype between different treatments, uppercase letters indicate significant differences between genotypes subjected to the same treatments. Statistical analyses were performed by using two-way ANOVA and Bonferroni's post-test (*p*-value < 0.05).

4.3. Defense response to *Pseudomonas syringae*

In addition to hyponasty, TGA1, 4 are crucial regulators for local and systemic resistance against the hemi-biotrophic pathogen *Pseudomonas syringae* pv. *maculicola* (*Psm*). An important marker gene for defense responses is *FLAVIN-DEPENDENT-MONOOXYGENASE 1* (*FMO1, AT1G19250*). FMO1 converts pipecolic acid (Pip) to N-hydroxy pipecolic acid (NHP), which is crucial for the establishment of SAR (Hartmann *et al.,* 2018). Similar to the *tga1 tga4* mutant, the *35S:HA-ROXY9* overexpressor line fails to induce *FMO1* expression in *Psm*-infected SAR leaves (Nair, unpublished), suggesting a repression of TGA1, 4 by ROXY9. To verify this hypothesis, the expression of *FMO1* was analyzed in the loss-of-function mutant *roxy6789* under SAR conditions as well as after local infection.

Moreover, bacterial growth assays showed that *35S:HA-ROXY9* is even more susceptible to *Psm* infection than the *tga1 tga4* mutant (Jung, 2016). The higher susceptibility of *tga1 tga4* was also observed by Sun *et al.,* 2018. These experiments were repeated with the *roxy6789* mutant and the bacterial titer was determined.

4.3.1. *FMO1* expression is not regulated by ROXY6, 7, 8, 9 in *Psm*-infected SAR leaves

In order to perform SAR experiments, local leaves of 4.5-week-old plants were infiltrated with *Psm* or the mock control ($MgCl_2$). After two days, upper leaves were infiltrated with *Psm.* These upper leaves were harvested after 8 h, RNA was isolated, cDNA synthesized and the *FMO1* expression was determined by qRT-PCRs.

As expected, *FMO1* is induced in *Psm*-infected SAR leaves in Col-0 but not the *tga1 tga4* mutant. The *roxy6789* shows a slightly higher *FMO1* expression after *Psm*/*Psm* treatment compared to the WT, but there is no statistical difference (Figure 13, Supplementary Figure S1). These results suggest that ROXY6, 7, 8, 9 play at most a minor role in the control of SAR. The *35S:HA-ROXY9* overexpressor line most likely shows an artificial regulation due to unphysiologically high levels of ROXY9.

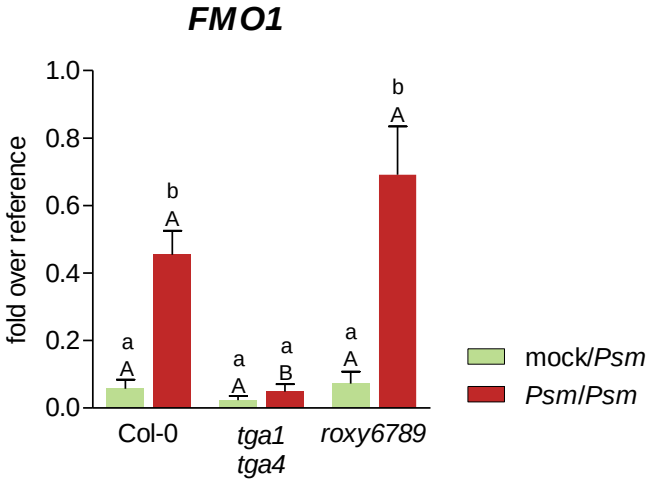

Figure 13: *FMO1* expression is not regulated by ROXY6, 7, 8, 9 in *Psm*-infected SAR leaves. Lower leaves of 4.5-week-old *A. thaliana* plants were infiltrated with $MgCl_2$ (green, mock treatment) or infiltrated with *Psm* (red, OD_{600} = 0.005). After 48 h, upper leaves were infiltrated with *Psm*. The upper leaves were collected after 8 hours, RNA was isolated and cDNA synthesized. Expression of *FMO1* was analyzed by qRT-PCR in the genotypes Col-0, *tga1 tga4* and *roxy6789*, *UBQ5* was used as a reference gene. Mean values of four to six biological replicates are shown. Error bars represent the standard error of the mean. Lowercase letters indicate statistically significant differences within a genotype between different treatments, uppercase letters indicate significant differences between genotypes subjected to the same treatments. Statistical analysis was performed by using two-way ANOVA and Bonferroni's post-test (*p*-value < 0.05). Two independent experiments were performed with similar results.

4.3.2. *roxy6789* might have elevated *FMO1* and *DLO1* expression after local infection

Since the involvement of ROXY9 in *FMO1* expression upon SAR conditions could not be shown in *roxy6789*, local leaves were analyzed. For this, leaves of 4-week-old plants were infiltrated with *Psm* or the mock control and samples were harvested after 8 h. After isolation of RNA and cDNA synthesis, qRT-PCRs were performed. In addition to *FMO1*, the expression of *DMR6-LIKE OXYGENASE 1* (*DLO1, AT4G10500*) was analyzed. *DLO1* encodes for a SA hydroxylase which is involved in SA catabolism (Zhang *et al.,* 2003) and the expression is activated by TGA1, 4 (Budimir *et al.,* 2021).

Col-0 did not show an induction of either *FMO1* or *DLO1* after pathogen treatment (Figure 14). Still, the expression levels of both genes were reduced in the *tga1 tga4* mutant, even though the difference is not statistically significant. In the *roxy6789* mutant, *FMO1* and *DLO1* transcript levels were elevated in mock control as well as after *Psm* treatment. The expression varied greatly between the replicates, but a statistical difference was determined in the *Psm*-treated samples for both genes compared to Col-0 and *tga1 tga4*. This indicates that ROXY6, 7, 8 and 9 might be involved in the regulation of *FMO1* and *DLO1* and thus in the defense responses against local *Psm* infection.

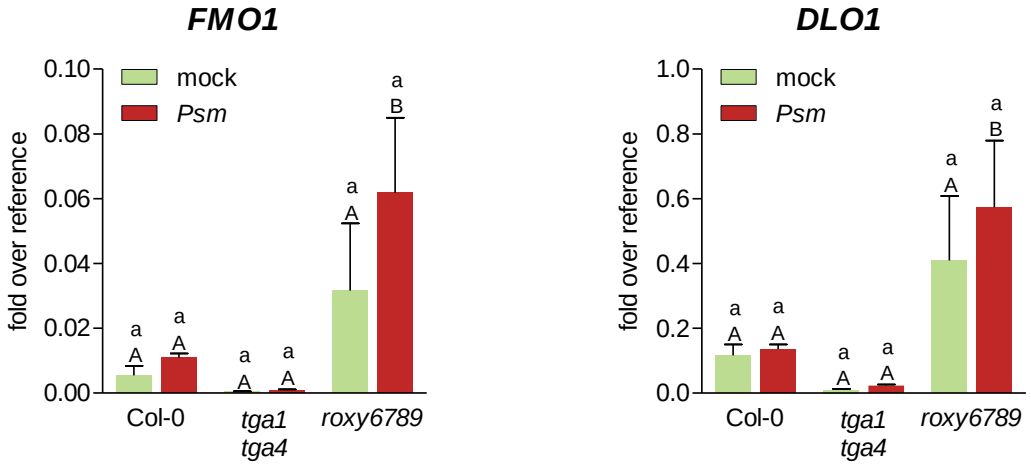

Figure 14: *roxy6789* might have elevated *FMO1* and *DLO1* expression in *A. thaliana* leaves after local *Psm* infection. Leaves of 4-week-old *A. thaliana* plants were infiltrated with $MgCl_2$ (green, mock treatment) or with *Psm* (red, OD_{600} = 0.001). Leaf material was collected 8 h after the treatment, RNA was isolated and cDNA synthesized. Expression of *FMO1* and *DLO1* was analyzed by qRT-PCR in the genotypes Col-0, *tga1 tga4* and *roxy6789*, *UBQ5* was used as a reference gene. Mean values of four to six biological replicates are shown. Error bars represent the standard error of the mean. Lowercase letters indicate statistically significant differences within a genotype between different treatments, uppercase letters indicate significant differences between genotypes subjected to the same treatments. Statistical analyses were performed by using two-way analysis of variance (ANOVA) and Bonferroni's post-test. Two independent experiments were performed with similar results (p-value < 0.05).

4.3.3. *roxy6789* might be more resistant to *P. syringae* in bacterial growth assays

The growth of bacteria in the plant leaves can be determined by bacterial growth assays. Leaves of 4-week old plants were infiltrated with *Psm*. After 72 h, the bacteria were isolated from the leaves and plated on King's B plates. Two days later, the amount of grown colonies was determined and the colony forming units (cfu) per cm^2 were calculated.

In total, four experiments were performed with Col-0, *tga1 tga4* and *roxy6789*. All of the experiments show different results and are shown in Figure 15. In two experiments, the published higher resistance of *tga1 tga4* was reproduced (Experiment 1 and 2; Sun *et al.,* 2018), whereby it was only statistically significant in Experiment 1. The *roxy6789* mutant showed a higher resistance in three experiments (Experiment 1, 2 and 3), two of which show a significant difference to Col-0 (Experiment 1 and 3). The forth experiment did not show any differences between the testes genotypes.

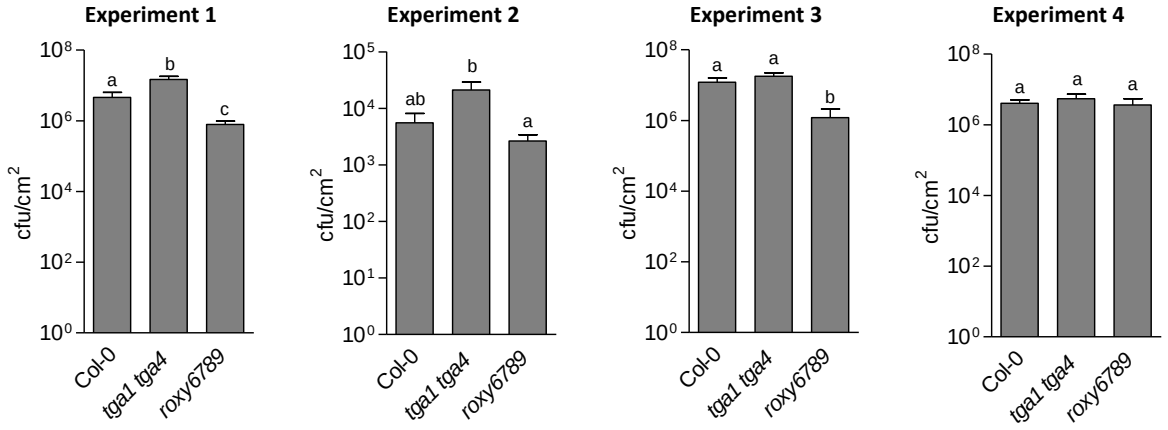

Figure 15: *roxy6789* might be more resistant to *Psm* infection. Leaves of 4-week-old *A. thaliana* plants were infiltrated with *Psm* (OD_{600} = 0.005). Leaf discs were collected 72 h after the treatment, bacteria were isolated and plated. After incubation of the plates for two days at 29°C, bacterial colonies were counted and the colony forming units (cfu) per cm^2 were calculated. Four independently performed experiments with the genotypes Col-0, *tga1 tga4* and *roxy6789* are shown. Mean values of ten to twelve biological replicates are shown. Error bars represent the standard error of the mean. Letters indicate statistically significant differences of the logarithmic values. Statistical analyses were performed by using one-way ANOVA and Tukey's post-test (*p*-value < 0.05).

In addition, a bioluminescence assay with transgenic *P. syringae* pv. *tomatoe* DC3000 (*Pst*) *lux* was performed. This method was developed by Matsumoto *et al.,* 2022 and allows easy and reliable analysis of bacterial growth in leaves. Similar to the bacterial growth assays, *Pst lux* were infiltrated into leaves of 4-week-old plants. Samples were collected directly after the infiltration (Day 0) and after three day (Day 3). The bioluminescence was measured and relative light units (RLU) per cm^2 were calculated.

The samples collected on Day 0 serve as a background control and the amount of luminescence is similar in Col-0, *tga1 tga4* and *roxy6789* in both experiments (Figure 16). After three days, the *tga1 tga4* mutant show higher susceptibility than Col-0. The *roxy6789* mutant is more resistant to *Pst* infection in one experiment (Experiment 1).

Taken together with the gene expression data, ROXY6, 7, 8, 9 might be involved in negatively regulating resistance against *Psm* and *Pst,* even if the higher resistance of *roxy6789* was not detectable in all experiments.

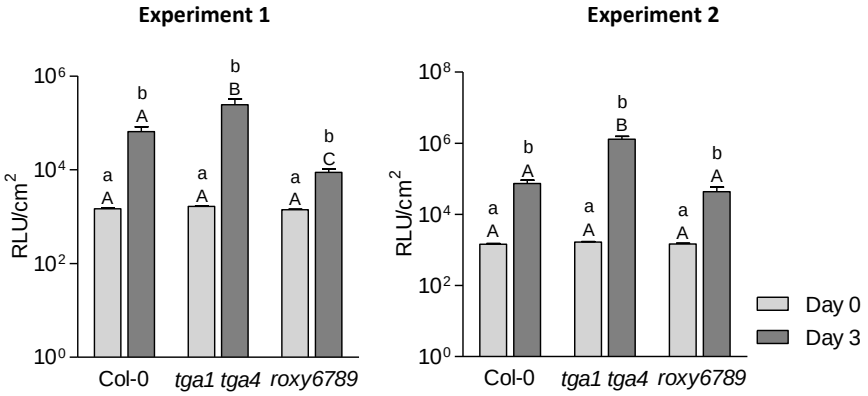

Figure 16: *roxy6789* might be more resistant to *Pst* infection. Leaves of 4-week-old *A. thaliana* plants were infiltrated with *Pst*. Leaf discs were collected immediately after the treatment (Day 0) or after 3 days. The bioluminescence was measured and the relative light units (RLU) per cm^2 were calculated. Two independent experiments were performed. Mean values of 30 biological replicates are shown. Error bars represent the standard error of the mean. Lowercase letters indicate statistically significant differences within a genotype between different timepoints, uppercase letters indicate significant differences between genotypes. Statistical analyses were performed with logarithmic values by using two-way ANOVA and Bonferroni's post-test (*p*-value < 0.05).

4.4. Autoregulation of ROXY9

4.4.1. ROXY6, 7, 8, 9 repress the expression of *ROXY9*

For the hyponastic growth as well as the pathogen infections, no highly regulated target genes were identified for *roxy6789*. Previous studies showed that the expression of *ROXY8* and *ROXY9* is activated by TGA1, 4 and repressed in a negative feedback loop by ROXY8, 9 (Li *et al.,* 2019). The *roxy6789* mutant contains a 7 bp deletion in the *ROXY9* coding region resulting in a *ROXY9* transcript but a non-functional protein due to the frameshift and pre-mature stop codon. That is why the *ROXY9* expression can be analyzed in the *roxy6789* mutant. For this, RNA was isolated from leaves of 4-week old plants, cDNA was synthesized and qRT-PCRs were performed.

ROXY9 expression was completely abolished in *tga1 tga4* and elevated in *roxy6789* compared to the WT (Figure 17), suggesting that *ROXY9* is activated by TGA1, 4 and repressed by ROXY6, 7, 8, 9. The triple mutants *roxy689* and *roxy679* have higher *ROXY9* levels than Col-0, but lower than *roxy6789.* The *roxy79* mutant shows WT-like *ROXY9* expression, indicating an additive effect of ROXY6, 7, 8, 9.

Additionally, the expression of *ROXY6*, *ROXY7* and *ROXY8* was analyzed. Similar to *ROXY9*, the coding region of *ROXY6, 7* and *8* contains bp deletions or insertions, leading to a transcript but non-functional protein. Also *ROXY8* is activated by TGA1 and 4 and repressed by ROXY6, 7, 8 and 9. In contrast, *ROXY6* is activated by TGA1, 4 but not regulated by ROXY6, 7, 8, 9 and *ROXY7* is repressed by ROXY6, 7, 8, 9 but not regulated by TGA1, 4.

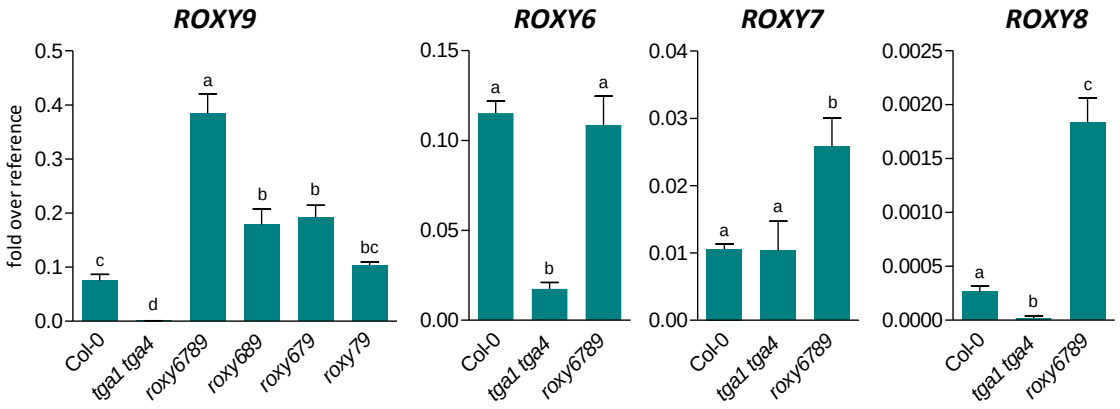

Figure 17: *ROXY9* expression is activated by TGA1, 4 and repressed by ROXY6, 7, 8, 9. Leaves of 4-week-old *A. thaliana* plants were collected, RNA was isolated and cDNA synthesized. The expression of *ROXY6*, *ROXY7*, *ROXY8* and *ROXY9* was analyzed by qRT-PCR, *UBQ5* was used as a reference gene. Mean values of four to six biological replicates are shown. Error bars represent the standard error of the mean. Expression of *ROXY9* was analyzed by qRT-PCR, *UBQ5* was used as reference gene. Letters indicate statistically significant differences values with. Statistical analyses were performed by using one-way ANOVA and Tukey's post-test (*p*-value < 0.05).

4.5. Gene expression upon nitrate starvation

Even though *ROXY9* itself was identified as a target gene which can be used as a marker gene for mechanistic studies, we wanted to identify genes with physiological relevance. Previous studies had shown that the expression of *ROXY6*, *ROXY8* and *ROXY9* is induced in the shoots upon nitrogen (N) starvation. Subsequently, the ROXYs travel to the roots, where they activate the expression of e.g. *NRT2.1* (*AT1G08090*) and *CEPH* (*CEPD INDUCED PHOSPHATASE, AT4G32950*) (Ohkubo *et al.,* 2017; Ota *et al.,* 2020; Ohkubo *et al.,* 2021). *NRT2.1* encodes for a high-affinity nitrate transporter which is activated by CEPH through dephosphorylation (Ohkubo *et al.,* 2021). In addition, TGA1 is much higher expressed in the roots than in the shoots (Budimir, 2019) and can bind to the promoter region of *NRT2.1* (Alvarez *et al.,* 2014), suggesting a joint regulation of *NRT2.1* by ROXY6, 7, 8, 9 and TGA1, 4. This is why we decided to analyze gene expression upon N starvation.

4.5.1. Expression of ROXY6, 8, 9 is induced in shoots upon nitrogen starvation

To analyze gene expression upon N starvation, seedlings were grown for 7 days on full nutrition (FN) plates under constant light conditions and then transferred to either FN or low nitrogen (LN) conditions. After 2 days, root and shoot material was separately collected.

First of all, the expression pattern of *ROXY6, 7, 8* and *9* was analyzed in our experimental setup. In roots, *ROXY7, ROXY8* and *ROXY9* are hardly expressed in both FN and LN conditions (Figure 18). Only minor *ROXY6* amounts were detected in sufficient N supply, which are induced upon N starvation. In contrast, the shoots have higher expression levels for all tested genes. In FN conditions, *ROXY6, ROXY7* and *ROXY9* are expressed to a similar extent, whereas *ROXY8* is only weakly expressed. The expression of *ROXY6, ROXY8* and *ROXY9* is induced in LN conditions, whereby the amount of *ROXY8* and *ROXY9* increases drastically. Overall, *ROXY9* under N starvation conditions has a much higher expression than the other ALWL-free ROXYs, suggesting that ROXY9 plays the major role in gene regulation under N limiting conditions, whereas at least ROXYs 6, 7 and 9 have similar contribution in FN conditions.

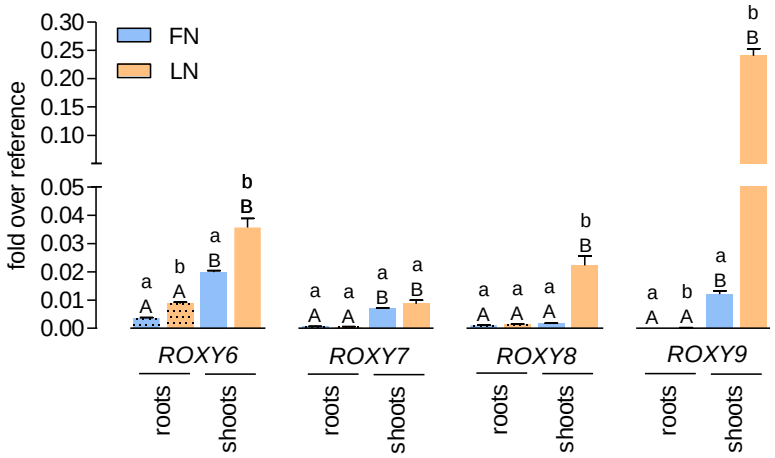

Figure 18: Expression of *ROXY6, ROXY7, ROXY8* and *ROXY9* in *A. thaliana* roots and shoots in sufficient nitrogen supply and upon nitrogen starvation conditions. 7-day old seedlings grown on full nutrition (FN) plates under constant light conditions (70 µmol photons s^{-1} m^{-2}) were transferred to either FN (blue) or low nitrogen (LN, orange) plates. Two days later, roots or shoots were separately collected, RNA was isolated and cDNA synthesized. Expression of *ROXY6, ROXY7, ROXY8* and *ROXY9* was analyzed in the wild type Col-0 by qRT-PCR, *UBQ5* was used as a reference gene. Mean values of four to five biological replicates are shown. Error bars represent the standard error of the mean. Lowercase letters indicate statistically significant differences within the tissue between the conditions, uppercase letters indicate significant differences within treatment between the tissues. Statistical analyses were performed individually for each gene with the logarithmic values by using two-way ANOVA and Bonferroni's post-test (p-value < 0.05).

4.5.2. ROXY6, 7, 8, 9 activate *PER10* and *CLE3* expression upon nitrogen starvation

Published transcriptome analysis with root material from ROXY6, ROXY8 and ROXY9 overexpression lines show that *PEROXIDASE 10* (*PER10, AT1G49570*) and *CLAVATA3/EMBRYO SURROUNDING REGION-RELATED 3* (*CLE3, AT1G06225*) are highly upregulated when grown in low nitrate conditions (Ohkubo *et al.,* 2021). In addition, the expression of *PER10* is repressed by TGA1, 4 in roots of soil grown plants (Pelizaeus, 2019). As *CLE3* has 6 TGACG motifs in the promoter region 2 kb upstream of the transcription start site, it is likely that TGAs regulate its expression as well. These findings prompted us to further analyze the expression of *PER10* and *CLE3* in Col-0, *tga1 tga4* and *roxy6789* roots under sufficient N supply versus N limiting conditions.

In FN conditions, the *tga1 tga4* mutant has higher expression of *PER10* than Col-0 (Figure 19), meaning that TGA1, 4 represses the expression. No difference in *PER10* expression is detected in FN conditions between in Col-0 and *roxy6789*. Upon N starvation, *PER10* expression is induced in Col-0, but not in *roxy6789*, showing that ROXY6, 7, 8, 9 activate *PER10*. In addition, the *PER10* expression of in *tga1 tga4* mutant is as high as in the WT. These results suggest that ROXY6, 7, 8, 9 are activating the gene expression of *PER10* in LN conditions, whereas TGA1, 4 repress the expression in FN conditions. Moreover, an activator needs to be active in the *tga1 tga4* mutant in FN conditions, which is less active in LN conditions. In the *roxy6789* mutant, the repressive effect of TGA1, 4 on *PER10* is quite strong. The induction of *PER10* in the WT under N limiting conditions can be explained with the higher amounts of ROXYs which interfere with the negative effect of TGA1, 4.

Similar to *PER10*, *CLE3* expression is higher in the *tga1 tga4* mutant in FN conditions. Thus, TGA1, 4 repress the gene expression of *CLE3*. No transcript was detected in *roxy6789* mutant in both conditions, indicating that ROXY6, 7, 8, 9 activate the *CLE3* expression. In contrast to *PER10*, *CLE3* is not induced upon N starvation in Col-0. In the *tga1 tga4* mutant, the *CLE3* transcript decreases in LN conditions to the WT level. At least in FN conditions, ROXY6, 7, 8, 9 interfere the repressive mechanism of TGA1, 4 in order to activate gene expression. In LN conditions, ROXY6, 7, 8, 9 seem to activate *CLE3* expression independent of TGA1, 4.

For the statistical analyses, log transformation was performed as it makes the data more symmetrical, leading to a more accurate evaluation of data with low fold over references. However, statistical analyses are not possible for *CLE3* expression as no *CLE3* transcript was detected in the *roxy6789* mutant.

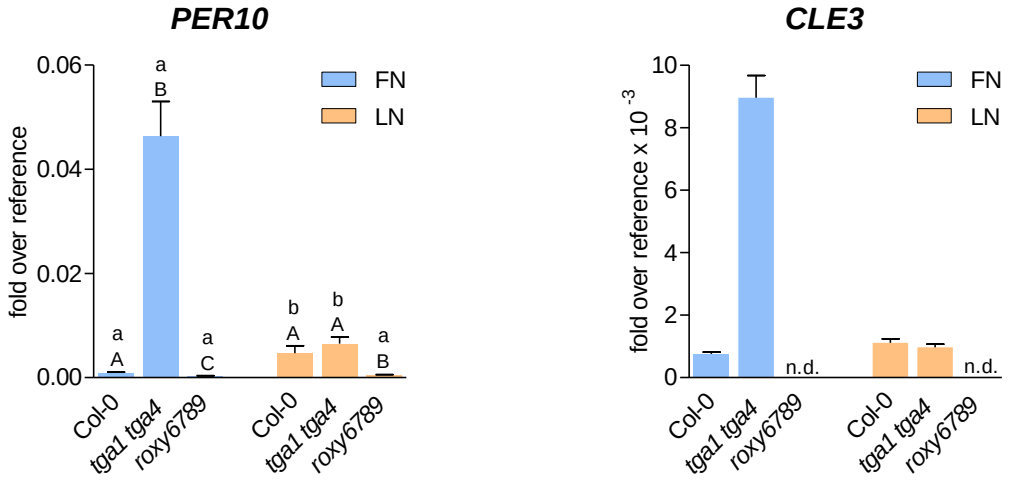

Figure 19: ROXY6, 7, 8, 9 activate the expression of *PER10* and *CLE3* in *A. thaliana* roots upon nitrogen starvation by interfering with the repressive mechanism of TGA1, 4. 7-day old seedlings grown on full nutrition (FN) plates under constant light conditions (70 µmol photons s^{-1} m^{-2}) were transferred to either FN or low nitrogen (LN) plates. Two days later, roots were collected, RNA was isolated and cDNA synthesized. Expression of *PER10* and *CLE3* was analyzed by qRT-PCR, *UBQ5* was used as a reference gene. Mean values of four to five biological replicates are shown. Error bars represent the standard error of the mean. n.d.: not detected. Lowercase letters indicate statistically significant differences within the genotype between the treatments, uppercase letters indicate significant differences within treatment between the genotypes. Statistical analyses were performed with the logarithmic values of the *PER10* expression by using two-way ANOVA and Bonferroni's post-test (*p*-value < 0.05). Three independent experiments were performed with similar results.

The induction of *PER10* upon LN treatment in Col-0 was detected in five out of six experiments. In those experiments, in which no induction was detected, the difference between WT and *roxy6789* in LN conditions was not significant. To identify target genes, which are more robustly regulated, transcriptome analysis was performed. This also allows the detection of genes, which are activated by TGA1, 4 and repressed by ROXY6, 7, 8, 9, since TGA1, 4 are described as activators rather than repressors.

4.5.3. Identification of new target genes via transcriptome analysis

The transcriptome analysis was performed with RNA from Col-0 and *roxy6789* roots grown under LN conditions. In total, four Col-0 and four *roxy6789* samples were sent for sequencing to the Next Genome Sequencing Integrative Genomics Core Unit (NIG), University Göttingen. One sample consists out of four to five RNA replicates from one experiment.

To control data distribution, a Principal Component Analysis (PCA) was performed (Supplementary Figure S2a). Samples from the same genotype and treatment have a similar transcriptome dataset and cluster together. The analysis revealed however, that one Col-0 replicate behaves differently from the others. Further analysis identified a contamination with leaf material. Therefore, this dataset was excluded in all subsequent analysis. In a new PCA analysis, the remaining replicates of one genotype cluster together (Supplementary Figure S2b). The remaining replicates revealed that 212 genes were higher expressed and 350 genes were lower expressed in *roxy6789* compared to Col-0 (logarithmic fold change to the base 2 (log_2 FC) > 1, adjusted *p*-value (*p*.adj) < 0.05, Dataset 1).

4.5.3.1. ROXY6, 7, 8, 9 repress the expression of 212 genes in roots subjected to nitrogen starvation

First of all, the 212 genes, which were less expressed in the *roxy6789* mutant were analyzed, as these might be regulated through a repression of the transcriptional activators TGA1, 4 by ROXY6, 7, 8, 9. Gene Ontology (GO) term analysis for biological processes surprisingly showed that N starvation-responsive genes were not enriched in this subset compared to the *Arabidopsis* genome (Figure 20). Instead, many photosynthesis-related genes are over 5-fold enriched.

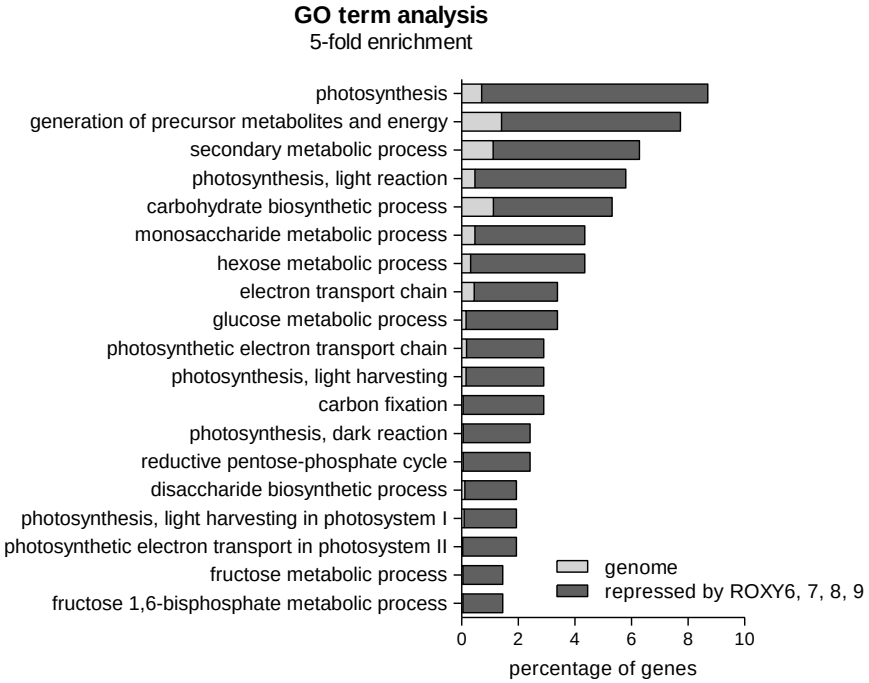

Figure 20: Photosynthesis-related genes are repressed by ROXY6, 7, 8, 9 upon nitrogen starvation. Gene Ontology (GO) term analysis was performed with the 212 genes that are higher expressed (log_2 FC > 1, *p*.adj < 0.05) in *roxy6789* compared to Col-0 upon nitrogen starvation according to transcriptome data**.** GO terms with a 5-fold enrichment are shown. Statistical analysis was performed using Fisher test and False discovery rate (FDR) < 0.05.

In addition, motif enrichment analysis was performed with the Motif Mapper software (Berendzen *et al.,* 2010). With this method, enriched transcription factor binding sites in the promoter region of a data set can be identified. Within the 212 genes, which are repressed by ROXY6, 7, 8, 9, no significant changes were detected for the TGA-factor binding sites TGACG, TGACGTCA and TACGTA (Table 26). Still, it is noteworthy that the TGACG and TGACGTCA motifs are rather depleted than enriched. This suggests that ROXY6, 7, 8, 9 either repress at least a subset of these genes independent of TGA factors or that these genes are indirectly regulated by the ROXY/TGA module.

Interestingly, the MYC2 transcription factor binding site CACGTG (Boter *et al.,* 2004; Dombrecht *et al.,* 2007) was 1.64 fold enriched and the gibberellin (GA)-responsive element TATCCAC (Gubler & Jacobsen, 1992) was even enriched by a factor of 2.18. MYC2, as well as the closest homologues MYC3 and MYC4, are important for jasmonic acid (JA)-responsive gene expression (Lorenzo *et al.,* 2004; Fernández-Calvo *et al.,* 2011). JA is important for response to wounding and regulation of defense mechanisms against necrotrophic pathogens (Glazebrook, 2005) and GA regulates plant growth and development (Koornneef & van der Veen, 1980; Richards *et al.,* 2001). This suggests that ROXY6, 7, 8, 9 might be involved in regulation of gene expression during biotic or abiotic stresses.

Table 26: TGA factor binding sites are not enriched in the 212 ROXY6, 7, 8, 9-repressed genes. Motif mapper analysis was performed with the 212 genes that are higher expressed (log_2 FC > 1, *p*.adj < 0.05) in *roxy6789* compared to Col-0 upon nitrogen starvation according to transcriptome data. Enrichments were calculated compared to a set of randomly chosen promoters from the whole *A. thaliana* genome.

Motif	Number of motifs in 212 ROXY9-repressed genes	Number of motifs in genome	*p*-value	enrichment
TGACG	159	183.7	-0.0510	0.87
TGACGTCA	1	2.8	-0.1539	0.36
TACGTA	48	38.0	0.0643	1.26
CACGTG	64	39.1	0.0001	1.64
TATCCAC	49	22.5	0.0000	2.18

Even though TGA binding sites were not enriched, we wanted to identify genes, which are activated by TGA1, 4 and repressed by ROXY6, 7, 8, 9. For this purpose, the ten most upregulated genes in *roxy6789* compared to Col-0 were taken into account (Table 27). All promoter regions of these genes contain at least one TGACG motif, suggesting that TGA factors might be involved in the activation of these genes. Only two of the genes have been described in roots. *SWEET11* (*AT3G48740*) encodes for a sugar efflux transporter located in the plasma membrane of the phloem (Chen *et al.,* 2012b). Even though *SWEET11* is mainly expressed in shoots, water shortage induces the expression in roots (Durand *et al.,* 2016). The expression of *AUXIN-INDUCED IN ROOT CULTURES 1* (*AIR1*, *AT4G12550*) is induced upon treatment of *Arabidopsis* roots with auxin (Neuteboom *et al.,* 1999), but no function of AIR1 has been described. In contrast, the function of TERMINAL FLOWER LOCUS 1 (TFL1, AT5G03840), INDOLE GLUCOSINOLATE O-METHYLTRANSFERASE 1 (IGMT1, AT1G21100) and PEROXIDASE71 (PER71, AT5G64120) has been described in shoots. TFL1 is an important regulator of inflorescence meristem identity and flowering time (Shannon & Meeks-Wagner, 1991; Ratcliffe *et al.,* 1998). IGMT1 converts the most abundant glucosinolate in leaves, indole-3-yl-methylglucosinolate, to 4-methoxyindole-3-yl-methylglucosinolate (Pfalz *et al.,* 2011) and PER71 negatively influences the shoot growth most likely though repressing cell expansion (Raggi *et al.,* 2015). Still, we decided to analyze the expression of these five genes in Col-0, *tga1 tga4* and *roxy6789* roots under FN and LN conditions, as they might have additional functions.

Table 27: Ten most upregulated genes in *roxy6789* roots upon nitrogen starvation compared to Col-0 based on transcriptome data. The logarithmic fold change to base 2 (log_2) was calculated by DESeq2 Galaxy Tool. Number of TGACG motifs was counted in the region 2 kb upstream of the transcription start site. Analyzed genes in this study by qRT-PCR are highlighted in grey. TPM: transcript per million.

	TPM Col-0	TPM *roxy6789*	log_2FC	TGACG motifs
AT4G39675	1.98	38.79	-3.16	1
SWEET11	0.18	6.03	-2.70	3
TFL1	2.10	17.87	-2.49	1
AT1G52100	0.21	2.02	-2.22	1
GDPD3	0.07	1.19	-2.22	1
AT4G29905	39.61	222.61	-2.19	2
IGMT1	4.50	23.42	-2.18	3
AT1G49500	7.34	38.52	-2.14	1
PER71	31.68	179.93	-2.09	1
AIR1	26.69	152.68	-2.04	1

4.5.3.2. *TFL1* and *PER71* expression is activated by TGA1, 4 under FN conditions

Both *TFL1* and *PER71* show lower expression in the *tga1 tga4* mutant and higher expression in the *roxy6789* mutant in FN conditions (Figure 21). Thus, they are activated by TGA1, 4 and repressed by ROXY6, 7, 8, 9. Upon N starvation, *TFL1* and *PER71* expression is reduced in Col-0 compared to FN conditions. No difference is detectable between Col-0 and *tga1 tga4*, most likely because ROXY6, 7, 8, 9 fully repress the function of TGA1, 4. Also *IGMT1* and *AIR1* expression is activated by TGA1, 4 and repressed by ROXY6, 7, 8, 9 in sufficient N supply (Supplementary Figure S3). However, the differences between the genotypes are more striking for *TFL1* and *PER1*. Moreover, in LN conditions, no repressive effect of ROXY6, 7, 8 9 on *IGMT1* was observed. This finding varies from the transcriptome data, thus *IGMT1* was not considered a suitable target gene.

In contrast to the previously described genes, *SWEET11* is not regulated by TGA1, 4 in neither FN nor LN conditions. Still, ROXY6, 7, 8, 9 repress the expression in both conditions, so that *SWEET11* is a suitable marker gene to analyze the repressive mechanism of ROXY6, 7, 8, 9.

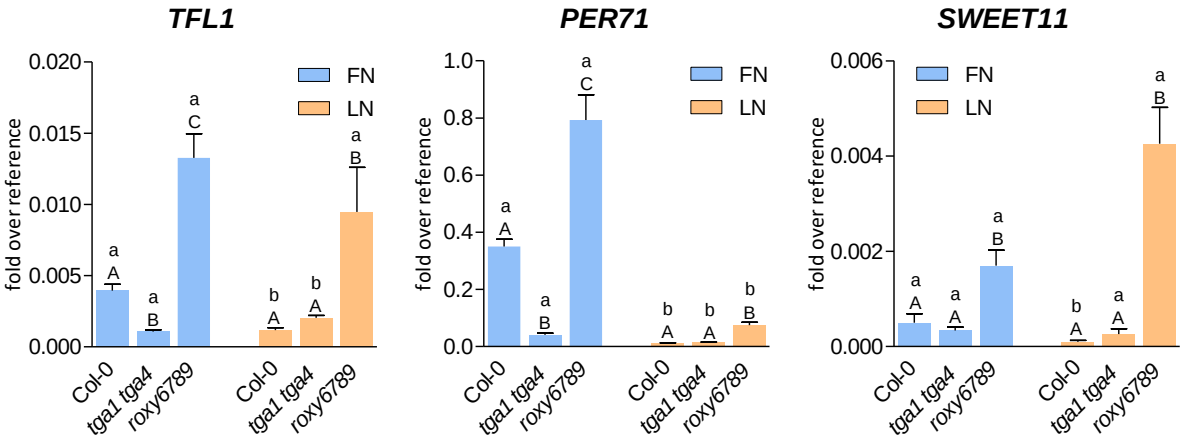

Figure 21: ROXY6, 7, 8, 9 repress the expression of *TFL1, PER71* and *SWEET11* in *A. thaliana* roots. 7-day old seedlings grown on full nutrition (FN) plates under constant light conditions (70 µmol photons s^{-1} m^{-2}) were transferred to either FN or low nitrogen (LN) plates. Two days later, roots were collected, RNA was isolated and cDNA synthesized. Expression of *TFL1, PER71* and *SWEET11* was analyzed by qRT-PCR, *UBQ5* was used as a reference gene. Mean values of four to five biological replicates are shown. Error bars represent the standard error of the mean. Lowercase letters indicate statistically significant differences within the genotype between the treatments, uppercase letters indicate significant differences within treatment between the genotypes. Statistical analyses were performed with the logarithmic values by using two-way ANOVA and Bonferroni's post-test (*p*-value < 0.05). Three independent experiments were performed with similar results.

4.5.3.3. ROXY6, 7, 8, 9 activate the expression of 350 genes upon nitrogen starvation

Besides the 212 genes, which are repressed by ROXY6, 7, 8, 9 in LN conditions, the transcriptome analysis revealed 350 genes which are activated by ROXY6, 7, 8, 9 (log_2 FC > 1, p.adj < 0.05). Within this dataset, nitrogen and nitrate responses are over 5-fold enriched compared to the genome (Figure 22, displayed in red). This suggests that ROXY6, 7, 8, 9 are important for the regulation of N starvation responses and nitrate uptake.

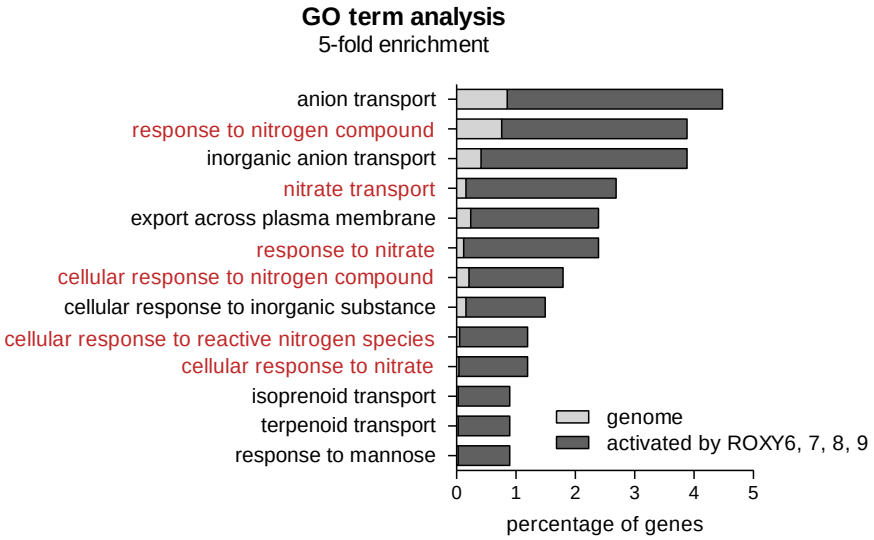

Figure 22: Nitrogen-related genes are activated by *roxy6789* upon nitrogen starvation. Gene Ontology (GO) term analysis was performed with the 350 genes that are lower expressed (log_2 FC > 1, *p*.adj < 0.05) in *roxy6789* compared to Col-0 upon nitrogen starvation according to transcriptome data**.** GO terms related to nitrogen are displayed in red. Statistical analysis was performed using Fisher test and False discovery rate (FDR) < 0.05.

In addition to the GO term analysis, motif mapper analysis was performed. The TGA binding motifs TGACG, TGACGTCA and TACGTA are enriched in within the 350 ROXY-activated genes compared to the genome (Table 28). Thus, TGA factors are most likely involved in the regulation of these genes. Furthermore, the WRKY DNA-BINDING PROTEIN 50 (WRKY50) binding site GACTTTTC (Hussain *et al.,* 2018) and the SUCROSE-RESPONSIVE ELEMENT 2 (SURE2) binding site AATACTAAT (Grierson *et al.,* 1994) are enriched. WRKY50 has been shown to interact with TGA2 and 5 to regulate *PR1* expression in leaves (Hussain *et al.,* 2018). Maybe WRKY50 has additional functions in roots upon N starvation. SURE2 proteins have a putative role in sucrose-responsiveness (Grierson *et al.,* 1994).

Table 28: TGA factor binding sites are enriched in the 350 ROXY6, 7, 8, 9-activated genes. Motif mapper analysis was performed with the 350 genes that are lower expressed (log_2 FC > 1, *p*.adj < 0.05) in *roxy6789* compared to Col-0 upon nitrogen starvation according to transcriptome data. Enrichments were calculated compared to a set of randomly chosen promoters from the whole *A. thaliana* genome.

Motif	Number of motifs in 350 ROXY-activated genes	Number of motifs in genome	*p*-value	enrichment
TGACG	335	298.2	0.0192	1.12
TGACGTCA	9	4.7	0.0294	1.93
TACGTA	78	62.4	0.0359	1.25
GACTTTTC	30	18.2	0.0037	1.65
AATACTAAT	21	12.6	0.0099	1.66

To analyze whether TGA1, 4 are involved in the regulation of genes which are activated by ROXY6, 7, 8, 9, target genes for qRT-PCRs were chosen. Again, the ten most differentially expressed genes in *roxy6789* compared to Col-0 were taken into account (Table 29). Among them are five genes, which have been described as nitrate-responsive. *NRT2.2* (*AT1G08100*) and *NRT2.4* (*AT5G60770*) encode high-affinity nitrate transporters (Zhuo *et al.,* 1999; Kiba *et al.,* 2012), similar to *NRT2.1*, the previously described target gene of ROXY6, 8, 9 (Ohkubo *et al.,* 2017). Even though *NRT2.1* was not among the ten genes activated by ROXY6, 7, 8, 9, we decided to analyze the expression in our experimental setup as well. Also *CEPH* was previously identified as being activated ROXY6, 8, 9 (Ohkubo *et al.,* 2021). The ammonium transporter AMT1-5 (AT3G24290) has been shown to accumulate in roots grown under N starvation conditions (Yuan *et al.,* 2007). *NIN-LIKE PROTEIN 3* (*NLP3*, *AT4G38340*) encodes for a nitrate-responsive transcription factor. Recently, the closely related NLP7 was described to have an additional function as nitrate receptor (Liu *et al.,* 2022).

Besides these genes, *USUALLY MULTIPLE ACIDS MOVE IN AND OUT TRANSPORTERS 35* (*UMAMIT35*, *AT1G60050*) and *RAD-LIKE 3* (*RL3*, *AT4G36570*) were chosen for qRT-PCR analysis. UMAMIT35 is a transporter, which exports several amino acid out of the cytosol (Zhao *et al.,* 2021). *RAD* and *RAD-LIKE* genes have so far only been characterized in *Antirrhinum majus*, where they maintain floral asymmetry (Baxter *et al.,* 2007). As *A. thaliana* has symmetric flowers, *RL3* might have a different function.

Except for *NLP3*, all these genes have at least one TGACG motif in their promoter region in the region 2 kb upstream of the transcription start site, suggesting that these genes are regulated by TGA factors in addition to ROXY6, 7, 8, 9.

Table 29: Ten most downregulated genes in *roxy6789* roots compared to Col-0 based on transcriptome data. The logarithmic fold change to base 2 (log_2) was calculated by DESeq2 Galaxy Tool. Number of TGACG motifs was counted in the region 2 kb upstream of the transcription start site. Analyzed genes in this study by qRT-PCR are highlighted in grey. TPM: transcript per million.

	TPM Col-0	TPM *roxy6789*	log_2FC	TGACG motifs
NRT2.2	127.66	3.31	4.59	4
UMAMIT35	19.19	0.57	4.47	3
NRT2.4	121.67	4.59	4.26	1
ATL7	5.83	0.15	3.55	✘
AMT1-5	9.87	0.34	3.51	2
RL3	15.23	0.92	3.35	1
NLP3	22.47	1.89	3.34	✘
OCT1	11.02	0.82	3.32	1
CEPH	140.96	10.42	3.22	3
AT4G37220	19.44	1.57	3.19	✘

4.5.3.4. TGA1, 4 contribute only weakly to the activation of *NRT2.2* and *NRT2.4* in LN conditions

Expression of *NRT2.2, NRT2.4, NRT2.1, NLP3*, *AMT1-5* and *CEPH* is highly induced in Col-0 under N limiting conditions (Figure 23, Supplementary Figure S4). In FN conditions, TGA1, 4 seems to slightly contribute to the expression of these target genes, as the expression is higher than in the WT. Upon N starvation, the *tga1 tga4* mutant shows similar induction as in Col-0. In the *roxy6789* mutant, the gene expression of *NRT2.2, NRT2.4, NLP3*, *AMT1-5* and *CEPH* is only weakly induced, clearly showing that ROXY6, 7, 8 and 9 activate the expression of these genes. In contrast, *NRT2.1* expression is still moderately induced in *roxy6789* mutant in LN conditions, but compared to Col-0, it is reduced by about factor 2 (Supplementary Figure S4). This supports the published data (Ohkubo *et al.,* 2017; Ota *et al.,* 2020), but as especially *NRT2.2* and *NRT2.4* show drastic differences in the expression between Col-0 and *roxy6789*, we focused on these genes for further analysis.

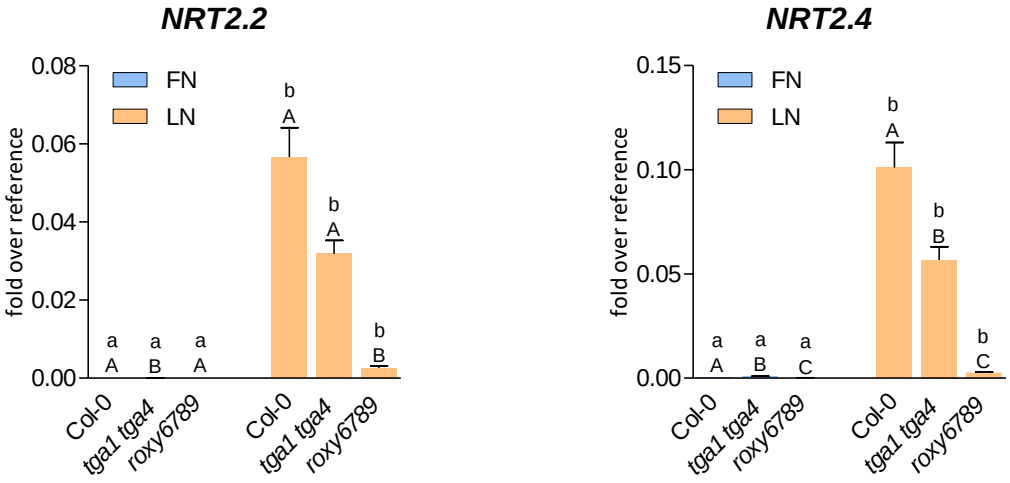

Figure 23: ROXY6, 7, 8, 9 activate the expression of *NRT2.2* and *NRT2.4* in *A. thaliana* roots. 7-day old seedlings grown on full nutrition (FN) plates under constant light conditions (70 µmol photons s^{-1} m^{-2}) were transferred to either FN or low nitrogen (LN) plates. Two days later, roots were collected, RNA was isolated and cDNA synthesized. Expression of *NRT2.2* and *NRT2.4* was analyzed by qRT-PCR, *UBQ5* was used as a reference gene. Mean values of four to five biological replicates are shown. Error bars represent the standard error of the mean. Lowercase letters indicate statistically significant differences within the genotype between the treatments, uppercase letters indicate significant differences within treatment between the genotypes. Statistical analyses were performed with the logarithmic values by using two-way ANOVA and Bonferroni's post-test (*p*-value < 0.05). Three independent experiments were performed with similar results.

4.5.3.5. *UMAMIT35* and *RL3* are activated by ROXY6, 7, 8, 9 and repressed by TGA1, 4 in FN conditions

In FN conditions, *UMAMIT35* and *RL3* are higher expressed in the *tga1 tga4* mutant and lower expressed in the *roxy6789* mutant compared to Col-0 (Figure 24). This shows that *UMAMIT35* and *RL3* are activated by ROXY6, 7, 8, 9, most likely through interfering with the repressive mechanism of TGA1, 4.

Upon N starvation, both genes are induced in the Col-0, but not in *roxy6789*, indicating that ROXY6, 7, 8, 9 are also required for the activation of these genes in LN conditions. In the *tga1 tga4* mutant, the expression of *UMAMIT35* is similar to the WT levels, suggesting that TGA1, 4 is fully repressed by ROXY6, 7, 8, 9. The *RL3* expression is lower in the *tga1 tga4* mutant compared to the WT. Thus TGA1, 4 contributes to the expression under LN conditions.

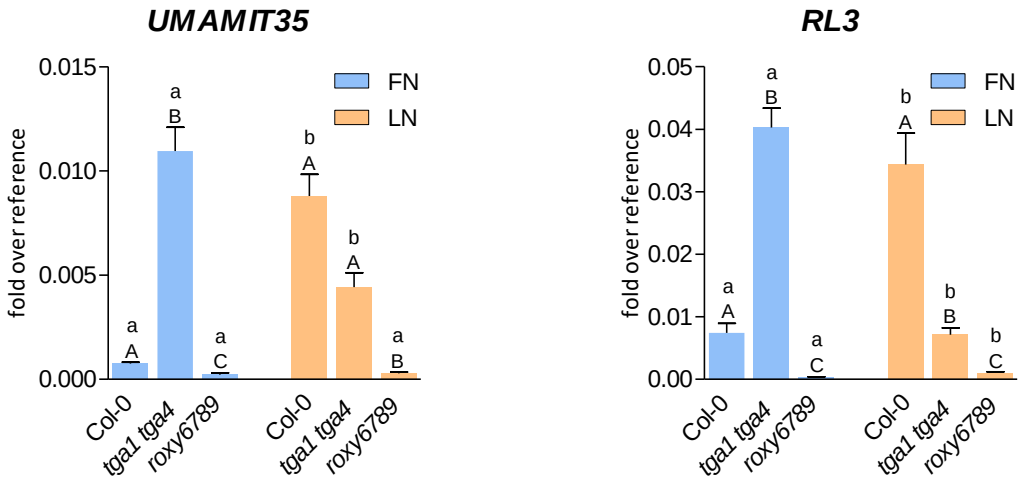

Figure 24: ROXY6, 7, 8, 9 activate the expression of *UMAMIT35* and *RL3* in *A. thaliana* roots by interfering with the repressive mechanism of TGA1, 4. 7-day old seedlings grown on full nutrition (FN) plates under constant light conditions (70 µmol photons s^{-1} m^{-2}) were transferred to either FN or low nitrogen (LN) plates. Two days later, roots were collected, RNA was isolated and cDNA synthesized. Expression of *UMAMIT35* and *RL3* was analyzed by qRT-PCR, *UBQ5* was used as a reference gene. Mean values of four to five biological replicates are shown. Error bars represent the standard error of the mean. Lowercase letters indicate statistically significant differences within the genotype between the treatments, uppercase letters indicate significant differences within treatment between the genotypes. Statistical analyses were performed with the logarithmic values by using two-way ANOVA and Bonferroni's post-test (*p*-value < 0.05). Three independent experiments were performed with similar results.

4.5.4. ROXY6, 7, 8, 9 and TGA1, 4 function in one pathway to regulate gene expression

As described in the previous section, *TFL1* and *PER71* were identified to be activated by TGA1, 4 and repressed by ROXY6, 7, 8, 9; suggesting that ROXY6, 7, 8, 9 repress TGA1, 4. In contrast, *PER10*, *CLE3*, *RL3* and *UMAMIT35* are activated by ROXY6, 7, 8, 9, and repressed by TGA1, 4, most likely through repression of TGA1, 4 by ROXY6, 7, 8, 9. To validate that ROXY6, 7, 8 and 9 function in one pathway with TGA1, 4 to control the expression of these genes, the respective mutants *roxy6789* and *tga1 tga4* were crossed with the help of the technician Ronald Scholz. After genotyping 400 plants in the second generation and 280 plants in the third generation, we finally identified the *tga1 tga4 roxy6 roxy7 roxy8 roxy9* (*tga14roxy6789*) hexuple mutant.

As representation, *PER71* and *UMAMIT35* are depicted in Figure 25, the other target genes can be found in Supplementary Figure S5. For all target genes, the *tga14roxy6789* mutant behaves like the *tga1 tga4* mutant in both N sufficient and N limiting supply. This is especially striking for *PER71, UMAMIT35* and *TFL1* in LN conditions, as the *tga1 tga4* mutant has WT-like gene expression. Still,

TGA1, 4 are involved in the regulation of the expression, as the *tga14roxy6789* does not show the increased gene expression of *roxy6789*. This confirms that ROXY6, 7, 8, 9 functions in one pathway with TGA1, 4 in order to control the gene expression of *TFL1*, *PER71*, *PER10*, *CLE3*, *RL3* and *UMAMIT35*.

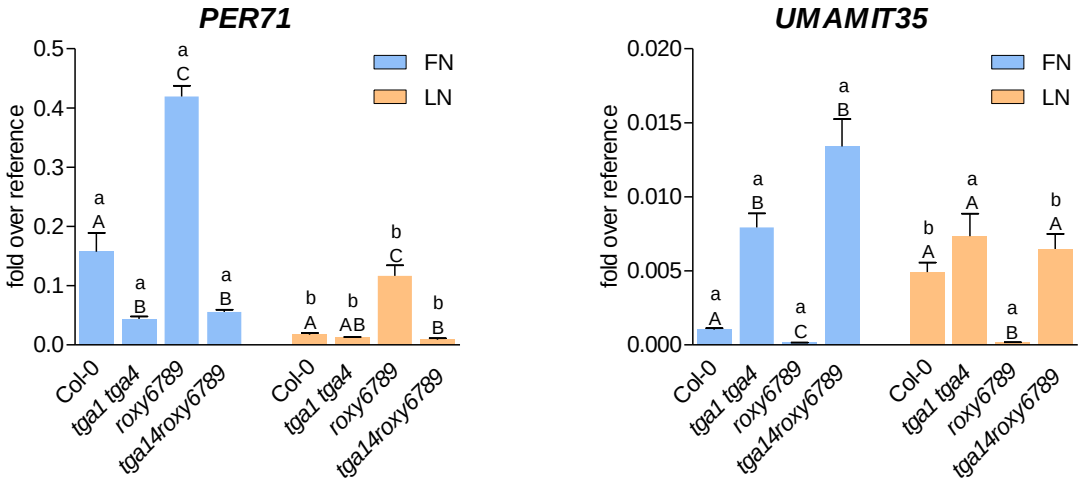

Figure 25: ROXY6, 7, 8, 9 and TGA1, 4 function in one pathway to regulate the expression of *PER71* and *UMAMIT35*. 7-day old seedlings grown on full nutrition (FN) plates under constant light conditions (70 µmol photons s^{-1} m^{-2}) were transferred to either FN or low nitrogen (LN) plates. Two days later, roots were collected, RNA was isolated and cDNA synthesized. Expression of *PER71* and *UMAMIT35* was analyzed by qRT-PCR, *UBQ5* was used as a reference gene. Mean values of four to five biological replicates are shown. Error bars represent the standard error of the mean. Lowercase letters indicate statistically significant differences within the genotype between the treatments, uppercase letters indicate significant differences within treatment between the genotypes. Statistical analyses were performed with the logarithmic values by using two-way ANOVA and Bonferroni's post-test (*p*-value < 0.05). Two independent experiments were performed with similar results.

4.5.5. ROXY6, 7, 8, 9 interfere with the repressive mechanism of TGA1, 4 in order to activate *NRT2.2* and *NLP3* expression

Even though the expression of *NRT2.2* and *NLP3* is similar in the WT and *tga1 tga4*, we analyzed the expression in the *tga14roxy6789* mutant to rule out that TGA1, 4 are involved in the regulation of these genes.

Surprisingly, upon N starvation, *NRT2.2* and *NLP3* expression in the hexuple mutant is WT- and *tga1 tga4*-like (Figure 26), suggesting that TGA1, 4 is not the activator of *NRT2.2* and *NLP3* but functions as a repressor, which is in turn repressed by ROXY6, 7, 8, 9. For this reason the *tga1 tga4* mutant does not show a difference in gene expression. Additionally, this indicates that *NRT2.2* and *NLP3* are induced by another activator. Besides, *NLP3* does not contain a TGACG motif in the promoter region. In order to interfere with the gene expression, TGA1, 4 might activate another repressor.

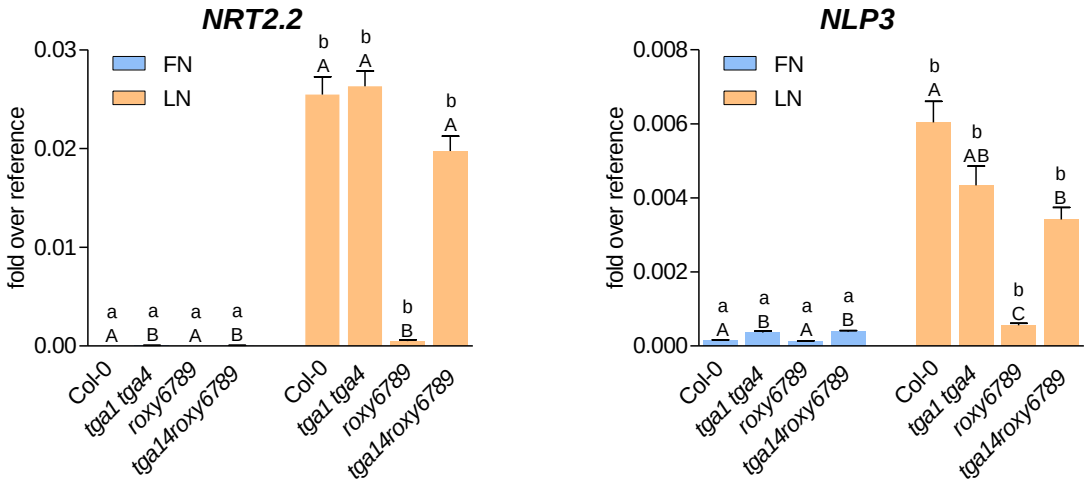

Figure 26: ROXY6, 7, 8, 9 activate the expression of *NRT2.2* and *NLP3* by interfering with the repressive mechanism of TGA1, 4. 7-day old seedlings grown on full nutrition (FN) plates under constant light conditions (70 µmol photons s^{-1} m^{-2}) were transferred to either FN or low nitrogen (LN) plates. Two days later, roots were collected, RNA was isolated and cDNA synthesized. Expression of *NRT2.2* and *NLP3* was analyzed by qRT-PCR, *UBQ5* was used as a reference gene. Mean values of four to five biological replicates are shown. Error bars represent the standard error of the mean. Lowercase letters indicate statistically significant differences within the genotype between the treatments, uppercase letters indicate significant differences within treatment between the genotypes. Statistical analyses were performed with the logarithmic values by using two-way ANOVA and Bonferroni's post-test (*p*-value < 0.05). Two independent experiments were performed with similar results.

4.5.6. Clade II TGA factors repress *PER71* and *SWEET11* expression upon nitrogen starvation

As most of the analyzed genes contain at least one TGACG motif in the 2 kb region upstream of the transcription start site, we wondered if other TGA factors are involved in the regulation in addition or instead of Clade I TGAs 1, 4. TGA factors from Clade II (TGA2, 5, 6) and Clade III (TGA3, 7) are involved in the regulation of stress responses, thus they might regulate gene expression upon N starvation as well. To test whether these TGAs are involved, the *tga2 tga5 tga6* (*tga256*)*, tga3 tga7* (*tga37*) and *tga2 tga3 tga5 tga6* (*tga2356*) mutants were analyzed. Most of the experiments were performed by Hannah Knerich as part of her bachelor thesis. However, the experimental design and the statistical analyses were prepared as part of this dissertation.

First of all, the expression of *PER71, TFL1* and *SWEET11* was analyzed, which is repressed by ROXY6, 7, 8, 9 In FN conditions, *PER71* and *TFL1* are not regulated by neither TGA2, 5, 6 nor TGA3, 7 (Figure 27, Supplementary Figure S6). In contrast, *SWEET11* is repressed by TGA2, 5, 6. Upon LN treatment, *PER71* and *SWEET11,* but not *TFL1*, are elevated in the *tga256 and tga2356* mutants, suggesting that clade II TGAs repress *PER71* and *SWEET11* in addition to ROXY6, 7, 8, 9. As TGA2, 5, 6 and ROXY6, 7, 8, 9 can interact with each other (Zander *et al.,* 2012; Uhrig *et al.,* 2017), they might form a repressive complex in order to regulate the gene expression.

Next, the expression of genes, which are activated by ROXY6, 7, 8, 9 was analyzed in the respective TGA mutants. The expression of *UMAMIT35* is elevated in the *tga256* and *tga2356* mutants in FN conditions compared to the WT and the *tga37* mutant (Figure 27). Upon N starvation *UMAMIT35* expression is induced in all genotypes to the same extent. This shows that TGA2, 5, 6 repress *UMAMIT35* in sufficient but not limited N supply. ROXY6, 7, 8, 9 might therefore interfere with the repressive mechanism of these TGAs in addition to TGA1, 4 in order to activate the gene expression in LN conditions.

NRT2.2, *NRT2.4*, *NLP3* and *RL3* expression is induced in LN conditions in the WT and the analyzed mutants to the same extent (Figure 27, Supplementary Figure S6), suggesting that clade II and clade III TGA factors are not involved in the regulation of the expression. However, TGA2, 5, 6 and TGA3, 7 might function in a similar manner as TGA1, 4 as repressors in order to regulate *NRT2.2 NRT2.4*, *NLP3* and *RL3* expression. In LN conditions, TGA1, 4 is completely repressed by ROXY6, 7, 8, 9 and thus the *tga1 tga4* mutant does not differ from the WT. To further investigate this hypothesis, the respective mutants *tga256* and *tga37* need to be crossed with the *roxy6789* mutant as well.

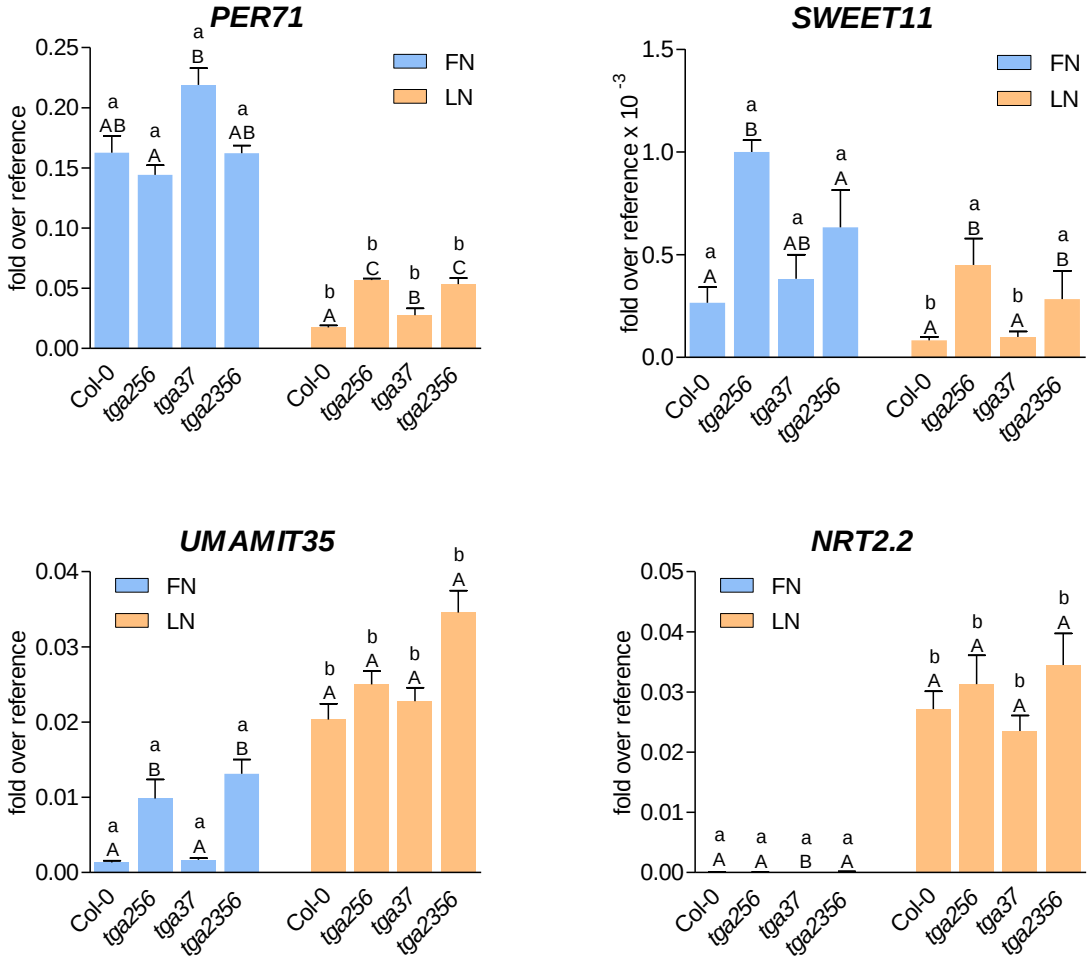

Figure 27: TGA2, 5, 6 repress the expression of *PER71* and *SWEET11* in *A. thaliana* roots upon nitrogen starvation. 7-day old seedlings grown on full nutrition (FN) plates under constant light conditions (70 µmol photons s^{-1} m^{-2}) were transferred to either FN or low nitrogen (LN) plates. Two days later, roots were collected, RNA was isolated and cDNA synthesized. Expression of *PER71* and *SWEET11* was analyzed by qRT-PCR, *UBQ5* was used as a reference gene. Mean values of four to five biological replicates are shown. Error bars represent the standard error of the mean. Lowercase letters indicate statistically significant differences within the genotype between the treatments, uppercase letters indicate significant differences within treatment between the genotypes. Statistical analyses were performed with the logarithmic values by using two-way ANOVA and Bonferroni's post-test (*p*-value < 0.05). Two independent experiments were performed with similar results.

4.5.7. ROXY10-15 have a negative influence on *UMAMIT35* expression under sufficient nitrogen supply

In contrast to the ALWL-free ROXYs 6, 7, 8 and 9, the expression of the ALWL-containing ROXYs 10, 11, 12, 13, 14, 15, 16, 17, 18 were repressed upon N starvation (Jung *et al.,* 2018). Moreover, adding nitrate leads to the upregulation of ROXY11, 12, 13, 15, 17 (Patterson *et al.,* 2016). This is why we decided to investigate the influence of some of these ROXYs on the ROXY9 target gene expression as well. ROXY11, 12, 13, 14 and 15 are located next to each other in the genome. By using CRISPR-Cas9, Jelena Budimir knocked out the whole cluster. Additionally, ROXY10 was mutated by the technician Ronny Scholz, resulting in the *roxy10, 11-15* (*roxy10-15*) mutant.

In our experimental setup, *ROXY10, ROXY11, ROXY12, ROXY13, ROXY14* and *ROXY15* are hardly expressed in roots independent of the N levels (Supplementary Figure S7). In shoots, the tested genes are higher expressed in sufficient N supply compared to N limiting conditions, which is in line with the published data. To fulfil a role in roots, we have to postulate that ROXY10-15 are transported from the shoots to the roots in a similar manner like ROXY6, 7, 8, 9.

The expression of *UMAMIT35* is elevated in FN conditions in the *roxy10-15* mutant compared to Col-0 and *roxy6789* (Figure 28). The *roxy6789* mutant shows weaker expression of *UMAMIT35* than the WT, even though this difference is not statistically significant. Still, the results indicate that ROXY10-15 function in a reciprocal manner to ROXY6, 7, 8, 9. All other analyzed target genes in FN and LN conditions behaved WT-like in the *roxy10-15* mutant (Figure 28, Supplementary Figure S8), suggesting that ROXY10-15 are either not involved in the regulation of these genes or other ALWL-containing ROXYs can compensate the loss of ROXY10-15.

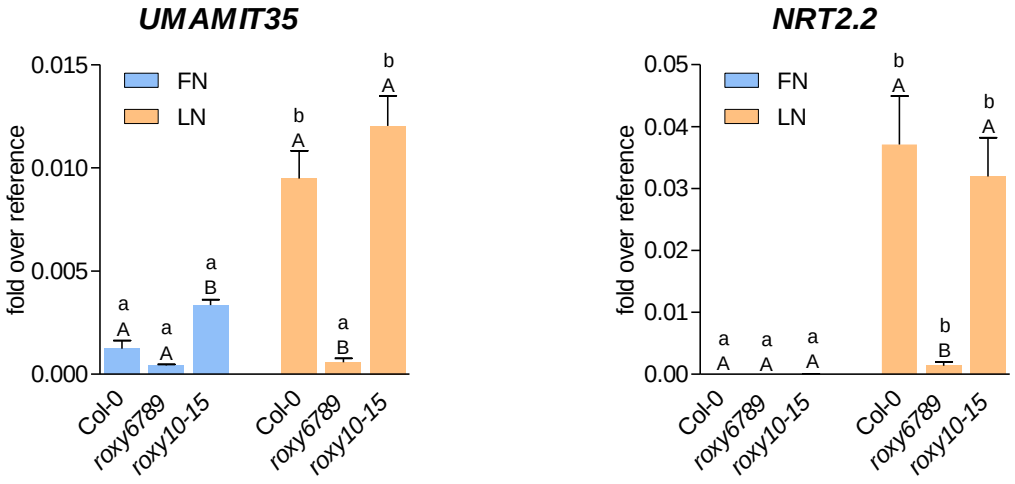

Figure 28: ROXY10-15 have a negative influence on *UMAMIT35* expression *A. thaliana* roots under sufficient nitrogen supply. 7-day old seedlings grown on full nutrition (FN) plates under constant light conditions (70 µmol photons s^{-1} m^{-2}) were transferred to either FN or low nitrogen (LN) plates. Two days later, roots were collected, RNA was isolated and cDNA synthesized. Expression of *UMAMIT35* and *NRT2.2* was analyzed by qRT-PCR, *UBQ5* was used as a reference gene. Mean values of four to five biological replicates are shown. Error bars represent the standard error of the mean. Lowercase letters indicate statistically significant differences within the genotype between the treatments, uppercase letters indicate significant differences within treatment between the genotypes. Statistical analyses were performed with the logarithmic values by using two-way ANOVA and Bonferroni's post-test (*p*-value < 0.05).

4.5.8. CEPR1 is required for regulation of target gene expression upon nitrogen starvation

Upon N starvation, CEP1 is formed in the roots. After transfer to the shoot through the xylem, CEP1 binds to CEPR1 to activate the expression of *ROXY6, ROXY8, ROXY9*. ROXY6, 8, 9 travel to the roots to activate gene expression (Tabata *et al.,* 2014; Ohkubo *et al.,* 2017; Ota *et al.,* 2020). Consequently, the *cepr1* mutant is impaired in the activation of *NRT2.1* expression in roots after CEP1 treatment (Tabata *et al.,* 2014). We wanted to analyze if CEPR1 also contributes to the expression of ROXY6, 7, 8, 9 target genes when grown under N starvation conditions. The *cepr1-3* mutant is impaired in the induction of ROXY6, 7, 8, 9-activated *NRT2.2* and *UMAMIT35* in LN conditions (Figure 29). In contrast, CEPR1-mediated processes repress *TFL1*, which is negatively regulated by ROXY6, 7, 8, 9. This shows that CEPR1 is required for the regulation of ROXY6, 7, 8, 9 target genes under N limiting conditions.

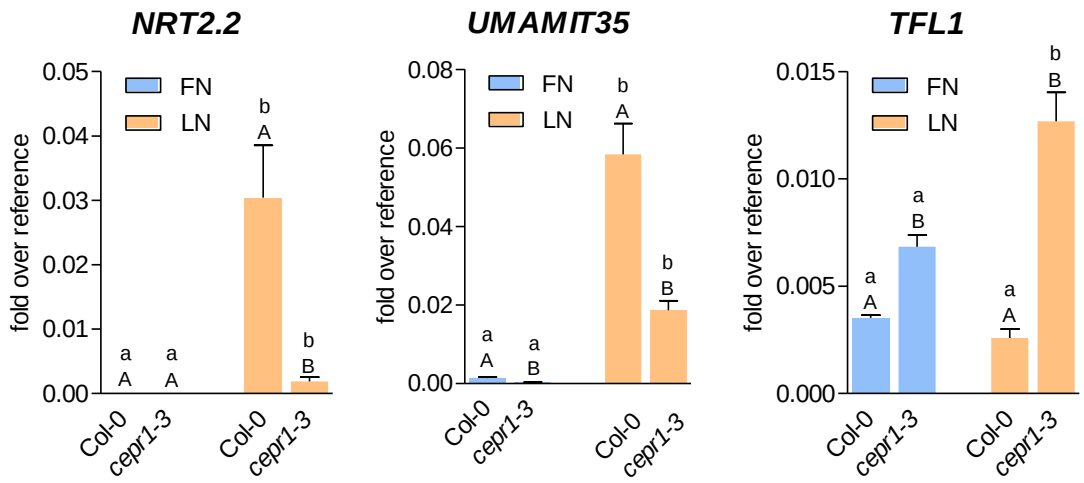

Figure 29: CEPR1 regulates the expression of *NRT2.2*, *UMAMIT35* and *TFL1* in *A. thaliana* roots. 7-day old seedlings grown on full nutrition (FN) plates under constant light conditions (70 µmol photons s^{-1} m^{-2}) were transferred to either FN or low nitrogen (LN) plates. Two days later, roots were collected, RNA was isolated and cDNA synthesized. Expression of *NRT2.2*, *UMAMIT35* and *TFL1* was analyzed by qRT-PCR, *UBQ5* was used as a reference gene. Mean values of four to five biological replicates are shown. Error bars represent the standard error of the mean. Lowercase letters indicate statistically significant differences within the genotype between the treatments, uppercase letters indicate significant differences within treatment between the genotypes. Statistical analyses were performed with the logarithmic values by using two-way ANOVA and Bonferroni's post-test (*p*-value < 0.05).

Next, we wanted to analyze, whether CEPR1 regulates target gene expression through the activation of *ROXY9* expression in the shoots. As expected, the expression of *ROXY9* is induced in the Col-0 upon N starvation (Figure 30a,). Surprisingly, a similar induction occurs in the *cepr1-3* mutant, indicating that CEPR1 is not required to activate *ROXY9* expression in these conditions. As CEPR1 is activated by CEP1, we questioned whether CEP1 can still activate *ROXY9* expression. For this, Col-0 seedlings were grown for seven days on FN plates and then transferred to either FN or FN containing CEP1 (FN+CEP1). The expression of *ROXY9* is induced in the WT when grown on FN+CEP1 (Figure 30a), consistent with the published data (Ohkubo *et al.,* 2017). This suggests that activation of CEPR1 is required for the induction of other processes that regulate N starvation-dependent genes.

a.

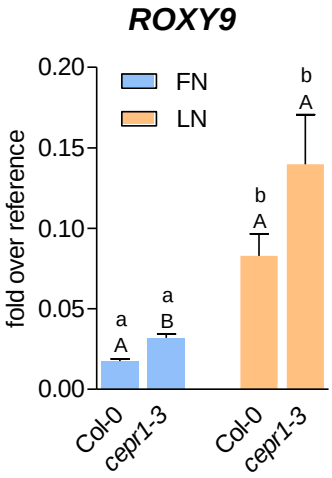

b.

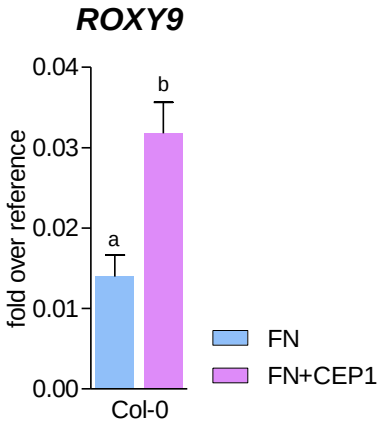

Figure 30: CEP and CEPR1 do not activate the expression of *ROXY9* in *A. thaliana* roots. 7-day old seedlings grown on full nutrition (FN) plates under constant light conditions (70 µmol photons s^{-1} m^{-2}) were transferred to either FN, FN containing 1 µM CEP1 (FN+CEP1) or low nitrogen (LN) plates. Shoot material was collected after two days, RNA was isolated and cDNA synthesized. Expression of *ROXY9* was analyzed by qRT-PCR, *UBQ5* was used as a reference gene. Mean values of four to six biological replicates are shown. Error bars represent the standard error of the mean. Lowercase letters indicate statistically significant differences within the genotype between the treatments, uppercase letters indicate significant differences within treatment between the genotypes. **a.** Statistical analysis was performed with the logarithmic values by using two-way ANOVA and Bonferroni's post-test (*p*-value < 0.05). **b.** Statistical analysis was performed with the logarithmic values by using an unpaired students t-test (*p*-value < 0.05).

4.5.10. Induction of *NRT2.2* does not require basal nitrogen amounts

As NRT2.2 is a nitrate transporter, low N levels might be required for the induction. To test this, we analyzed the gene expression in the absence of nitrogen. Seedlings were grown on FN plates for 7 days before they were transferred to either FN plates or no nitrogen (NN) plates. Roots were harvested, RNA was isolated, cDNA synthesized and qRT-PCR analyses were performed.

In Col-0, *NRT2.2* expression is induced in NN conditions, indicating that nitrogen is not required for the induction of *NRT2.2*. This induction is abolished in the *roxy6789* mutant, showing that ROXY6, 7, 8, 9 are required for the *NRT2.2* gene expression. Also the other tested target genes *NLP3*, *UMAMIT35*, *TFL1*, and *PER71* do not show a difference in NN conditions compared to LN (Supplementary Figure S9). *NLP3* and *UMAMIT35* are activated in the absence of N whereas *TFL1* and *PER71* are repressed.

Only *RL3* behaves differently in NN and LN conditions. While *RL3* is activated under N limiting conditions, it is repressed in the absence of nitrogen. This suggests that the activation of gene expression requires the right nitrogen concentration.

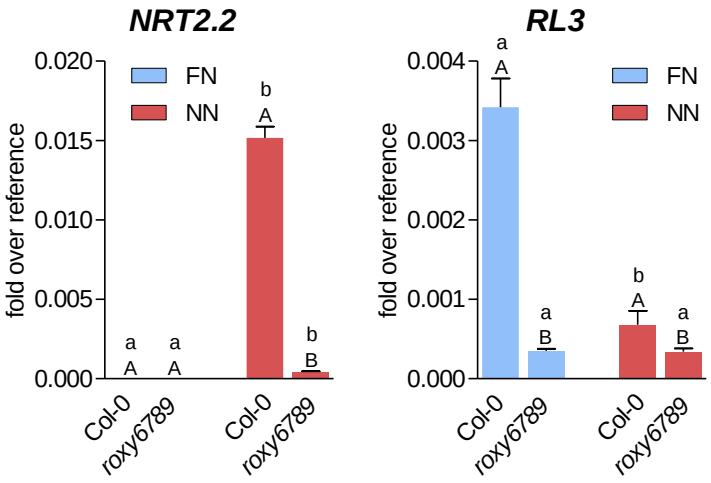

Figure 31: Induction of *NRT2.2* does not require basal nitrogen amounts. 7-day old seedlings grown on full nutrition (FN) plates under constant light conditions (70 µmol photons s^{-1} m^{-2}) were transferred to either FN or no nitrogen (NN) plates. Two days later, roots were collected, RNA was isolated and cDNA synthesized. Expression of *NRT2.2* was analyzed by qRT-PCR, *UBQ5* was used as a reference gene. Mean values of four to five biological replicates are shown. Error bars represent the standard error of the mean. Lowercase letters indicate statistically significant differences within the genotype between the treatments, uppercase letters indicate significant differences within treatment between the genotypes. Statistical analyses were performed with the logarithmic values by using two-way ANOVA and Bonferroni's post-test (*p*-value < 0.05).

5. Results Part II – Mechanism of action of ROXY9

After successful characterization of the *roxy6789* mutant, the mechanism of action of ROXY9 was investigated. To this aim, the influence of the redox state of TGAs was analyzed, the importance of the ROXY-specific active site motif was elucidated and a TurboID-approach was used to identify new interaction partners of ROXY9.

5.1. The repressive mechanism of ROXY6, 7, 8, 9 does not involve redox modulation of TGA1

TGA1 and TGA4 contain four conserved cysteines of which two can form intramolecular disulfide bridges (Després *et al.,* 2003). As class I GRXs are involved in reduction and oxidation of disulfide bridges, ROXYs might have a similar function and thus might be involved in the redox modulation of the TGAs. This is why we decided to analyze whether the redox state of TGA1 is important for the expression of ROXY6, 7, 8, 9 target genes.

To this aim, *tga1 tga4* complementation lines with WT TGA1 and a version of TGA1 in which all cysteines are mutated (C172N, C260N, C266S, C287S), so that it cannot be oxidized, were analyzed (Budimir *et al.,* 2021). We named the WT TGA complementation TGA1ox and the mutated version TGA1red.

The expression of *ROXY9* in leaves of 4-week old plants is activated by TGA1, 4 and repressed by ROXY6, 7, 8, 9 (Figure 17). Thus, the *roxy6789* mutant shows the derepressed level of *ROXY9*, whereas the expression of *ROXY9* is partially repressed in Col-0. Also in this experiment, the *ROXY9* expression is abolished in the *tga1 tga4* mutant and the empty vector control (Figure 32a). The TGA1ox and TGA1red complementation lines can complement the *tga1 tga4* phenotype to the same extent, revealing that oxidation of TGA1 does not lead to inactivation. If the repression of TGA1 was due to oxidation, the reduced TGA1, 4 should show hyperinduction, similar to the *roxy6789* mutant.

In addition to the *ROXY9* expression in leaves, *PER71* and *UMAMIT35* expression in roots upon N starvation was analyzed. *PER71* is activated by TGA1, 4 and repressed by ROXY6, 7, 8, 9 (Figure 21). The TGA1ox and TGA1red complementation lines can restore the reduced *PER71* expression in the *tga1 tga4* mutant to the same extent (Figure 32b).

Expression of *UMAMIT35* is repressed by TGA1, 4 and activated by ROXY6, 7, 8, 9 through interfering with the function of TGA1, 4 (Figure 24). Both TGA1 complementation lines are able to mediate this repression to a similar extent (Figure 32b). This shows that the repressive mechanism of ROXY6, 7, 8, 9 does not involve redox modulation of TGA1.

a.

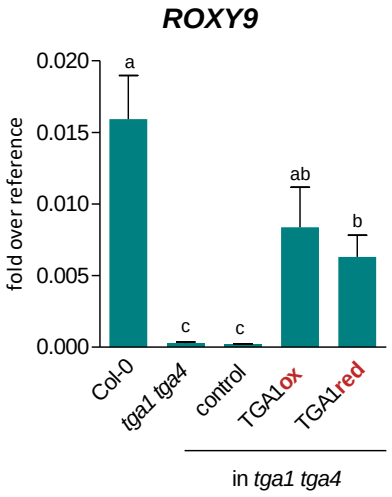

b.

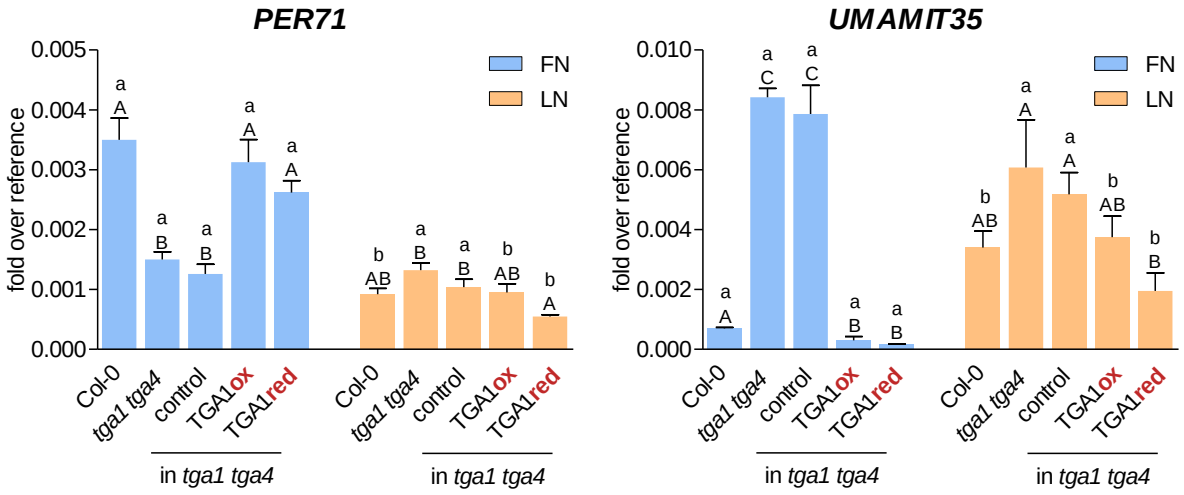

Figure 32: The repressive mechanism of ROXY6, 7, 8, 9 does not involve redox modulation of TGA1. a. Leaves of 4-week old *A. thaliana* plants were collected, RNA was isolated and cDNA synthesized. Expression of *ROXY9* was analyzed by qRT-PCR, *UBQ5* was used as a reference gene. Mean values of three to six biological replicates are shown. Error bars represent the standard error of the mean. Letters indicate statistically significant differences of the from the $\log_2$ values. Statistical analysis was performed by using one-way ANOVA and Tukey's post-test (*p*-value < 0.05). Three independent experiments were performed with similar results. **b.** 7-day old *A. thaliana* seedlings grown on full nutrition (FN) plates under constant light conditions (70 µmol photons s^{-1} m^{-2}) were transferred to either FN or low nitrogen (LN) plates. Two days later, roots were collected, RNA was isolated and cDNA synthesized. Expression of *PER71* and *UMAMIT35* was analyzed by qRT-PCR, *UBQ5* was used as a reference gene. Mean values of four to five biological replicates are shown. Error bars represent the standard error of the mean. Lowercase letters indicate statistically significant differences within the genotype between the treatments, uppercase letters indicate significant differences within treatment between the genotypes. Statistical analyses were performed with the logarithmic values by using two-way ANOVA and Bonferroni's post-test (*p*-value < 0.05).

5.2. Analysis of the importance of the ROXY-specific active site motif

To further elucidate how ROXY9 can regulate gene expression, the active site motif was analyzed. For this, *roxy6789* was complemented with ROXY9 wild type active site motif CCLC Y as well as with ROXY9 active site variants.

The first cysteine of the active site motif is highly conserved among all described GRX across species (Lillig *et al.,* 2008). It is the catalytically active cysteine and required for Fe-S cluster binding and transfer (Rouhier *et al.,* 2002; Feng *et al.,* 2006; Rouhier *et al.,* 2007). Thus, we hypothesize that the first cysteine of the ROXY9 active site motif CYS21 has important functions as well. Recent studies showed that CYS21 might be involved in Fe-S-cluster binding and is required for the formation of an internal disulfide bridge with CYS24. However, only weak reductase activity was detected (Mrozek, 2022). Still, CYS21 might be important for regulation of gene expression by ROXY9.

Besides the highly conserved first cysteine, the cysteine at the second position of the ROXY9 active site motif, CYS22, is conserved throughout all ROXYs in *A. thaliana*. So far, little is known about the function of this cysteine. According to the modelled structure, it is located on the surface, suggesting that it might be an interface for the interaction with other proteins or subject to post-translational modifications.

The tyrosine directly after the ROXY-specific active site motif, TYR25, is only present in ROXYs without ALWL motif, the other 17 ROXY members have a histidine located at this position. Thus, the tyrosine might be important for specific functions of ALWL-free ROXYs.

To analyze the importance of CYS21 and CYS22 for the function of ROXY9, *roxy6789* complementation lines were generated in which they were exchanged to serine (SCLC and CSLC). Besides, TYR25 was altered to an alanine (CCLCA). In addition to these active site variants, the ROXY9 active site motif was replaced by catalytically active class I CPYC consensus sequence. Previous studies showed that all these variants of ROXY9 can interact with TGA1 in the yeast-two hybrid system (Li *et al.,* 2019; Mörk, 2021). Recent biochemical analysis revealed that including a linker region between the HA-tag and ROXY9 prevents artificial aggregate formation (Mrozek, unpublished). Thus, a HA-L-ROXY9 construct was used for the generation of the complementation lines. As ROXY6, 7, 8 and 9 function in an additive manner, the expression of *HA-L-ROXY9* was introduced under control of a *35S* promoter to mimic the expression level of ROXY6, 7, 8 and 9. With this, we additionally analyzed whether ROXY9 is sufficient to complement the loss of the four ALWL-free ROXYs.

By using the floral dipping method, the coding region for HA-L-ROXY9 with wild type or altered active site motif was introduced into the *roxy6789* mutant. In the primary transformants (T1 generation), the amount of transgenic *ROXY9* was determined and lines with low expression levels were chosen for the next generation. In addition, the amount of endogenous *ROXY9* was determined in the T1 generation. Due to the autoregulation of ROXY9, the level of endogenous *ROXY9* reveals the functionality of the construct and whether the active site motif is involved in the repression *ROXY9*.

Apart from transcript analysis, western blots were performed with protein extracts derived from T1 leaf samples. Lines with similar protein expression were chosen for analysis of target gene expression upon N starvation and sufficient N supply in the T2 generation. In parallel, selected lines were self-fertilized to obtain homozygous plants, which were used to analyze the fresh weight and leaf-to-petiole ratio of the complementation lines.

5.2.1. ROXY9 active site variants can repress *ROXY9* in the T1 generation

By analyzing the amount of endogenous and transgenic *ROXY9* in the T1 generation, first insights into the importance of the active site motif can be collected. For this, leaf samples were harvested after growth for 4-5 weeks in long day (16/8 h light regime) conditions. After RNA extraction and cDNA synthesis, qRT-PCRs were performed.

In total, 37 to 38 independent lines per active site variant were analyzed as well as 20 control lines (*roxy6789* with *35S*:HA). The individual expression levels of each line can be found in Supplementary Figure S10. The results show that ROXY9 with the wild type CCLC active site version can repress the expression of endogenous *ROXY9,* as the expression levels are clearly reduced compared to the HA control (Figure 33a). This indicates that the HA-L-ROXY9 protein is expressed and functional. Similarly, ROXY9 with the active site variants SCLC and CSLC can complement *roxy6789* to the same extent as the CCLC version. Also the CCLCA and CPYC active site versions can repress endogenous *ROXY9*, however not as efficiently as the wild type version. Analysis of transgenic *ROXY9* reveals that this is not due to the fact that these active site variants are less expressed. In contrast, the 38 independent lines with the CPYC active site version have the highest transgenic *ROXY9* expression whereas the CCLC version is expressed the lowest.

These results show that the first and second cysteine of the active site motif are not required for the autoregulation of ROXY9. As the first cysteine is important for oxidoreductase activity and Fe-S cluster binding in other GRX, we can furthermore conclude that the repression of *ROXY9* is working in a different manner. As the CPYC active site variant is not as efficient as the WT ROXY9, it might be that the general structure of the active site is required for the functionality of ROXY9.

In addition to transcript analysis, western blots were performed with samples from lines with low transgenic *ROXY9* expression. 6 independent lines per active site variant were identified with similar protein expression (Figure 33b). Fully developed and dehumidified seeds of these lines were collected (T2 seeds) and used for further experiments.

a.

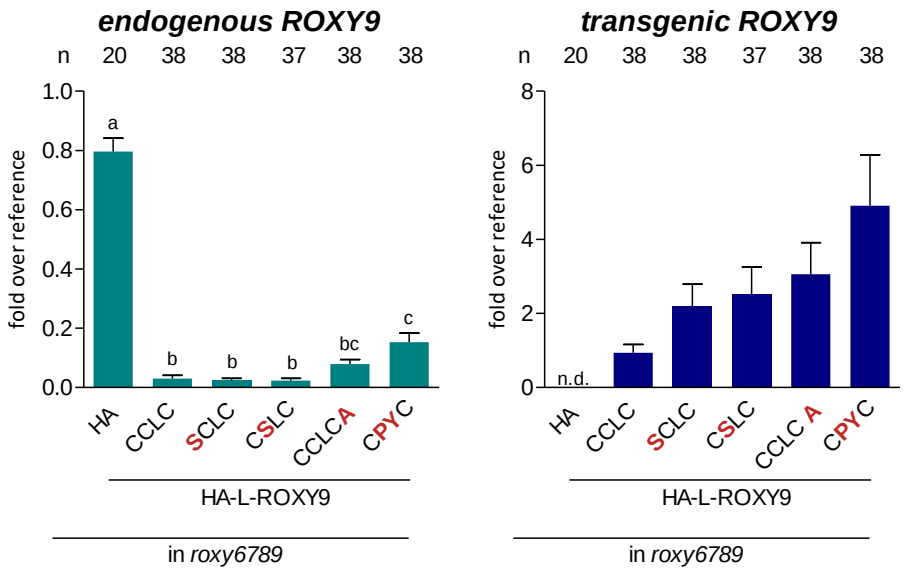

b.

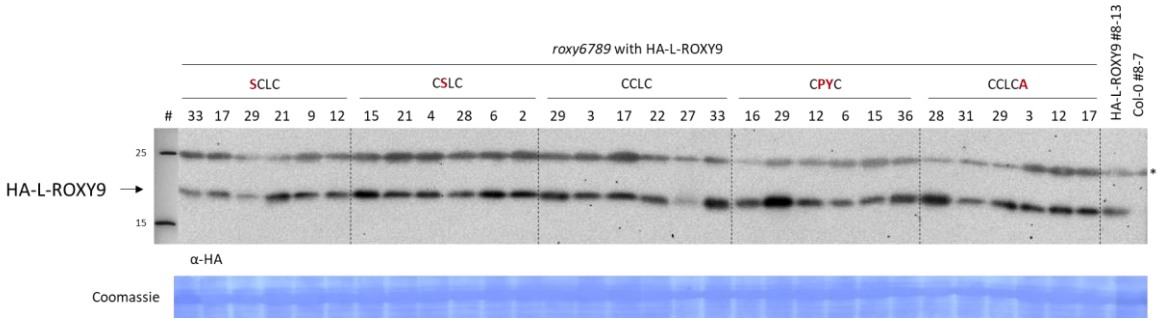

Figure 33: The first and second cysteine of the ROXY9 active site motif are not required for the autoregulation of ROXY9 in *A. thaliana* leaves. *roxy6789* was stably transformed with HA-L-ROXY9 active site variants by flower dipping. Leaves of the T1 generation were collected, RNA and proteins were isolated and cDNA was synthesized. **a.** Expression of endogenous and transgenic *ROXY9* was analyzed by qRT-PCR, *UBQ5* was used as a reference gene. Mean values of 20 to 38 independent lines are shown. Error bars represent the standard error of the mean. n.d.: not detected. Letters indicate statistically significant differences between the genotypes. Statistical analyses were performed with by using two-way ANOVA and Bonferroni's post-test (p-value < 0.05). **b.** For the detection of HA-L-ROXY9 in western blot analysis, α-HA was used as primary antibody and α-rabbit linked to peroxidase was used as secondary antibody. *: unspecific

5.2.2. The ROXY-specific active site motif is not required for the regulation of target gene expression upon nitrogen starvation

Next, target gene expression upon N starvation and sufficient N supply was analyzed in the complementation lines. For this, the 6 lines with low transgenic *ROXY9* amounts and similar protein expression in the T1 generation were chosen. Per independent line, four FN plates were prepared with 13 seeds of the T2 generation per plate. Seedlings were transferred to either FN or LN plates after seven days, resulting in two plates per line and condition. After two days, roots and shoots were separately collected and the material of two plates were pooled per line. The samples were ground in liquid N and the powder was divided for protein extraction and RNA isolation. Western blot analyses were performed and 5 lines per construct with similar protein amount were chosen for subsequent qRT-PCR analysis (Figure 34). As the CCLCA active site variant had less protein expression in 4 out of 6 lines, this active site variant was discarded for further analysis.

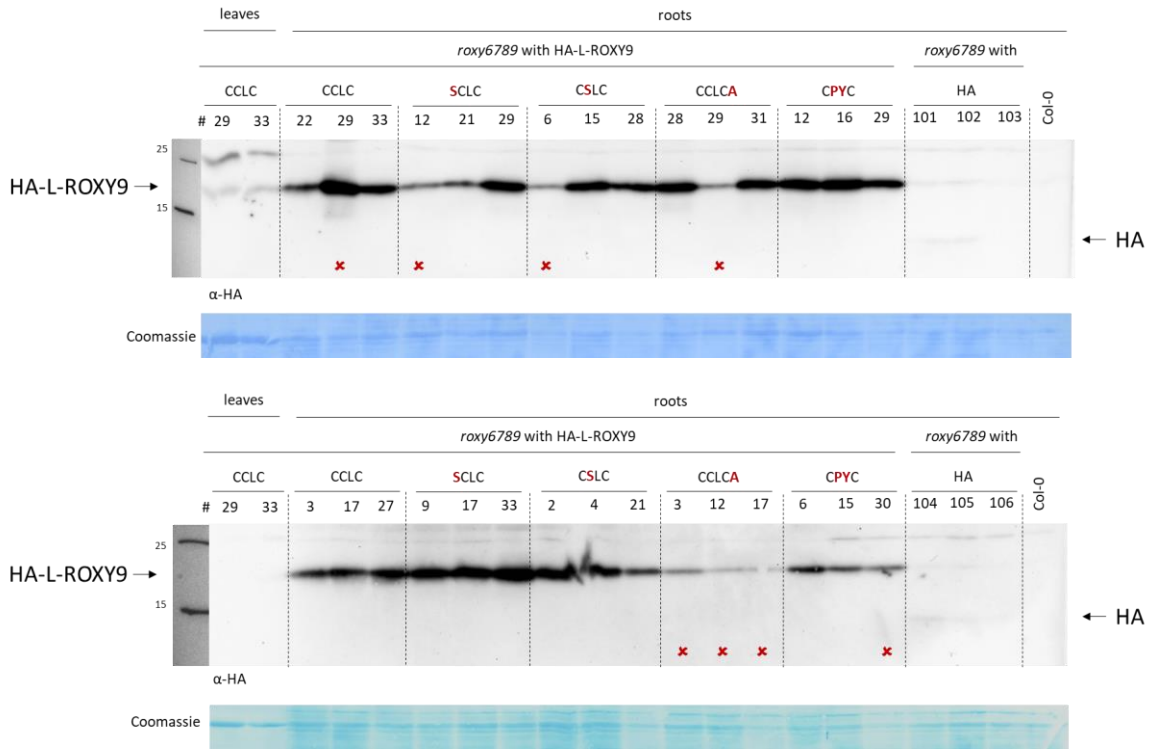

Figure 34: Western blot analysis of stably transformed *roxy6789* with HA-L-ROXY9 active site variants. 7-day old seedlings grown on full nutrition (FN) plates under constant light conditions (70 µmol photons s^{-1} m^{-2}) were transferred to low nitrogen plates. Two days later, roots were collected and proteins were extracted from 6 independent lines per active site variant. For the detection of HA-L-ROXY9 in western blot analysis, α-HA was used as primary antibody and α-rabbit linked to peroxidase was used as secondary antibody. The lines marked with ✖ were excluded in qRT-PCR analysis as they had too high or too low protein amount.

As shown before, the expression of *NRT2.2, NRT2.4*, *AMT1-5* and *NLP3* is activated in response to LN conditions in Col-0 (Figure 35, Supplementary Figure S11). This activation is impaired in the *roxy6789* HA control. The HA-L-ROXY9 CCLC, SCLC and CSLC active site variants can restore the *NRT2.2* and *NLP3* expression upon N starvation to the same extent. The expression of *NRT2.4* and *AMT1-5* is higher in the CCLC variant, but SCLC and CSLC are also able to rescue the expression suggesting that the CCLC version is more efficient than the other variants. The CPYC active site variant fails to induce *NRT2.2, NRT2.4*, *AMT1-5* and *NLP3* expression. Under N sufficient conditions, the active site variants CCLC, SCLC and CSLC show elevated *NRT2.2, NRT2.4*, *AMT1-5* and *NLP3* levels, most likely due to the artificially high expression of ROXY9 in these conditions. As the expression of these genes is induced in the active site variants in LN conditions, ROXY9 alone is not sufficient to induce the expression and the N starvation is required.

The *TFL1* and *PER71* expression is elevated in the HA control compared to Col-0 in FN and LN conditions, whereby the *TFL1* expression is not significantly different in sufficient N supply. The ROXY9 active site variants CCLC, SCLC and CSLC are able to reduce the expression of *TFL1* and *PER71* expression to the WT-levels. CPYC shows elevated gene expression similar to the HA control.

The expression of *UMAMIT35* is highly elevated in FN conditions in the HA-L-ROXY9 CCLC active site variant and to a lesser extent in the SCLC and CSLC active site variants. The CPYC variant has similar expression levels like the HA control. Upon N starvation, *UMAMIT35* is induced in the WT, but not in the active site variants. This shows that ROXY9 is sufficient to activate *UMAMIT35* though interfering with the repressive mechanism of TGA1, 4. In Col-0, the expression of *UMAMIT35* is regulated by the

amount of ROXY9 present in the roots. Even though the SCLC and CSLC active site variants show elevated gene expression, they are not as efficient as the ROXY9 version with the WT active site variant.

These results show that ROXY9 can compensate the loss of all four ROXYs without ALWL motif. Moreover, the first and second cysteine of the active site motif are not important for the regulation of gene expression upon N starvation, indicating that oxidoreductase activity and Fe-S cluster binding are not involved. Still, the active site motif is to some extent important as the CPYC active site variant is not functional.

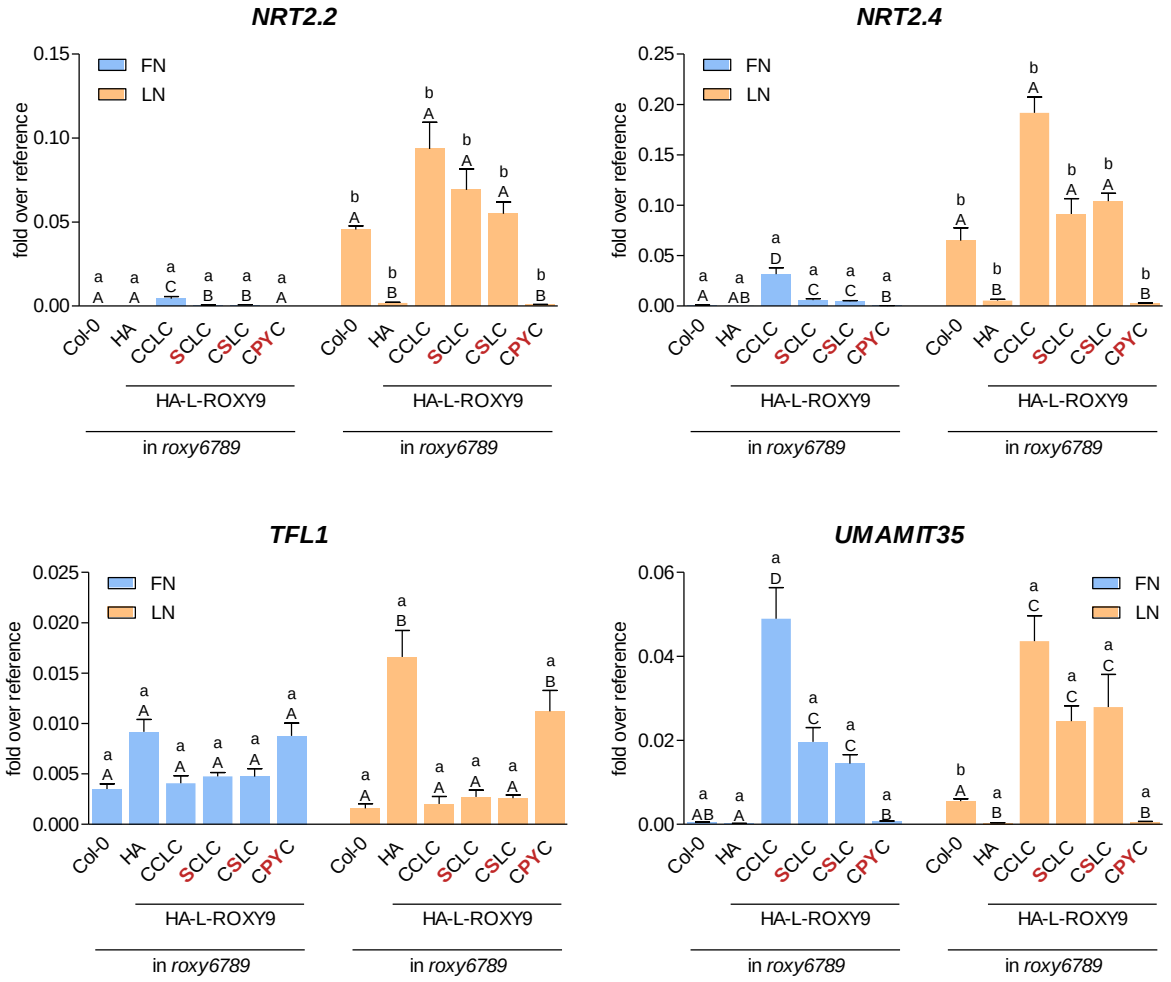

Figure 35: The first and second cysteine of the ROXY9 active site motif are not required for the regulation of *NRT2.2, NRT2.4, TFL1* and *UMAMIT35* expression in *A. thaliana* roots upon nitrogen starvation. 7-day old T2 seedlings grown on full nutrition (FN) plates under constant light conditions (70 µmol photons s^{-1} m^{-2}) were transferred to either FN or low nitrogen (LN) plates. Two days later, roots were collected, RNA was isolated and cDNA synthesized. Expression of *NRT2.2, NRT2.4, TFL1 and UMAMIT35* was analyzed in 5 independent lines per *roxy6789* active site variant by qRT-PCR, *UBQ5* was used as a reference gene. Mean values of four to five biological replicates are shown. Error bars represent the standard error of the mean. Lowercase letters indicate statistically significant differences within the genotype between the treatments, uppercase letters indicate significant differences within treatment between the genotypes. Statistical analyses were performed with the logarithmic values by using two-way ANOVA and Bonferroni's post-test (*p*-value < 0.05).

5.2.3. HA-L-ROXY9 active site variants can complement the biomass and petiole length of *roxy6789*

After obtaining homozygous ROXY9 active site variants in the *roxy6789* background, the biomass and petiole length was determined. Here, we focused on the role of the first cysteine, CYS21, thus active site variants SCLC as well as the WT CCLC motif and the HA control was analyzed. Plants were grown for 4 weeks in a 12/12 h light regime before the fresh weight was measured and the petiole length was determined. Statistical analyses were performed, but are not incorporated in the diagrams for greater clarity. Instead, results of statistical analyses can be found in Supplementary Table S2 and Supplementary Table S3. Additionally, material for protein extraction was collected and a western blot was performed.

The *roxy6789* mutant has reduced biomass compared to Col-0. The HA controls (#4-8, #101-8, #102-8) also have reduced biomass, however, the difference to Col-0 is not statistically significant. The independent CCLC (#2-1, #27-5) and two out of three SCLC active site variants (#9-3, #37-5) have a higher fresh weight than the WT. The third SCLC line, #12-2, as well as one CSLC line (#6-1) have a similar fresh weight as Col-0, but due to the high variation in the fresh weight, there is no significant difference to the HA controls. Only one CSLC line (#15-3) cannot complement the reduced fresh weight of *roxy6789* and has a similar biomass as the HA lines. Western blot analysis reveal that CSLC line #15-3 has reduced HA-L-ROXY9 protein amounts compared to the other lines. This might explain, why no complementation can be observed. However, also CCLC line #2-1 and SCLC line #12-2 have reduced protein levels and are still able to rescue the biomass, whereby CCLC #2-1 has a higher biomass than the SCLC line. This leads to the conclusion that the active site variants SCLC and CSLC are in principle functional like the WT CCLC version, however higher protein amounts might be needed. Still, it shows that for the fresh weight the first and second cysteine of the ROXY9 active site motif is not required.

For the leaf-to-petiole ratio, a similar tendency is detectable. However, the differences between the different genotypes are even weaker than for the fresh weight. The *roxy6789* mutant as well as the HA lines #4-8, #101-8, #102-8 have a reduced leaf-to petiole ratio compared to Col-0. All HA-L-ROXY9 lines except SCLC #12-2 are able to restore the leaf-to petiole, indicating that Cys21 and Cys22 of ROXY9 are not required for the regulation of the petiole length.

Overall, these results show that robust differences greater than 2-fold are required for optimal analysis of the complementation lines. Still, taken together with the previous experiments, no involvement of the first and second cysteine in the function of ROXY9 was detected. Thus, oxidoreductase activity and Fe-S cluster binding are not required for the regulation of the biomass, the petiole length or gene expression.

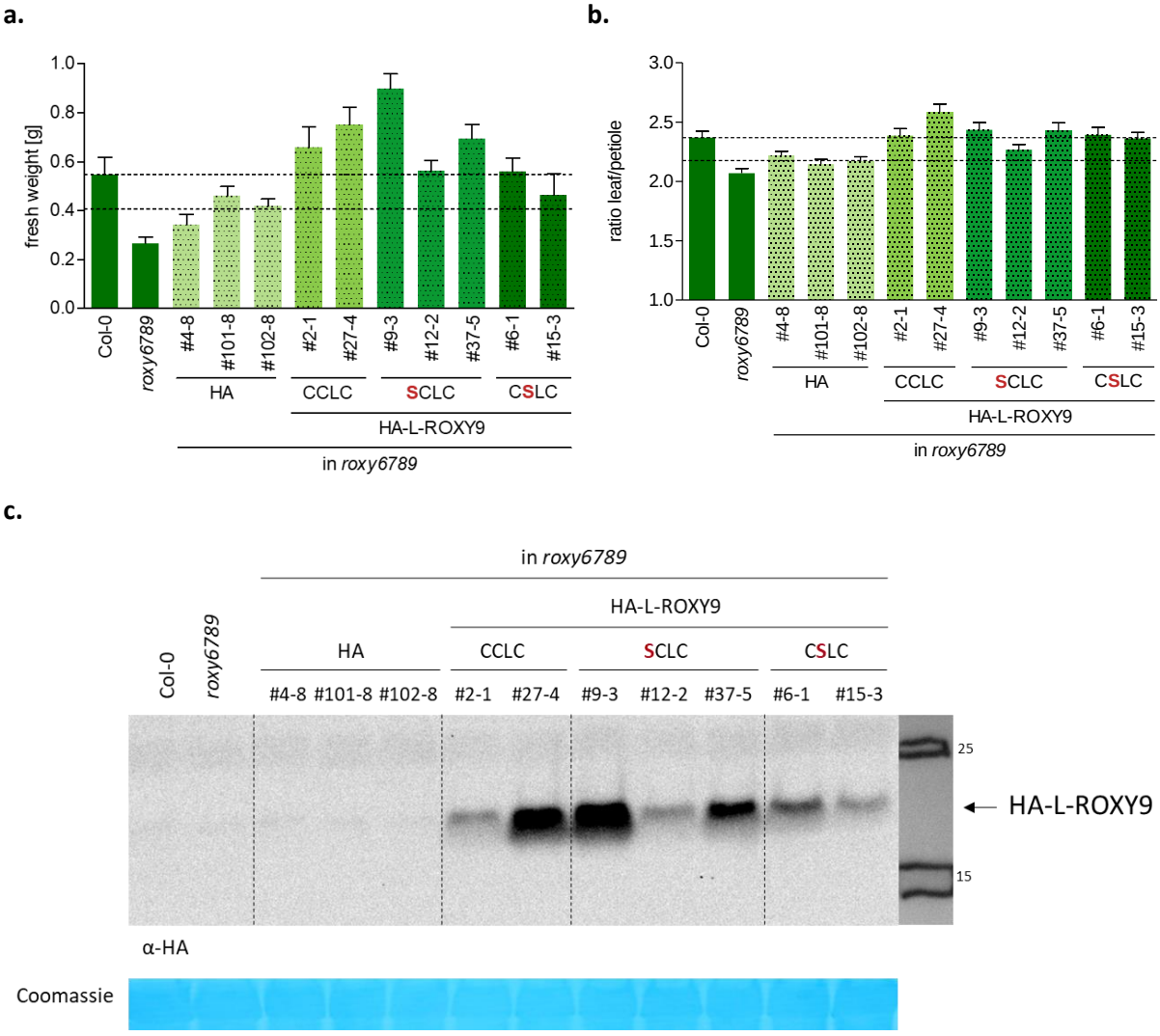

Figure 36: The first and second cysteine of the ROXY9 active site motif are not required for the regulation of fresh weight and the leaf-to-petiole ratio. Stably transformed *roxy6789* with HA-L-ROXY9 active site variants were grown for 4 weeks in 12/12 h light regime. **a.** Fresh weight of the whole rosette was measured. Mean values of 12 biological replicates per line are shown. Error bars represent the standard error of the mean. Dotted line indicates the mean fresh weight of Col-0 and all HA control lines. **b**. Pictures of all leaves of four plants per line were taken. The length of the leaves and petioles was measures with the ImageJ software and the leaf-to-petiole ratio was calculated. Mean values of around 50 leaf-to-petiole ratios are shown, error bars represent the standard error of the mean. Dotted line indicates the mean leaf-to-petiole ratio of Col-0 and all HA control lines. **c.** For the detection of HA-L-ROXY9 in western blot analysis, α-HA was used as primary antibody and α-rabbit linked to peroxidase was used as secondary antibody. *: unspecific

5.3. Identification of new interaction partners of ROXY9

A TurboID approach was chosen to identify new interaction partners of ROXY9. The biotin ligase Turbo is a modified and improved version of BioID isolated from *E. coli* (Branon *et al.,* 2018). In the presence of biotin, molecules within a 10 nm range of Turbo get biotinylated (May *et al.,* 2020). In contrast to a pull down approach, the TurboID method also allows identification of proteins which are only transiently in close proximity to the ligase. The biotinylated proteins can be isolated by using streptavidin-coated beads, which bind to biotin with a high affinity. Known interacting proteins can then detected by western blot analysis by using specific antibodies and new interaction partners can be identified by liquid chromatography coupled with mass spectrometry (LCMS).

For the identification of new interaction partners, ROXY9 was C-terminally fused to HA-tagged Turbo. Additionally, a HA-Turbo control was generated. The coding regions of these constructs under control of the *UBIQUITIN10* (*UBQ10*) promoter were stably transformed into the *roxy6789* mutant by using the flower dipping method. In the T1 generation, the amount of HA-Turbo-ROXY9 and HA-Turbo was determined in western blot analysis and the lines with the highest expression were chosen for the next generation. After selection on basta plates and self-fertilization, homozygous lines were identified. The subsequent experiments were performed with two independent HA-Turbo-ROXY9 lines as well as with two independent HA-Turbo control lines.

5.3.1. Stably expressed HA-Turbo-ROXY9 can complement the growth phenotype and the endogenous *ROXY9* expression

To test the functionality of the HA-Turbo-ROXY9 protein, the biomass and endogenous *ROXY9* expression was analyzed. As expected, HA-Turbo-ROXY9, but not the HA-Turbo control, can restore the fresh weight to WT-like levels (Figure 37). Additionally, HA-Turbo-ROXY9 is able to repress the endogenous *ROXY9* expression. These results indicate that the fusion protein is indeed functional.

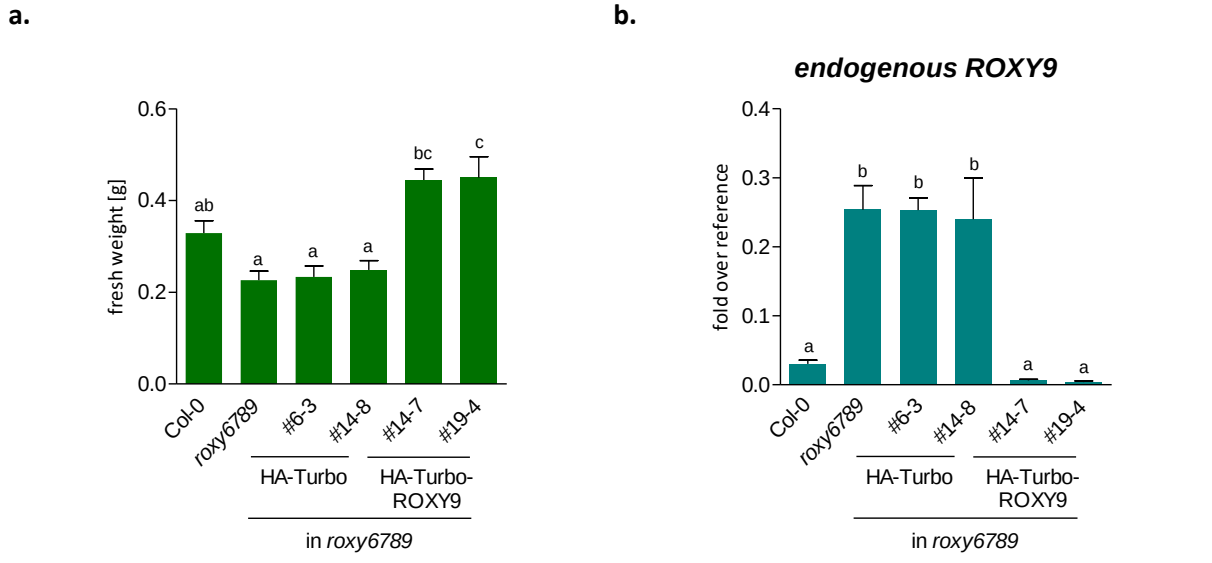

Figure 37: Stably transformed HA-Turbo-ROXY9 can complement the *roxy6789* phenotype. Plants were grown for 4 weeks in 12/12 h light regime **a.** Fresh weight of the rosette was measured. Mean values of 12 biological replicates per line are shown. Error bars represent the standard error of the mean. Letters indicate statistically significant differences between the genotypes. Statistical analysis was performed by one-way ANOVA and Tukey's post-test (p-value < 0.05). **b.** Leaves of 4-week-old *A. thaliana* plants were collected, RNA was isolated and cDNA synthesized. Expression of endogenous *ROXY9* was analyzed by qRT-PCR, *UBQ5* was used as a reference gene. Mean values of three to six biological replicates are shown. Error bars represent the standard error of the mean. Letters indicate statistically significant differences of the from the $\log_2$ values. Statistical analysis was by one-way ANOVA and Tukey's post-test (p-value < 0.05).

5.3.2. HA-Turbo-ROXY9 biotinylates TGA1 in roots

In addition to the capability of complementing the *roxy6789* phenotype, we analyzed whether the Turbo ligase in the construct is able to biotinylate known interaction partners. For this, *A. thaliana* plants were grown for 4 weeks before the roots were cleaned in water and submerged in biotin solution. The proteins of the roots were isolated and excessive biotin was removed by a desalting column. Before the streptavidin pull down, a minor amount was kept as an input reference. In western blot analysis, the input control as well as the eluate of the pull down was analyzed. By using the TGA1 antibody, we were able to detect TGA1 in the pull downs of HA-Turbo-ROXY9 (Figure 38). This shows that TGA1 is biotinylated in roots by HA-Turbo-ROXY9.

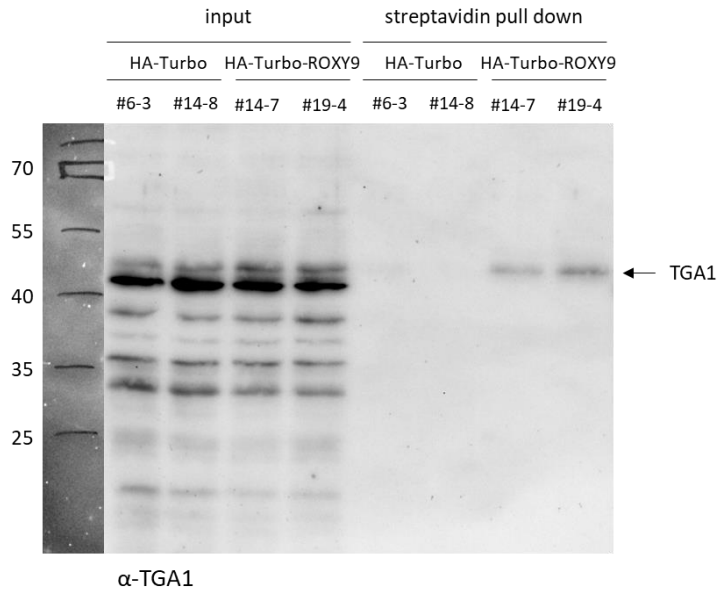

Figure 38: HA-Turbo-ROXY9 biotinylates TGA1 in roots. Roots of 4-week-old *A. thaliana* plants expressing HA-Turbo or HA-Turbo-ROXY9 were submerged in 200 µM biotin solution. After 3 hours, roots of 20 plants per genotype were collected, proteins were extracted, the free biotin was removed by desalting and a streptavidin pull down was performed. Before the pull down, an input control was kept aside. For the detection, α-TGA1 was used as primary antibody and α-rabbit linked to peroxidase was used as secondary antibody.

5.3.3. TOPLESS and TOPLESS-RELATED proteins are biotinylated *in vivo* by HA-Turbo-ROXY9

In order to identify new interaction partners, the biotinylated proteins were digested with trypsin, purified and analyzed by LCMS by the LCMS Protein Analytics Service Unit, University Göttingen. For this, the proteins were. The LCMS data was mapped to the *A. thaliana* proteome, differences between HA-Turbo and HA-Turbo-ROXY9 were identified and plotted in a volcano plot (Figure 39).

Overall, not many proteins were detected (Supplementary Table S1). Still, TOPLESS (TPL, AT1G15750), TOPLESS-RELATED 1 (TPR1, AT1G80490) and TPR2 (AT3G16830) are enriched in the fraction isolated from *roxy6789* expressing HA-Turbo-ROXY9 compared to the lines expressing HA-Turbo (Figure 39), indicating that these proteins are located in close proximity to ROXY9. Surprisingly, TGA1 and ROXY9 itself was not among the enriched fraction. As western blot analysis shows that TGA1 can by biotinylated by HA-Turbo-ROXY9, it is most likely below the detection limit. Moreover, ROXY9 itself might not be accessible for biotinylation. Instead, some unspecifically biotinylated proteins are enriched in the plants expressing the HA-Turbo control. To obtain reliable results, this experiment needs to be repeated with more root material. However, collecting more material might not be realizable. Additionally, the extraction and pull down protocols could be optimized. As this is quite time consuming, it was not feasible within the frame of this thesis.

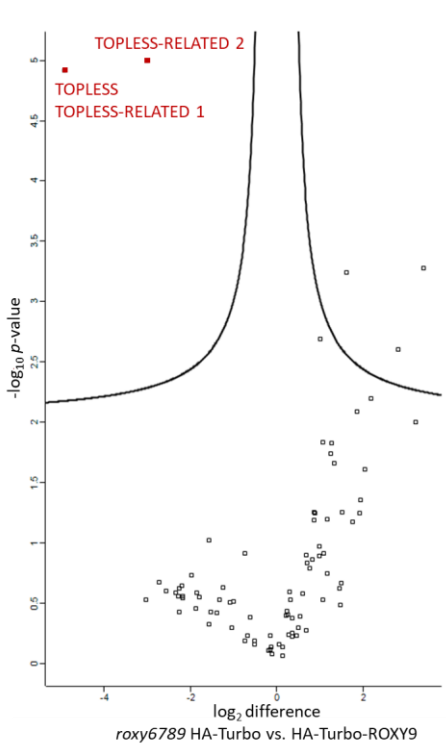

Figure 39: TOPLESS and TOPLESS-RELATED proteins are biotinylated *in vivo* by HA-Turbo-ROXY9. Roots of 4-week-old *A. thaliana* plants expressing HA-Turbo or HA-Turbo-ROXY9 were submerged in 200 µM biotin solution. After 3 hours, roots of 20 plants per genotype were collected, proteins were extracted, the free biotin was removed by desalting and a streptavidin pull down was performed. The proteins were digested with trypsin and purified. Two biological replicates were analyzed twice via LCMS. After mapping the data to the *A. thaliana* proteome, a volcano plot was generated. The upper left corner shows significantly enriched proteins in the HA-Turbo-ROXY9 sample set (FDR < 0.05).

Still, we identified TPL, TPR1 and TPR2 in close proximity to ROXY9. TPL is a transcriptional co-repressor which can interact with ROXY-type GRX via the C-terminal ALWL motif. Lacking the ALWL motif, ROXY9 cannot directly interact with TPL (Uhrig *et al.,* 2017). Other known interactors of TPL include JAZMONATE ZIM DOMAIN (JAZ) 5, 6, 8 (Arabidopsis Interactome Mapping Consortium, 2011; Causier *et al.,* 2012; Moreno *et al.,* 2013) and NOVEL INTERACTOR OF JAZ (NINJA; Pauwels *et al.,* 2010). NINJA itself is also a transcriptional co-repressor and can interact with several JAZ proteins (Pauwels *et al.,* 2010). JAZ, NINJA and TOPLESS are important regulators for JA-mediated responses to wounding or attack by necrotrophic pathogens. Under basal conditions, JAZ, NINJA and TPL repress among others the MYC transcription factors 2, 3 and 4. Upon wounding or in response to combat necrotrophic pathogens, JA-Ile is produced. This leads to the degradation of JAZ resulting in the derepression of MYC and thus the activation of target genes (Glazebrook, 2005). Previous studies in our department showed that ROXY9 can interact with JAZ4, 6, 7, 8, 9, 10 in a yeast-two-hybrid system (Willmer, 2014). Thus, ROXY9, JAZ, NINJA and TPL might form a repressive complex in order to regulate the expression of e.g. *TFL1*, *PER71* and *SWEET11*.

Unfortunately, the *tpl-1* mutant has severe growth defects (Long *et al.,* 2002) and thus could not be analyzed in our experimental setup. Instead, we decided to analyze JAZ and NINJA mutants. The *A. thaliana* genome encodes for 13 JAZ, a knock-out of all JAZ proteins is most likely lethal. However, the *jaz decuple* (*jazD*) mutant, lacking JAZ1-7, 9, 10, and 13, shows a normal growth phenotype (Guo *et al.,* 2018). The *ninja-1* mutant was identified in a β-glucuronidase (GUS) reporter assay and still contains the *JAZ10:GUS* construct (Acosta *et al.,* 2013). By comparing the mutant to the respective WT, we were nevertheless able to investigate the influence of NINJA on ROXY9 target gene expression. As part of her bachelor thesis, Hannah Knerich performed the experiments with these mutants. In

addition, the *myc2-2 myc3 myc4* (*myc234*) mutant was analyzed, as the MYC binding site CACGTG was enriched in our transcriptome data in the subset of 212 genes repressed by ROXY6, 7, 8, 9.

5.3.4. JAZ1-7, 9, 10, 13 and NINJA regulate the expression of *TFL1, PER71* and *PER10*

First, the expression of TGA1, 4 activated and ROXY6, 7, 8, 9 repressed *TFL1* and *PER71* was analyzed. In the *jazD* and *ninja-1* mutants, the expression of *TFL1* and *PER71* is reduced compared to Col-0 under N sufficient and N starvation conditions (Figure 40, Supplementary Figure S12). In contrast to our expectation, JAZ1-7, 9, 10, 13 and NINJA activate *TFL1* and *PER71*, thus they do not form a repressive complex with ROXY6, 7, 8, 9. Instead, they might interfere with the repressive mechanism of ROXY9. The *myc234* mutant only shows slightly reduced *PER71* levels in FN conditions compared to the WT. No difference was detected between in LN conditions. Also the *TFL1* expression is comparable between Col-0 and *myc234*, suggesting that *PER71* and *TFL1* expression is independent of MYC2, 3, 4.

Both the *jazD* and *ninja-1* mutant show elevated *PER10* expression. This suggests that JAZ1-7, 9, 10, 13 and NINJA repress ROXY6, 7, 8, 9. Without JAZ and NINJA, *PER10* is activated by ROXY6, 7, 8, 9 though interfering with the repressive mechanism of TGA1, 4. This regulation is independent of MYC2, 3, 4, as the *PER10* expression in the *myc234* mutant is WT-like.

In addition, the expression of *UMAMIT35* and *NRT2.2* was analyzed. There is no difference in the between the WT and *jazD*, *ninja-1* or *myc234*, thus *UMAMIT35* and *NRT2.2* are not regulated by JAZ1-7, 9, 10, 13, NINJA or MYC2, 3, 4.

These results show that even though the MYC binding site was enriched in the transcriptome analysis, MYC2, 3, 4 are not involved in the regulation of ROXY target gene expression. However, JAZ and NINJA might be required to incorporate JA signaling.

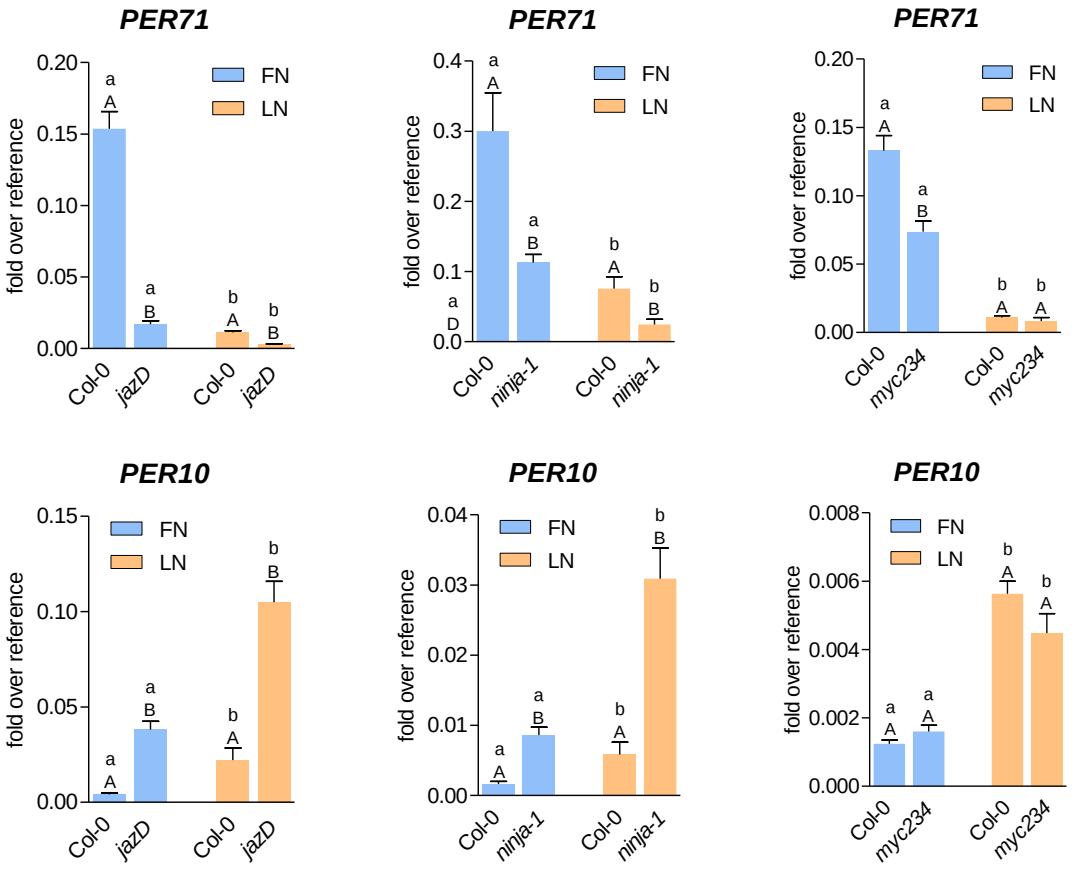

Figure 40: JAZ1-7, 9, 10, 13 and NINJA regulate the expression of *PER71* and *PER10* in *A. thaliana* roots. 7-day old seedlings grown on full nutrition (FN) plates under constant light conditions (70 µmol photons s^{-1} m^{-2}) were transferred to either FN or low nitrogen (LN) plates. Two days later, roots were collected, RNA was isolated and cDNA synthesized. Expression of *PER71* and *PER10* was analyzed by qRT-PCR, *UBQ5* was used as a reference gene. Mean values of four to five biological replicates are shown. Error bars represent the standard error of the mean. Lowercase letters indicate statistically significant differences within the genotype between the treatments, uppercase letters indicate significant differences within treatment between the genotypes. Statistical analyses were performed with the logarithmic values by using two-way ANOVA and Bonferroni's post-test (*p*-value < 0.05). Three independent experiments were performed with similar results.

6. Results Part III – Distinct roles of clade I and II TGA factors in the establishment of SAR

TGA1, 4 are not only involved in the regulation of genes under N starvation conditions, but they are also involved in the activation of genes related to the immune response systemic acquired resistance (SAR; Sun *et al.,* 2018). SAR is largely dependent on salicylic acid (SA), which is synthesized from isochorismate by ISOCHORISMATE SYNTHASE 1 (ICS1; Wildermuth *et al.,* 2001) and AVRPPHB SUSCEPTIBLE 3 (PBS3; Rekhter *et al.,* 2019; Torrens-Spence *et al.,* 2019). Both genes are induced in SAR leaves upon the arrival of the mobile signal N-hydroxy pipecolic acid (NHP). Induction of SA and NHP synthesis genes in systemic leaves occurs at basal SA levels and can be observed in the absence of pathogen-induced SA as in the *salicylic acid induction 2-2* (*sid2*) mutant. This induction requires the SA receptor NPR1, and transcription factors TGA1, 4 and TGA2, 5, 6 (Nair *et al.,* 2021). Interestingly, most of the *in vitro* TGACG binding activity of leaf extracts consists of TGA2, 5, 6, which is easily detectable by Western blot analysis (Cheng *et al.,* 2009). In contrast, TGA1, 4 levels seem to be much lower and restricted to the vascular tissue (Wang *et al.,* 2019). No heterodimers are observed between different clades of TGAs (Niggeweg *et al.,* 2000). Therefore, the question arose, why the above mentioned genes require both clades of TGAs and whether some upstream regulatory factors might be regulated by only e.g. clade I TGA factors. This factor might then act in concert with clade II TGA factors at further target genes. To identify genes that are differentially regulated by the two classes of TGA factors at resting SA levels, we performed transcriptome analysis in *Psm*-infected SAR leaves using *sid2*, *sid2 tga1 tga4* (*sid2 tga14*) and *sid2 tga2 tga5 tga6* (*sid2 tga256*) mutant plants.

6.1. Transcriptome analysis

For the transcriptome analysis, lower leaves of *sid2*, *sid2 tga14* and *sid2 tga256* were infiltrated with *Psm*. As control, some *sid2* plants were left untreated. After 48 h, the upper SAR leaves were infiltrated with *Psm* as well. Untreated *sid2* plants were left untreated again. After 48 h, *Psm*-treated SAR leaves (*Psm*/*Psm*) of all genotypes and of the untreated *sid2* leaves (untr/untr) were collected and RNA was extracted. Four experiments were performed in which five RNA replicates per genotype and treatment were pooled as one sample. The RNA sequencing was performed by the Next Genome Sequencing Integrative Genomics Core Unit (NIG), University Göttingen.

Principal Component Analysis (PCA) revealed that one *sid2* untr/untr replicate does not cluster with the other replicates (Supplementary Figure S13), thus it was excluded in all subsequent analysis. Anew PCA without this replicate shows that samples from the same genotype and treatment cluster together (Figure 41). The data points of *sid2* untr/untr and *Psm*/*Psm* show a clear separation, indicating that transcriptional changes occur upon *Psm*/*Psm* treatment. The *sid2 tga256 Psm*/*Psm* data points cluster between *sid2* untr/untr and *Psm*/*Psm*, suggesting that TGA2, 5, 6 are responsible for some of the transcriptional changes in *Psm*-infected SAR leaves. The data points of *sid2 tga14 Psm*/*Psm* lie in the same principal components 1 (PC1) range as *sid2 tga256 Psm*/*Psm*, but vary in PC2. This could mean that TGA1, 4 have similar as well as distinct roles compared to TGA2, 5, 6.

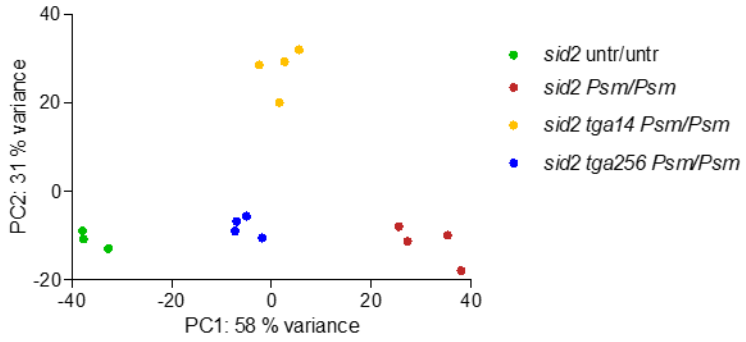

Figure 41: Principal component analysis (PCA) of transcriptome data. Lower leaves of 4.5-week-old *A. thaliana* plants were infiltrated with *Psm* or left untreated. After 48 h, upper leaves were infiltrated with *Psm* or left untreated. The upper leaves were collected after 8 hours, RNA was isolated. Per treatment, RNA of five plants was pooled and sent for RNA sequencing. PCA were performed with the obtained transcriptome data.

6.1.1. Most SAR-induced genes are regulated by clade I or clade II TGA factors

The transcriptome analysis led to the identification of 4184 genes (logarithmic fold change to the base 2 ($\log_2$ FC) > 1, adjusted *p*-value (*p*.adj) < 0.05, Dataset 2) that were induced in *Psm*-infected SAR leaves of *sid2* plants. MarVis cluster analysis was performed to visualize the expression of these *Psm*-induced genes as function of TGA1, 4 and/or TGA2, 5, 6. This software clusters genes with similar expression patterns together and uses color codes for the relative expression levels. High relative expression is depicted in red whereas low expression levels are blue.

Genes which are activated by TGAs 1, 4 and TGA2, 5, 6 are assorted to cluster 7, 8, 9 and 10 (Figure 42). Especially the 531 genes of cluster 10 are highly induced and stringently depend on both clades of TGAs. It includes known TGA-dependent genes like *FMO1*, *DLO1*, *PBS3* (*AT5G13320*), *PR1* (*AT2G14610*) and *ORA59 (AT1G06160)* (Zhang *et al.,* 2003; Lindermayr *et al.,* 2010; Zander *et al.,* 2014; Nair *et al.,* 2021; Budimir *et al.,* 2021).

251 genes in cluster 6 are activated by TGA1, 4 but not regulated by TGA2, 5, 6. This cluster contains *SARD1* (*SAR DEFICIENT 1*, *AT1G73805*), which is a key transcription factor regulating SAR genes (Zhang *et al.,* 2010). This finding might already explain why so many genes are regulated in a TGA1, 4-dependent manner. SARD1 in turn might regulate downstream genes in combination with clade II TGAs at TGACG-containing promoters.

The large cluster 5 contains 798 genes that are not as highly induced compared to those of clusters 7 to 10. Still, the influence of both TGA clades is visible, but might not be statistically significant. Cluster 4 contains genes that require only clade II TGAs for activation. Genes in clusters 1 to 3 are repressed by clade I TGAs but not influenced by TGA2, 5, 6. These clusters include genes of the detoxification pathway like *CYP81D11* (*AT3G28740*) and *NAC032* (*AT1G77450*) that are expressed in a clade II-dependent manner when stimuli like toxic chemicals are applied (Fode *et al.,* 2008; Köster *et al.,* 2012).

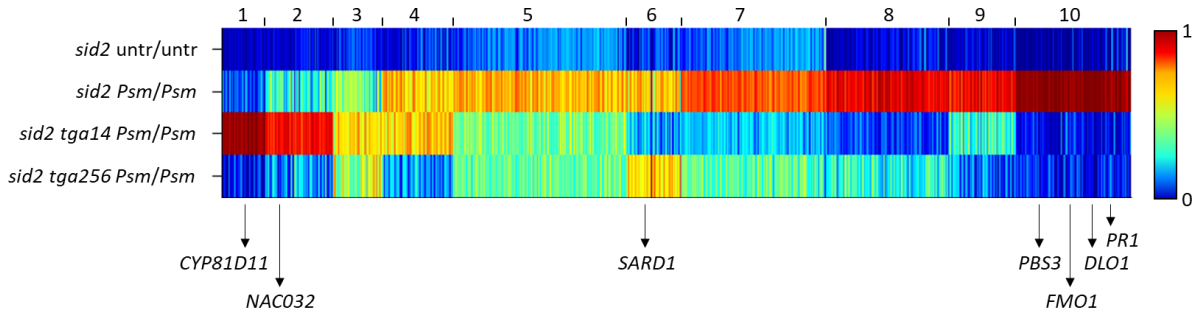

Figure 42: MarVis clustering analysis of 4184 SAR-induced genes according to transcriptome data. Lower leaves of 4.5-week-old *A. thaliana* plants were infiltrated with *Psm* or left untreated. After 48 h, upper leaves were infiltrated with *Psm* or left untreated. The upper leaves were collected after 8 hours and RNA was isolated. Per treatment, RNA of 5 plants was pooled and sent for RNA sequencing. The results were mapped against the *A. thaliana* genome and quantified. Low relative expression is depicted in blue, high relative expression in red. Prominent genes that have already been described as being regulated by TGAs are indicated.

In addition, Venn diagrams were generated to determine genes that are differentially expressed in the three genotypes. In contrast to the MarVis clustering, Venn diagrams take statistical significant differences into account, but miss the degree of regulation as it defines differentially expressed genes because of a given threshold. This is beneficial to identify robustly regulated genes. 1965 genes were lower expressed in *sid2 tga14 Psm*/*Psm* compared to *sid2 Psm*/*Psm* and 2409 were lower expressed in *sid2 tga256 Psm*/*Psm* ($\log_2$ FC > 1, *p*.adj < 0.05). Of the 4184 SAR-induced genes, 676 genes are activated by either clade I and 598 genes are activated by clade II TGAs in the *sid2* background. 1191 genes are regulated by both clades (Figure 43a). 1719 genes are induced in *Psm*-infected SAR leaves but not significantly activated by TGA1, 4 or TGA2, 5, 6. 740 of these genes are assorted to cluster 5, indicating that they are weakly activated by the TGAs, but miss the threshold for robustly regulated genes.

In addition, genes which are repressed were analyzed. TGA2, 5, 6 repress 2038 genes whereas TGA1, 4 repress 3204 genes ($\log_2$ FC > 1, *p*.adj < 0.05). Only a minority of these genes are induced in *sid2 Psm*/Psm, namely 18 for TGA2, 5, 6; 353 for TGA1, 4 and 37 are repressed by TGA1, 4 and TGA2, 5, 6 (Figure 43b). 338 out of the 353 TGA1, 4-repressed and SAR-induced genes are assorted to clusters 1 and 2 in the MarVis analysis. Clusters 1 and 2 contain additional 175 genes, but these genes are enriched to a lesser extent than $\log_2$ FC > 1. To identify in which biological processes the 353 genes are involved, GO term enrichment analysis was performed. Compared to the genome, the subset is enriched in nitrogen- and JA-responsive genes (Supplementary Figure S14).

Next, genes which are activated by one clade and repressed by the other one were determined. Only 14 genes are activated by TGA1, 4 and repressed by TGA2, 5, 6, two of these genes are additionally induced after *Psm*/*Psm* treatment ($\log_2$ FC > 1, *p*.adj < 0.05, Supplementary Figure S15a). TGA2, 5, 6 activated 130 genes, which are repressed by TGA1, 4. Out of these genes, 102 are also SAR-induced ($\log_2$ FC > 1, *p*.adj < 0.05, Supplementary Figure S15b). This shows that most of the genes are not reciprocally regulated by clade I and II TGAs.

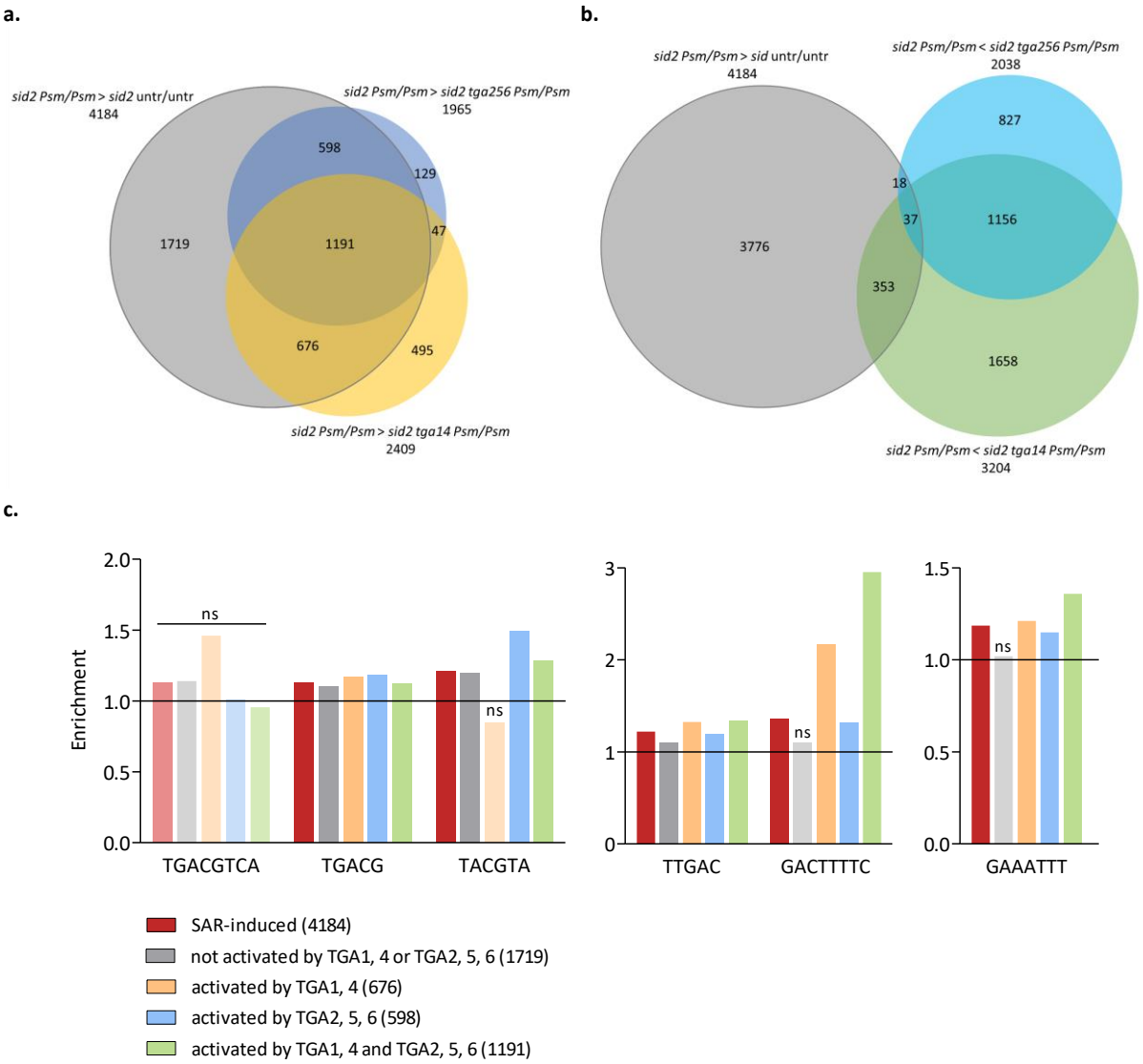

Figure 43: Schematic representation of transcriptome data. Lower leaves of 4.5-week-old *A. thaliana* plants were infiltrated with *Psm* or left untreated. After 48 h, upper leaves were infiltrated with *Psm* or left untreated. The upper leaves were collected after 8 hours and RNA was isolated. Per treatment, RNA of 5 plants was pooled and sent for RNA sequencing. The results were mapped against the *A. thaliana* genome and quantified. **a.-b.** Venn diagrams were generated to analyze the SAR-inducible genes in the *sid2* mutant and genes, which are differentially expressed in the *sid2 tga1 tga4* or *sid2 tga2 tga5 tga6* mutant compared to *sid2* (log_2 fold change (FC) > 1, adjusted p-value (*p*.adj) < 0.05). **c.** Motif mapper analysis was performed with the 4184 SAR-inducible genes (log_2 FC > 1, *p*.adj < 0.05) according to transcriptome data. TGACGTCA, TGACG and TACTGA are TGA factor binding sites, TTGAC is a WRKY transcription factor binding site, GACTTTTC is specific for WRKY50 and GAAATTT is a SARD1 binding site. Enrichments were calculated compared to a set of randomly chosen promoters from the whole *A. thaliana* genome (*p*-value < 0.05), which is normalized to 1 and indicated by the line. ns: not significant.

In addition, motif enrichment analysis was performed with the Motif Mapper software. This method allows the identification of enriched transcription factor binding sites in the promoter region of a data set compared to the genome. The TGACGTCA palindrome is enriched in the 676 SAR-inducible TGA1, 4-activated genes (Figure 43d). Due to the low number of TGACGTCA motifs, the difference is not significant (Supplementary Table S4), but it still suggests that TGA1, 4 preferably targets promoters containing the palindrome. This was also shown before by Budimir *et al.,* 2021, as the TGACGTCA motif is specifically enriched in promoter regions of SA-induced TGA1, 4-regulated genes. The TGA-factor binding sites TGACG and TACGTA were enriched in the promoter regions of the 4184 SAR-inducible genes (*p*-value < 0.05, Figure 43d). Also within the subset of 1719 genes, which are not activated by TGA1, 4 or TGA2, 5, 6, the TGACG motif is enriched to the same extent as in the subset of genes, which

are activated by TGA1, 4 or TGA2, 5, 6. This indicates that also these genes can be regulated by the TGAs. Either the regulation is by TGA1, 4 or TGA2, 5, 6 is too weak so that the there is no statistical significant difference, the regulation by TGA1, 4 or TGA2, 5, 6 does not occur in these conditions or other TGA factors of clade III to V are involved. Besides the TGA binding sites, the WRKY transcription factor binding site TTGAC (Rushton *et al.,* 1996; Maleck *et al.,* 2000) was significantly enriched within the promoter regions of SAR induced genes. The difference in the enrichment does not vary much between the different tested subsets of genes. However, the WRKY50 binding motif GACTTTTC is over 2-fold enriched within the promoter regions of the 676 TGA1, 4-activated genes and the 1191 genes activated by clade I and II TGAs. This suggests that WRKY50 and TGA1, 4 might regulate the expression of some genes together. The SARD1 binding site GAAATTT (Wang *et al.,* 2011) is enriched in the promoter regions of the 4184 SAR-induced genes as well as in the subset of genes, which are activated by either or both TGA clades. This indicates that many TGA activated genes are also regulated by SARD1. This is consistent with the previous findings that *SARD1* expression is regulated by clade I TGAs with the speculation that *SARD1* might also regulate genes together with clade II TGAs.

6.2. Identification of differentially regulated transcription factor encoding genes by clade I and II TGAs in *Psm*-infected SAR leaves

Within the 676 SAR-inducible TGA1, 4-activated genes, we identified 15 genes encoding for transcription factors (Table 30). Most of them are highly upregulated in *Psm*/*Psm* conditions and strictly regulated by clade I TGAs. Apart from two genes, all contain at least one TGACG motif in their promoter region, suggesting that TGA1, 4 can directly activate the expression of these transcriptional regulators. Among them is SARD1, an important regulator of SAR (Zhang *et al.,* 2010), which is known to be activated by TGA1, 4 (Sun *et al.,* 2018).

Besides, seven WRKY transcription are activated upon *Psm*/*Psm* treatment in the *sid* mutant and TGA1, 4-induced. Many *WRKYs* are expressed in response to pathogen and are involved in the regulation of pathogen defense responses (Eulgem & Somssich, 2007). The most strictly TGA1, 4-regulated is WRKY51 (AT5G64810), which promotes resistance against *Pst* (Gao *et al.,* 2011).

Table 30: Transcription factors regulated by TGA1, 4 in *Psm*-infected SAR according to transcriptome data. The logarithmic fold change to base 2 (log_2) was calculated by DESeq2 Galaxy Tool. Number of TGACG motifs was counted in the region 2 kb upstream of the transcription start site. Analyzed genes in this study by qRT-PCR are highlighted in grey. TPM: transcript per million. *: one of the motifs is a TGACGTCA palindrome

	TPM ***sid2*** untr/untr	**TPM** ***sid2*** *Psm/Psm*	**TPM** ***sid2 tga14*** *Psm/Psm*	**TPM** ***sid2 tga256*** *Psm/Psm*	**log_2FC** ***sid2 tga14* vs. *sid2 tga256***	**TGACG motifs**
WRKY51	4.83	87.80	8.53	98.89	-3.37	2*
MYB90	0.02	0.62	0.01	0.20	-2.35	2
NAC036	46.16	108.52	21.14	98.71	-2.13	×
SARD1	36.63	203.68	50.76	231.61	-2.09	2*
WRKY46	11.12	234.83	38.66	173.66	-2.05	3
TGA4	5.11	12.40	2.47	10.38	-1.99	7*
WRKY70	246.96	563.84	135.13	568.18	-1.97	2
WRKY63	0.06	7.13	1.13	3.91	-1.66	5
WRKY71	0.05	1.42	0.38	1.24	-1.61	2
GATA5	23.55	57.75	12.04	36.85	-1.55	2
NAC090	3.36	18.44	3.16	9.53	-1.50	2
TGA1	4.10	18.10	3.22	9.21	-1.42	2
WRKY60	4.83	72.43	26.51	65.36	-1.23	1
WRKY53	8.09	141.72	40.56	88.57	-1.06	×
HSFA8	41.75	109.58	31.61	68.49	-1.05	3

26 genes encoding for transcription factors were identified as being mainly regulated by TGA2, 5, 6 but to a lesser extent by TGA1, 4 after *Psm*/*Psm* treatment. All of these genes are highly induced upon *Psm*/*Psm* in *sid2* (Table 31). These genes are found in cluster 4, which already shows that the genes are not as stringently regulated by TGA2, 5, 6 as compared to cluster 10.

Within this subset, there are ten NAC transcription factors, three ETHYLENE-RESPONSIVE FACTORs (ERFs) and three MYB transcription factors. Several NAC factors negatively regulate defense responses to *P. syringae* infection and promote the activation of the JA-pathway (Bu *et al.,* 2008; Zheng *et al.,*

2012; Yuan *et al.,* 2019). Many ERFs are induced upon JA or ET treatment and activate defense responses against necrotrophic pathogens (Büttner & Singh, 1997; Lorenzo *et al.,* 2004; Oñate-Sánchez *et al.,* 2007; Pré *et al.,* 2008; Meng *et al.,* 2013) while members of the MYB family mediate responses against wounding and confer resistance against herbivory (Cheong *et al.,* 2002; Johnson & Dowd, 2004; de Vos *et al.,* 2006). Thus, it is unlikely that these transcription factors promote resistance to the plant in SAR conditions.

Table 31: Transcription factors are only regulated by TGA2, 5, 6 in *Psm*-infected SAR according to transcriptome data. The logarithmic fold change to base 2 (log_2) was calculated by DESeq2 Galaxy Tool. Number of TGACG motifs was counted in the region 2 kb upstream of the transcription start site. TPM: transcript per million.

	TPM ***sid2*** untr/untr	**TPM** ***sid2*** *Psm/Psm*	**TPM** ***sid2 tga14*** *Psm/Psm*	**TPM** ***sid2 tga256*** *Psm/Psm*	**log_2FC** ***tga14* vs.** ***tga256***	**TGACG motifs**
TGA5	6.72	24.09	12.11	0.04	7.31	1
NAC059	0.43	1.49	5.45	0.22	4.24	1
NAC032	3.74	41.30	71.07	4.43	3.98	3
ERF020	0.04	7.45	11.51	0.68	3.92	2
ERF12	0.14	0.62	2.70	0.18	3.70	7
MYB108	0.10	2.21	4.97	0.41	3.53	3
NAC002	6.35	48.21	105.37	9.22	3.50	×
WRKY61	0.00	0.93	0.63	0.06	3.10	×
NAC055	0.04	21.31	14.24	1.69	3.02	3
ERF113	0.19	40.03	71.32	10.19	2.80	3
NAC092	0.73	37.67	19.24	2.75	2.62	1
NAC047	0.21	42.58	23.15	4.38	2.36	2
BHLH167	0.77	219.10	177.21	35.63	2.34	×
MYB14	0.02	3.52	3.05	0.64	2.21	2
TGA10	0.01	0.21	0.18	0.03	2.11	1
NAC003	1.19	31.16	18.70	4.36	2.10	2
NAC087	0.26	6.37	5.39	1.27	2.06	2
NAC025	0.00	0.47	0.22	0.03	1.95	1
MYB13	0.75	7.94	4.95	1.27	1.93	4
GT-3A	0.00	6.61	7.22	1.94	1.92	3
NAC075	0.63	2.50	2.61	0.81	1.71	2
WRKY28	0.88	66.36	85.15	28.03	1.64	2
BHLH117	0.47	1.80	2.05	0.74	1.48	3
BHLH51	0.40	4.96	6.20	2.39	1.41	3
TGA9	0.02	0.17	0.12	0.04	1.26	×
WRKY26	2.01	13.23	12.65	6.19	1.07	1

The expression of a large number of transcription factors is activated by both TGA1, 4 and TGA2, 5, 6 in *Psm*/*Psm* conditions (Table 32). However, only few genes are highly induced upon SAR conditions and robustly regulated by both TGA clades, like *WRKY75* (*AT5G13080*) and *WRKY31* (*AT4G22070*). WRKY75 promotes SA synthesis by activating the expression of *ICS1* (Guo *et al.,* 2017). The role of WRKY31 has not been analyzed so far. Besides, *ORA59* is activated by TGA1, 4 and TGA2, 5, 6 in *Psm*-infected SAR leaves. ORA59 is the major transcription factor in JA/ET signaling (Pré *et al.,* 2008)

Table 32: Transcription factors regulated by TGA1, 4 and TGA2, 5, 6 in *Psm*-infected SAR according to transcriptome data. The logarithmic fold change to base 2 (log_2) was calculated by DESeq2 Galaxy Tool. Number of TGACG motifs was counted in the region 2 kb upstream of the transcription start site. TPM: transcript per million.

	TPM *sid2* untr/untr	**TPM *sid2*** *Psm/Psm*	**TPM *sid2 tga14*** *Psm/Psm*	**TPM *sid2 tga256*** *Psm/Psm*	**log_2FC *sid2* vs. *sid2 tga14***	**log_2FC *sid2* vs. *sid2 tga256***	**TGACG motifs**
NAC061	1.74	77.41	0.96	4.35	5.88	3.91	1
ERF14	0.00	4.07	0.12	0.56	4.53	2.66	1
WRKY55	0.75	93.30	4.36	17.55	4.22	2.34	×
ERF096	0.00	14.97	0.63	0.43	4.21	4.61	1
JUB1	1.24	85.51	3.93	3.61	4.14	4.29	×
MYB122	0.04	23.49	1.25	0.97	4.13	4.51	×
WRKY75	0.69	237.29	15.90	9.52	3.75	4.50	6
NAC085	0.10	0.50	0.02	0.10	3.69	2.23	1
MYB86	0.09	2.58	0.17	0.15	3.62	3.82	2
ERF1B	0.72	26.82	2.06	7.77	3.61	1.78	1
WRKY72	0.05	2.60	0.25	0.73	3.34	1.83	6
TAF14	0.89	9.60	0.97	3.38	3.23	1.50	3
WRKY41	0.07	7.63	0.87	1.88	3.03	2.01	2
ERF2	19.30	95.59	11.15	46.56	2.97	1.03	1*
MYB51	13.28	177.38	21.90	63.28	2.93	1.49	×
ORA59	0.69	5.11	0.62	0.98	2.89	2.33	2
HSFB1	12.56	593.06	80.15	136.22	2.80	2.11	2
WRKY31	0.01	19.24	2.77	1.85	2.68	3.26	2
NAC016	0.79	12.14	1.92	4.99	2.59	1.30	×
NAC104	1.02	4.75	0.84	1.30	2.41	1.87	2
HSFB3	0.08	2.79	0.51	1.10	2.35	1.36	1
WRKY33	35.93	508.25	97.64	193.83	2.34	1.41	4
WRKY40	3.11	259.14	54.31	108.92	2.21	1.27	4
OFP18	1.20	3.27	0.73	1.58	2.08	1.06	3
WRKY30	1.23	190.74	43.70	73.14	2.08	1.39	2
NAC053	8.86	76.55	18.22	30.64	2.03	1.35	3
BZIP60	50.49	482.16	119.89	230.69	1.97	1.08	3
BHLH92	0.05	6.24	1.49	0.42	1.95	3.66	4
WRKY8	1.74	108.75	29.67	26.07	1.83	2.07	2
AT2G01818	0.63	3.86	1.05	1.84	1.76	1.08	1
AT3G12910	0.09	8.56	2.55	3.96	1.72	1.14	3

	TPM *sid2* untr/untr	**TPM *sid2*** *Psm/Psm*	**TPM *sid2 tga14*** *Psm/Psm*	**TPM *sid2 tga256*** *Psm/Psm*	**log_2FC *sid2* vs. *sid2 tga14***	**log_2FC *sid2* vs. *sid2 tga256***	**TGACG motifs**
HSFB2A	2.45	36.04	11.24	11.75	1.64	1.62	2
OFP17	0.66	10.79	3.48	2.24	1.58	2.25	×
NAC081	42.55	423.62	142.41	158.38	1.54	1.44	5*
MYB109	2.23	15.96	5.40	6.24	1.54	1.37	4
WRKY45	0.53	41.53	14.19	4.22	1.50	3.26	×
NAC048	0.26	2.93	1.01	0.85	1.49	1.77	3
NAC029	1.85	52.44	17.95	13.07	1.45	1.96	1
OFP2	0.55	7.27	2.56	0.76	1.45	3.19	2
BHLH168	0.03	14.04	4.90	0.99	1.42	3.68	×
MYB85	0.12	1.07	0.37	0.41	1.40	1.33	×
WRKY36	0.24	2.06	0.76	0.53	1.38	1.94	1
WRKY6	5.22	154.86	60.04	34.87	1.34	2.16	2
NAC046	1.85	15.86	7.48	6.71	1.05	1.26	2
MYB7	1.73	18.49	8.65	9.15	1.05	1.04	×
HHO3	38.01	139.94	66.45	68.74	1.05	1.05	3

6.2.1. Clade I TGAs activate *WRKY51* expression in *Psm*-infected SAR leaves

Next, we focused on WRKY51 and its closest paralogue WRKY50 (AT5G26170). The expression of *WRKY51* is highly induced in *Psm*-infected SAR leaves and activated by TGA1, 4 but not by TGA2, 5, 6 (Table 30). The binding motif of WRKY50, GACTTTTC, is over 2-fold enriched within the promoter regions of the 676 TGA1, 4-activated genes and the 1191 genes activated by clade I and II TGAs. Since WRKY50 has been described to promote the binding of clade II TGAs to their target sites (Hussain *et al.,* 2018), it is – apart from or in addition to SARD1 – a good candidate that might contribute to the expression of the large group of genes that are regulated by both clades of TGAs. The promoter region of *WRKY51* contains two TGACG motifs, one of them being a TGACGTCA palindrome, suggesting a direct regulation by TGA1, 4. As many promoter regions of SAR-induced genes contain TTGAC WRKY binding sites, it is likely that WRKY transcription factors are involved in their activation. Previous studies revealed that the *wrky51* mutant is more susceptible to *Psm* DC3000 infection (Gao *et al.,* 2011).

To analyze whether *WRKY51* might be involved in the establishment of SAR in the *sid2* background, qRT-PCR analyses were performed. In contrast to the transcriptome data, the *Psm*/*Psm*-treated plants were compared to mock/*Psm* treated plants. In *sid2* plants, *WRKY51* expression is higher induced upon *Psm*/*Psm* treatment compared to mock/*Psm* treatment (Figure 44). The observed hyperinduction in *Psm*/*Psm*-treated plants compared to mock/*Psm*-treated plants is due to the priming effect in SAR leaves. This induction is also detected in the *sid2 tga256* mutant, indicating that TGA2, 5, 6 are not required for the expression of *WRKY51*. In the *sid2 tga14* mutant, *WRKY51* expression is completely abolished after mock/*Psm* and *Psm*/*Psm* treatment. Thus, TGA1, 4 activate *WRKY51* in *Psm*-infected SAR leaves in the *sid2* background.

Since WRKY50 missed the thresholds in the transcriptome analysis, we analyzed its expression in the *sid2*, *sid2 tga14* and *sid2 tga256* mutants after *Psm*/*Psm* treatment as well. Similar to the *WRKY51* expression, *WRKY50* is hyperinduced in *Psm*-infected SAR leaves compared to mock/*Psm* treatment in the *sid2* mutant and to a lesser extent in the *sid2 tga256* mutant, but not in the *sid2 tga14* mutant. This suggests that WRKY50 might have a similar function as WRKY51.

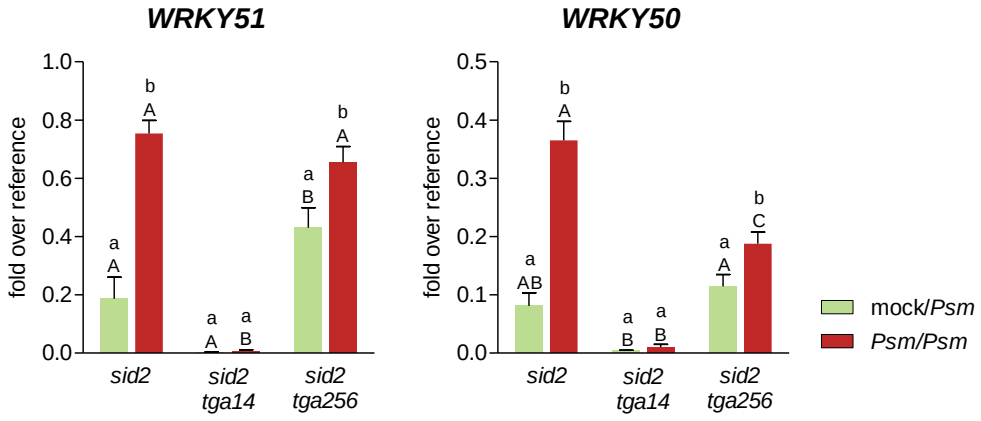

Figure 44: *WRKY51* and *WRKY50* expression is activated by TGA1, 4 in *Psm*-infected SAR leaves. Lower leaves of 4.5-week-old *A. thaliana* plants were infiltrated with $MgCl_2$ (green, mock treatment) or infiltrated with *Psm* (red, OD_{600} = 0.005). After 48 h, upper leaves were infiltrated with *Psm*. The upper leaves were collected after 8 hours, RNA was isolated and cDNA synthesized. Expression of *WRKY51* and *WRKY50* was analyzed by qRT-PCR, *UBQ5* was used as a reference. Mean values of four to six biological replicates are shown. Error bars represent the standard error of the mean. Lowercase letters indicate statistically significant differences within a genotype between different treatments, uppercase letters indicate significant differences between genotypes subjected to the same treatments. Statistical analyses were performed by using two-way ANOVA and Bonferroni's post-test (*p*-value < 0.05). Two independent experiments were performed with similar results.

6.2.2. *WRKY51* expression is activated by TGA1, 4 after NHP but not after SA treatment in the *sid2* background

As NHP is required for the establishment of SAR, we wanted to analyze whether NHP treatment induces *WRKY51* as well. To this aim, 4.5-week-old plants were infiltrated with NHP or $MgCl_2$ as mock control. The infiltrated leaves were harvested after 8 h. In addition, we investigated, whether SA leads to *WRKY51* expression as well. For this, 4-week-old plants were sprayed with 1 mM SA and leaves were harvested after 8 h. Water spraying served as control. The *sid2-2 npr1-1* (*sid2 npr1*) mutant was included in these experiments, as NPR1 is also required for the establishment of SAR. The NHP infiltration experiment was conducted by Isha Goyal in the frame of her dissertation, however, the qRT-PCR analysis was performed as part of this thesis.

The expression of *WRKY51* is induced upon NHP treatment in the *sid2* and *sid2 tga256* mutants (Figure 45). No induction is detected for the *sid2 tga14* mutant, indicating that TGA1, 4 activate *WRKY51* in an NHP dependent manner. This is different for *SARD1* which is not induced in the *sid2 tga256* mutant (Nair *et al.,* 2021). The *sid2 npr1* mutant shows weak activation of *WRKY51* after NHP treatment, but expression levels are much lower compared to *sid2*. This shows that NPR1 plays a role in the activation of *WRKY51* in NHP treated plants.

After SA treatment, *WRKY51* expression is induced in *sid2*, *sid2 tga14* and *sid2 tga256*, but not in *sid2 npr1*. This shows that the expression of *WRKY51* is regulated in a different manner, depending on the treatment by either NHP or SA. TGA1, 4 only activate *WRKY51* in response to NHP, but not in response to SA. Still, NPR1 is important for induction by both treatments.

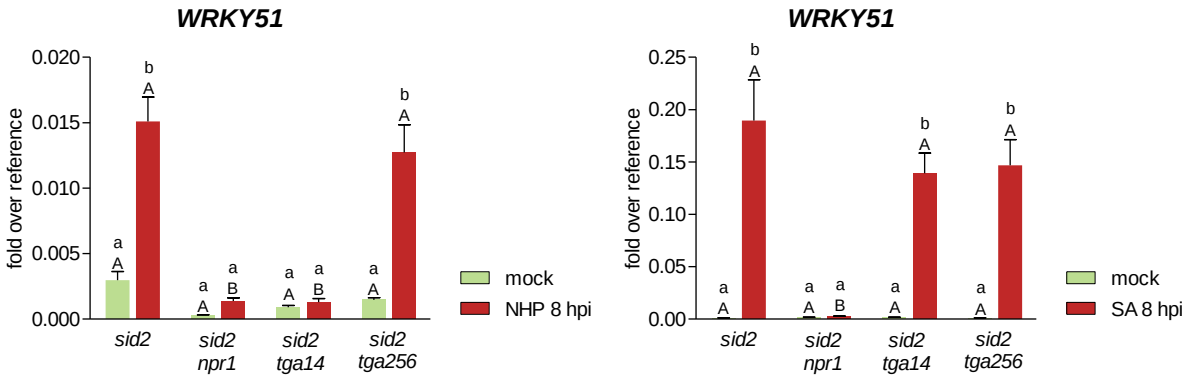

Figure 45: *WRKY51* expression is activated by TGA1, 4 after NHP, but not after SA treatment. a. Lower leaves of 4.5-week old *A. thaliana* plants were infiltrated with $MgCl_2$ (green, mock treatment) or infiltrated with 1 mM NHP (red). **b.** 1 mM SA (red) or water (green, mock treatment) was sprayed onto the rosette of 4.5-week old *A. thaliana* plants. Leaves were harvested after 8 hours, RNA was isolated and cDNA synthesized. Expression of *WRKY51* was analyzed by qRT-PCR, *UBQ5* was used as a reference. Mean values of four to six biological replicates are shown. Error bars represent the standard error of the mean. Lowercase letters indicate statistically significant differences within a genotype between different treatments, uppercase letters indicate significant differences between genotypes subjected to the same treatments. Statistical analyses were performed by using two-way ANOVA and Bonferroni's post-test (p-value < 0.05). Two independent experiments were performed with similar results.

In addition to these genotypes, Isha Goyal analyzed the *WRKY51* expression after NHP treatment in the *sid2-2 NahG* line. *NahG* encodes for a SA hydroxylase, which leads to the decrease of SA. The results reveal that basal SA levels are required for the activation of *WRKY51* after NHP treatment.

6.2.3. WRKY50, 51 is not required for induction of *FMO1* in *Psm*-infected SAR leaves

After having identified *WRKY51* as being induced in a TGA1, 4-, but not TGA2, 5, 6-dependent manner in *Psm*-infected SAR leaves and after NHP treatment, we wanted to analyze the *FMO1* expression in the respective mutants. For this, the technician Ronald Scholz crossed the *wrky50-1 wrky51-1* double mutant with *sid2-2*. After analyzing 320 plants, homozygous *sid2-2 wrky50-1 wrky51-1* (*sid2 wrky5051*) were identified, but no *sid2-2 wrky51-1* (*sid2 wrky51*). To obtain homozygous *sid2 wrky51* mutants, the plants were sprayed with SA prior to flowering. This might suggest that WRKY51 is involved in SA responses.

In contrast to our expectations, *sid2 wrky51* and *sid2 wrky5051* are able to induce *FMO1* expression after *Psm*/*Psm* treatment (Figure 46a). Likewise, after NHP infiltration, *FMO1* is induced in *sid2 wrky5051* to the same extent as in the *sid2* mutant (Figure 46b). Thus, WRKY51 is not the missing link in understanding, why *FMO1* expression depends on clade I TGA factors, although its promoter does not have a functional TGA binding site.

In addition to *FMO1*, *SARD1* and *PR1* expression was analyzed in *Psm*-infected SAR leaves. The promoter region of *SARD1* has no WRKY50 binding site whereas *PR1* has three. However, no difference was detected in the *sid2 wrky51* and *sid2 wrky5051* mutants compared to the respective *sid2* control (Supplementary Figure S16). To identify in what processes WRKY50, 51 are involved in after *Psm*/*Psm* treatment as well as after NHP treatment, RNA was sent for sequencing to the NIG. Unfortunately, the transcriptome data was not ready for analysis before the submission deadline of this thesis.

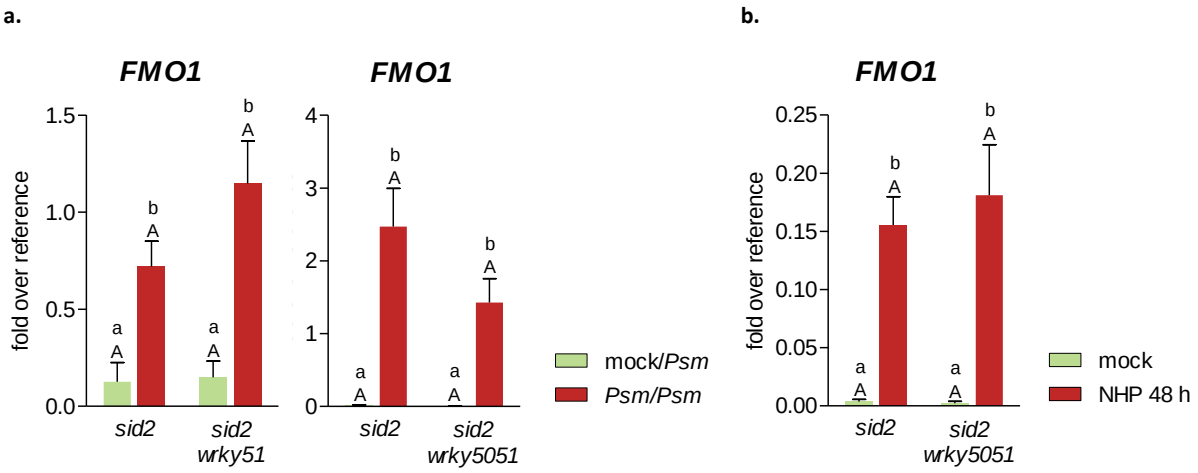

Figure 46: *FMO1* expression is not regulated by WRKY51 in *Psm*-infected SAR leaves. a. Lower leaves of 4.5-week-old *A. thaliana* plants were infiltrated with $MgCl_2$ (green, mock treatment) or infiltrated with *Psm* (red, OD_{600} = 0.005). After 48 h, upper leaves were infiltrated with *Psm*. The upper leaves were collected after 8 hours, RNA was isolated and cDNA synthesized. Expression of *FMO1* was analyzed by qRT-PCR, *UBQ5* was used as a reference. Mean values of eight to nine biological replicates are shown. Error bars represent the standard error of the mean. Lowercase letters indicate statistically significant differences within a genotype between different treatments, uppercase letters indicate significant differences between genotypes subjected to the same treatments. Statistical analyses were performed by using two-way ANOVA and Bonferroni's post-test. **b.** Lower leaves of 4.5-week old *A. thaliana* plants were infiltrated with $MgCl_2$ (green, mock treatment) or infiltrated with 1 mM NHP (red). Leaves were harvested after 8 hours, RNA was isolated and cDNA synthesized. Expression of *FMO1* was analyzed by qRT-PCR, *UBQ5* was used as a reference. Mean values of six to eight biological replicates are shown. Error bars represent the standard error of the mean. Lowercase letters indicate statistically significant differences within a genotype between different treatments, uppercase letters indicate significant differences between genotypes subjected to the same treatments. Statistical analysis was performed by using two-way ANOVA and Bonferroni's post-test (p-value < 0.05).

7. Discussion

7.1. Regulation of gene expression by ROXYs without the conserved ALWL motif upon nitrogen starvation

TGA transcription factors are important regulatory components in numerous processes, such as pathogen defense (Zhang *et al.,* 2003; Kesarwani *et al.,* 2007; Zander *et al.,* 2010), development (Chuang *et al.,* 1999; Hepworth *et al.,* 2005; Murmu *et al.,* 2010) or detoxification (Mueller *et al.,* 2008; Fode *et al.,* 2008). In order to regulate some of these stress responses, ROXY-type GRX interact with and repress the activity of TGAs (Xing *et al.,* 2005; Ndamukong *et al.,* 2007; Li *et al.,* 2009; Murmu *et al.,* 2010; Zander *et al.,* 2012; Li *et al.,* 2019). The genome of *A. thaliana* encodes 21 ROXYs which can be further divided into proteins encoding for a C-terminal ALWL motif and ROXYs without the ALWL motif. The ALWL motif recruits the transcriptional co-repressor TOPLESS (Uhrig *et al.,* 2017). Formation of a TGA/ROXY/TPL complex at the respective promoter regions represents most likely one of the mechanisms how ROXY-mediated repression can work. ROXY6, 7, 8, 9 are the only ROXYs without ALWL motif. Ectopically expressed ROXY8 or ROXY9 can repress the function of TGA1, 4 (Li *et al.,* 2019). How this mechanism is mediated is unknown.

In this study, we wanted to unravel how these ROXYs without ALWL motif can regulate gene expression. Upon nitrogen (N) starvation, the expression of at least *ROXY6*, *8* and *9* is induced in the shoots. After traveling to the roots, gene expression of e.g. *NRT2.1* is activated (Ohkubo *et al.,* 2017; Ota *et al.,* 2020). As TGA1, 4 can bind to the promoter region of *NRT2.1* (Alvarez *et al.,* 2014), ROXY6, 7, 8, 9 and TGA1, 4 might regulate the expression together. Additional target genes of ROXY6, 7, 8, 9 in roots upon N starvation conditions were identified by transcriptome analysis. To explore how the expression is regulated, further qRT-PCR analyses with additional genotypes were performed.

7.1.1. ROXY6, 7, 8, 9 and TGA1, 4 function in one pathway to regulate gene expression

Unambiguous evidence for our conclusion that ROXY6, 7, 8, 9 function in one pathway to regulate target gene expression was provided by the *tga14roxy6789* hexuple mutant, which abolished the function of ROXY6, 7, 8, 9 either as negative or positive regulators of gene expression (Figure 25, Figure 26, Supplementary Figure S5). This means that TGAs function downstream of the ROXYs, or in other words, TGAs are epistatic to ROXY6, 7, 8, 9. The same observation has been made in the case of the genetic interaction between ROXY1 and the TGA factor PAN. While the *roxy1* mutant has in average 2.5 petals and the *pan* mutant has five petals, the *roxy1 pan* double mutant has five petals (Li *et al.,* 2009).

Our transcriptome analysis, in which we compared Col-0 and the *roxy6789* mutant under LN conditions, we identified 350 genes that were activated by ROXY6, 7, 8, 9 and 220 genes that were repressed by the ALWL-free ROXYs (Dataset 1). When we compared the expression pattern of highly regulated target genes in Col-0, *tga1 tga4* and *roxy6789* we found the following correlations (Table 33).

Table 33: Regulation of gene expression by ROXY6, 7, 8, 9.

ROXY6, 7, 8, 9 as activators in LN conditions (e.g. *UMAMIT35*, *NRT2.2*)	**ROXY6, 7, 8, 9 as repressors in LN conditions (e.g. *PER71*, *TFL1*)**
Induction of target genes in LN conditions	Repression of target genes in LN conditions
Repressive effect of TGA1, 4 preferentially seen in FN conditions	Activating effect of TGA1, 4 preferentially seen in FN conditions
TGACG motif enriched	TGACG motif rather depleted than enriched
Activation of the JA pathway promotes expression of at least some of these genes	Activation of the JA pathway interferes with expression of at least some of these genes

Genes, that require ROXY6, 7, 8, 9 for activation, are repressed by TGAs in FN conditions, like *UMAMIT35* (Figure 24). This group of genes is induced upon N starvation. TGA1, 4 represses these genes only under N sufficient conditions. Under these conditions, a still unknown activator is required for *UMAMIT35* expression. The repressive effect of TGA1, 4 is fully abolished upon LN-induced expression of ROXY6, 7, 8, 9, leading to the induction of gene expression. Depending on the experiment and the target gene, we observe the tendency that the repressive activity of TGA1, 4 is not only derepressed but that TGA1, 4 turns into an activator under LN conditions. TGACG motifs are enriched in the promoter regions of the genes in this group (Table 28), indicating that the ROXY/TGA complex can directly regulate at least a subset of the 350 genes (Figure 47), while other genes may be indirectly regulated. Indeed, Alvarez *et al.,* 2014 showed by chromatin immunoprecipitation experiments that TGA1 can bind to the promoter regions of *NRT2.1* and *NRT2.2*.

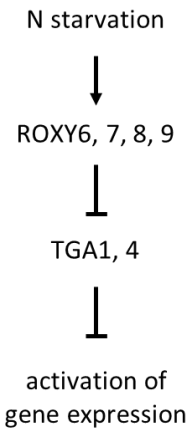

Figure 47: Proposed model for the activation of gene activation by ROXY6, 7, 8, 9. The expression of ROXY6, 7, 8, 9 is induced upon nitrogen (N) starvation. ROXY6, 7, 8, 9 interfere with the repressive mechanism of TGA1, 4 to activate gene expression.

The model shown in Figure 47 matches almost perfectly for *UMAMIT35*, but for other promoters, additional regulators influence the expression and hide or obscure the described regulation. A prominent example is represented by *NRT2.2*, which is highly induced in LN conditions even in the *tga14roxy6789* mutant (Figure 26). Still, it is not induced in *roxy6789*, indicating that TGA1, 4 function as repressors. Moreover, an activator that is only active under LN conditions dominates the induction, so that the repressive effect of TGA1, 4 cannot be observed in FN conditions.

Genes that are repressed by ROXY6, 7, 8, 9 require TGA1, 4 for activation in FN conditions and are downregulated upon N starvation, like *PER71* and *TFL1* (Figure 21). The TGACG motif is rather depleted

in the promoter regions of these genes (Table 26), suggesting an indirect regulation. Assuming that the primary regulation works like shown in Figure 47, we have to postulate that TGA1, 4 repress a repressor of this set of genes. The LN-induced ROXY6, 7, 8, 9 interfere with the repression of TGA1, 4, thus this repressor is more highly expressed and downregulates gene expression (Figure 48).

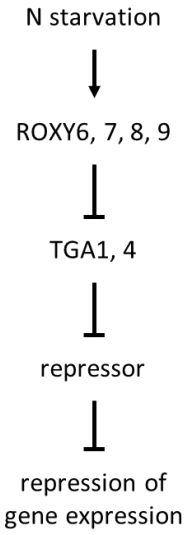

Figure 48: Proposed model for the repression of gene activation by ROXY6, 7, 8, 9. The expression of ROXY6, 7, 8, 9 is induced upon nitrogen (N) starvation. ROXY6, 7, 8, 9 interfere with the repressive mechanism of TGA1, 4 to activate gene expression.

A similar regulatory principle which is based on the regulated repression of a repressive mechanism has been described before with regard to seed germination. Seed germination is the default pathway when the two antagonistic plant hormones ABA and GA are missing (Koornneef *et al.,* 1982). This can be compared to the constitutive expression of *UMAMIT35* or the LN-induced expression of *NRT2.2* in the absence of TGA1, 4 and ROXY6, 7, 8, 9. While abscisic acid (ABA) represses seed germination, GA represses the synthesis of ABA, which is required to induce germination (Koornneef *et al.,* 1982; Piskurewicz *et al.,* 2008). The regulation of germination is tightly connected to environmental conditions through this ABA/GA module. In unfavorable conditions such as high temperature (Toh *et al.,* 2008) and far-red light (Yamaguchi *et al.,* 1998; Oh *et al.,* 2006), endogenous GA synthesis is repressed. This leads to the derepression of ABA and subsequent block of germination.

As mentioned above, the epistatic relationship between ROXY6, 7, 8, 9 and TGA1, 4 is the same as the epistatic relationship between ROXY1 and PAN. However, PAN directly binds to AGAMOUS and activates its expression (Das *et al.,* 2009), while TGA1, 4 negatively regulate their target genes. Thus, in the ROXY1/PAN system, ROXY1 represses a transcriptional activator in a manner that requires the ALWL motif at the C-terminus. Since TGA1, 4 have been described as transcriptional activators in the shoot, the question arises, which mechanism turns this activator into a repressor.

7.1.2. ROXY10-15 function as antagonists to ROXY6, 7, 8, 9 to control *UMAMIT35* expression

ROXY6, 7, 8, 9 are the only members of the ALWL-free ROXYs. While their expression is induced upon N starvation, the expression of at least nine ALWL-containing ROXYs (ROXY10-18) is repressed (Jung *et al.,* 2018). Studies with ectopically expressed ROXY9 and ROXY15 revealed an antagonistic relationship. ROXY9 was shown to activate *NRT2.1* expression in N sufficient conditions, which is consistent with our model that ROXY6, 7, 8, 9 activate the gene expression by releasing the repressive effect of TGA1, 4. In contrast, ROXY15 functions as repressor (Jung *et al.,* 2018). Our loss-of-function analysis of the

ROXY15 and the related ROXYs 10-14 revealed that *UMAMIT35* is partially derepressed in the *roxy10-15* mutant in FN conditions (Figure 28). The repression might be mediated by a repressive complex of TGA1, 4, ROXY10-15 and TPL. LN-induced ROXY6, 7, 8, 9 might displace ROXY10-15 in order to interfere with the repressive mechanism However, derepression in the *roxy10-15* mutant was not as pronounced as in the *tga1 tga4* mutant. Due to potential functional redundancy, other ALWL-containing ROXYs might be involved in the repression of *UMAMIT35*. Moreover, they might compensate the loss of ROXY10-15 leading to WT-like expression of the other target genes in the *roxy10-15* mutant (Figure 28, Supplementary Figure S8). In our experimental setup, *ROXY10-15* are mainly expressed in shoots (Supplementary Figure S7). Similar to ROXY6, 7, 8, 9, ROXY10-15 might travel from the shoots to the roots to control gene expression.

7.1.3. The ROXY/TGA module might incorporate environmental signals

While the ROXY/TGA regulatory module is required to mediate N-supply-regulated expression of e.g. *UMAMIT35* and *PER71*, other genes like *NRT2.2* contain the module, but deletion of the module does not affect gene expression. As mentioned above, an independent LN-induced activating principle is installed for the regulation.

This activating principle might be realized by members of the NLP family which induce nitrate-related gene expression in the absence of reduced nitrogen like ammonium or glutamine. Thus, they might function as activator of *NRT2.2* and *NLP3*. There are nine NLPs encoded in the *A. thaliana* genome. In a recent study, transcriptome analysis identified 3103 genes that are activated by transiently overexpressed NLP1-9 in mesophyll protoplasts (Liu *et al.,* 2022). We compared this dataset with our transcriptome data and identified 71 ROXY6, 7, 8, 9-activated genes which are also activated by NLP1-9 (Figure 49). Among these genes are *NRT2.2*, *NLP3* and *UMAMIT35*. This suggests that NLPs activate at least a subset of ROXY6, 7, 8, 9-induced genes. As the analysis by Liu *et al.,* 2022, was performed with mesophyll protoplasts, NLP1-9 might regulate additional genes in roots upon N starvation.

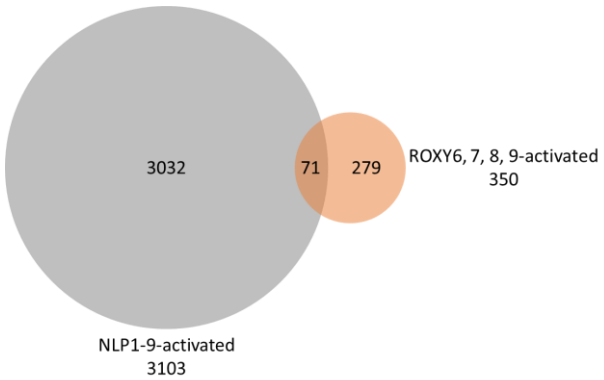

Figure 49: Schematic representation of transcriptome data. Venn diagram was generated with 3103 NLP1-9-activated genes ($log_2 > 1$, $P < 0.05$) identified in Liu *et al.,* 2022, and 350 ROXY6, 7, 8, 9-activated genes in low nitrogen conditions (log_2 FC > 1, *p*.adj < 0.05) according to transcriptome data from this study.

In this study, we identified that *NRT2.2*, *NLP3* and *UMAMIT35* expression is induced in the absence of external nitrate (Figure 31). However, NLP7 requires nitrate for its activation. Binding nitrate leads to conformational changes and derepression of NLP7 (Liu *et al.,* 2022). NLP7 is activated by subsequent nitrate-dependent phosphorylation (Liu *et al.,* 2017a). The nitrate binding domain of NLP7 is highly conserved among all NLPs (Liu *et al.,* 2022). Unless endogenous nitrate levels, which might still be present in the plants transferred from high nitrate to medium without nitrate, are sufficient for the activation, NLPs are most likely not the primary activators under our conditions. However,

independent from the identity of the LN-induced activation mechanism, the question remains, why the dispensable ROXY/TGA module is still functional.

One hypothesis is that the ROXY/TGA module might be important to integrate environmental conditions into N starvation-dependent gene expression. Nitrate is the main source of nitrogen and its uptake is mostly mediated by the seven members of the NRT2 family under N limiting conditions (Cerezo *et al.,* 2001; Kiba *et al.,* 2012; Lezhneva *et al.,* 2014). Additional roles have been described for some members. Lack of NRT2.1, for example, leads to enhanced lateral root formation in response to high sucrose levels (Little *et al.,* 2005), enhanced resistance to *Pst* (Camañes *et al.,* 2012) and reduced ethylene production (Zheng *et al.,* 2013). NRT2.6 contributes to the resistance against the phytopathogenic bacterium *Erwinia amylovora* (Dechorgnat *et al.,* 2012). This shows how tightly connected nitrate signaling and other environmental conditions are. Thus, it can be imagined that the LN-induced expression of e.g. the high-affinity nitrate transporters has to be adapted to further environmental clues. In this scenario, ROXYs, which might respond to these environmental cues even in the shoot, can mediate their integration. To further elaborate the ROXY/TGA regulation, low nitrogen levels could be combined with other abiotic or biotic conditions.

7.1.4. CEPR1 is required for target gene expression

Previous studies showed that CEP1 is produced upon N starvation in roots (Tabata *et al.,* 2014). After traveling to the shoots, CEP1 binds to the leucine rich receptor kinases CEPR1 and CEPR2 and expression of *ROXY6*, *8* and *9* is activated (Tabata *et al.,* 2014; Ohkubo *et al.,* 2017; Ohkubo *et al.,* 2021). ROXY6, 8, 9 are transported to the roots and induce gene expression. In our experimental setup, we were able to show that CEPR1 regulates the expression of *NRT2.2*, *UMAMIT35* and *TFL1* in roots upon N starvation (Figure 29). However, under our experimental conditions this is not due to reduced transcription of *ROXY9* in the shoots (Figure 30). As ROXY9 needs to travel from the shoots to the roots, CEPR1 might be involved in this process. The closest homologue of CEPR1, CEPR2, has been shown to phosphorylate target proteins such as the low-affinity nitrate transporter NRT1.2 (Zhang *et al.,* 2021) and ABA-receptors PYRABACTIN RESISTANCE 1-LIKE (PYL) 2, 4 (Yu *et al.,* 2019). CEPR1 might facilitate the transport of ROXY9 through phosphorylation of either ROXY9 or unknown target proteins. Alternatively, it might be important for the expression of another regulatory component that is required for the induction of N starvation-regulated genes. For example, micro RNAs (miRNAs) could be involved. In legumes, the expression of miR2111s is activated in the shoot by CEP1 and upon N starvation (Gautrat *et al.,* 2020). MiR2111s have been shown to move from the shoot to the root to promote nodule formation (Okuma *et al.,* 2020). Similarly, CEP1- or N starvation-induced miRNAs could function as shoot-to-root signal in *A. thaliana* to induce gene expression.

7.1.5. ROXY6, 7, 8, 9, might integrate JA signaling into nitrogen starvation responses

By using the TurboID approach, the transcriptional co-repressors TOPLESS (TPL), TOPLESS-RELATED (TPR) 2 and TPR4 were identified as being in close proximity to ROXY9 in roots (Figure 39). Both TPL and ROXY9 can interact with several JAZ proteins (Arabidopsis Interactome Mapping Consortium, 2011; Causier *et al.,* 2012; Moreno *et al.,* 2013; Willmer, 2014). Additionally, JAZ and TPL can interact with NINJA, which thus serves as adaptor protein for the recruitment of TPL to JAZ. The major role of JAZ, NINJA and TPL is regulating JA-mediated responses to wounding or to combat necrotrophic pathogens (Glazebrook, 2005) and to limit especially root growth under conditions that trigger JA-Ile synthesis (Pauwels *et al.,* 2010). In unchallenged conditions, MYC2, 3, 4 is repressed by JAZ, NINJA and TPL. In response to wounding or attack by necrotrophic pathogen, JA-Ile is produced leading to the

degradation of JAZ, mediated by CORONATINE INSENSITIVE1 (COI1). MYC2, 3, 4 are derepressed and activate gene expression (Glazebrook, 2005).

We hypothesized that ROXY9, JAZ, NINJA and TPL form a repressive complex in order to regulate target gene expression. As the *tpl-1* mutant shows abnormal growth under normal conditions (Long *et al.,* 2002), we analyzed mutants with compromised JAZ, NINJA or MYC expression. We discovered that e.g. *PER10*, a gene which is activated in LN conditions, is repressed by JAZ and NINJA in both FN and LN conditions (Figure 40). This repression is independent of MYC2, 3, 4 and might be mediated through the recruitment to the promoter by the ROXY/TGA complex. As JA signaling leads to the degradation of JAZ, we assume that the repressive effect of the JAZ1-7, 9, 10, 13 is resolved in response to wounding or necrotrophic pathogens. Thus, expression of N starvation-induced genes can be further enhanced, not only und LN, but also under FN conditions (Figure 50). In the case of LN-repressed genes, we observe that at least *PER71* is less expressed in the mutants that mimic constitutive activation of the JA pathway. This opposite effect is consistent with our findings that the ROXY/TGA module represses the expression of a repressor of the LN-repressed genes. Thus, higher activation of this repressor upon JA-mediated activation of JAZ degradation would lead to reduced expression of target genes. These observations are also included in Table 33.

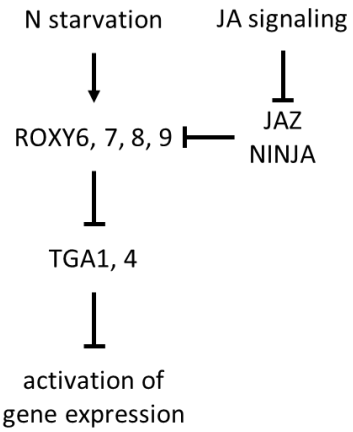

Figure 50: Schematic representation on how JA signaling might be integrated into regulation of gene expression by ROXY6, 7, 8, 9. JAZ and NINJA negatively regulate the activation of gene expression by repressing ROXY6, 7, 8, 9. JAZ is degraded in jasmonic acid (JA) signaling.

A link between N and JA signaling has been reported before. JA induces the expression of low-affinity nitrate transporter *NRT1.8* in a COI1-dependent manner. In contrast, *NRT1.5* is repressed by COI1 in the presence of JA (Zhang *et al.,* 2014). Both NRT1.8 and NRT1.5 mediate nitrate transport between roots and shoots in response to environmental signals such as salt stress, drought or exposure to heavy metals (Lin *et al.,* 2008; Li *et al.,* 2010; Chen *et al.,* 2012a). This suggests a crosstalk between JA signaling and N starvation-responsive gene expression, which might be mediated through ROXY-dependent recruitment of the JA-responsive regulatory module to target promoters.

7.1.6. Oxidoreductase activity of ROXY9 is not required for regulation of target gene expression upon nitrogen starvation

GRXs have first been described as small enzymes which are able to modify the redox state of target proteins (Laurent *et al.,* 1964). The characteristic Cxx[C/S] active site motif mediates the oxidoreductase activity (Martin, 1995). According to the other conserved amino acids at the active site, GRX can be subdivided into three classes. The CPYC-type (Class I) is mainly involved in the reduction of disulfide bridges and oxidation of thiol groups (Holmgren, 1976; Gravina & Mieyal, 1993; Couturier *et al.,* 2013) whereas members of the CGFS-type (class II) are involved in Fe-S cluster binding and transfer (Rodríguez-Manzaneque *et al.,* 2002; Picciocchi *et al.,* 2007; Bandyopadhyay *et al.,* 2008; Iwema *et al.,* 2009). For these functions, the first cysteine of the active site motif is crucial (Rouhier *et al.,* 2002; Feng *et al.,* 2006; Rouhier *et al.,* 2007). Whereas class I and II are found in most of the so far characterized organisms, the CC-type GRXs (class III, ROXYs) are specific for land plants (Lemaire, 2004; Ziemann *et al.,* 2009). 21 CC-type GRXs are found in the genome of *A. thaliana*. So far, only little is known about the functional relevance of the ROXY specific CC[M/L][C/S/G] active site motif and whether it mediates oxidoreductase activities.

In this study, we analyzed the ROXY9 active site motif CCLC. For this, the *roxy6789* was complemented with a HA-tagged ROXY9 harboring a CCLC, SCLC, CSLC or CPYC active site. Initially, a CCLCA active site variant was planned as well, but as these lines expressed less proteins, it was excluded from further analysis (Figure 34). As a linker sequence between the HA-tag and the coding region for ROXY9 prevents artificial aggregate formation (Mrozek, unpublished), a HA-L-ROXY9 construct was used. We discovered that the first and second cysteine of ROXY9, CYS21 and CYS22, are not required for biomass production, petiole length and repression of endogenous *ROXY9* (Figure 33, Figure 36). When analyzing the regulation of several target genes upon N starvation, we observed clear induction or repression in those lines that contain either the SCLC or CSLC motif (Figure 35, Supplementary Figure S11). This excludes the proposed mechanism that ROXY9 acts through the redox modulation of a target protein. Consistently, we showed that the putative target protein TGA1 does not require its potentially redox-active cysteines to complement N starvation-induced gene expression in the *tga1 tga4* mutant (Figure 32). Nevertheless, a tendency that ROXY9 SCLC and CSLC variants are less active than the wild type protein was observed. Only the ROXY9 CPYC active site version is nonfunctional.

Still, it is remarkable that the CC motif is so conserved during evolution, while exchange of the last C of the active site has occurred in several *ROXY* genes. Since we expressed the transgene under the control of the ubiquitously expressed *35S* promoter, the ROXY9 variants are directly present in those cell types where they regulate the target genes. In contrast, the endogenous ROXYs are transported from the shoot to the roots. Thus, it cannot be excluded that the CC motif is important for this transport. Therefore, it is worthwhile to express ROXY9 and the corresponding active site variants under the *ROXY9* promoter. Since under our conditions *ROXY9* is much higher expressed than *ROXY6*, *ROXY7* or *ROXY8* (Figure 18), it is likely that expression of *ROXY9* alone will be sufficient to complement the *roxy6789* phenotype. Alternatively, redox modulation at the first cysteine might be needed to integrate environmental conditions such as oxidative into nitrate signaling. To test this hypothesis, buthionine sulfoximine (BSO), which inhibits GSH synthesis (Griffith & Meister, 1979), or ozone could be applied to the LN plates and the previously identified target genes could be used as a read out.

In contrast to our findings, previous studies with plants ectopically expressing ROXY9 demonstrate a relevance of the cysteines in the respective active site motifs (Li *et al.,* 2019). In this study, HA-ROXY9 without a linker sequence was expressed under control of the *35S* promoter in Col-0. The experimental

read out was ROXY9-mediated repression of TGA1, 4-dependent activation of hyponasty in low light stress. When altering the first or second cysteine of the ROXY9 active site motif to serine, the repressive mechanism was impaired. We have not explicitly tested the *35S:*HA-L-ROXY9 lines for their ability to interfere with the increased hyponastic growth of the *roxy6789* mutant. However, since the petiole length most likely contributes to hyponasty and no difference was observed between the HA-L-ROXY9 CCLC, SCLC and CSLC complementation lines (Figure 36), it is unlikely that the lines behave differently in hyponasty.

Why are the two conserved cysteines important when ectopically expressing the HA-ROXY9 protein under the *35S* promoter in Col-0, while they are not important when expressing the HA-L-ROXY9 protein in the *roxy6789* mutant? We have observed that the HA-ROXY9 plants are stunted, which is not observed when introducing the HA-L-ROXY9 construct into the *roxy6789* background. It might well be that the biggest difference between two constructs is the linker sequence between the HA-tag and the open reading frame. We have introduced this linker sequence because biochemical analysis of the recombinant protein had unraveled that the HA-tag leads to aggregation of the protein and that the cysteines in the active center cannot be oxidized by dithiane. These problems were solved by inserting a linker between the tag and the start codon. Because of the wild type-like growth phenotype, we would trust the results with the HA-L-tag more than the data from Li *et al.,* 2019. However, it seems counterintuitive that the conserved cysteines in the ROXY-specific active site are relevant for the activity of HA-ROXY9 with a tag that alters the redox properties of the protein, while they are dispensable for HA-L-ROXY9. While finishing this thesis, constructs without the tag were generated in the lab. Again, ROXY9 variants with the mutated cysteines were functional, although it appeared that the C/S variants in the first two positions were less efficient. Apparently the HA-tag diminishes the already weaker function of HA-ROXY9 SCLC or HA-ROXY CSLC, but to a lesser extent the function of HA-ROXY9.

Apart from ROXY9, the active site motif has been studied in ROXY1 and ROXY19. ROXY1 interferes with the function of PAN, a negative regulator of petal development, in order to maintain normal petal number (Xing *et al.,* 2005; Li *et al.,* 2009). In complementation experiments using the *35S* promoter, ROXY1 complemented the phenotype in 64 % of the transformants, while the ROXY1 SCMC variant failed to do so (4 %; Xing *et al.,* 2005). When the experiment was repeated with the endogenous promoter, the construct with the wild type protein showed 100 % complementation efficiency. The SCMC variant was also able to complement, although with a lower efficiency (70 %). These results are very similar to our results, that the first cysteine is not absolutely required, but that the protein loses its functionality to a certain degree (Ziemann, 2010). Thus, oxidoreductase activity or Fe-S binding does not seem to be required both for ROXY1 and ROXY9 function. In PAN, CYS340 seemed to be important in complementation experiments (Li *et al.,* 2009). However, it is not known whether this cysteine is redox modulated at all.

Another analysis has been made with plants expressing *35S:*HA-ROXY19. These lines are more susceptible to the chemical 2,3,5-triiodobenzoic acid (TIBA) due to repression of TGA2, 5, 6-activated detoxification genes such as *CYP81D11* and *NAC032* (Fode *et al.,* 2008; Huang *et al.,* 2016). The first active site cysteine is required for this negative regulation as mutation to serine led to a WT-like phenotype (Oberdiek, 2018). However, also this construct contains the HA-tag which might interfere with the ROXY function. Therefore, it might be possible that the anyways weaker activity of a SCMC derivative might be further diminished. Moreover, mutating the single cysteine of TGA2 into a serine did not alter its activity in complementation experiments (Findling *et al.,* 2018).

In contrast, a recent publication on maize ROXY homologue MALE STERILE CONVERTED ANTHER 1 (MSCA1) demonstrated an oxidoreductase activity. MSCA1 and its closest paralogues ZmGRX2 and ZmGRX5 share a CCMC active site motif and suppress meristem growth by repressing TGA factor FASCIATED EAR 4 (FEA4; Yang *et al.,* 2015; 2021). The interaction of MSCA1 and FEA4 relies on the first and/or last cysteine of the MSCA1 active site motif and the critical cysteine of FEA4, CYS321. Biochemical analysis revealed that MSCA1 can reduce FEA4. The MSCA1 SMCS version failed to alter the redox state of FEA4, indicating that the CCMC active site motif mediates the reduction. When altering the FEA4 CYS321 to serine, FEA4 became reduced to a lesser extent, revealing that CYS321 is the main target site for redox modulation by MSCA1 (Yang *et al.,* 2021). These findings demonstrate that at least this CC-type GRX is able to reduce oxidized TGA factors.

The interaction of MSCA1 and FEA4 relies on the active site motif and FEA CYS321 (Yang *et al.,* 2021). In contrast, the interaction of ROXY9 with TGA1, 4 is independent of the ROXY9 active site motif (Li *et al.,* 2019). Alignment of FEA4 to TGA1, 4 revealed that FEA4 CYS321 is conserved as CYS260 in TGA1 and CYS256 in TGA4 (Figure 51). Whether these cysteines are important for the interaction with ROXY9 has not been analyzed. Experiments with TGA1 active site complementation lines in this thesis showed that the four cysteines of TGA1 are not required for the expression of *ROXY9* or *PER71*. ROXY9 regulates the expression of these genes by repressing TGA1, 4, suggesting an intact interaction despite the altered cysteines. As the interaction of ROXY9 and TGA1, 4 functions differently to MSCA1 and FEA4, the repression is most likely also mediated through a different mechanism.

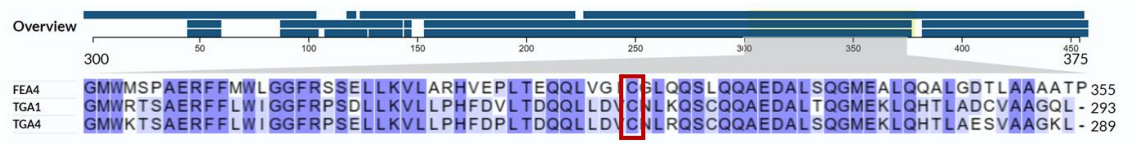

Figure 51: Alignment of ZmFEA4, AtTGA1 and AtTGA4. Protein sequences of ZmFEA4, AtTGA1 and AtTGA4 were aligned by Clustal Omega (1.2.4) multiple sequence alignment (Sievers *et al.,* 2011; Sievers & Higgins, 2018). CYS321 of FEA4 is conserved in TGA1 and TGA4, marked in red.

7.2. The role of WRKY50, 51 in the establishment of SAR remains to be elucidated

Apart from being involved in N starvation responses, TGA1, 4 are important regulatory components of systemic acquired resistance (SAR), which is the enhanced resistance to secondary pathogen attacks (Sun *et al.,* 2018). For the establishment of SAR, the expression of *ICS1*, *PBS3*, *ALD1* and *FMO1* is induced. ICS1 and PBS3 are part of the SA synthesis pathway (Wildermuth *et al.,* 2001; Rekhter *et al.,* 2019; Torrens-Spence *et al.,* 2019), while ALD1 and FMO1 are involved in the synthesis of NHP. Already at basal SA levels, like in the SA synthesis mutant *salicylic acid induction 2-2* (*sid2*), *Psm*/*Psm* infection or NHP treatment leads to the activation of SA and NHP synthesis genes. Clade I (TGA1, 4) and clade II (TGA2, 5, 6) TGA factors as well as NPR1 are required for this activation (Nair *et al.,* 2021).

Since some of the above mentioned target genes contain only one TGACG motif, and since TGAs to not form heterodimers (Niggeweg *et al.,* 2000), we were wondering why both clades of TGAs were required for the activation. We wanted to identify which regulatory factors are activated by only one clade of TGAs, e.g. clade I. This factor could function together with the more abundant clade II TGA factors and would explain why both clades are required to induce expression of SAR genes. In addition to the TGAs, SARD1 could be involved in the regulation (Figure 52).

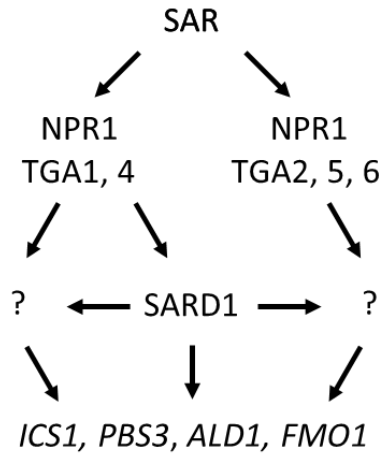

Figure 52: Clade I and II TGAs activate SAR-inducible gene expression. To induce systemic acquired resistance (SAR), NPR1 and TGA1, 4 activate *SARD1* expression. SARD1, NPR1 and TGA2, 5, 6 activate the expression of SAR-inducible genes, such as *ICS1*, *PBS3*, *ALD1* and *FMO1*. In this study, we wanted to identify additional transcription factors that are activated by clade I and/or II TGAs in SAR conditions and contribute to the induction of SAR genes. These unknown factors are indicated as question marks.

By using transcriptome analysis, we identified 4184 genes, which are induced in SAR conditions in the *sid2* mutant (Dataset 2). Visualization with the MarVis software revealed that most of these genes are regulated by TGA1, 4 and/or TGA2, 5, 6 (Figure 42). As the *sid2* mutant is impaired in the accumulation of pathogen-induced SA, these results indicate that basal SA levels are sufficient for the TGA-dependent regulation of gene expression in SAR conditions. This is especially striking as NPR1 is required for the establishment of SAR (Cao *et al.,* 1997) and NPR1 needs SA for its activation (Mou *et al.,* 2003). NPR1 interacts with TGAs to activate several SAR-induced genes (Dong, 2004; Ding *et al.,* 2018).

We identified not only *SARD1*, but also *WRKY51* as being activated by TGA1, 4 in *Psm*-infected SAR leaves. The closest homologue of WRKY51 is WRKY50, which has been shown to interact with clade II TGAs to synergistically activate *PR1* expression in transiently transformed protoplasts (Hussain *et al.,* 2018). Thus, WRKY50, 51 are interesting candidates which might contribute to the activation of gene

expression regulated by both TGA clades. The role of WRKY50, 51 has been studied first in the *suppressor of SA insensitivity2* (*ssi2*) background. The *ssi2* mutant accumulates SA, overexpresses *PR* genes and is more resistant to *Pst* infection (Shah *et al.,* 2001). Moreover, *ssi2* is unable to induce *PDF1.2* expression after JA treatment and is hypersusceptible to necrotrophic pathogens such as *B. cinerea* (Kachroo *et al.,* 2001). Mutation of *WRKY50* and *WRKY51* in the *ssi2* background can restore the *PDF1.2* expression and resistance to *B. cinerea*. Also the elevated SA levels were reduced in the *ssi2 wrky5051* mutant, although the expression of *PR* genes was not altered compared to the *ssi2* mutant (Gao *et al.,* 2011). Additionally, the *wrky51* mutant is more susceptible to *Pst* infection (Gao *et al.,* 2011). This suggests that WRKY50 and WRKY51 function as positive regulators of SA-mediated signaling.

As TGA1, 4 activate the expression of *WRKY50* and *WRKY51* in *Psm*-infected SAR leaves and after NHP treatment in the *sid2* background (Figure 44, Figure 45), we questioned whether WRKY50, 51 are involved in the activation of SAR genes as well. SARD1 is a crucial regulator for the establishment of SAR, however, its expression is independent of WRKY50, 51 in *Psm*/*Psm* conditions and after NHP treatment (Supplementary Figure S16). Likewise, *FMO1*, which is regulated by SARD1, is not affected in the *wrky5051* mutant. WRKY50, 51 in the *sid2* background are also not required for the activation of *PR1*, the previously described target gene of WRKY50 and TGA2, 5 in protoplasts.

The transcriptome analysis additionally revealed that no transcription factor is robustly regulated by only clade II TGAs (Table 31). The *FMO1* promoter only contains one TGACG motif which is dispensable for its activation (Nair *et al.,* 2021), suggesting that the expression of a transcription factor is induced by clade I and II TGAs and this factor in turn activates *FMO1* expression. SARD1 might also contribute to this regulation. Prime candidates for such a transcription factor are WRKY75 and WRKY31, as these are highly upregulated in SAR conditions in a TGA-dependent manner (Table 32). Especially the *WRKY75* promoter with six TGACG motifs might accommodate both clades of TGAs. WRKY75 binds to the promoter region of *ICS1* and promotes resistance to *Pst* infection (Guo *et al.,* 2017) whereas the function of WRKY31 has not been studied.

Our findings are summarized in Figure 53. In SAR conditions or in response to NHP treatment, the NPR1- and TGA1, 4-dependent expression of WRKY50, 51 is activated in the presence of basal SA levels. This activation is independent of SARD1 and CBP60g (Goyal, unpublished). Since clade II TGAs interact with WRKY50 (Hussain *et al.,* 2018), they might activate the expression of SAR-induced genes together. As key transcription factor in SAR, SARD1 might also be involved in the regulation of this gene expression. In order to identify genes which are regulated by WRKY50, 51 and might contribute to SAR, a transcriptome analysis is ongoing. Moreover, NPR1 and TGA2, 5, 6 might activate the expression of *WRKY75* and *WRKY31*. TGA1, 4 and SARD1 might be involved in the activation. WRKY75 and WRKY31 might induce *PBS3*, *ALD1* and *FMO1* expression.

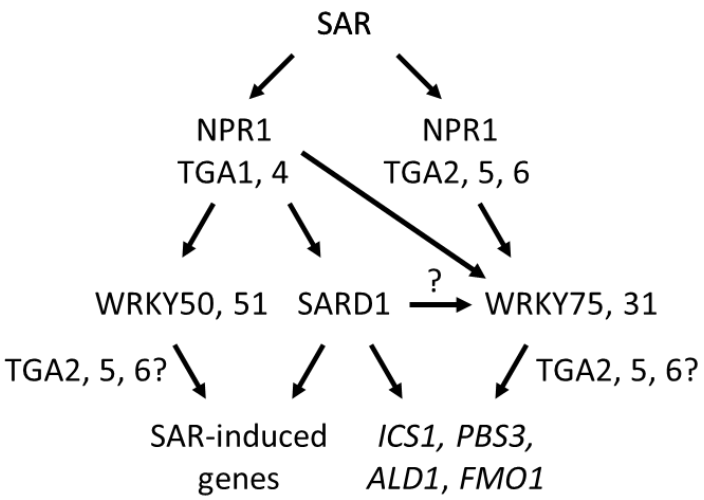

Figure 53: Proposed model for regulation of gene expression in SAR conditions by clade I and II TGAs. In SAR conditions, NPR1 and TGA1, 4 activate the expression of *SARD1*, *WRKY50* and *WRKY51*. Together with NPR1, TGA2, 5, 6 and SARD1, WRKY50, 51 might activate SAR-induced genes. Additionally, TGA1, 4 and TGA2, 5, 6 activate *WRKY75* and *WRKY31* expression, which could contribute to the expression of *ICS1*, *PBS3*, *ALD1* and *FMO1*.

8. Conclusion

In this study, we analyzed how TGA1, 4 and ROXY6, 7, 8, 9 regulate gene expression under different conditions. While only a weak influence of these proteins was detected in low light-induced gene expression and expression of defense-responsive genes, many target genes were discovered upon nitrogen starvation.

Our studies have revealed that the low nitrogen-induced ROXY6, 7, 8, 9 interfere with the repressive mechanism of TGA1, 4, which leads to the activation of the target genes upon N starvation (Figure 54). A not yet characterized activator contributes to the activation. This activation might be enhanced by JA treatment, which leads to the degradation of JAZ and thus interferes with the repression of ROXY function mediated by the JAZ/NINJA/TPL complex. In order to repress gene expression under N-limiting conditions, we postulate that ROXY6, 7, 8, 9/TGA1, 4 module activates the expression of a repressor, which mediates the repression of target gene expression.

The first and second cysteine of the active site motif are not required for the function of ROXY6, 7, 8, 9, thus it is concluded that neither oxidoreductase activity nor Fe-S cluster binding are involved in the regulation of gene expression by ROXY6, 7, 8, 9. However, the active site needs to be somewhat intact as revealed by our finding that the CPYC version is non-functional.

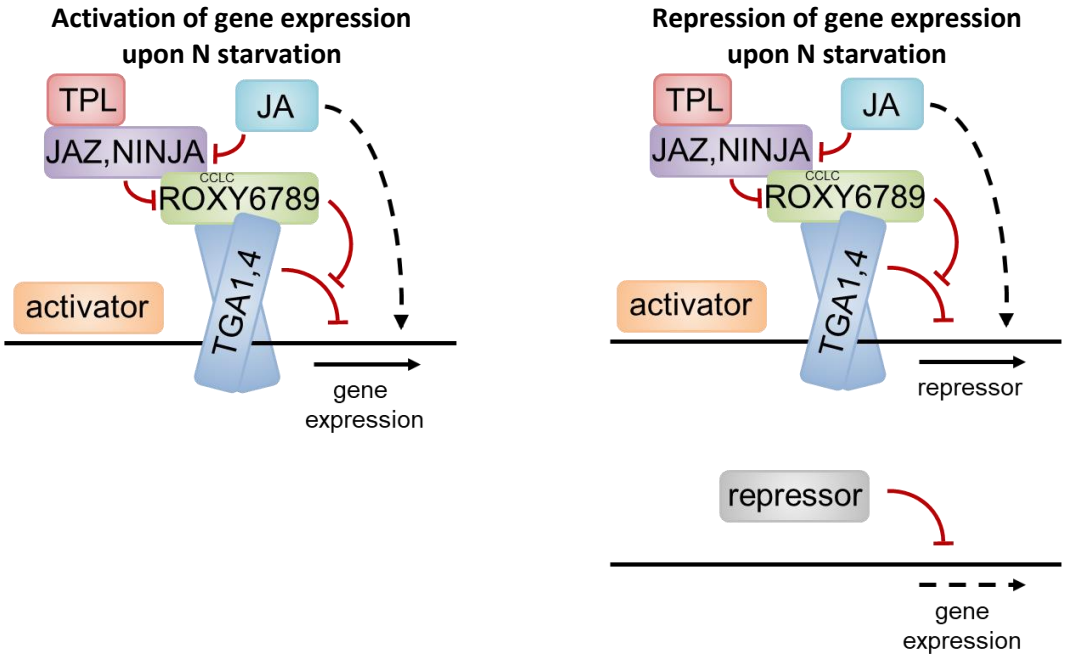

Figure 54: Proposed model for the regulation of ROXY6, 7, 8, 9 target genes upon nitrogen starvation. To induce gene expression upon nitrogen (N) starvation, ROXY6, 7, 8, 9 interfere with the repressive mechanism of TGA1, 4. An additional activator contributes to the activation. Through the recruitment of TOPLESS (TPL), JAZMONATE ZIM DOMAIN (JAZ) and NOVEL INTERACTOR OF JAZ (NINJA), ROXY6, 7, 8, 9 is repressed. Jasmonic acid (JA) treatment might enhance the gene expression as it leads to the degradation of JAZ. To repress gene expression, ROXY6, 7, 8, 9 activate the transcription of a repressor. The repressor then negatively regulates gene expression.

Besides, we investigated the differential roles of clade I and II TGAs in the establishment of systemic acquired resistance (SAR). In *Psm*-infected SAR leaves, NPR1 and TGA1, 4 activate the expression of *WRKY50*, *51* (Figure 55). SARD1 and WRKY50, 51 might activate some SAR-induced genes together. Additionally, both TGA clades activate *WRKY75* and *WRKY31* expression. SARD1 might also contribute to this activation. WRKY75, WRKY31 and SARD1 might activate the expression of *ICS1*, *PBS1*, *ALD1* and *FMO1*. TGA2, 5, 6 might also be directly involved in the activation of SAR-induced genes which contain a TGACG motif in the promoter region.

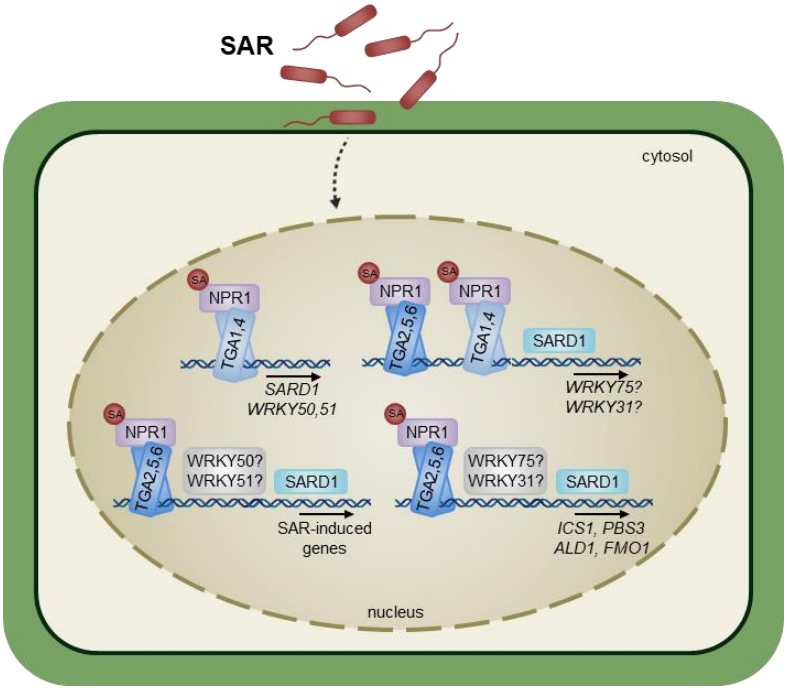

Figure 55: Proposed model for the regulation of gene expression by clade I and II TGAs in SAR conditions. TGA1, 4 and NPR1 activate the expression of *SARD1* and *WRKY50, 51* in SAR conditions. Some SAR-induced genes might be activated by SARD1 and WRKY50, 51. Clade I and II TGAs might activate *WRKY75* and *WRKY31* expression together with NPR1 and SARD1. WRKY75, WRKY31 and SARD1 might induce the expression of *ICS1*, *PBS3*, *ALD1* and *FMO1*. In addition, TGA2, 5, 6 might be involved in the activation of SAR-induced genes. SA: salicylic acid.

9. References

Acosta, I. F., Gasperini, D., Chételat, A., Stolz, S., Santuari, L., & Farmer, E. E. (2013). Role of NINJA in root jasmonate signaling. *Proceedings of the National Academy of Sciences, 110*(38), 15473–15478. https://doi.org/10.1073/pnas.1307910110.

Afgan, E., Baker, D., Batut, B., van den Beek, M., Bouvier, D., Cech, M., Chilton, J., Clements, D., Coraor, N., Gruning, B. A., Guerler, A., Hillman-Jackson, J., Hiltemann, S., Jalili, V., Rasche, H., Soranzo, N., Goecks, J., Taylor, J., Nekrutenko, A., & Blankenberg, D. (2018). The Galaxy platform for accessible, reproducible and collaborative biomedical analyses: 2018 update. *Nucleic Acids Research, 46*(W1), W537-W544. https://doi.org/10.1093/nar/gky379.

Alvarez, J. M., Riveras, E., Vidal, E. A., Gras, D. E., Contreras-Lopez, O., Tamayo, K. P., Aceituno, F., Gomez, I., Ruffel, S., Lejay, L., Jordana, X., & Rodrigo A. Gutiérrez (2014). Systems approach identifies TGA1 and TGA4 transcription factors as important regulatory components of the nitrate response of Arabidopsis thaliana roots. *The Plant Journal, 80*(1), 1–13. https://doi.org/10.1111/tpj.12618.

Anders, S., Pyl, P. T., & Huber, W. (2015). HTSeq—a Python framework to work with high-throughput sequencing data. *Bioinformatics, 31*(2), 166–169. https://doi.org/10.1093/bioinformatics/btu638.

Arabidopsis Interactome Mapping Consortium (2011). Evidence for network evolution in an Arabidopsis interactome map. *Science, 333*(6042), 601–607. https://doi.org/10.1126/science.1203877.

Araya, T., Miyamoto, M., Wibowo, J., Suzuki, A., Kojima, S., Tsuchiya, Y. N., Sawa, S., Fukuda, H., Wirén, N. von, & Takahashi, H. (2014). CLE-CLAVATA1 peptide-receptor signaling module regulates the expansion of plant root systems in a nitrogen-dependent manner. *Proceedings of the National Academy of Sciences, 111*(5), 2029–2034. https://doi.org/10.1073/pnas.1319953111.

Ashburner, M., Ball, C. A., Blake, J. A., Botstein, D., Butler, H., Cherry, J. M., Davis, A. P., Dolinski, K., Dwight, S. S., Eppig, J. T., Harris, Midori A., Hill, David P., Issel-Tarver, L., Kasarskis, A., Lewis, S., Matese, J. C., Richardson, J. E., Ringwald, M., Rubin, G. M., & Sherlock, G. (2000). Gene ontology: tool for the unification of biology. *Nature Genetics, 25*(1), 25–29. https://doi.org/10.1038/75556.

Azam, T., Przybyla-Toscano, J., Vignols, F., Couturier, J., Rouhier, N., & Johnson, M. K. (2020). The Arabidopsis Mitochondrial Glutaredoxin GRXS15 Provides 2Fe-2S Clusters for ISCA-Mediated 4Fe-4S Cluster Maturation. *International Journal of Molecular Sciences, 21*(23). https://doi.org/10.3390/ijms21239237.

Bandyopadhyay, S., Gama, F., Molina-Navarro, M. M., Gualberto, J. M., Claxton, R., Naik, S. G., Huynh, B. H., Herrero, E., Jacquot, J. P., Johnson, M. K., & Rouhier, N. (2008). Chloroplast monothiol glutaredoxins as scaffold proteins for the assembly and delivery of 2Fe-2S clusters. *The EMBO Journal, 27*(7), 1122–1133. https://doi.org/10.1038/emboj.2008.50.

Baxter, C. E., Costa, M. M. R., & Coen, E. S. (2007). Diversification and co-option of RAD-like genes in the evolution of floral asymmetry. *The Plant Journal, 52*(1), 105–113. https://doi.org/10.1111/j.1365-313X.2007.03222.x.

Behringer, C., Bartsch, K., & Schaller, A. (2011). Safeners recruit multiple signalling pathways for the orchestrated induction of the cellular xenobiotic detoxification machinery in Arabidopsis. *Plant, Cell & Environment, 34*(11), 1970–1985. https://doi.org/10.1111/j.1365-3040.2011.02392.x.

Bender, K. W., Wang, X., Cheng, G. B., Kim, H. S., Zielinski, R. E., & Huber, S. C. (2015). Glutaredoxin AtGRXC2 catalyses inhibitory glutathionylation of Arabidopsis BRI1-associated receptor-like kinase 1 (BAK1) in vitro. *The Biochemical Journal, 467*(3), 399–413. https://doi.org/10.1042/BJ20141403.

Berendzen, K. W., Weiste, C., Wanke, D., Kilian, J., Harter, K., & Dröge-Laser, W. (2010). Bioinformatic cis-element analyses performed in Arabidopsis and rice disclose bZIP-and MYB-related binding sites as potential AuxRE-coupling elements in auxin-mediated transcription. *BMC Plant Biology, 12*(1), 1–19. https://doi.org/10.1186/1471-2229-12-125.

Bertani, G. (1951). Studies on lysogenesis I. The mode of phage liberation by lysogenic Escherichia coli. *Journal of Bacteriology, 62*(2), 293–300. https://doi.org/10.1128/jb.62.3.293-300.1951.

Boter, M., Ruíz-Rivero, O., Abdeen, A., & Prat, S. (2004). Conserved MYC transcription factors play a key role in jasmonate signaling both in tomato and Arabidopsis. *Genes & Development, 18*(13), 1577–1591. https://doi.org/10.1101/gad.297704.

Branon, T. C., Bosch, J. A., Sanchez, A. D., Udeshi, N. D., Svinkina, T., Carr, S. A., Feldmann, J. L., Perrimon, N., & Ting, A. Y. (2018). Efficient proximity labeling in living cells and organisms with TurboID. *Nature Biotechnology, 36*(9), 880–887. https://doi.org/10.1038/nbt.4201.

Bu, Q., Jiang, H., Li, C.-B., Zhai, Q., Zhang, J., Wu, X., Sun, J., Xie, Q., & Li, C. (2008). Role of the Arabidopsis thaliana NAC transcription factors ANAC019 and ANAC055 in regulating jasmonic acid-signaled defense responses. *Cell Research, 18*(7), 756–767. https://doi.org/10.1038/cr.2008.53.

Budimir, J. (2019). Regulation of clade I TGA transcription factors of Arabidopsis thaliana during salicylic acid mediated defense response. *PhD Thesis, Georg-August Universität, Göttingen, Germany*.

Budimir, J., Treffon, K., Nair, A., Thurow, C., & Gatz, C. (2021). Redox-active cysteines in TGACG-BINDING FACTOR 1 (TGA1) do not play a role in salicylic acid or pathogen-induced expression of TGA1-regulated target genes in Arabidopsis thaliana. *New Phytologist, 230*(6), 2420–2432. https://doi.org/10.1111/nph.16614.

Büttner, M., & Singh, K. B. (1997). Arabidopsis thaliana ethylene-responsive element binding protein (AtEBP), an ethylene-inducible, GCC box DNA-binding protein interacts with an ocs element binding protein. *Proceedings of the National Academy of Sciences, 94*(11), 5961–5966. https://doi.org/10.1073/pnas.94.11.5961.

Camañes, G., Pastor, V., Cerezo, M., García-Andrade, J., Vicedo, B., García-Agustín, P., & Flors, V. (2012). A deletion in NRT2.1 attenuates Pseudomonas syringae-induced hormonal perturbation, resulting in primed plant defenses. *Plant Physiology, 158*(2), 1054–1066. https://doi.org/10.1104/pp.111.184424.

Campbell, A. (1961). Sensitive mutants of bacteriophage λ. *Virology, 14*(1). https://doi.org/10.1016/0042-6822(61)90128-3.

Cao, H., Glazebrook, J., Clarke, J. D., Volko, S., & Dong, X. (1997). The Arabidopsis NPR1 gene that controls systemic acquired resistance encodes a novel protein containing ankyrin repeats. *Cell, 88*(1), 57–63. https://doi.org/10.1016/S0092-8674(00)81858-9.

Carbon, S., & Mungall, C. (2018). Gene Ontology Data Reference. *Dataset*. https://doi.org/10.5281/zenodo.6363681.

Causier, B., Ashworth, M., Guo, W., & Davies, B. (2012). The TOPLESS interactome: a framework for gene repression in Arabidopsis. *Plant Physiology, 158*(1), 423–438. https://doi.org/10.1104/pp.111.186999.

Cerezo, M., Tillard, P., Filleur, S., Muños, S., Daniel-Vedele, F., & Gojon, A. (2001). Major alterations of the regulation of root NO(3)(-) uptake are associated with the mutation of Nrt2.1 and Nrt2.2 genes in Arabidopsis. *Plant Physiology, 127*(1), 262–271. https://doi.org/10.1104/pp.127.1.262.

Chapman, K., Taleski, M., Ogilvie, H. A., Imin, N., & Djordjevic, M. A. (2019). CEP–CEPR1 signalling inhibits the sucrose-dependent enhancement of lateral root growth. *Journal of Experimental Botany, 70*(15), 3955–3967. https://doi.org/10.1093/jxb/erz207.

Chen, C.-Z., Lv, X.-F., Li, J.-Y., Yi, H.-Y., & Gong, J.-M. (2012a). Arabidopsis NRT1.5 is another essential component in the regulation of nitrate reallocation and stress tolerance. *Plant Physiology, 159*(4), 1582–1590. https://doi.org/10.1104/pp.112.199257.

Chen, F., Li, Y., Li, X., Li, W., Xu, J., Cao, H., Wang, Z., Soppe, W. J. J., & Liu, Y. (2021). Ectopic expression of the Arabidopsis florigen gene FLOWERING LOCUS T in seeds enhances seed dormancy via the GA and DOG1 pathways. *The Plant Journal, 107*(3), 909–924. https://doi.org/10.1111/tpj.15354.

Chen, L.-Q., Qu, X.-Q., Hou, B.-H., Sosso, D., Osorio, S., Fernie, A. R., & Frommer, W. B. (2012b). Sucrose efflux mediated by SWEET proteins as a key step for phloem transport. *Science, 335*(6065), 207–211. https://doi.org/10.1126/science.1213351.

Cheng, N.-H. (2008). AtGRX4, an Arabidopsis chloroplastic monothiol glutaredoxin, is able to suppress yeast grx5 mutant phenotypes and respond to oxidative stress. *FEBS Letters, 582*(6), 848–854. https://doi.org/10.1016/j.febslet.2008.02.006.

Cheng, N.-H., Liu, J.-Z., Brock, A., Nelson, R. S., & Hirschi, K. D. (2006). AtGRXcp, an Arabidopsis chloroplastic glutaredoxin, is critical for protection against protein oxidative damage. *Journal of Biological Chemistry, 281*(36), 26280–26288. https://doi.org/10.1074/jbc.M601354200.

Cheng, N.-H., Liu, J.-Z., Liu, X., Wu, Q., Thompson, S. M., Lin, J., Chang, J., Whitham, S. A., Park, S., Cohen, J. D., & Hirschi, K. D. (2011). Arabidopsis monothiol glutaredoxin, AtGRXS17, is critical for temperature-dependent postembryonic growth and development via modulating auxin response. *Journal of Biological Chemistry, 286*(23), 20398–20406. https://doi.org/10.1074/jbc.M110.201707.

Cheng, Y. T., Germain, H., Wiermer, M., Bi, D., Xu, F., García, A. V., Wirthmueller, L., Després, C., Parker, J. E., Zhang, Y., & Li, X. (2009). Nuclear pore complex component MOS7/Nup88 is required for innate immunity and nuclear accumulation of defense regulators in Arabidopsis. *The Plant Cell, 21*(8), 2503–2516. https://doi.org/10.1105/tpc.108.064519.

Cheong, Y. H., Chang, H.-S., Gupta, R., Wang, X., Zhu, T., & Luan, S. (2002). Transcriptional profiling reveals novel interactions between wounding, pathogen, abiotic stress, and hormonal responses in Arabidopsis. *Plant Physiology, 129*(2), 661–677. https://doi.org/10.1104/pp.002857.

Choi, J., Huh, S. U., Kojima, M., Sakakibara, H., Paek, K.-H., & Hwang, I. (2010). The cytokinin-activated transcription factor ARR2 promotes plant immunity via TGA3/NPR1-dependent salicylic acid signaling in Arabidopsis. *Developmental Cell, 19*(2), 284–295. https://doi.org/10.1016/j.devcel.2010.07.011.

Chomczynski, P., & Mackey, K. (1995). Short technical report. Modification of the TRIZOL reagent procedure for isolation of RNA from Polysaccharide-and proteoglycan-rich sources. *Biotechniques, 19*(6), 942–945.

Chuang, C. F., Running, M. P., Williams, R. W., & Meyerowitz, E. M. (1999). The PERIANTHIA gene encodes a bZIP protein involved in the determination of floral organ number in Arabidopsis thaliana. *Genes & Development, 13*(3), 334–344. https://doi.org/10.1101/gad.13.3.334.

Clough, S. J., & Bent, A. F. (1998). Floral dip: a simplified method for Agrobacterium-mediated transformation of Arabidopsis thaliana. *The Plant Journal, 16*(6), 735–743. https://doi.org/10.1046/j.1365-313x.1998.00343.x.

Courey, A. J., Holtzman, D. A., Jackson, S. P., & Tjian, R. (1989). Synergistic activation by the glutamine-rich domains of human transcription factor Sp1. *Cell, 59*(5), 827–836. https://doi.org/10.1016/0092-8674(89)90606-5.

Couturier, J., Jacquot, J.-P., & Rouhier, N. (2013). Toward a refined classification of class I dithiol glutaredoxins from poplar: biochemical basis for the definition of two subclasses. *Frontiers in Plant Science, 4*, 518. https://doi.org/10.3389/fpls.2013.00518.

Couturier, J., Ströher, E., Albetel, A.-N., Roret, T., Muthuramalingam, M., Tarrago, L., Seidel, T., Tsan, P., Jacquot, J.-P., Johnson, M. K., Dietz, K.-J., Didierjean, C., & Rouhier, N. (2011). Arabidopsis chloroplastic glutaredoxin C5 as a model to explore molecular determinants for iron-sulfur cluster binding into glutaredoxins. *Journal of Biological Chemistry, 286*(31), 27515–27527. https://doi.org/10.1074/jbc.M111.228726.

Cox, M. C., Millenaar, F. F., Van Berkel, Y E, Peeters, A J, & Voesenek, L. A. (2003). Plant movement. Submergence-induced petiole elongation in Rumex palustris depends on hyponastic growth. *Plant Physiology, 132*(1), 282–291. https://doi.org/10.1104/pp.102.014548.

Das, P., Ito, T., Wellmer, F., Vernoux, T., Dedieu, A., Traas, J., & Meyerowitz, E. M. (2009). Floral stem cell termination involves the direct regulation of AGAMOUS by PERIANTHIA. *Development, 136*(10), 1605–1611. https://doi.org/10.1242/dev.035436.

de Vos, M., Denekamp, M., Dicke, M., Vuylsteke, M., van Loon, L., Smeekens, S. C., & Pieterse, C. M. (2006). The Arabidopsis thaliana Transcription Factor AtMYB102 Functions in Defense Against the Insect Herbivore Pieris rapae. *Plant Signaling & Behavior, 1*(6), 305–311. https://doi.org/10.4161/psb.1.6.3512.

Dechorgnat, J., Patrit, O., Krapp, A., Fagard, M., & Daniel-Vedele, F. (2012). Characterization of the Nrt2.6 gene in Arabidopsis thaliana: a link with plant response to biotic and abiotic stress. *PLoS One, 7*(8), e42491. https://doi.org/10.1371/journal.pone.0042491.

Deponte, M. (2013). Glutathione catalysis and the reaction mechanisms of glutathione-dependent enzymes. *Biochimica et Biophysica Acta (BBA)-General Subjects, 1830*(5), 3217–3266. https://doi.org/10.1016/j.bbagen.2012.09.018.

Després, C., Chubak, C., Rochon, A., Clark, R., Bethune, T., Desveaux, D., & Fobert, P. R. (2003). The Arabidopsis NPR1 disease resistance protein is a novel cofactor that confers redox regulation of DNA binding activity to the basic domain/leucine zipper transcription factor TGA1. *The Plant Cell, 15*(9), 2181–2191. https://doi.org/10.1105/tpc.012849.

Després, C., DeLong, C., Glaze, S., Liu, E., & Fobert, P. R. (2000). The Arabidopsis NPR1/NIM1 Protein Enhances the DNA Binding Activity of a Subgroup of the TGA Family of bZIP Transcription Factors. *The Plant Cell, 12*(2), 279–290. https://doi.org/10.1105/tpc.12.2.279.

Ding, P., Rekhter, D., Ding, Y., Feussner, K., Busta, L., Haroth, S., Xu, S., Li, X., Jetter, R., Feussner, I., & Zhang, Y. (2016). Characterization of a Pipecolic Acid Biosynthesis Pathway Required for Systemic Acquired Resistance. *The Plant Cell, 28*(10), 2603–2615. https://doi.org/10.1105/tpc.16.00486.

Ding, Y., Sun, T., Ao, K., Peng, Y., Zhang, Y., Li, X., & Zhang, Y. (2018). Opposite roles of salicylic acid receptors NPR1 and NPR3/NPR4 in transcriptional regulation of plant immunity. *Cell, 173*(6), 1454–1467. https://doi.org/10.1016/j.cell.2018.03.044.

Divi, U. K., Rahman, T., & Krishna, P. (2010). Brassinosteroid-mediated stress tolerance in Arabidopsis shows interactions with abscisic acid, ethylene and salicylic acid pathways. *BMC Plant Biology, 10*, 151. https://doi.org/10.1186/1471-2229-10-151.

Domagalska, M. A., Sarnowska, E., Nagy, F., & Davis, S. J. (2010). Genetic analyses of interactions among gibberellin, abscisic acid, and brassinosteroids in the control of flowering time in Arabidopsis thaliana. *PLoS One, 5*(11), e14012. https://doi.org/10.1371/journal.pone.0014012.

Dombrecht, B., Xue, G. P., Sprague, S. J., Kirkegaard, J. A., Ross, J. J., Reid, J. B., Fitt, G. P., Sewelam, N., Schenk, P. M., Manners, J. M., & Kazan, K. (2007). MYC2 differentially modulates diverse jasmonate-dependent functions in Arabidopsis. *The Plant Cell, 19*(7), 2225–2245. https://doi.org/10.1105/tpc.106.048017.

Dong, X. (2004). NPR1, all things considered. *Current Opinion in Plant Biology, 7*(5), 547–552. https://doi.org/10.1016/j.pbi.2004.07.005.

Durand, M., Porcheron, B., Hennion, N., Maurousset, L., Lemoine, R., & Pourtau, N. (2016). Water Deficit Enhances C Export to the Roots in Arabidopsis thaliana Plants with Contribution of Sucrose Transporters in Both Shoot and Roots. *Plant Physiology, 170*(3), 1460–1479. https://doi.org/10.1104/pp.15.01926.

Ellenberger, T. E., Brandl, C. J., Struhl, K., & Harrison, S. C. (1992). The GCN4 basic region leucine zipper binds DNA as a dimer of uninterrupted alpha helices: crystal structure of the protein-DNA complex. *Cell, 71*(7), 1223–1237. https://doi.org/10.1016/s0092-8674(05)80070-4.

Eulgem, T., & Somssich, I. E. (2007). Networks of WRKY transcription factors in defense signaling. *Current Opinion in Plant Biology, 10*(4), 366–371. https://doi.org/10.1016/j.pbi.2007.04.020.

Feng, Y., Zhong, N., Rouhier, N., Hase, T., Kusunoki, M., Jacquot, J. P., Jin, C., & Xia, B. (2006). Structural insight into poplar glutaredoxin C1 with a bridging iron− sulfur cluster at the active site. *Biochemistry, 45*(26), 7998–8008. https://doi.org/10.1021/bi060444t.

Fernández-Calvo, P., Chini, A., Fernández-Barbero, G., Chico, J. M., Gimenez-Ibanez, S., Geerinck, J., Eeckhout, D., Schweizer, F., Godoy, M., Franco-Zorrilla, José Manuel, Pauwels, Laurens, Witters, E., Puga, M. I., Paz-Ares, J., Goossens, A., Reymond, P., Jaeger, G. de, & Solano, R. (2011). The Arabidopsis bHLH transcription factors MYC3 and MYC4 are targets of JAZ repressors and act additively with MYC2 in the activation of jasmonate responses. *The Plant Cell, 23*(2), 701–715. https://doi.org/10.1105/tpc.110.080788.

Findling, S., Stotz, H. U., Zoeller, M., Krischke, M., Zander, M., Gatz, C., Berger, S., & Mueller, M. J. (2018). TGA2 signaling in response to reactive electrophile species is not dependent on cysteine modification of TGA2. *PLoS One, 13*(4), e0195398. https://doi.org/10.1371/journal.pone.0195398.

Fode, B., Siemsen, T., Thurow, C., Weigel, R., & Gatz, C. (2008). The Arabidopsis GRAS Protein SCL14 Interacts with Class II TGA Transcription Factors and Is Essential for the Activation of Stress-Inducible Promoters. *The Plant Cell, 20*(11), 3122–3135. https://doi.org/10.1105/tpc.108.058974.

Fry, S. C., Smith, R. C., Renwick, K. F., Martin, D. J., Hodge, S. K., & Matthews, K. J. (1992). Xyloglucan endotransglycosylase, a new wall-loosening enzyme activity from plants. *The Biochemical Journal, 282*(3), 821–828. https://doi.org/10.1042/bj2820821.

Gao, H., Subramanian, S., Couturier, J., Naik, S. G., Kim, S.-K., Leustek, T., Knaff, D. B., Wu, H.-C., Vignols, F., Huynh, B. H., Rouhier, N., & Johnson, M. K. (2013). Arabidopsis thaliana Nfu2 accommodates 2Fe-2S or 4Fe-4S clusters and is competent for in vitro maturation of chloroplast 2Fe-2S and 4Fe-4S cluster-containing proteins. *Biochemistry, 52*(38), 6633–6645. https://doi.org/10.1021/bi4007622.

Gao, Q.-M., Venugopal, S., Navarre, D., & Kachroo, A. (2011). Low Oleic Acid-Derived Repression of Jasmonic Acid-Inducible Defense Responses Requires the WRKY50 and WRKY51 Proteins. *Plant Physiology, 155*(1), 464–476. https://doi.org/10.1104/pp.110.166876.

Garcion, C., Lohmann, A., Lamodière, E., Catinot, J., Buchala, A., Doermann, P., & Métraux, J.-P. (2008). Characterization and biological function of the ISOCHORISMATE SYNTHASE2 gene of Arabidopsis. *Plant Physiology, 147*(3), 1279–1287. https://doi.org/10.1104/pp.108.119420.

Gatz, C. (2013). From pioneers to team players: TGA transcription factors provide a molecular link between different stress pathways. *Molecular Plant–Microbe Interactions, 26*(2), 151–159. https://doi.org/10.1094/MPMI-04-12-0078-IA.

Gautrat, P., Laffont, C., & Frugier, F. (2020). Compact Root Architecture 2 Promotes Root Competence for Nodulation through the miR2111 Systemic Effector. *Current biology : CB, 30*(7), 1339-1345.e3. https://doi.org/10.1016/j.cub.2020.01.084.

Gemayel, R., Chavali, S., Pougach, K., Legendre, M., Zhu, B., Boeynaems, S., van der Zande, E., Gevaert, K., Rousseau, F., Schymkowitz, J., Babu, M. M., & Verstrepen, K. J. (2015). Variable Glutamine-Rich Repeats Modulate Transcription Factor Activity. *Molecular Cell, 59*(4), 615–627. https://doi.org/10.1016/j.molcel.2015.07.003.

The Gene Ontology Consortium (2021). The Gene Ontology resource: enriching a GOld mine. *Nucleic Acids Research, 49*(D1), D325-D334. https://doi.org/10.1093/nar/gkaa1113.

Glazebrook, J. (2005). Contrasting mechanisms of defense against biotrophic and necrotrophic pathogens. *Annual Review of Phytopathology, 43*, 205–227. https://doi.org/10.1146/annurev.phyto.43.040204.135923.

Gómez-Mena, C., & Sablowski, R. (2008). ARABIDOPSIS THALIANA HOMEOBOX GENE1 establishes the basal boundaries of shoot organs and controls stem growth. *The Plant Cell, 20*(8), 2059–2072. https://doi.org/10.1105/tpc.108.059188.

Gravina, S. A., & Mieyal, J. J. (1993). Thioltransferase is a specific glutathionyl mixed disulfide oxidoreductase. *Biochemistry, 32*(13), 3368–3376. https://doi.org/10.1021/bi00064a021.

Grierson, C., Du, J. S., Torres Zabala, M. de, Beggs, K., Smith, C., Holdsworth, M., & Bevan, M. (1994). Separate cis sequences and trans factors direct metabolic and developmental regulation of a potato tuber storage protein gene. *The Plant Journal, 5*(6), 815–826.

Griffith, O. W., & Meister, A. (1979). Potent and specific inhibition of glutathione synthesis by buthionine sulfoximine (S-n-butyl homocysteine sulfoximine). *Journal of Biological Chemistry, 254*(16), 7558–7560. https://doi.org/10.1016/S0021-9258(18)35980-5.

Gubler, F., & Jacobsen, J. V. (1992). Gibberellin-responsive elements in the promoter of a barley high-pI alpha-amylase gene. *The Plant Cell, 4*(11), 1435–1441. https://doi.org/10.1105/tpc.4.11.1435.

Guo, P., Li, Z., Huang, P., Li, B., Fang, S., Chu, J., & Guo, H. (2017). A Tripartite Amplification Loop Involving the Transcription Factor WRKY75, Salicylic Acid, and Reactive Oxygen Species Accelerates Leaf Senescence. *The Plant Cell, 29*(11), 2854–2870. https://doi.org/10.1105/tpc.17.00438.

Guo, Q., Yoshida, Y., Major, I. T., Wang, K., Sugimoto, K., Kapali, G., Havko, N. E., Benning, C., & Howe, G. A. (2018). JAZ repressors of metabolic defense promote growth and reproductive fitness in Arabidopsis. *Proceedings of the National Academy of Sciences, 115*(45), E10768-E10777. https://doi.org/10.1073/pnas.1811828115.

Gutsche, N., & Zachgo, S. (2016). The N-Terminus of the Floral Arabidopsis TGA Transcription Factor PERIANTHIA Mediates Redox-Sensitive DNA-Binding. *PLoS One, 11*(4), e0153810. https://doi.org/10.1371/journal.pone.0153810.

Han, Q., Tan, W., Zhao, Y., Yang, F., Yao, X., Lin, H., & Zhang, D. (2022). Salicylic acid-activated BIN2 phosphorylation of TGA3 promotes Arabidopsis PR gene expression and disease resistance. *The EMBO Journal, 41*(19), e110682. https://doi.org/10.15252/embj.2022110682.

Hanahan, D. (1983). Studies on transformation of Escherischia coli with plasmids. *Journal of Molecular Biology, 166*(4), 557–580. https://doi.org/10.1016/S0022-2836(83)80284-8.

Hartmann, M., Kim, D., Bernsdorff, F., Ajami-Rashidi, Z., Scholten, N., Schreiber, S., Zeier, T., Schuck, S., Reichel-Deland, V., & Zeier, J. (2017). Biochemical Principles and Functional Aspects of Pipecolic Acid Biosynthesis in Plant Immunity. *Plant Physiology, 174*(1), 124–153. https://doi.org/10.1104/pp.17.00222.

Hartmann, M., Zeier, T., Bernsdorff, F., Reichel-Deland, V., Kim, D., Hohmann, M., Scholten, N., Schuck, S., Bräutigam, A., Hölzel, T., Ganter, C., & Zeier, J. (2018). Flavin Monooxygenase-Generated N-Hydroxypipecolic Acid Is a Critical Element of Plant Systemic Immunity. *Cell, 173*(2), 456-469. https://doi.org/10.1016/j.cell.2018.02.049.

Hepworth, S. R., Zhang, Y., McKim, S., Li, X., & Haughn, G. W. (2005). BLADE-ON-PETIOLE-Dependent Signaling Controls Leaf and Floral Patterning in Arabidopsis. *The Plant Cell, 17*(5), 1434–1448. https://doi.org/10.1105/tpc.104.030536.

Herrera-Vásquez, A., Fonseca, A., Ugalde, J. M., Lamig, L., Seguel, A., Moyano, T. C., Gutiérrez, R. A., Salinas, P., Vidal, E. A., & Holuigue, L. (2021). TGA class II transcription factors are essential to restrict oxidative stress in response to UV-B stress in Arabidopsis. *Journal of Experimental Botany, 72*(5), 1891–1905. https://doi.org/10.1093/jxb/eraa534.

Holmgren, A. (1976). Hydrogen donor system for Escherichia coli ribonucleoside-diphosphate reductase dependent upon glutathione. *Proceedings of the National Academy of Sciences, 73*(7), 2275–2279. https://doi.org/10.1073/pnas.73.7.2275.

Huang, L.-J., Li, N., Thurow, C., Wirtz, M., Hell, R., & Gatz, C. (2016). Ectopically expressed glutaredoxin ROXY19 negatively regulates the detoxification pathway in Arabidopsis thaliana. *BMC Plant Biology, 16*(1), 200. https://doi.org/10.1186/s12870-016-0886-1.

Hulsen, T., Vlieg, J. de, & Alkema, W. (2008). BioVenn – a web application for the comparison and visualization of biological lists using area-proportional Venn diagrams. *BMC Genomics, 9*(1), 1–6. https://doi.org/10.1186/1471-2164-9-488.

Huot, B., Yao, J., Montgomery, B. L., & He, S. Y. (2014). Growth-defense tradeoffs in plants: a balancing act to optimize fitness. *Molecular Plant, 7*(8), 1267–1287. https://doi.org/10.1093/mp/ssu049.

Hussain, R. M. F., Sheikh, A. H., Haider, I., Quareshy, M., & Linthorst, H. J. M. (2018). Arabidopsis WRKY50 and TGA Transcription Factors Synergistically Activate Expression of PR1. *Frontiers in Plant Science, 9*, 930. https://doi.org/10.3389/fpls.2018.00930.

Iwema, T., Picciocchi, A., Traore, D. A. K., Ferrer, J.-L., Chauvat, F., & Jacquamet, L. (2009). Structural basis for delivery of the intact Fe2S2 cluster by monothiol glutaredoxin. *Biochemistry, 48*(26), 6041–6043. https://doi.org/10.1021/bi900440m.

Izawa, T., Foster, R., & Chua, N. H. (1993). Plant bZIP protein DNA binding specificity. *Journal of Molecular Biology, 230*(4), 1131–1144. https://doi.org/10.1006/jmbi.1993.1230.

Jakoby, M., Weisshaar, B., Droge-Laser, W., Vincente-Carbajosa, J., Tiedemann, J., Kroj, T., & Parcy, F. (2002). bZIP transcription factors in Arabidopsis. *Trends in Plant Science, 7*(3), 106–111. https://doi.org/10.1016/S1360-1385(01)02223-3.

Jiang, W.-B., Huang, H.-Y., Hu, Y.-W., Zhu, S.-W., Wang, Z.-Y., & Lin, W.-H. (2013). Brassinosteroid regulates seed size and shape in Arabidopsis. *Plant Physiology, 162*(4), 1965–1977. https://doi.org/10.1104/pp.113.217703.

Johannessen, M., Delghandi, M. P., Seternes, O. M., Johansen, B., & Moens, U. (2004). Synergistic activation of CREB-mediated transcription by forskolin and phorbol ester requires PKC and depends on the glutamine-rich Q2 transactivation domain. *Cellular Signalling, 16*(10), 1187–1199. https://doi.org/10.1016/j.cellsig.2004.03.009.

Johnson, E. T., & Dowd, P. F. (2004). Differentially enhanced insect resistance, at a cost, in Arabidopsis thaliana constitutively expressing a transcription factor of defensive metabolites. *Journal of Agricultural and Food Chemistry, 52*(16), 5135–5138. https://doi.org/10.1021/jf0308049.

Jung, F. (2016). Analysis of the defense responses of Arabidopsis thaliana tga1,4 knockout mutants and plants ectopically expressing ROXY9 and establishment of a roxy9 knockout mutant. *Master Thesis, Georg-August Universität, Göttingen, Germany*.

Jung, J.-Y., Ahn, J. H., & Schachtman, D. P. (2018). CC-type glutaredoxins mediate plant response and signaling under nitrate starvation in Arabidopsis. *BMC Plant Biology, 18*(1), 281. https://doi.org/10.1186/s12870-018-1512-1.

Kachroo, P., Shanklin, J., Shah, J., Whittle, E. J., & Klessig, D. F. (2001). A fatty acid desaturase modulates the activation of defense signaling pathways in plants. *Proceedings of the National Academy of Sciences, 98*(16), 9448–9453. https://doi.org/10.1073/pnas.151258398.

Kaever, A., Landesfeind, M., Feussner, K., Mosblech, A., Heilmann, I., Morgenstern, B., Feussner, I., & Meinicke, P. (2015). MarVis-Pathway: integrative and exploratory pathway analysis of non-targeted metabolomics data. *Metabolomics, 11*(3), 764–777. https://doi.org/10.1007/s11306-014-0734-y.

Kaever, A., Lingner, T., Feussner, K., Göbel, C., Feussner, I., & Meinicke, P. (2009). MarVis: a tool for clustering and visualization of metabolic biomarkers. *BMC Bioinformatics, 10*, 92. https://doi.org/10.1186/1471-2105-10-92.

Katagiri, F., Lam, E., & Chua, N. H. (1989). Two tobacco DNA-binding proteins with homology to the nuclear factor CREB. *Nature, 340*(6236), 727–730. https://doi.org/10.1038/340727a0.

Katzen, F. (2007). Gateway® recombinational cloning: a biological operating system. *Expert Opinion on Drug Discovery, 2*(4), 571–589. https://doi.org/10.1517/17460441.2.4.571.

Kesarwani, M., Yoo J., & Dong X. (2007). Genetic interactions of TGA transcription factors in the regulation of pathogenesis-related genes and disease resistance in Arabidopsis. *Plant Physiology, 144*(1), 336–346. https://doi.org/10.1104/pp.106.095299.

Khan, M., Ragni, L., Tabb, P., Salasini, B. C., Chatfield, S., Datla, R., Lock, J., Kuai, X., Després, C., Proveniers, M., Yongguo, C., Xiang, D., Morin, H., Rullière, J.-P., Citerne, S., Hepworth, S. R., & Pautot, V. (2015). Repression of Lateral Organ Boundary Genes by PENNYWISE and POUND-FOOLISH Is Essential for Meristem Maintenance and Flowering in Arabidopsis. *Plant Physiology, 169*(3), 2166–2186. https://doi.org/10.1104/pp.15.00915.

Kiba, T., Feria-Bourrellier, A. B., Lafouge, F., Lezhneva, L., Boutet-Mercey, S., Orsel, M., Bréhaut, V., Miller, A., Daniel-Vedele, F., Sakakibara, H., & Krapp, A. (2012). The Arabidopsis nitrate transporter NRT2. 4 plays a double role in roots and shoots of nitrogen-starved plants. *The Plant Cell, 24*(1), 245–258.

Kim, T.-W., Park, C. H., Hsu, C.-C., Zhu, J.-Y., Hsiao, Y., Branon, T., Xu, S.-L., Ting, A. Y., & Wang, Z.-Y. (2019). Application of TurboID-mediated proximity labeling for mapping a GSK3 kinase signalling network in Arabidopsis. *bioRxiv*, 636324. https://doi.org/10.1101/636324.

Kim, Y.-W., Youn, J.-H., Roh, J., Kim, J.-M., Kim, S.-K., & Kim, T.-W. (2022). Brassinosteroids enhance salicylic acid-mediated immune responses by inhibiting BIN2 phosphorylation of clade I TGA transcription factors in Arabidopsis. *Molecular Plant, 15*(6), 991–1007. https://doi.org/10.1016/j.molp.2022.05.002.

King, E. O., Ward, M. K., & Raney, D. E. (1954). Two simple media for the demonstration of pyocyanin and fluorescin. *Journal of Laboratory and Clinical Medicine, 44*(2), 301–307. https://doi.org/10.5555/uri:pii:002221435490222X.

Knuesting, J., Riondet, C., Maria, C., Kruse, I., Bécuwe, N., König, N., Berndt, C., Tourrette, S., Guilleminot-Montoya, J., Herrero, E., Gaymard, F., Balk, J., Belli, G., Scheibe, R., Reichheld, J.-P., Rouhier, N., & Rey, P. (2015). Arabidopsis glutaredoxin S17 and its partner, the nuclear factor Y subunit C11/negative cofactor 2α, contribute to maintenance of the shoot apical meristem under long-day photoperiod. *Plant Physiology, 167*(4), 1643–1658. https://doi.org/10.1104/pp.15.00049.

Koini, M. A., Alvey, L., Allen, T., Tilley, C. A., Harberd, N. P., Whitelam, G. C., & Franklin, K. A. (2009). High temperature-mediated adaptations in plant architecture require the bHLH transcription factor PIF4. *Current Biology, 19*(5), 408–413. https://doi.org/10.1016/j.cub.2009.01.046.

Koncz, C., & Schell, J. (1984). The promoter of TL-DNA gene 5 controls the tissue-specific expression of chimaeric genes carried by a novel type of Agrobacterium binary vector. *Molecular and General Genetics, 204*(3), 383–396. https://doi.org/10.1007/BF00331014.

Konishi, M., & Yanagisawa, S. (2013). Arabidopsis NIN-like transcription factors have a central role in nitrate signalling. *Nature Communications, 4*(1), 1–9. https://doi.org/10.1038/ncomms2621.

Koornneef, M., Jorna, M. L., Brinkhorst-van der Swan, D. L., & Karssen, C. M. (1982). The isolation of abscisic acid (ABA) deficient mutants by selection of induced revertants in non-germinating gibberellin sensitive lines of Arabidopsis thaliana (L.) heynh. *Theoretical and Applied Genetics, 61*(4), 385–393. https://doi.org/10.1007/BF00272861.

Koornneef, M., & van der Veen, J. H. (1980). Induction and analysis of gibberellin sensitive mutants in Arabidopsis thaliana (L.) heynh. *Theoretical and Applied Genetics, 58*(6), 257–263. https://doi.org/10.1007/BF00265176.

Köster, J., Thurow, C., Kruse, K., Meier, A., Iven, T., Feussner, I., & Gatz, C. (2012). Xenobiotic- and jasmonic acid-inducible signal transduction pathways have become interdependent at the Arabidopsis CYP81D11 promoter. *Plant Physiology, 159*(1), 391–402. https://doi.org/10.1104/pp.112.194274.

Laurent, T. C., Moore, E. C., & Reichard, P. (1964). Enzymatic synthesis of deoxyribonucleotides: IV. Isolation and characterization of thioredoxin, the hydrogen donor from Escherichia coli B. *Journal of Biological Chemistry, 239*(10), 3436–3444.

Lemaire, S. D. (2004). The glutaredoxin family in oxygenic photosynthetic organisms. *Photosynthesis Research, 79*, 305–318. https://doi.org/10.1023/B:PRES.0000017174.60951.74.

Lezhneva, L., Kiba, T., Feria-Bourrellier, A.-B., Lafouge, F., Boutet-Mercey, S., Zoufan, P., Sakakibara, H., Daniel-Vedele, F., & Krapp, A. (2014). The Arabidopsis nitrate transporter NRT2.5 plays a role in nitrate acquisition and remobilization in nitrogen-starved plants. *The Plant Journal, 80*(2), 230–241. https://doi.org/10.1111/tpj.12626.

Li, J.-Y., Fu, Y.-L., Pike, S. M., Bao, J., Tian, W., Zhang, Y., Chen, C.-Z., Zhang, Y., Li, H.-M., Huang, J., Li, L.-G., Schroeder, J. I., Gassmann, W., & Gong, J.-M. (2010). The Arabidopsis nitrate transporter NRT1.8 functions in nitrate removal from the xylem sap and mediates cadmium tolerance. *The Plant Cell, 22*(5), 1633–1646. https://doi.org/10.1105/tpc.110.075242.

Li, N., Muthreich, M., Huang, L.-J., Thurow, C., Sun, T., Zhang, Y., & Gatz, C. (2019). TGACG-BINDING FACTORs (TGAs) and TGA-interacting CC-type glutaredoxins modulate hyponastic growth in Arabidopsis thaliana. *New Phytologist, 221*(4), 1906–1918. https://doi.org/10.1111/nph.15496.

Li, S., Lauri, A., Ziemann, M., Busch, A., Bhave, M., & Zachgo, S. (2009). Nuclear activity of ROXY1, a glutaredoxin interacting with TGA factors, is required for petal development in Arabidopsis thaliana. *The Plant Cell, 21*(2), 429–441. https://doi.org/10.1105/tpc.108.064477.

Lillig, C. H., Berndt, C., & Holmgren, A. (2008). Glutaredoxin systems. *Biochimica et Biophysica Acta (BBA)-General Subjects, 1780*(11), 1304–1317. https://doi.org/10.1016/j.bbagen.2008.06.003.

Lin, S.-H., Kuo, H.-F., Canivenc, G., Lin, C.-S., Lepetit, M., Hsu, P.-K., Tillard, P., Lin, H.-L., Wang, Y.-Y., Tsai, C.-B., Gojon, A., & Tsay, Y.-F. (2008). Mutation of the Arabidopsis NRT1.5 nitrate transporter causes defective root-to-shoot nitrate transport. *The Plant Cell, 20*(9), 2514–2528. https://doi.org/10.1105/tpc.108.060244.

Lindermayr, C., Sell, S., Müller, B., Leister, D., & Durner, J. (2010). Redox regulation of the NPR1-TGA1 system of Arabidopsis thaliana by nitric oxide. *The Plant Cell, 22*, 2894-2907. https://doi.org/10.1105/tpc.109.066464.

Little, D. Y., Rao, H., Oliva, S., Daniel-Vedele, F., Krapp, A., & Malamy, J. E. (2005). The putative high-affinity nitrate transporter NRT2.1 represses lateral root initiation in response to nutritional cues. *Proceedings of the National Academy of Sciences, 102*(38), 13693–13698. https://doi.org/10.1073/pnas.0504219102.

Liu, K.-H., Liu, M., Lin, Z., Wang, Z. F., Chen, B., Liu, C., Guo, A., Konishi, M., Yanagisawa, S., Wagner, G., & Sheen, J. (2022). NIN-like protein 7 transcription factor is a plant nitrate sensor. *Science, 377*(6613), 1419–1425. https://doi.org/10.1126/science.add1104.

Liu, K.-H., Niu, Y., Konishi, M., Wu, Y., Du, H., Sun Chung, H., Li, L., Boudsocq, M., McCormack, M., Maekawa, S., Ishida, T., Zhang, C., Shokat, K., Yanagisawa, S., & Sheen, J. (2017a). Discovery of nitrate-CPK-NLP signalling in central nutrient-growth networks. *Nature, 545*(7654), 311–316. https://doi.org/10.1038/nature22077.

Liu, S., Ziegler, J., Zeier, J., Birkenbihl, R. P., & Somssich, I. E. (2017b). Botrytis cinerea B05. 10 promotes disease development in Arabidopsis by suppressing WRKY33-mediated host immunity. *Plant, Cell & Environment, 40*(10), 2189–2206. https://doi.org/10.1111/pce.13022.

Liu, X., Liu, S., Feng, Y., Liu, J.-Z., Chen, Y., Pham, K., Deng, H., Hirschi, K. D., Wang, X., & Cheng, N. (2013). Structural insights into the N-terminal GIY-YIG endonuclease activity of Arabidopsis glutaredoxin AtGRXS16 in chloroplasts. *Proceedings of the National Academy of Sciences, 110*(23), 9565–9570. https://doi.org/10.1073/pnas.1306899110.

Long, J. A., Woody, S., Poethig, S., Meyerowitz, E. M., & Barton, M. K. (2002). Transformation of shoots into roots in Arabidopsis embryos mutant at the TOPLESS locus. *Development, 129*(12), 2797–2806. https://doi.org/10.1242/dev.129.12.2797.

Lorenzo, O., Chico, J. M., Saénchez-Serrano, J. J., & Solano, R. (2004). JASMONATE-INSENSITIVE1 encodes a MYC transcription factor essential to discriminate between different jasmonate-regulated defense responses in Arabidopsis. *The Plant Cell, 16*(7), 1938–1950. https://doi.org/10.1105/tpc.022319.

Love, M. I., Huber, W., & Anders, S. (2014). Moderated estimation of fold change and dispersion for RNA-seq data with DESeq2. *Genome Biology, 15*(12), 1–21. https://doi.org/10.1186/s13059-014-0550-8.

Maleck, K., Levine, A., Eulgem, T., Morgan, A., Schmid, J., Lawton, K. A., Dangl, J. L., & Dietrich, R. A. (2000). The transcriptome of Arabidopsis thaliana during systemic acquired resistance. *Nature Genetics, 26*(4), 403–410. https://doi.org/10.1038/82521.

Martin, J. L. (1995). Thioredoxin—a fold for all reasons. *Structure, 3*(3), 245–250. https://doi.org/10.1016/S0969-2126(01)00154-X.

Martins, L., Knuesting, J., Bariat, L., Dard, A., Freibert, S. A., Marchand, C. H., Young, D., Dung, N. H. T., Voth, W., Debures, A., Saez-Vasquez, J., Lemaire, S. D., Lill, R., Messens, J., Scheibe, R., Reichheld, J.-P., & Riondet, C. (2020). Redox Modification of the Iron-Sulfur Glutaredoxin GRXS17 Activates Holdase Activity and Protects Plants from Heat Stress. *Plant Physiology, 184*(2), 676–692. https://doi.org/10.1104/pp.20.00906.

Maß, L., Holtmannspötter, M., & Zachgo, S. (2020). Dual-color 3D-dSTORM colocalization and quantification of ROXY1 and RNAPII variants throughout the transcription cycle in root meristem nuclei. *The Plant Journal, 104*(5), 1423–1436. https://doi.org/10.1111/tpj.14986.

Matsumoto, A., Schlüter, T., Melkonian, K., Takeda, A., Nakagami, H., & Mine, A. (2022). A versatile Tn7 transposon-based bioluminescence tagging tool for quantitative and spatial detection of bacteria in plants. *Plant Communications, 3*(1), 100227. https://doi.org/10.1016/j.xplc.2021.100227.

May, D. G., Scott, K. L., Campos, A. R., & Roux, K. J. (2020). Comparative application of BioID and TurboID for protein-proximity biotinylation. *Cells, 9*(5), 1070. https://doi.org/10.3390/cells9051070.

Meng, X., Xu, J., He, Y., Yang, K.-Y., Mordorski, B., Liu, Y., & Zhang, S. (2013). Phosphorylation of an ERF transcription factor by Arabidopsis MPK3/MPK6 regulates plant defense gene induction and fungal resistance. *The Plant Cell, 25*(3), 1126–1142. https://doi.org/10.1105/tpc.112.109074.

Mi, H., Muruganujan, A., Casagrande, J. T., & Thomas, P. D. (2013). Large-scale gene function analysis with the PANTHER classification system. *Nature Protocols, 8*(8), 1551–1566. https://doi.org/10.1038/nprot.2013.092.

Michaud, O., Fiorucci, A. S., Xenarios, I., & Fankhauser, C. (2017). Local auxin production underlies a spatially restricted neighbor-detection response in Arabidopsis. *Proceedings of the National Academy of Sciences, 114*(28), 7444–7449. https://doi.org/10.1073/pnas.170227611.

Millenaar, F. F., van Zanten, M., Cox, M. C., Pierik, R., Voesenek, L. A., & Peeters, A. J. (2009). Differential petiole growth in Arabidopsis thaliana: photocontrol and hormonal regulation. *New Phytologist, 184*(1), 141–152. https://doi.org/10.1111/j.1469-8137.2009.02921.x.

Mohnike, L., Rekhter, D., Huang, W., Feussner, K., Tian, H., Herrfurth, C., Zhang, Y., & Feussner, I. (2021). The glycosyltransferase UGT76B1 modulates N-hydroxy-pipecolic acid homeostasis and plant immunity. *The Plant Cell, 33*(3), 735–749. https://doi.org/10.1093/plcell/koaa045.

Moreno, J. E., Shyu, C., Campos, M. L., Patel, L. C., Chung, H. S., Yao, J., He, S. Y., & Howe, G. A. (2013). Negative feedback control of jasmonate signaling by an alternative splice variant of JAZ10. *Plant Physiology, 162*(2), 1006–1017. https://doi.org/10.1104/pp.113.218164.

Mörk, K. (2021). Transkriptanalyse und Analyse der Suszeptibilität gegen Pseudomonas syringae von transgenen Arabidopsis thaliana Linien, die ROXY9 bzw.ROXY9 Varianten mit Aminosäuremutationen im aktiven Zentrum überexprimieren. *Bachelor Thesis, Georg-August Universität, Göttingen, Germany*.

Moseler, A., Aller, I., Wagner, S., Nietzel, T., Przybyla-Toscano, J., Mühlenhoff, U., Lill, R., Berndt, C., Rouhier, N., Schwarzländer, M., & Meyer, A. J. (2015). The mitochondrial monothiol glutaredoxin S15 is essential for iron-sulfur protein maturation in Arabidopsis thaliana. *Proceedings of the National Academy of Sciences, 112*(44), 13735–13740. https://doi.org/10.1073/pnas.1510835112.

Mou, Z., Fan, W., & Dong, X. (2003). Inducers of plant systemic acquired resistance regulate NPR1 function through redox changes. *Cell, 113*(7), 935–944. https://doi.org/10.1016/S0092-8674(03)00429-X.

Mrozek, P. (2022). Functional characterization of Arabidopsis thaliana CC-type glutaredoxin ROXY9. *PhD Thesis, Georg-August Universität, Göttingen, Germany*.

Mueller, S., Hilbert, B., Dueckershoff, K., Roitsch, T., Krischke, M., Mueller, M. J., & Berger, S. (2008). General detoxification and stress responses are mediated by oxidized lipids through TGA transcription factors in Arabidopsis. *The Plant Cell, 20*(3), 758–785. https://doi.org/10.1105/tpc.107.054809.

Müller-Schüssele, S. J., Bohle, F., Rossi, J., Trost, P., Meyer, A. J., & Zaffagnini, M. (2021). Plasticity in plastid redox networks: evolution of glutathione-dependent redox cascades and glutathionylation sites. *BMC Plant Biology, 21*(1), 322. https://doi.org/10.1186/s12870-021-03087-2.

Murmu, J., Bush, M. J., DeLong, C., Li, S., Xu, M., Khan, M., Malcolmson, C., Fobert, P. R., Zachgo, S., & Hepworth, S. R. (2010). Arabidopsis basic leucine-zipper transcription factors TGA9 and TGA10 interact with floral glutaredoxins ROXY1 and ROXY2 and are redundantly required for anther development. *Plant Physiology, 154*(3), 1492–1504. https://doi.org/10.1104/pp.110.159111.

Muthreich, M. (2014). Characterization of clade I TGA transcription factors in Arabidopsis thaliana with respect to biotic stress. *PhD Thesis, Georg-August Universität, Göttingen, Germany*.

Nair, A., Goyal, I., Voß, E., Mrozek, P., Prajapati, S., Thurow, C., Tietze, L., Tittmann, K., & Gatz, C. (2021). N-hydroxypipecolic acid-induced transcription requires the salicylic acid signaling pathway at basal SA levels. *Plant Physiology, 187*(4), 2803–2819. https://doi.org/10.1093/plphys/kiab433.

Návarová, H., Bernsdorff, F., Döring, A.-C., & Zeier, J. (2012). Pipecolic acid, an endogenous mediator of defense amplification and priming, is a critical regulator of inducible plant immunity. *The Plant Cell, 24*(12), 5123–5141. https://doi.org/10.1105/tpc.112.103564.

Ndamukong, I., Abdallat, A. A., Thurow, C., Fode, B., Zander, M., Weigel, R., & Gatz, C. (2007). SA-inducible Arabidopsis glutaredoxin interacts with TGA factors and suppresses JA-responsive PDF1. 2 transcription. *The Plant Journal, 50*(1), 128–139. https://doi.org/10.1111/j.1365-313X.2007.03039.x.

Neuteboom, L. W., Ng, J. M., Kuyper, M., Clijdesdale, O. R., Hooykaas, P. J., & van der Zaal, B. J. (1999). Isolation and characterization of cDNA clones corresponding with mRNAs that accumulate during auxin-induced lateral root formation. *Plant Molecular Biology, 39*(2), 273–287.

Niggeweg, R., Thurow, C., Weigel, R., Pfitzner, U., & Gatz, C. (2000). Tobacco TGA factors differ with respect to interaction with NPR1, activation potential and DNA-binding properties. *Plant Molecular Biology, 42*(5), 775–788. https://doi.org/10.1023/A:1006319113205.

Nolan, T. M., Vukašinović, N., Liu, D., Russinova, E., & Yin, Y. (2020). Brassinosteroids: Multidimensional Regulators of Plant Growth, Development, and Stress Responses. *The Plant Cell, 32*(2), 295–318. https://doi.org/10.1105/tpc.19.00335.

Oberdiek, J. (2018). Funktionale Analyse des CC-Typ Glutaredoxin ROXY19 in Arabidopsis thaliana. *PhD Thesis, Georg-August Universität, Göttingen, Germany*.

Oh, E., Yamaguchi, S., Kamiya, Y., Bae, G., Chung, W.-I., & Choi, G. (2006). Light activates the degradation of PIL5 protein to promote seed germination through gibberellin in Arabidopsis. *The Plant Journal, 47*(1), 124–139. https://doi.org/10.1111/j.1365-313X.2006.02773.x.

Ohkubo, Y., Kuwata, K., & Matsubayashi, Y. (2021). A type 2C protein phosphatase activates high-affinity nitrate uptake by dephosphorylating NRT2.1. *Nature Plants, 7*(3), 310–316. https://doi.org/10.1038/s41477-021-00870-9.

Ohkubo, Y., Tanaka, M., Tabata, R., Ogawa-Ohnishi, M., & Matsubayashi, Y. (2017). Shoot-to-root mobile polypeptides involved in systemic regulation of nitrogen acquisition. *Nature Plants, 3*(4), 1–6. https://doi.org/10.1038/nplants.2017.29.

Okuma, N., Soyano, T., Suzaki, T., & Kawaguchi, M. (2020). MIR2111-5 locus and shoot-accumulated mature miR2111 systemically enhance nodulation depending on HAR1 in Lotus japonicus. *Nature Communications, 11*(1), 5192. https://doi.org/10.1038/s41467-020-19037-9.

Oñate-Sánchez, L., Anderson, J. P., Young, J., & Singh, K. B. (2007). AtERF14, a member of the ERF family of transcription factors, plays a nonredundant role in plant defense. *Plant Physiology, 143*(1), 400–409. https://doi.org/10.1104/pp.106.086637.

Ota, R., Ohkubo, Y., Yamashita, Y., Ogawa-Ohnishi, M., & Matsubayashi, Y. (2020). Shoot-to-root mobile CEPD-like 2 integrates shoot nitrogen status to systemically regulate nitrate uptake in Arabidopsis. *Nature Communications, 11*(1), 1–9. https://doi.org/10.1038/s41467-020-14440-8.

Pantazopoulou, C. K., Bongers, F. J., Kupers, J. J., Reinen, E., Das, D., Evers, J. B., Anten, N. P. R., & Pierik, R. (2017). Neighbor detection at the leaf tip adaptively regulates upward leaf movement through spatial auxin dynamics. *Proceedings of the National Academy of Sciences, 114*(28), 7450–7455. https://doi.org/10.1073/pnas.1702275114.

Patterson, K., Walters, L. A., Cooper, A. M., Olvera, J. G., Rosas, M. A., Rasmusson, A. G., & Escobar, M. A. (2016). Nitrate-Regulated Glutaredoxins Control Arabidopsis Primary Root Growth. *Plant Physiology, 170*(2), 989–999. https://doi.org/10.1104/pp.15.01776.

Pauwels, L., Barbero, G. F., Geerinck, J., Tilleman, S., Grunewald, W., Pérez, A. C., Chico, J. M., Bossche, R. V., Sewell, J., Gil, E., García-Casado, G., Witters, E., Inzé, D., Long, J. A., Jaeger, G. de, Solano, R., & Goossens, A. (2010). NINJA connects the co-repressor TOPLESS to jasmonate signalling. *Nature, 464*(7289), 788–791. https://doi.org/10.1038/nature08854.

Pelizaeus, A. M. (2019). Pseudomonas syringae-inducible gene expression in Arabidopsis thaliana roots. *Master Thesis, Georg-August Universität, Göttingen, Germany*.

Pfalz, M., Mikkelsen, M. D., Bednarek, P., Olsen, C. E., Halkier, B. A., & Kroymann, J. (2011). Metabolic engineering in Nicotiana benthamiana reveals key enzyme functions in Arabidopsis indole glucosinolate modification. *The Plant Cell, 23*(2), 716–729. https://doi.org/10.1105/tpc.110.081711.

Picciocchi, A., Saguez, C., Boussac, A., Cassier-Chauvat, C., & Chauvat, F. (2007). CGFS-type monothiol glutaredoxins from the cyanobacterium Synechocystis PCC6803 and other evolutionary distant model organisms possess a glutathione-ligated 2Fe-2S cluster. *Biochemistry, 46*(51), 15018–15026. https://doi.org/10.1021/bi7013272.

Pierik, R., Millenaar, F. F., Peeters, A. J., & Voesenek, L. A. (2005). New perspectives in flooding research: the use of shade avoidance and Arabidopsis thaliana. *Annals of Botany, 96*(4), 533–540. https://doi.org/10.1093/aob/mci208.

Piskurewicz, U., Jikumaru, Y., Kinoshita, N., Nambara, E., Kamiya, Y., & Lopez-Molina, L. (2008). The gibberellic acid signaling repressor RGL2 inhibits Arabidopsis seed germination by stimulating abscisic acid synthesis and ABI5 activity. *The Plant Cell, 20*(10), 2729–2745. https://doi.org/10.1105/tpc.108.061515.

Polko, J. K., van Zanten, M., van Rooij, J. A., Maree, A. F., Voesenek, L. A., Peeters, A. J., & Pierik, R. (2012). Ethylene-induced differential petiole growth in Arabidopsis thaliana involves local microtubule reorientation and cell expansion. *New Phytologist, 193*(2), 339–348. https://doi.org/10.1111/j.1469-8137.2011.03920.x.

Pré, M., Atallah, M., Champion, A., de Vos, M., Pieterse, C. M. J., & Memelink, J. (2008). The AP2/ERF domain transcription factor ORA59 integrates jasmonic acid and ethylene signals in plant defense. *Plant Physiology, 147*(3), 1347–1357. https://doi.org/10.1104/pp.108.117523.

Quaedvlieg, N., Dockx, J., Rook, F., Weisbeek, P., & Smeekens, S. (1995). The homeobox gene ATH1 of Arabidopsis is derepressed in the photomorphogenic mutants cop1 and det1. *The Plant Cell, 7*(1), 117–129. https://doi.org/10.1105/tpc.7.1.117.

Raggi, S., Ferrarini, A., Delledonne, M., Dunand, C., Ranocha, P., Lorenzo, G. de, Cervone, F., & Ferrari, S. (2015). The Arabidopsis class III peroxidase AtPRX71 negatively regulates growth under physiological conditions and in response to cell wall damage. *Plant Physiology, 169*(4), 2513–2525. https://doi.org/10.1104/pp.15.01464.

Rappsilber, J., Ishihama, Y., & Mann, M. (2003). Stop and go extraction tips for matrix-assisted laser desorption/ionization, nanoelectrospray, and LC/MS sample pretreatment in proteomics. *Analytical Chemistry, 75*(3), 663–670. https://doi.org/10.1021/ac026117i.

Ratcliffe, O. J., Amaya, I., Vincent, C. A., Rothstein, S., Carpenter, R., Coen, E. S., & Bradley, D. J. (1998). A common mechanism controls the life cycle and architecture of plants. *Development, 125*(9), 1609–1615. https://doi.org/10.1242/dev.125.9.1609.

Rekhter, D., Lüdke, D., Ding, Y., Feussner, K., Zienkiewicz, K., Lipka, V., Wiermer, M., Zhang, Y., & Feussner, I. (2019). Isochorismate-derived biosynthesis of the plant stress hormone salicylic acid. *Science, 365*(6452), 498–502. https://doi.org/10.1126/science.aaw1720.

Rey, P., Becuwe, N., Tourrette, S., & Rouhier, N. (2017). Involvement of Arabidopsis glutaredoxin S14 in the maintenance of chlorophyll content. *Plant, Cell & Environment, 40*(10), 2319–2332. https://doi.org/10.1111/pce.13036.

Richards, D. E., King, K. E., Ait-Ali, T., & Harberd, N. P. (2001). How gibberellin regulates plant growth and development: a molecular genetic analysis of gibberellin signaling. *Annual Review of Plant Biology, 52*(1), 67–88.

Rindermann, K. (2010). The Role of Arabidopsis Class-II TGA Transcription Factors in PAMP-mediated Defense Responses. *PhD Thesis, Georg-August Universität, Göttingen, Germany*.

Riondet, C., Desouris, J. P., Montoya, J. G., Chartier, Y., Meyer, Y., & Reichheld, J.-P. (2012). A dicotyledon-specific glutaredoxin GRXC1 family with dimer-dependent redox regulation is functionally redundant with GRXC2. *Plant, Cell & Environment, 35*(2), 360–373. https://doi.org/10.1111/j.1365-3040.2011.02355.x.

Rodríguez-Manzaneque, M. T., Tamarit, J., Bellí, G., Ros, J., & Herrero, E. (2002). Grx5 is a mitochondrial glutaredoxin required for the activity of iron/sulfur enzymes. *Molecular Biology of the Cell, 13*(4), 1109–1121. https://doi.org/10.1091/mbc.01-10-0517.

Rouhier, N., Gelhaye, E., & Jacquot, J. P. (2002). Exploring the active site of plant glutaredoxin by site-directed mutagenesis. *FEBS Letters, 511*(1-3), 145–149. https://doi.org/10.1016/S0014-5793(01)03302-6.

Rouhier, N., Gelhaye, E., & Jacquot, J.-P. (2004). Plant glutaredoxins: still mysterious reducing systems. *Cellular and Molecular Life Sciences, 61*(11), 1266–1277. https://doi.org/10.1007/s00018-004-3410-y.

Rouhier, N., Unno, H., Bandyopadhyay, S., Masip, L., Kim, S. K., Hirasawa, M., Gualberto, J. M., Lattard, V., Kusunoki, M., Knaff, D. B., Georgiou, G., Hase, T., Johnson, M. K., & Jacquot, J. P. (2007). Functional, structural, and spectroscopic characterization of a glutathione-ligated [2Fe–2S] cluster in poplar glutaredoxin C1. *Proceedings of the National Academy of Sciences, 104*(18), 7379-7384. https://doi.org/10.1073/pnas.0702268104.

Rouhier, N., Couturier, J., Johnson, M. K., & Jacquot, J.-P. (2010). Glutaredoxins: roles in iron homeostasis. *Trends in Biochemical Sciences, 35*(1), 43–52. https://doi.org/10.1016/j.tibs.2009.08.005.

Rouhier, N., Lemaire, S. D., & Jacquot, J.-P. (2008). The role of glutathione in photosynthetic organisms: emerging functions for glutaredoxins and glutathionylation. *Annual Review of Plant Biology, 59*, 143–166. https://doi.org/10.1146/annurev.arplant.59.032607.092811.

Rouina, H., Tseng, Y. H., Nataraja, K. N., Uma Shaanker, R., & Oelmüller, R. (2021). Arabidopsis Restricts Sugar Loss to a Colonizing Trichoderma harzianum Strain by Downregulating SWEET11 and-12 and Upregulation of SUC1 and SWEET2 in the Roots. *Microorganisms, 9*(6), 1246. https://doi.org/10.3390/microorganisms9061246.

Ruffel, S., Chaput, V., Przybyla-Toscano, J., Fayos, I., Ibarra, C., Moyano, T., Fizames, C., Tillard, P., O'Brien, J. A., Gutiérrez, R. A., Gojon, A., & Lejay, L. (2021). Genome-wide analysis in response to nitrogen and carbon identifies regulators for root AtNRT2 transporters. *Plant Physiology, 186*(1), 696–714. https://doi.org/10.1093/plphys/kiab047.

Rushton, P. J., Torres, J. T., Parniske, M., Wernert, P., Hahlbrock, K., & Somssich, I. E. (1996). Interaction of elicitor-induced DNA-binding proteins with elicitor response elements in the promoters of parsley PR1 genes. *The EMBO Journal, 15*(20), 5690–5700. https://doi.org/10.1002/j.1460-2075.1996.tb00953.x.

Scheible, W.-R., Morcuende, R., Czechowski, T., Fritz, C., Osuna, D., Palacios-Rojas, N., Schindelasch, D., Thimm, O., Udvardi, M. K., & Stitt, M. (2004). Genome-wide reprogramming of primary and secondary metabolism, protein synthesis, cellular growth processes, and the regulatory infrastructure of Arabidopsis in response to nitrogen. *Plant Physiology, 136*(1), 2483–2499. https://doi.org/10.1104/pp.104.047019.

Shah, J., Kachroo, P., Nandi, A., & Klessig, D. F. (2001). A recessive mutation in the Arabidopsis SSI2 gene confers SA- and NPR1-independent expression of PR genes and resistance against bacterial and oomycete pathogens. *The Plant Journal, 25*(5), 563–574. https://doi.org/10.1046/j.1365-313x.2001.00992.x.

Shannon, S., & Meeks-Wagner, D. R. (1991). A mutation in the Arabidopsis TFL1 gene affects inflorescence meristem development. *The Plant Cell, 3*(9), 877–892. https://doi.org/10.1105/tpc.3.9.877.

Shearer, H. L., Cheng, Y. T., Wang, L., Liu, J., Boyle, P., Despres, C., Zhang, Y., Li, X., & Fobert, P. R. (2012). Arabidopsis clade I TGA transcription factors regulate plant defenses in an NPR1-independent fashion. *Molecular Plant–Microbe Interactions, 25*, 1459–1468. https://doi.org/10.1094/MPMI-09-11-0256.

Shearer, H. L., Wang, L., DeLong, C., Despres, C., & Fobert, P. R. (2009). NPR1 enhances the DNA binding activity of the Arabidopsis bZIP transcription factor TGA7. *Botany, 87*(6), 561–570. https://doi.org/10.1139/B08-143.

Shevchenko, A., Wilm, M., Vorm, O., & Mann, M. (1996). Mass spectrometric sequencing of proteins from silver stained polyacrylamide gels. *Analytical Chemistry, 68*(5), 850–858. https://doi.org/10.1021/ac950914h.

Shigeto, J., Itoh, Y., Hirao, S., Ohira, K., Fujita, K., & Tsutsumi, Y. (2015). Simultaneously disrupting AtPrx2, AtPrx25 and AtPrx71 alters lignin content and structure in Arabidopsis stem. *Journal of Integrative Plant Biology, 57*(4), 349–356. https://doi.org/10.1111/jipb.12334.

Sievers, F., & Higgins, D. G. (2018). Clustal Omega for making accurate alignments of many protein sequences. *Protein Science, 27*(1), 135–145. https://doi.org/10.1002/pro.3290.

Sievers, F., Wilm, A., Dineen, D., Gibson, T. J., Karplus, K., Li, W., Lopez, R., McWilliam, H., Remmert, M., Söding, J., Thompson, J. D., & Higgins, D. G. (2011). Fast, scalable generation of high-quality protein multiple sequence alignments using Clustal Omega. *Molecular Systems Biology, 7*, 539. https://doi.org/10.1038/msb.2011.75.

Spoel, S. H., Koornneef, A., Claessens, S. M. C., Korzelius, J. P., van Pelt, J. A., Mueller, M. J., Buchala, A. J., Métraux, J.-P., Brown, R., Kazan, K., van Loon, L. C., Dong, X., & Pieterse, C. M. J. (2003). NPR1 modulates cross-talk between salicylate- and jasmonate-dependent defense pathways through a novel function in the cytosol. *The Plant Cell, 15*(3), 760–770. https://doi.org/10.1105/tpc.009159.

Spoel, S. H., Mou, Z., Tada, Y., Spivey, N. W., Genschik, P., & Dong, X. (2009). Proteasome-mediated turnover of the transcription coactivator NPR1 plays dual roles in regulating plant immunity. *Cell, 137*(5), 860–872. https://doi.org/10.1016/j.cell.2009.03.038.

Ströher, E., Grassl, J., Carrie, C., Fenske, R., Whelan, J., & Millar, A. H. (2016). Glutaredoxin S15 Is Involved in Fe-S Cluster Transfer in Mitochondria Influencing Lipoic Acid-Dependent Enzymes, Plant Growth, and Arsenic Tolerance in Arabidopsis. *Plant Physiology, 170*(3), 1284–1299. https://doi.org/10.1104/pp.15.01308.

Sun, T., Busta, L., Zhang, Q., Ding, P., Jetter, R., & Zhang, Y. (2018). TGACG-BINDING FACTOR 1 (TGA1) and TGA4 regulate salicylic acid and pipecolic acid biosynthesis by modulating the expression of SYSTEMIC ACQUIRED RESISTANCE DEFICIENT 1 (SARD1) and CALMODULIN-BINDING PROTEIN 60g (CBP60g). *New Phytologist, 217*(1), 344–354. https://doi.org/10.1111/nph.14780.

Sun, T., Zhang, Y., Li, Y., Zhang, Q., Ding, Y., & Zhang, Y. (2015). ChIP-seq reveals broad roles of SARD1 and CBP60g in regulating plant immunity. *Nature Communications, 6*, 10159. https://doi.org/10.1038/ncomms10159.

Tabata, R., Sumida, K., Yoshii, T., Ohyama, K., Shinohara, H., & Matsubayashi, Y. (2014). Perception of root-derived peptides by shoot LRR-RKs mediates systemic N-demand signaling. *Science, 346*(6207), 343–346. https://doi.org/10.1126/science.1257800.

Tatematsu, K., Kumagai, S., Muto, H., Sato, A., Watahiki, M. K., Harper, R. M., Liscum, E., & Yamamoto, K. T. (2004). MASSUGU2 encodes Aux/IAA19, an auxin-regulated protein that functions together with the transcriptional activator NPH4/ARF7 to regulate differential growth responses of hypocotyl and formation of lateral roots in Arabidopsis thaliana. *The Plant Cell, 16*(2), 379–393. https://doi.org/10.1105/tpc.018630.

Tian, H., Wu, Z., Chen, S., Ao, K., Huang, W., Yaghmaiean, H., Sun, T., Xu, F., Zhang, Y., Wang, S., Li, X., & Zhang, Y. (2021). Activation of TIR signalling boosts pattern-triggered immunity. *Nature, 598*(7881), 500–503. https://doi.org/10.1038/s41586-021-03987-1.

Toh, S., Imamura, A., Watanabe, A., Nakabayashi, K., Okamoto, M., Jikumaru, Y., Hanada, A., Aso, Y., Ishiyama, K., Tamura, N., Iuchi, S., Kobayashi, M., Yamaguchi, S., Kamiya, Y., Nambara, E., & Kawakami, N. (2008). High temperature-induced abscisic acid biosynthesis and its role in the inhibition of gibberellin action in Arabidopsis seeds. *Plant Physiology, 146*(3), 1368–1385. https://doi.org/10.1104/pp.107.113738.

Torrens-Spence, M. P., Bobokalonova, A., Carballo, V., Glinkerman, C. M., Pluskal, T., Shen, A., & Weng, J.-K. (2019). PBS3 and EPS1 Complete Salicylic Acid Biosynthesis from Isochorismate in Arabidopsis. *Molecular Plant, 12*(12), 1577–1586. https://doi.org/10.1016/j.molp.2019.11.005.

Treffon, K. (2019). Functional analysis of the Arabidopsis thaliana glutaredoxin ROXY9. *PhD Thesis, Georg-August Universität, Göttingen, Germany*.

Uhrig, J. F., Huang, L.-J., Barghahn, S., Willmer, M., Thurow, C., & Gatz, C. (2017). CC-type glutaredoxins recruit transcriptional co-repressor TOPLESS to TGA-dependent target promoters in Arabidopsis thaliana. *Biochimica et Biophysica Acta (BBA)-Gene Regulatory Mechanisms, 1860*(2), 218–226. https://doi.org/10.1016/j.bbagrm.2016.11.001.

Ukuwela, A. A., Bush, A. I., Wedd, A. G., & Xiao, Z. (2018). Glutaredoxins employ parallel monothiol-dithiol mechanisms to catalyze thiol-disulfide exchanges with protein disulfides. *Chemical Science, 9*(5), 1173–1183. https://doi.org/10.1039/C7SC04416J.

van Zanten, M., Voesenek, L. A., Peeters, A. J., & Millenaar, F. F. (2009). Hormone- and light-mediated regulation of heat-induced differential petiole growth in Arabidopsis. *Plant Physiology, 151*(3), 1446–1458. https://doi.org/10.1104/pp.109.144386.

Vandenbussche, F., Vriezen, W. H., Smalle, J., Laarhoven, L. J., Harren, F. J., & van der Straeten, D. (2003). Ethylene and auxin control the Arabidopsis response to decreased light intensity. *Plant Physiology, 133*(2), 517–527. https://doi.org/10.1104/pp.103.022665.

Vogelmann, K., Drechsel, G., Bergler, J., Subert, C., Philippar, K., Soll, J., Engelmann, J. C., Engelsdorf, T., Voll, L. M., & Hoth, S. (2012). Early senescence and cell death in Arabidopsis saul1 mutants involves the PAD4-dependent salicylic acid pathway. *Plant Physiology, 159*(4), 1477–1487. https://doi.org/10.1104/pp.112.196220.

Wang, L., Tsuda, K., Truman, W., Sato, M., Le Nguyen, V., Katagiri, F., & Glazebrook, J. (2011). CBP60g and SARD1 play partially redundant critical roles in salicylic acid signaling. *The Plant Journal, 67*(6), 1029–1041. https://doi.org/10.1111/j.1365-313X.2011.04655.x.

Wang, Y., Salasini, B. C., Khan, M., Devi, B., Bush, M., Subramaniam, R., & Hepworth, S. R. (2019). Clade I TGACG-Motif Binding Basic Leucine Zipper Transcription Factors Mediate BLADE-ON-PETIOLE-Dependent Regulation of Development. *Plant Physiology, 180*(2), 937–951. https://doi.org/10.1104/pp.18.00805.

Whalen, M. C., Innes, R. W., Bent, A. F., & Staskawicz, B. J. (1991). Identification of Pseudomonas syringae pathogens of Arabidopsis and bacterial locus determining avirulence on both Arabidopsis and soybean. *The Plant Cell, 3*(1), 49–59. https://doi.org/10.1105/tpc.3.1.49.

Wildermuth, M. C., Dewdney, J., Wu, G., & Ausubel, F. M. (2001). Isochorismate synthase is required to synthesize salicylic acid for plant defence. *Nature, 414*(6863), 562–565. https://doi.org/10.1038/35107108.

Willmer, M. (2014). Struktur-Funktions-Analyse von ROXY-Glutaredoxinen und TIFY-Domänen-Proteinen in Arabidopsis thaliana. *Bachelor Thesis, Georg-August Universität, Göttingen, Germany*.

Wu, Y., Di Zhang, Chu, J. Y., Boyle, P., Wang, Y., Brindle, I. D., Luca, V. de, & Després, C. (2012). The Arabidopsis NPR1 protein is a receptor for the plant defense hormone salicylic acid. *Cell Reports, 1*(6), 639–647. https://doi.org/10.1016/j.celrep.2012.05.008.

Xing, S., Rosso, M. G., & Zachgo, S. (2005). ROXY1, a member of the plant glutaredoxin family, is required for petal development in Arabidopsis thaliana. *Development, 132*(7), 1555–1565. https://doi.org/10.1242/dev.01725.

Yamaguchi, S., Smith, M. W., Brown, R. G., Kamiya, Y., & Sun, T. (1998). Phytochrome regulation and differential expression of gibberellin 3beta-hydroxylase genes in germinating Arabidopsis seeds. *The Plant Cell, 10*(12), 2115–2126. https://doi.org/10.1105/tpc.10.12.2115.

Yang, F., Bui, H. T., Pautler, M., Llaca, V., Johnston, R., Lee, B., Kolbe, A., Sakai, H., & Jackson, D. (2015). A maize glutaredoxin gene, abphyl2, regulates shoot meristem size and phyllotaxy. *The Plant Cell, 27*(1), 121–131. https://doi.org/10.1105/tpc.114.130393.

Yang, R. S., Xu, F., Wang, Y. M., Zhong, W. S., Dong, L., Shi, Y. N., Tang, T. J., Sheng, H. J., Jackson, D., & Yang, F. (2021). Glutaredoxins regulate maize inflorescence meristem development via redox control of TGA transcriptional activity. *Nature Plants, 7*(12), 1589–1601. https://doi.org/10.1038/s41477-021-01029-2.

Ye, Q., Zhu, W., Li, L., Zhang, S., Yin, Y., Ma, H., & Wang, X. (2010). Brassinosteroids control male fertility by regulating the expression of key genes involved in Arabidopsis anther and pollen development. *Proceedings of the National Academy of Sciences, 107*(13), 6100–6105. https://doi.org/10.1073/pnas.0912333107.

Yu, J., Zhang, N.-N., Yin, P.-D., Cui, P.-X., & Zhou, C.-Z. (2008). Glutathionylation-triggered conformational changes of glutaredoxin Grx1 from the yeast Saccharomyces cerevisiae. *Proteins, 72*(3), 1077–1083. https://doi.org/10.1002/prot.22096.

Yu, Z., Di Zhang, Xu, Y., Jin, S., Zhang, L., Zhang, S., Yang, G., Huang, J., Yan, K., Wu, C., & Zheng, C. (2019). CEPR2 phosphorylates and accelerates the degradation of PYR/PYLs in Arabidopsis. *Journal of Experimental Botany, 70*(19), 5457–5469. https://doi.org/10.1093/jxb/erz302.

Yuan, L., Loqué, D., Kojima, S., Rauch, S., Ishiyama, K., Inoue, E., Takahashi, H., & Wirén, N. von (2007). The organization of high-affinity ammonium uptake in Arabidopsis roots depends on the spatial arrangement and biochemical properties of AMT1-type transporters. *The Plant Cell, 19*(8), 2636–2652. https://doi.org/10.1105/tpc.107.052134.

Yuan, X., Wang, H., Cai, J., Li, D., & Song, F. (2019). NAC transcription factors in plant immunity. *Phytopathology Research, 1*(1). https://doi.org/10.1186/s42483-018-0008-0.

Zaffagnini, M., Fermani, S., Marchand, C. H., Costa, A., Sparla, F., Rouhier, N., Geigenberger, P., Lemaire, S. D., & Trost, P. (2019). Redox Homeostasis in Photosynthetic Organisms: Novel and Established Thiol-Based Molecular Mechanisms. *Antioxidants & redox signaling, 31*(3), 155–210. https://doi.org/10.1089/ars.2018.7617.

Zaffagnini, M., Michelet, L., Massot, V., Trost, P., & Lemaire, S. D. (2008). Biochemical characterization of glutaredoxins from Chlamydomonas reinhardtii reveals the unique properties of a chloroplastic CGFS-type glutaredoxin. *Journal of Biological Chemistry, 283*(14), 8868–8876. https://doi.org/10.1074/jbc.M709567200.

Zander, M., Chen, S., Imkampe, J., Thurow, C., & Gatz, C. (2012). Repression of the Arabidopsis thaliana jasmonic acid/ethylene-induced defense pathway by TGA-interacting glutaredoxins depends on their C-terminal ALWL motif. *Molecular Plant, 5*(4), 831–840. https://doi.org/10.1093/mp/ssr113.

Zander, M., La Camera, S., Lamotte, O., Métraux, J.-P., & Gatz, C. (2010). Arabidopsis thaliana class-II TGA transcription factors are essential activators of jasmonic acid/ethylene-induced defense responses. *The Plant Journal, 61*(2), 200–210. https://doi.org/10.1111/j.1365-313X.2009.04044.x.

Zander, M., Thurow, C., & Gatz, C. (2014). TGA Transcription Factors Activate the Salicylic Acid-Suppressible Branch of the Ethylene-Induced Defense Program by Regulating ORA59 Expression. *Plant Physiology, 165*(4), 1671–1683. https://doi.org/10.1104/pp.114.243360.

Zeilmaker, T., Ludwig, N. R., Elberse, J., Seidl, M. F., Berke, L., van Doorn, A., Schuurink, R., Snel, B., & van den Ackerveken, G. (2015). DOWNY MILDEW RESISTANT 6 and DMR 6-LIKE OXYGENASE 1 are partially redundant but distinct suppressors of immunity in Arabidopsis. *The Plant Journal, 81*(2), 210–222. https://doi.org/10.1111/tpj.12719.

Zhang, G.-B., Yi, H.-Y., & Gong, J.-M. (2014). The Arabidopsis ethylene/jasmonic acid-NRT signaling module coordinates nitrate reallocation and the trade-off between growth and environmental adaptation. *The Plant Cell, 26*(10), 3984–3998. https://doi.org/10.1105/tpc.114.129296.

Zhang, L., Yu, Z., Xu, Y., Yu, M., Ren, Y., Zhang, S., Yang, G., Huang, J., Yan, K., Zheng, C., & Wu, C. (2021). Regulation of the stability and ABA import activity of NRT1.2/NPF4.6 by CEPR2-mediated phosphorylation in Arabidopsis. *Molecular Plant, 14*(4), 633–646. https://doi.org/10.1016/j.molp.2021.01.009.

Zhang, Y., Fan, W., Kinkema, M., Li, X., & Dong, X. (1999). Interaction of NPR1 with basic leucine zipper protein transcription factors that bind sequences required for salicylic acid induction of the

PR-1 gene. *Proceedings of the National Academy of Sciences, 96*(11), 6523–6528. https://doi.org/10.1073/pnas.96.11.6523.

Zhang, Y., Tessaro, M. J., Lassner, M., & Li, X. (2003). Knockout analysis of Arabidopsis transcription factors TGA2, TGA5, and TGA6 reveals their redundant and essential roles in systemic acquired resistance. *The Plant Cell, 15*(11), 2647–2653. https://doi.org/10.1105/tpc.014894.

Zhang, Y., Xu, S., Ding, P., Wang, D., Cheng, Y. T., He, J., Gao, M., Xu, F., Li, Y., Zhu, Z., Li, X., & Zhang, Y. (2010). Control of salicylic acid synthesis and systemic acquired resistance by two members of a plant-specific family of transcription factors. *Proceedings of the National Academy of Sciences, 107*(42), 18220–18225. https://doi.org/10.1073/pnas.1005225107.

Zhao, C., Pratelli, R., Yu, S., Shelley, B., Collakova, E., & Pilot, G. (2021). Detailed characterization of the UMAMIT proteins provides insight into their evolution, amino acid transport properties, and role in the plant. *Journal of Experimental Botany, 72*(18), 6400–6417. https://doi.org/10.1093/jxb/erab288.

Zheng, D., Han, X., An, Y. I., Guo, H., Xia, X., & Yin, W. (2013). The nitrate transporter NRT2.1 functions in the ethylene response to nitrate deficiency in Arabidopsis. *Plant, Cell & Environment, 36*(7), 1328–1337. https://doi.org/10.1111/pce.12062.

Zheng, X.-Y., Spivey, N. W., Zeng, W., Liu, P.-P., Fu, Z. Q., Klessig, D. F., He, S. Y., & Dong, X. (2012). Coronatine promotes Pseudomonas syringae virulence in plants by activating a signaling cascade that inhibits salicylic acid accumulation. *Cell Host & Microbe, 11*(6), 587–596. https://doi.org/10.1016/j.chom.2012.04.014.

Zhuo, D., Okamoto, M., Vidmar, J. J., & Glass, A. D. (1999). Regulation of a putative high-affinity nitrate transporter (Nrt2; 1At) in roots of Arabidopsis thaliana. *The Plant Journal, 17*(5), 563–568.

Ziemann, M., Bhave, M., & Zachgo, S. (2009). Origin and diversification of land plant CC-type glutaredoxins. *Genome Biology and Evolution, 1*, 265–277. https://doi.org/10.1093/gbe/evp025.

Ziemann, M. (2010). Glutaredoxin family genes in plant development. *PhD Thesis, Swinburne University of Technology, Melbourne, Australia*.

Abbreviations

Abbreviation	Description
A. thaliana	*Arabidopsis thaliana*
A. tumefaciens	*Agrobacterium tumefaciens*
ACC	1-aminocyclopropane-1-carboxylic acid
AIR1	AUXIN-INDUCED IN ROOT CULTURES 1
ALD1	AGD2-LIKE DEFENSE RESPONSE PROTEIN 1
AMT1-5	AMMONIUM TRANSPORTER 1-5
ANOVA	analysis of variance
ARR2	ARABIDOPSIS TYPE-B RESPONSE REGULATOR2
ATH1	ARABIDOPSIS THALIANA HOMEOBOX GENE 1
attL	attachment L site
attR	attachment R site
B. cinerea	*Botrytis cinerea*
BAK1	BR-INSENSITIVE 1-ASSOCIATED RECEPTOR-LIKE KINASE
BIN2	BR-INSENSITIVE 2
BOP	BLADE-ON-PETIOLE
bp	base pair
BR	brassinosteroid
bZIP	basic leucine zipper
Cas9	CRISPR associated protein 9
CBP60g	CALMODULIN-BINDING PROTEIN 60g
cDNA	Complementary cDNA
CEP	C-TERMINALLY ENCODED PEPTIDE
CEPH	CEP DEPENDENT PHOSPHATASE
CFU	colony forming units
CIAP	Calf Intestine Alkaline Phosphatase
CLE3	CLAVATA3/EMBRYO SURROUNDING REGION-RELATED 3
Col-0	*A. thaliana* ecotype Columbia-0; WT
CRISPR	clustered regularly interspaced short palindromic repeats
CYP81D11	CYTOCHROM P450 FAMILY PROTEIN 81D11
Cys	cysteine
DLO1	DMR6-LIKE OXYGENASE 1
DNA	desoxyribonucleinacid
dNTP	desoxyribonucleoside triphosphate
dYT	double Yeast Tryptone
E. coli	*Escherichia coli*
e.g.	exempli gratia, for example
EDS5	ENHANCED DISEASE SUSCEPTIBILITY 5
EPS1	ENHANCED PSEUDOMONAS SUSCEPTIBILITY 1
ERF	ETHYLENE-RESPONSIVE FACTOR
et al.	*et alii*, and others
ET	ethylene
FC	fold change
Fe-S	iron sulfur cluster
FEA4	FASCIATED EAR 4

Abbreviation	Description
FMO1	FLAVIN-DEPENDENT MONOOXYGENASE 1
FN	full nutrition
fwd	forward
g	gram
GA	giberellin
gDNA	genomic DNA
GFP	green fluorescent protein
GO	gene onthology
GRX	glutaredoxin
GSH	glutathione
GSSG	glutathione disulfide
GSTU	GLUTATHIONE S-TRANSFERASE
GUS	β-glucuronidase
GW7	Gateway™ casette with 35S terminator
H_2O	water
HA	human influenza hemagglutinin
hpi	hours post infection
HR	hypersensitive response
HRP	horseradish peroxidase
IAA19	INDOLE-ACETIC-3-ACID INDUCIBLE 19
ICS1	ISOCHORISMATE SYNTHASE 1
IDCR	Ionic Detergent Compatibility Reagent
IGMT1	INDOLE GLUCOSINOLATE O-METHYLTRANSFERASE 1
IP	immunoprecipitation
ISCA	IRON SULFUR CLUSTER ASSEMBLY
JA	jasmonic acid
JAZ	JAZMONATE ZIM DOMAIN
kb	kilo base
kDa	kilo dalton
kV	kilovolt
λ	bacteriophage λ
LB	Lysogeny Broth
LB	left border
LCMS	liquid chromatography coupled with mass spectrometry
LD	long day
LL	low light
LL → NL	backshift from LL to NL
LN	low nitrogen
µF	microfarad
MarVis	Marker Visualization
miRNA	microRNA
MSCA1	MALE STERILE CONVERTED ANTHER 1
MtN19	MEDICAGO TRUNCATULA NODULIN 19
N. benthamiana	*Nicotiana benthamiana*
NAC	NAC DOMAIN CONTAINING PROTEIN
nahG	salicylate hydroxylase

Abbreviation	Description
NHP	N-hydroxy pipecolic acid
NIG	Next Genome Sequencing Integrative Genomics Core Unit
NINJA	NOVEL INERACTOR OF JAZ
NL	normal light
NLP	NIN-LIKE PROTEIN
NN	no nitrogen
NPR1	NONEXPRESSOR OF PATHOGENESIS-RELATED GENES 1
NRT	NITRATE TRANSPORTER
Ω	ohm
OD_{xx}	Optical Density at wavelength xx
ORA59	OCTADECANOID-RESPONSIVE ARABIDOPSIS APETALA2/ETHYLENE RESPONSE FACTOR DOMAIN PROTEIN 59
p.adj	adjusted *p*-value
PAN	TGACG motif binding bZIP transcription factor PERIANTHIA
PBS3	AVRPPHB SUSCEPTIBLE 3
PCA	principal component analysis
PCR	polymerase chain reaction
PDF1.2	PLANT DEFENSIN 1.2
PER	PEROXIDASE
Pip	pipecolic acid
PPA_1	A_1-phytoprostanes
PR	PATHOGENESIS-RELATED
Psm	*Pseudomonas syringae* pv. *maculicola* ES4326
Pst	*Pseudomonas syringae* pv. *tomatoe* DC3000
PTI	PAMP-triggered immunity
pv.	pathovar
PYL	PYRABACTIN RESISTANCE 1-LIKE
Q1, Q2	leucine rich regions in TGA factors
qRT-PCR	quantitative real time PCR
RB	right border
rev	reverse
RL3	RAD-LIKE3
RLU	relative luminescence units
RNA	ribonucleinacid
ROXY	CC-type glutaredoxin
RPK	reads per kilobases
rpm	rounds per minute
SA	salicylic acid
SAR	systemic acquired resistance
SARD	SAR DEFICINET
SCL14	SCARECROW-LIKE 14
SD	short day
SEM	standard error of the mean
SURE2	SUCROSE-RESPONSIVE ELEMENT 2
SWEET11	SUCROSE EFFLUX TRANSPORTER
T35S	35S terminator

Abbreviation	Description
TAIR	The Arabidopsis Information Resource
TF	transcription factor
TFL1	TERMINAL FLOWER LOCUS 1
TGA	TGACG MOTIF BINDING TRANSCRIPTION FACTOR
TIBA	2,3,5-triiodobenzoic acid
TPL	TOPLESS
TPM	transcript per million
TPR	TOPLESS-RELATED PROTEIN
TSS	transcription start site
U	units
UBQ	UBIQUITIN
UMAMIT35	USUALLY MULTIPLE ACIDS MOVE IN AND OUT TRANSPORTERS 35
untr	untreated
UV	ultraviolet
WRKY	WRKY DNA-BINDING PROTEIN
WT	*A. thaliana* ecotype Col-0, wild type
WT	wild type, Col-0
X-Gal	5-bromo-4-chloro-3-indolyl-β-D-galactopyranoside
XTH8	XYLOGLUCAN ENDOTRANS-GLUCOSYLASE/HYDROLASE 8
YEB	Yeast Extract Broth
YPAD	Yeast Extract Peptone Adenine Dextrose

Supplement

Supplementary Figures

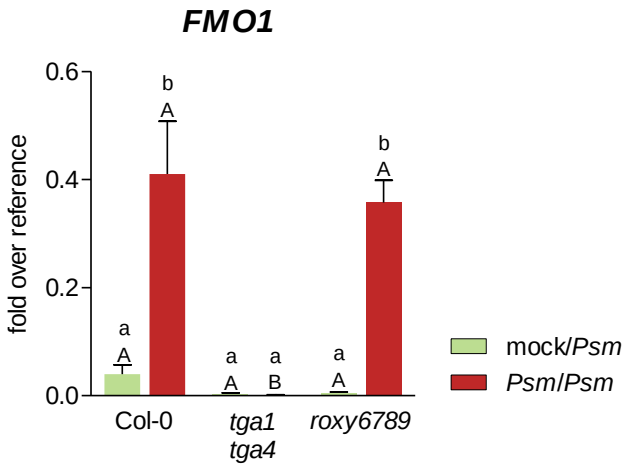

Supplementary Figure S1: *FMO1* expression is not regulated by ROXY6, 7, 8, 9 in *Psm*-infected SAR leaves. Lower leaves of 4.5-week-old *A. thaliana* plants were infiltrated with $MgCl_2$ (green, mock treatment) or infiltrated with *Psm* (red, OD_{600} = 0.005). After 48 h, upper leaves were infiltrated with *Psm*. The upper leaves were collected after 8 hours, RNA was isolated and cDNA synthesized. Expression of *FMO1* was analyzed by qRT-PCR in the genotypes Col-0, *tga1 tga4* and *roxy6789*, *UBQ5* was used as a reference gene. Mean values of four to six biological replicates are shown. Error bars represent the standard error of the mean. Lowercase letters indicate statistically significant differences within a genotype between different treatments, uppercase letters indicate significant differences between genotypes subjected to the same treatments. Statistical analysis was performed by using two-way ANOVA and Bonferroni's post-test (*p*-value < 0.05).

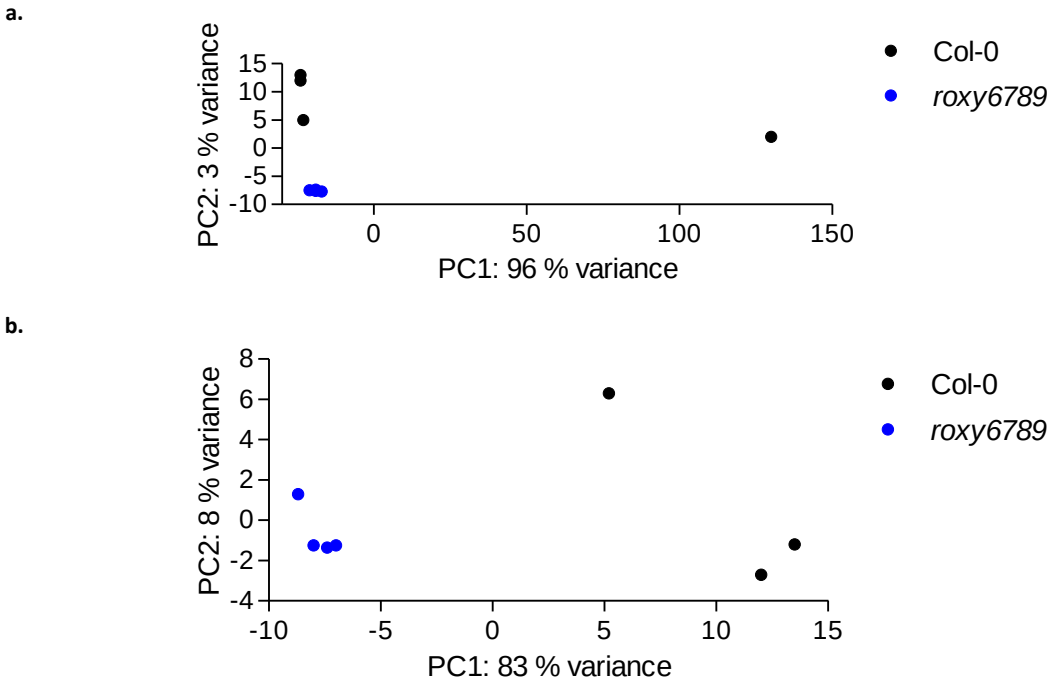

Supplementary Figure S2: Principal component analysis of transcriptome data. 7-day old seedlings grown on full nutrition (FN) plates under constant light conditions (70 µmol photons s^{-1} m^{-2}) were transferred to either FN or low nitrogen (LN) plates. Two days later, roots were collected, RNA was isolated. Per treatment, RNA of 5 replicates was pooled and sent for RNA sequencing.

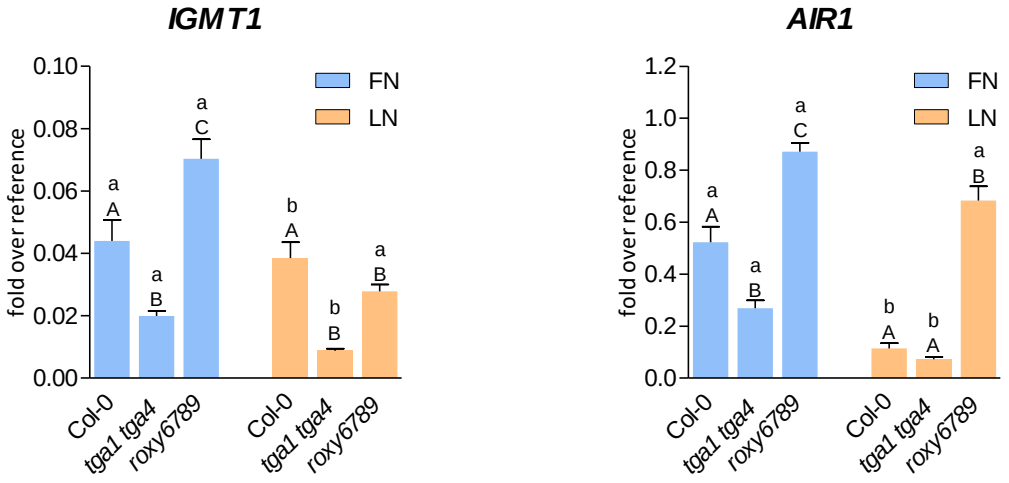

Supplementary Figure S3: The expression of *IGMT1* and *AIR1* is activated by TGA1, 4 and repressed by ROXY6, 7, 8, 9. 7-day old seedlings grown on full nutrition (FN) plates under constant light conditions (70 µmol photons s^{-1} m^{-2}) were transferred to either FN or low nitrogen (LN) plates. Two days later, roots were collected, RNA was isolated and cDNA synthesized. Expression of *IGMT1* and *AIR1* was analyzed by qRT-PCR, *UBQ5* was used as a reference gene. Mean values of four to five biological replicates are shown. Error bars represent the standard error of the mean. Lowercase letters indicate statistically significant differences within the genotype between the treatments, uppercase letters indicate significant differences within treatment between the genotypes. Statistical analyses were performed with the logarithmic values by using two-way ANOVA and Bonferroni's post-test (*p*-value < 0.05). Three independent experiments were performed with similar results.

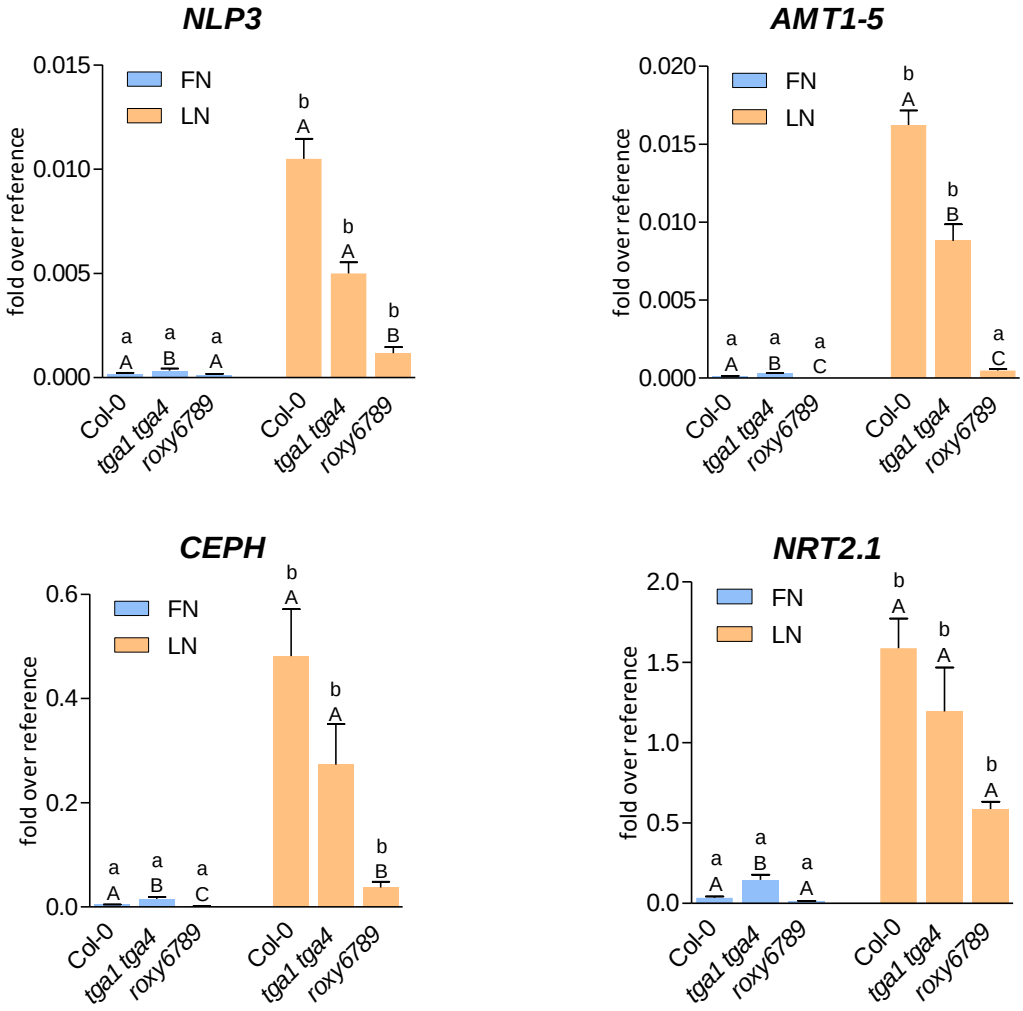

Supplementary Figure S4: ROXY6, 7, 8, 9 activates the expression of *NLP3*, *AMT1-5*, *CEPH* and *NRT2.1* in *A. thaliana* roots. 7-day old seedlings grown on full nutrition (FN) plates under constant light conditions (70 µmol photons s^{-1} m^{-2}) were transferred to either FN or low nitrogen (LN) plates. Two days later, roots were collected, RNA was isolated and cDNA synthesized. Expression of *NLP3*, *AMT1-5*, *CEPH* and *NRT2.1* was analyzed by qRT-PCR, *UBQ5* was used as a reference gene. Mean values of four to five biological replicates are shown. Error bars represent the standard error of the mean. Lowercase letters indicate statistically significant differences within the genotype between the treatments, uppercase letters indicate significant differences within treatment between the genotypes. Statistical analyses were performed with the logarithmic values by using two-way ANOVA and Bonferroni's post-test (p-value < 0.05). Three independent experiments were performed with similar results.

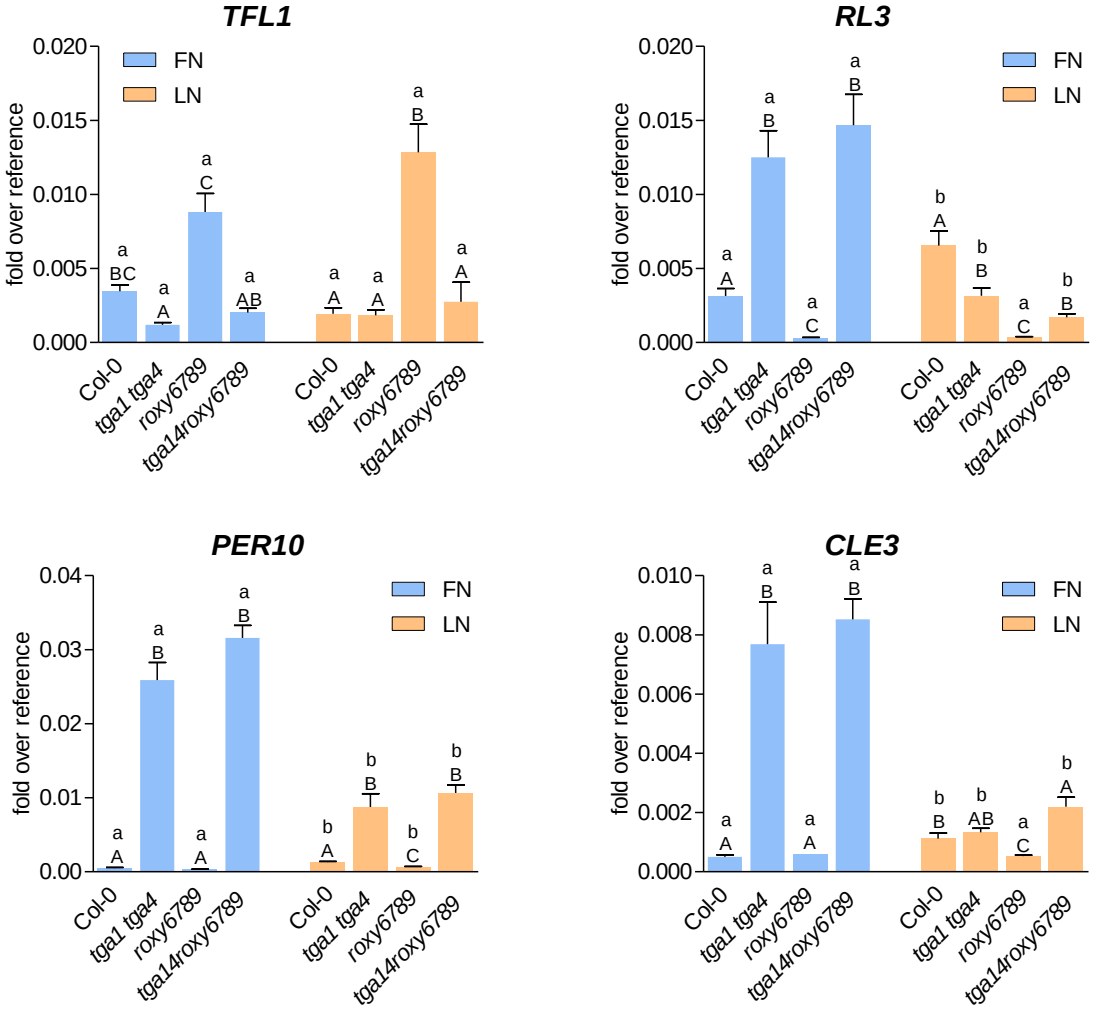

Supplementary Figure S5: ROXY6, 7, 8, 9 and TGA1, 4 function in one pathway in order to control the expression of *TFL1*, *RL3*, *PER10* and *CLE3* expression in *A. thaliana* roots. 7-day old seedlings grown on full nutrition (FN) plates under constant light conditions (70 µmol photons s^{-1} m^{-2}) were transferred to either FN or low nitrogen (LN) plates. Two days later, roots were collected, RNA was isolated and cDNA synthesized. Expression of *TFL1*, *RL3*, *PER10* and *CLE3* was analyzed by qRT-PCR, *UBQ5* was used as a reference gene. Mean values of four to five biological replicates are shown. Error bars represent the standard error of the mean. Lowercase letters indicate statistically significant differences within the genotype between the treatments, uppercase letters indicate significant differences within treatment between the genotypes. Statistical analyses were performed with the logarithmic values by using two-way ANOVA and Bonferroni's post-test (*p*-value < 0.05). Two independent experiments were performed with similar results.

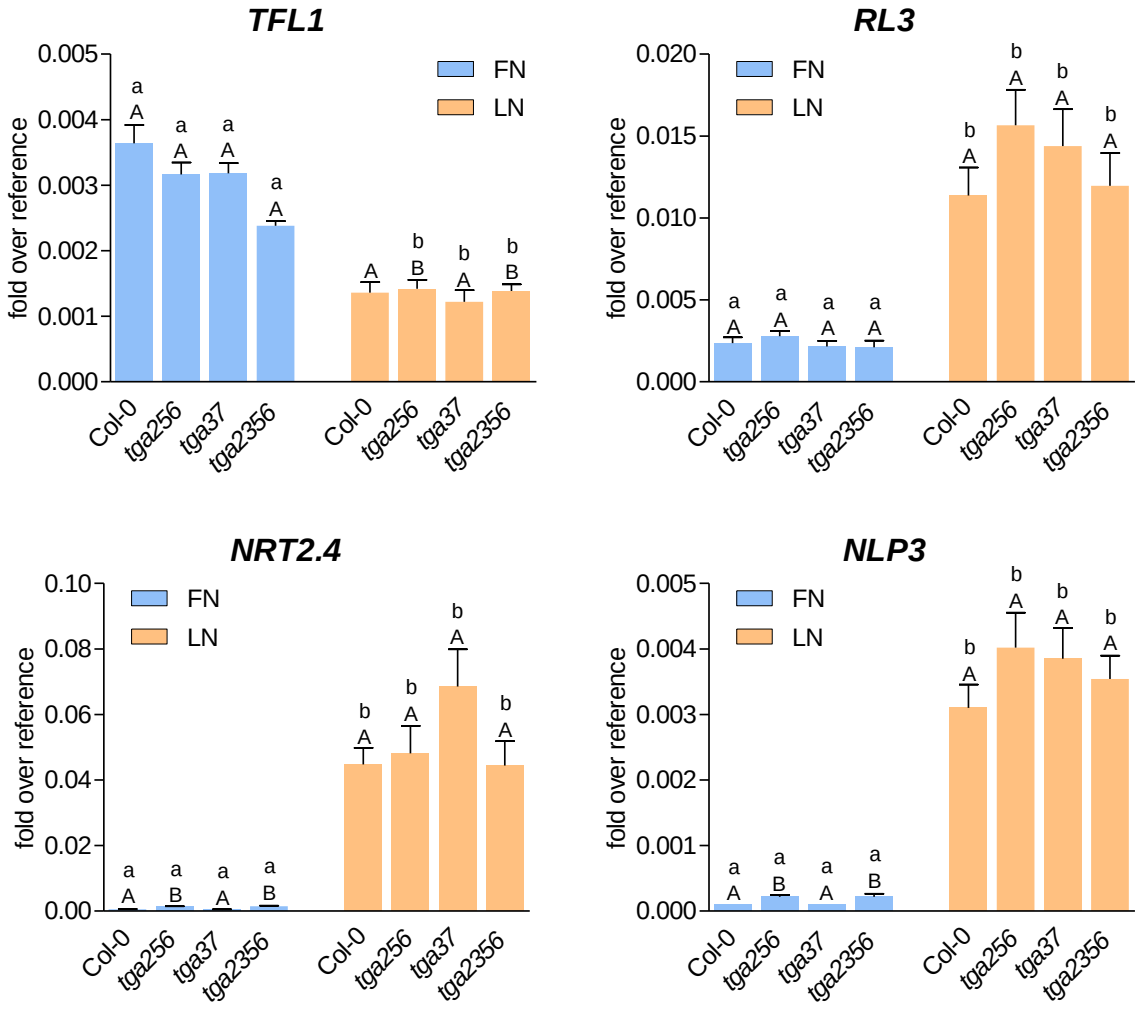

Supplementary Figure S6: The expression of *TFL1, NRT2.2, NRT2.4, NLP3, UMAMIT35* and *RL3* is not regulated by clade II and III TGA factors. 7-day old seedlings grown on full nutrition (FN) plates under constant light conditions (70 µmol photons s^{-1} m^{-2}) were transferred to either FN or low nitrogen (LN) plates. Two days later, roots were collected, RNA was isolated and cDNA synthesized. Expression of *TFL1, NRT2.2, NRT2.4, NLP3, UMAMIT35* and *RL3* was analyzed by qRT-PCR, *UBQ5* was used as a reference gene. Mean values of four to five biological replicates are shown. Error bars represent the standard error of the mean. Lowercase letters indicate statistically significant differences within the genotype between the treatments, uppercase letters indicate significant differences within treatment between the genotypes. Statistical analyses were performed with the logarithmic values by using two-way ANOVA and Bonferroni's post-test (*p*-value < 0.05). Two independent experiments were performed with similar results.

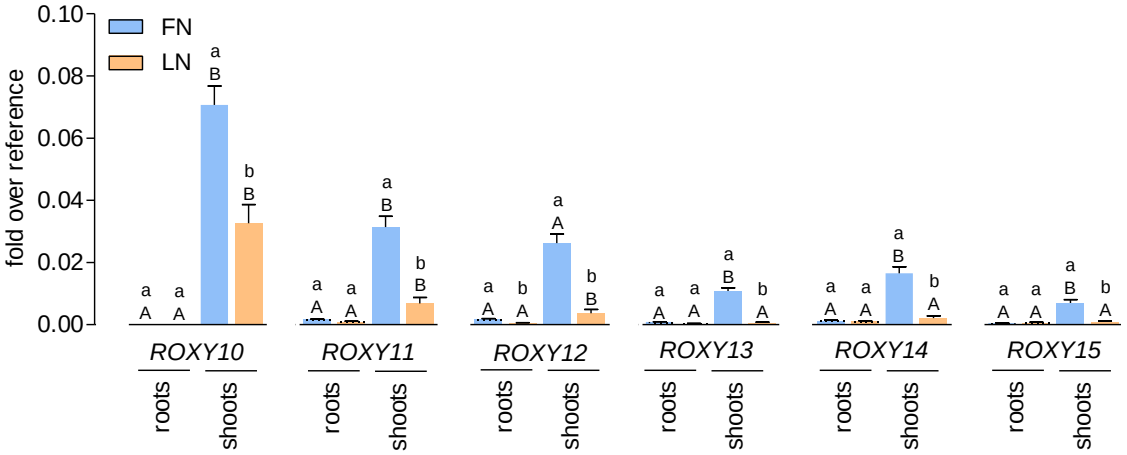

Supplementary Figure S7: Expression of *ROXY10, ROXY11, ROXY12, ROXY13, ROXY14* and *ROXY15* in *A. thaliana* roots and shoots in sufficient nitrogen supply and upon nitrogen starvation conditions. 7-day old seedlings grown on full nutrition (FN) plates under constant light conditions (70 µmol photons s^{-1} m^{-2}) were transferred to either FN or low nitrogen (LN) plates. Two days later, roots or shoots were separately collected, RNA was isolated and cDNA synthesized. Expression of *ROXY10, ROXY11, ROXY12, ROXY13, ROXY14* and *ROXY15* was analyzed in the wild type Col-0 by qRT-PCR, *UBQ5* was used as a reference gene. Mean values of four to five biological replicates are shown. Error bars represent the standard error of the mean. Lowercase letters indicate statistically significant differences within the tissue between the conditions, uppercase letters indicate significant differences within treatment between the tissues. Statistical analyses were performed individually for each gene with the logarithmic values by using two-way ANOVA and Bonferroni's post-test (*p*-value < 0.05).

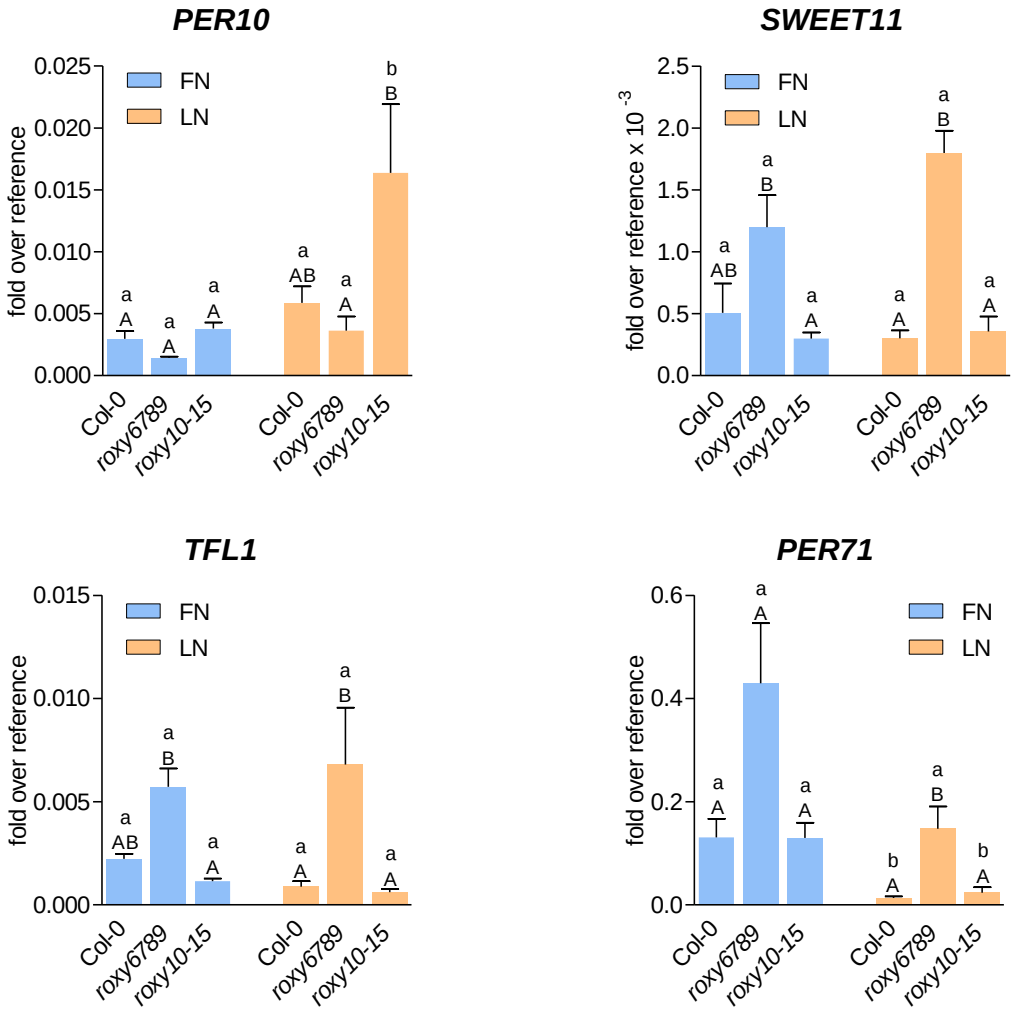

Supplementary Figure S8: The expression of *PER10, SWEET11, TFL1,* and *PER71* is not regulated by ROXY10-15. 7-day old seedlings grown on full nutrition (FN) plates under constant light conditions (70 µmol photons s^{-1} m^{-2}) were transferred to either FN or low nitrogen (LN) plates. Two days later, roots were collected, RNA was isolated and cDNA synthesized. Expression of *PER10, SWEET11, TFL1* and *PER71* was analyzed by qRT-PCR, *UBQ5* was used as a reference gene. Mean values of four to five biological replicates are shown. Error bars represent the standard error of the mean. Lowercase letters indicate statistically significant differences within the genotype between the treatments, uppercase letters indicate significant differences within treatment between the genotypes. Statistical analyses were performed with the logarithmic values by using two-way ANOVA and Bonferroni's post-test (p-value < 0.05).

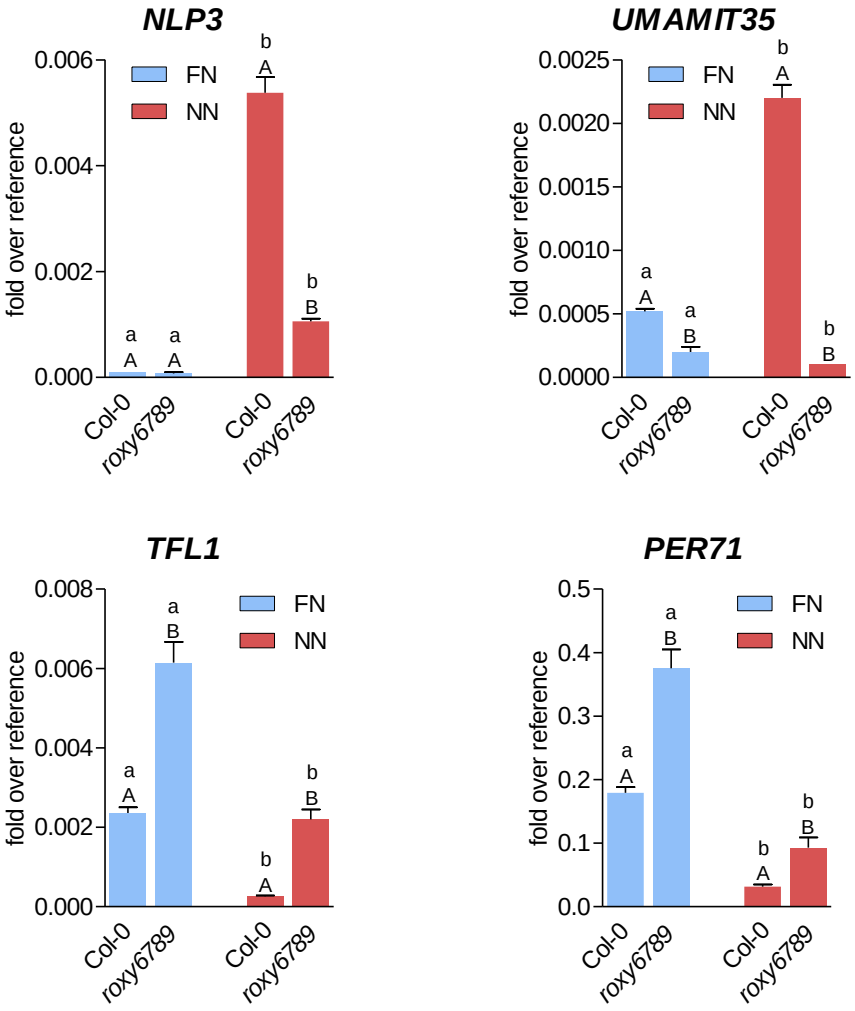

Supplementary Figure S9: Induction of *NRT2.2* does not require nitrogen. 7-day old seedlings grown on full nutrition (FN) plates under constant light conditions (70 µmol photons s^{-1} m^{-2}) were transferred to either FN or no nitrogen (NN) plates. Two days later, roots were collected, RNA was isolated and cDNA synthesized. Expression of *NRT2.2* was analyzed by qRT-PCR, *UBQ5* was used as a reference gene. Mean values of four to five biological replicates are shown. Error bars represent the standard error of the mean. Lowercase letters indicate statistically significant differences within the genotype between the treatments, uppercase letters indicate significant differences within treatment between the genotypes. Statistical analyses were performed with the logarithmic values by using two-way ANOVA and Bonferroni's post-test (*p*-value < 0.05).

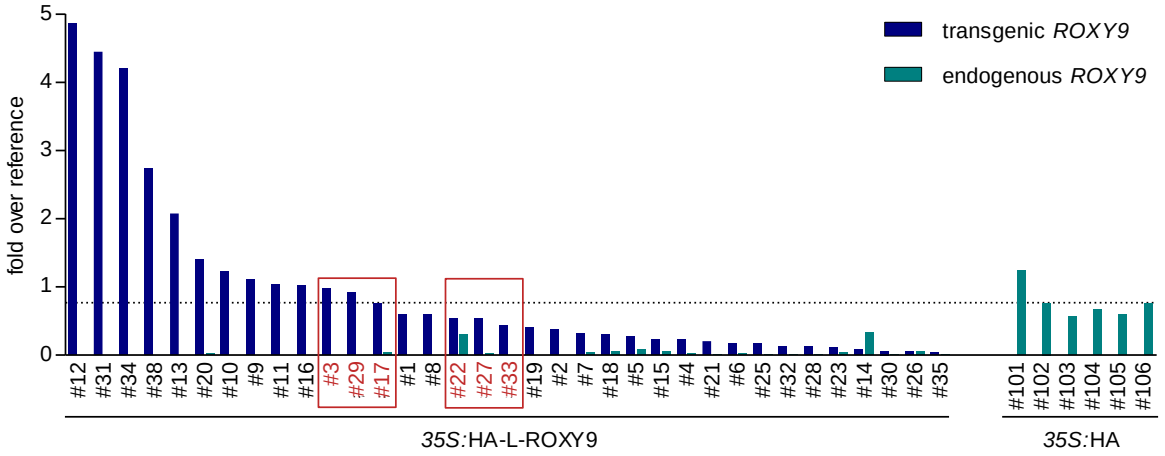
transgenic ROXY9
endogenous ROXY9
fold over reference
0
1
2
3
4
5
#12 #31 #34 #38 #13 #20 #10 #9 #11 #16 #3 #29 #17 #1 #8 #22 #27 #33 #19 #2 #7 #18 #5 #15 #4 #21 #6 #25 #32 #28 #23 #14 #30 #26 #35
#101 #102 #103 #104 #105 #106
35S:HA-L-ROXY9
35S:HA

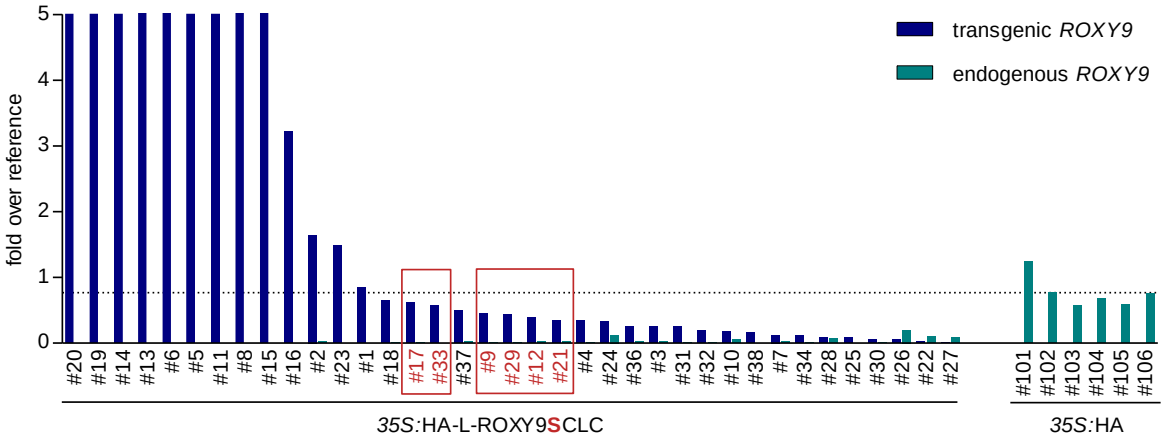
transgenic ROXY9
endogenous ROXY9
fold over reference
0
1
2
3
4
5
#20 #19 #14 #13 #6 #5 #11 #8 #15 #16 #2 #23 #1 #18 #17 #33 #37 #9 #29 #12 #21 #4 #24 #36 #3 #31 #32 #10 #38 #7 #34 #28 #25 #30 #26 #22 #27
#101 #102 #103 #104 #105 #106
35S:HA-L-ROXY9SCLC
35S:HA

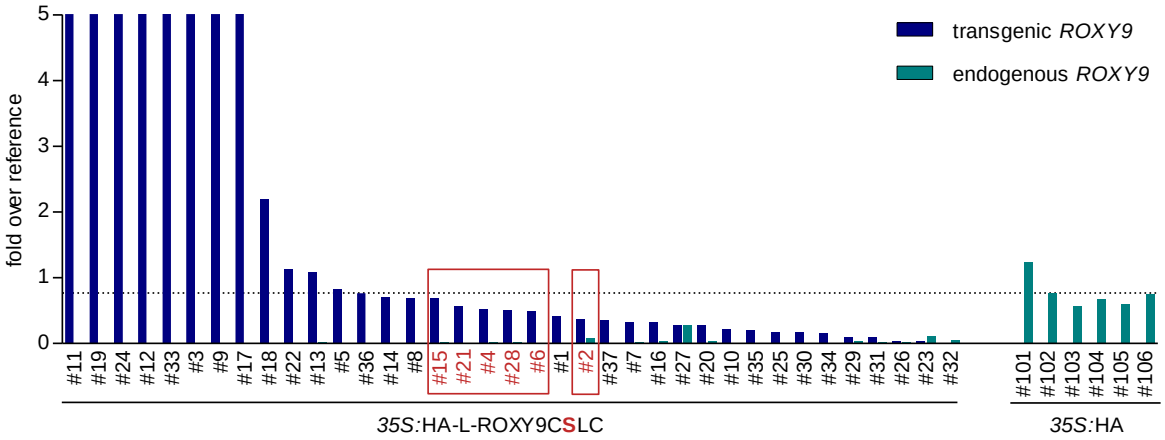
transgenic ROXY9
endogenous ROXY9
fold over reference
0
1
2
3
4
5
#11 #19 #24 #12 #33 #3 #9 #17 #18 #22 #13 #5 #36 #14 #8 #15 #21 #4 #28 #6 #1 #2 #37 #7 #16 #27 #20 #10 #35 #25 #30 #34 #29 #31 #26 #23 #32
#101 #102 #103 #104 #105 #106
35S:HA-L-ROXY9CSLC
35S:HA

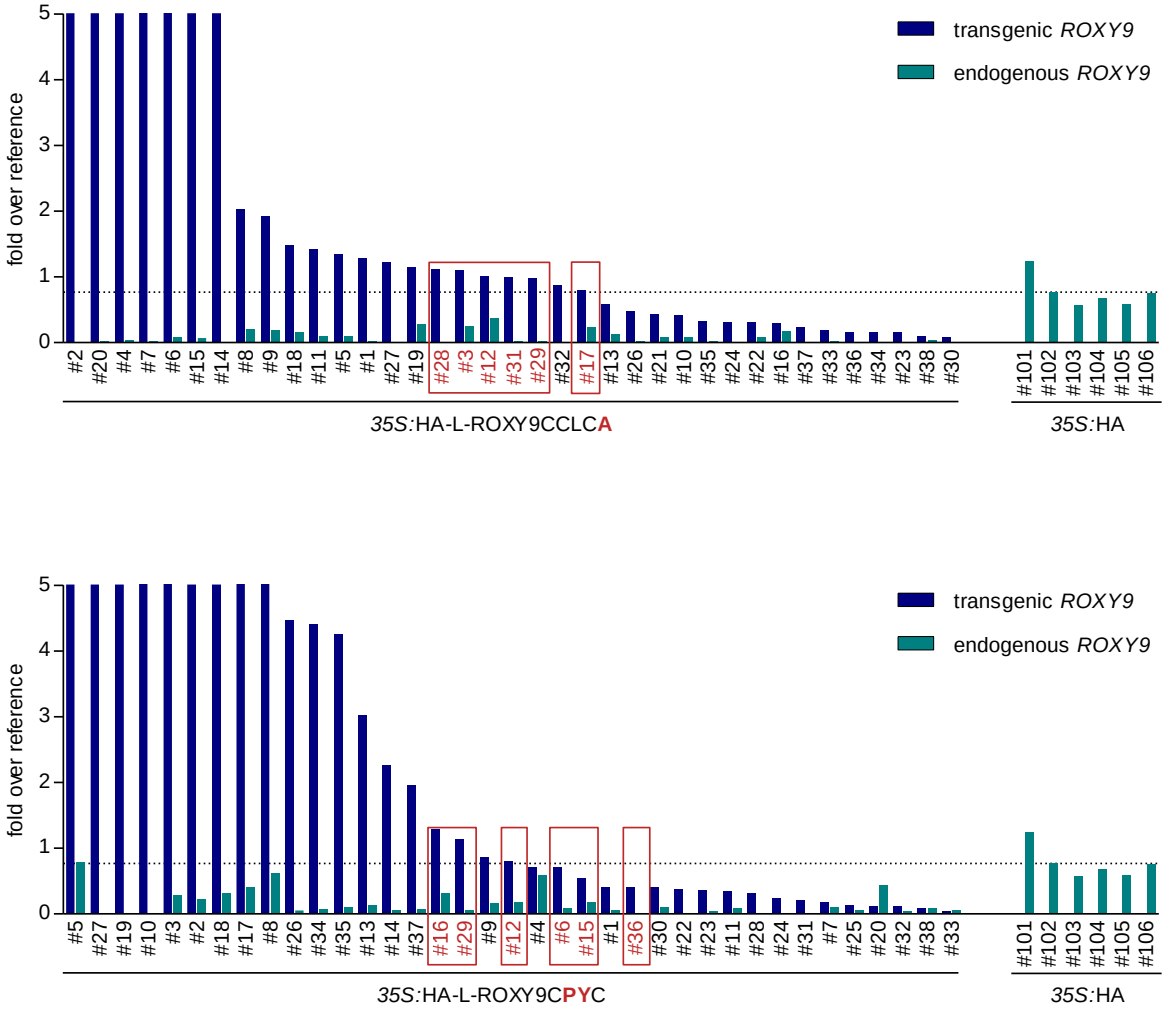

Supplementary Figure S10: Expression of transgenic and endogenous *ROXY9* in leaves of primary transformants. *roxy6789* was stably transformed with HA-L-ROXY9 active site variants by flower dipping. Leaves of the T1 generation were collected, RNA and proteins were isolated and cDNA was synthesized. Expression of endogenous and transgenic *ROXY9* was analyzed by qRT-PCR, *UBQ5* was used as a reference gene. Lines marked in red were chosen for subsequent analysis.

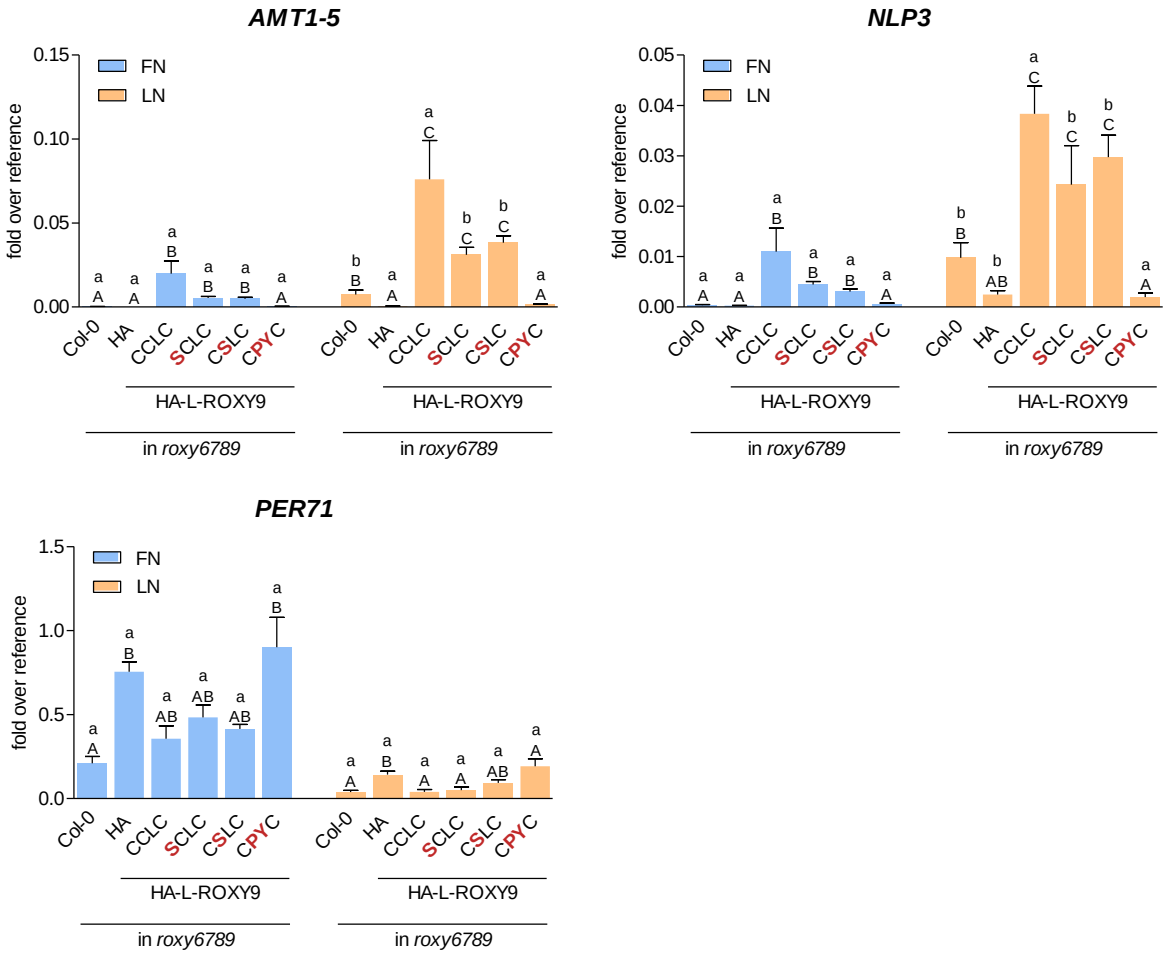

Supplementary Figure S11: The first and second cysteine of the ROXY9 active site motif are not required for the regulation of *NLP3, AMT1-5* and *PER71* expression in *A. thaliana* roots upon nitrogen starvation. 7-day old T2 seedlings grown on full nutrition (FN) plates under constant light conditions (70 µmol photons s^{-1} m^{-2}) were transferred to either FN or low nitrogen (LN) plates. Two days later, roots were collected, RNA was isolated and cDNA synthesized. Expression of *NLP3, AMT1-5* and *PER71* was analyzed in 4-5 independent lines per *roxy6789* active site variant by qRT-PCR, *UBQ5* was used as a reference gene. Mean values of four to five biological replicates are shown. Error bars represent the standard error of the mean. Lowercase letters indicate statistically significant differences within the genotype between the treatments, uppercase letters indicate significant differences within treatment between the genotypes. Statistical analyses were performed with the logarithmic values by using two-way ANOVA and Bonferroni's post-test (p-value < 0.05).

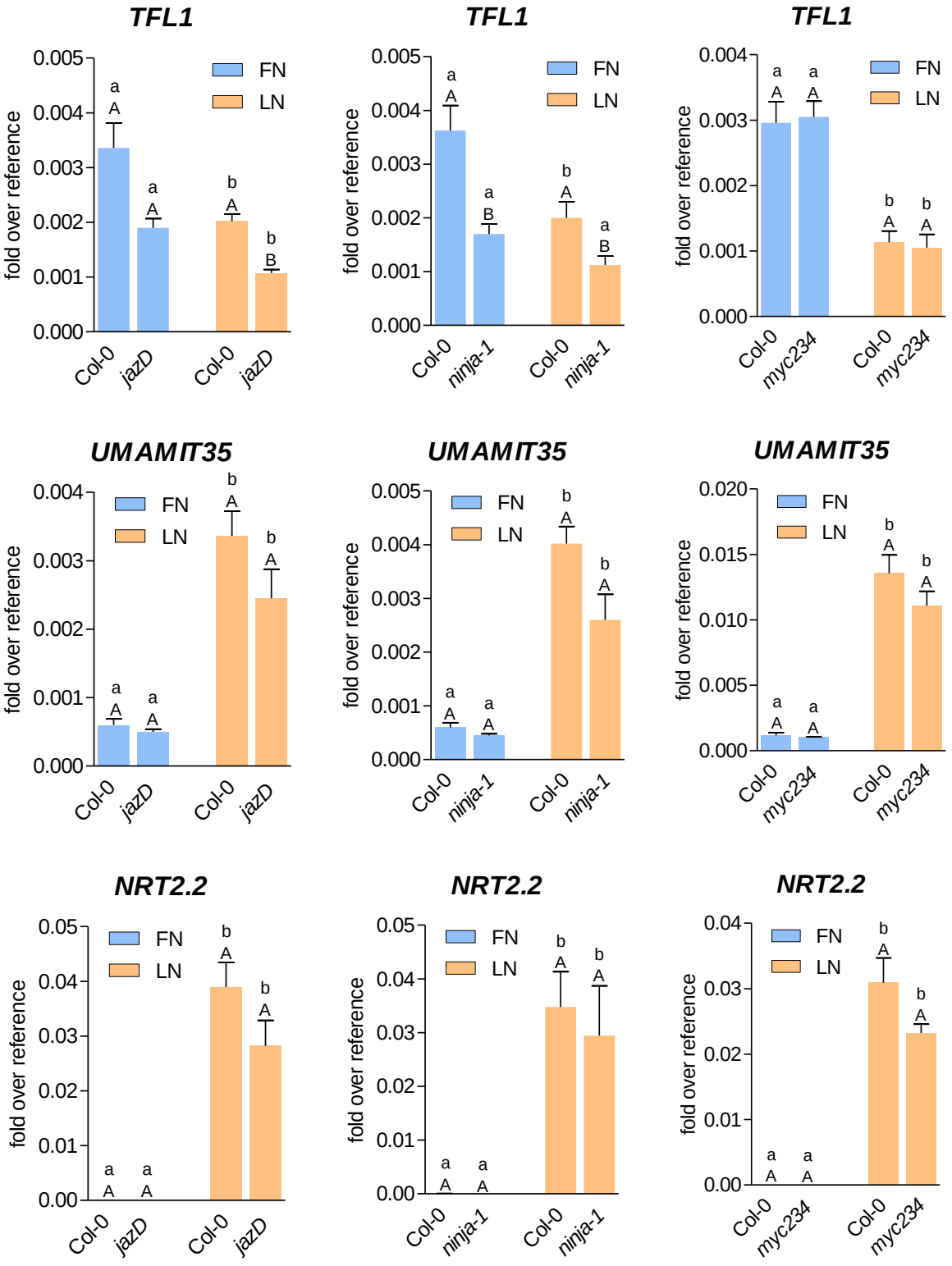

Supplementary Figure S12: The expression of *TFL1* is activated by JAZ1-7, 9, 10 and NINJA. 7-day old seedlings grown on full nutrition (FN) plates under constant light conditions (70 µmol photons s^{-1} m^{-2}) were transferred to either FN or low nitrogen (LN) plates. Two days later, roots were collected, RNA was isolated and cDNA synthesized. Expression of *TFL1, UMAMIT35* and *NRT2.2* was analyzed by qRT-PCR, *UBQ5* was used as a reference gene. Mean values of four to five biological replicates are shown. Error bars represent the standard error of the mean. Lowercase letters indicate statistically significant differences within the genotype between the treatments, uppercase letters indicate significant differences within treatment between the genotypes. Statistical analyses were performed with the logarithmic values by using two-way ANOVA and Bonferroni's post-test (*p*-value < 0.05). Three independent experiments were performed and similar results were obtained.

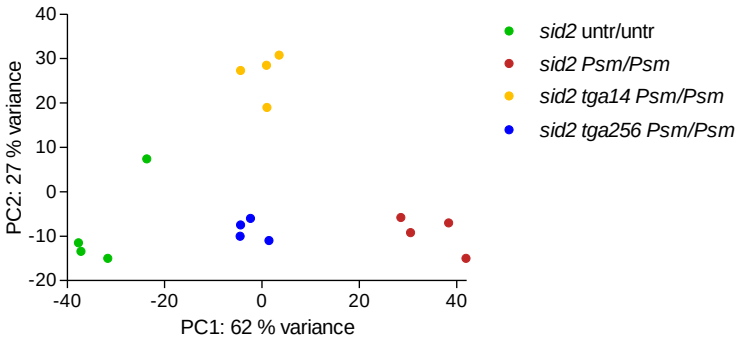

Supplementary Figure S13: Principal component analysis of transcriptome data. Lower leaves of 4.5-week-old *A. thaliana* plants were infiltrated with *Psm* or left untreated. After 48 h, upper leaves were infiltrated with *Psm* or left untreated. The upper leaves were collected after 8 hours, RNA was isolated. Per treatment, RNA of 5 plants was pooled and sent for RNA sequencing.

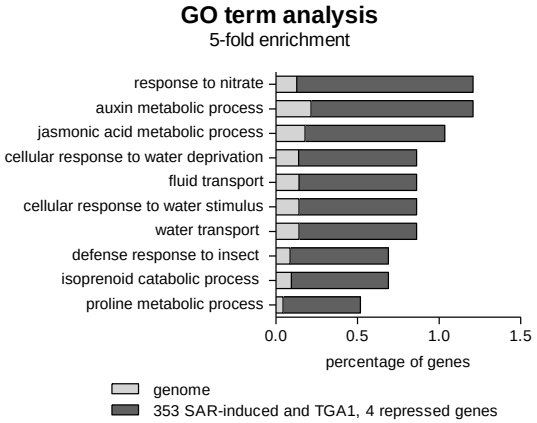

Supplementary Figure S14: Nitrate- and JA-responsive genes are repressed by TGA1, 4 in *Psm*-infected SAR leaves. Gene Ontology (GO) term analysis was performed with the 353 genes that are higher expressed (log_2 FC > 1, *p*.adj < 0.05) in *sid2 tga14* compared to *sid2* after *Psm*/*Psm* treatment according to transcriptome data**.** GO terms with a 5-fold enrichment are shown. Statistical analysis was performed using Fisher test and False discovery rate (FDR) < 0.05.

a.

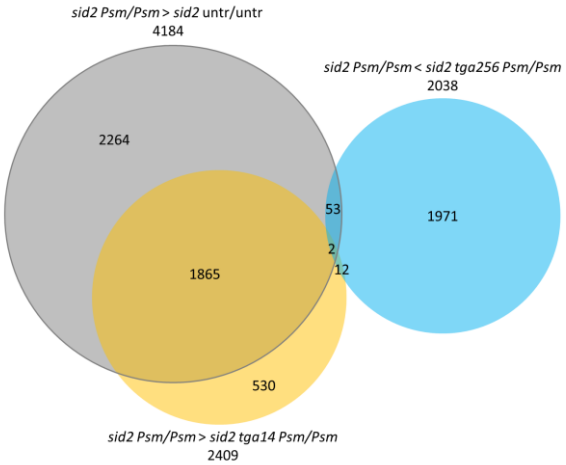

b.

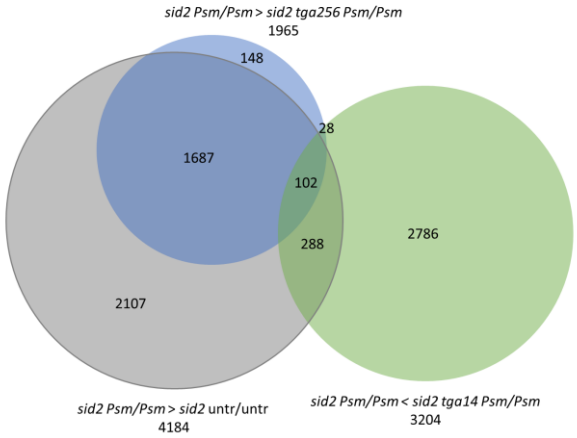

Supplementary Figure S15: Schematic representation of transcriptome data. Lower leaves of 4.5-week-old *A. thaliana* plants were infiltrated with *Psm* or left untreated. After 48 h, upper leaves were infiltrated with *Psm* or left untreated. The upper leaves were collected after 8 hours and RNA was isolated. Per treatment, RNA of 5 plants was pooled and sent for RNA sequencing. The results were mapped against the *A. thaliana* genome and quantified. Venn diagrams were generated to analyze the SAR-inducible genes in the *sid2* mutant and genes, which are differentially expressed in the *sid2 tga1 tga4* or *sid2 tga2 tga5 tga6* mutant compared to *sid2* (log_2 fold change (FC) > 1, adjusted p-value (p.adj) < 0.05).

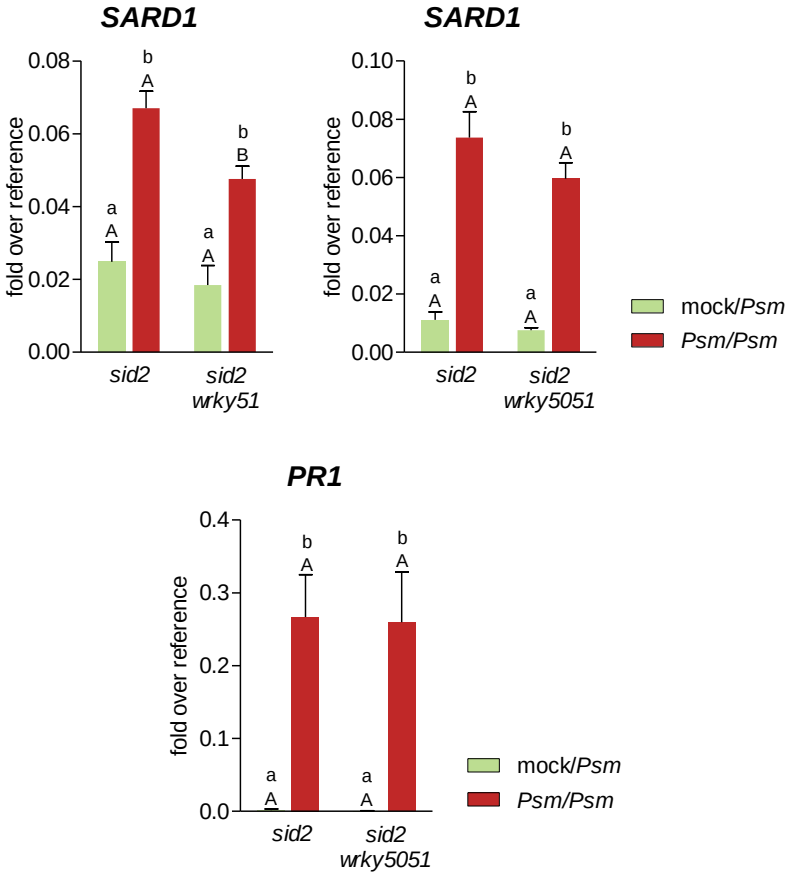

Supplementary Figure S16: *SARD1* and *PR1* expression is not regulated by WRKY51 in *Psm*-infected SAR leaves. Lower leaves of 4.5-week-old *A. thaliana* plants were infiltrated with $MgCl_2$ (green, mock treatment) or infiltrated with *Psm* (red, OD_{600} = 0.005). After 48 h, upper leaves were infiltrated with *Psm*. The upper leaves were collected after 8 hours, RNA was isolated and cDNA synthesized. Expression of *SARD1* and *PR1* was analyzed by qRT-PCR, *UBQ5* was used as a reference. Mean values of eight to nine biological replicates are shown. Error bars represent the standard error of the mean. Lowercase letters indicate statistically significant differences within a genotype between different treatments, uppercase letters indicate significant differences between genotypes subjected to the same treatments. Statistical analyses were performed by using two-way ANOVA and Bonferroni's post-test.

Supplementary Tables

Supplementary Table S1: Number of detected proteins by LCMS. Roots of 4-week-old *A. thaliana* plants expressing HA-Turbo or HA-Turbo-ROXY9 were submerged in 200 µM biotin solution. After 3 hours, roots of 20 plants per genotype were collected, proteins were extracted, the free biotin was removed by desalting and a streptavidin pull down was performed. The proteins were digested with trypsin and purified. Two biological replicates were analyzed twice via LCMS and the data was mapped to the *A. thaliana* proteome.

	Replicate, LCMS run	Detected proteins
roxy6789 with HA-Turbo	1, 1	351
	1, 2	413
	2, 1	118
	2, 2	110
roxy6789 with HA-Turbo-ROXY9	1, 1	113
	1, 2	103
	2, 1	173
	2, 2	201

Supplementary Table S2: Statistical analysis of fresh weight data obtained from stably transformed *roxy6789* with HA-L-ROXY9 active site variants. Plants were grown for 4 weeks in 12/12 h light regime. Fresh weight of the whole rosette was measured of 12 biological replicates per line. Statistical analysis was performed by using one-way ANOVA and Tukey's post-test. *p*-value: * < 0.05, ** < 0.001, *** < 0.0001 ns: not significant; *p*-value > 0.05

Comparison	Significant difference
Col-0 vs roxy6789	*
Col-0 vs HA #4-8	ns
Col-0 vs HA #101-8	ns
Col-0 vs HA #102-8	ns
Col-0 vs ROXY9CCLC #2-1	ns
Col-0 vs ROXY9CCLC #27-4	ns
Col-0 vs ROXY9SCLC #9-3	**
Col-0 vs ROXY9SCLC #12-2	ns
Col-0 vs ROXY9SCLC #37-5	ns
Col-0 vs ROXY9CSLC #6-1	ns
Col-0 vs ROXY9CSLC #15-3	ns
roxy6789 vs HA #4-8	ns
roxy6789 vs HA #101-8	ns
roxy6789 vs HA #102-8	ns
roxy6789 vs ROXY9CCLC #2-1	***
roxy6789 vs ROXY9CCLC #27-4	***
roxy6789 vs ROXY9SCLC #9-3	***
roxy6789 vs ROXY9SCLC #12-2	*
roxy6789 vs ROXY9SCLC #37-5	***
roxy6789 vs ROXY9CSLC #6-1	*
roxy6789 vs ROXY9CSLC #15-3	ns
HA #4-8 vs HA #101-8	ns
HA #4-8 vs HA #102-8	ns
HA #4-8 vs ROXY9CCLC #2-1	*
HA #4-8 vs ROXY9CCLC #27-4	***

Comparison	Significant difference
HA #4-8 vs ROXY9SCLC #9-3	***
HA #4-8 vs ROXY9SCLC #12-2	ns
HA #4-8 vs ROXY9SCLC #37-5	**
HA #4-8 vs ROXY9CSLC #6-1	ns
HA #4-8 vs ROXY9CSLC #15-3	ns
HA #101-8 vs HA #102-8	ns
HA #101-8 vs ROXY9CCLC #2-1	ns
HA #101-8 vs ROXY9CCLC #27-4	*
HA #101-8 vs ROXY9SCLC #9-3	***
HA #101-8 vs ROXY9SCLC #12-2	ns
HA #101-8 vs ROXY9SCLC #37-5	ns
HA #101-8 vs ROXY9CSLC #6-1	ns
HA #101-8 vs ROXY9CSLC #15-3	ns
HA #102-8 vs ROXY9CCLC #2-1	ns
HA #102-8 vs ROXY9CCLC #27-4	**
HA #102-8 vs ROXY9SCLC #9-3	***
HA #102-8 vs ROXY9SCLC #12-2	ns
HA #102-8 vs ROXY9SCLC #37-5	*
HA #102-8 vs ROXY9CSLC #6-1	ns
HA #102-8 vs ROXY9CSLC #15-3	ns
ROXY9CCLC #2-1 vs ROXY9CCLC #27-4	ns
ROXY9CCLC #2-1 vs ROXY9SCLC #9-3	ns
ROXY9CCLC #2-1 vs ROXY9SCLC #12-2	ns
ROXY9CCLC #2-1 vs ROXY9SCLC #37-5	ns
ROXY9CCLC #2-1 vs ROXY9CSLC #6-1	ns
ROXY9CCLC #2-1 vs ROXY9CSLC #15-3	ns
ROXY9CCLC #27-4 vs ROXY9SCLC #9-3	ns
ROXY9CCLC #27-4 vs ROXY9SCLC #12-2	ns
ROXY9CCLC #27-4 vs ROXY9SCLC #37-5	ns
ROXY9CCLC #27-4 vs ROXY9CSLC #6-1	ns
ROXY9CCLC #27-4 vs ROXY9CSLC #15-3	*
ROXY9SCLC #9-3 vs ROXY9SCLC #12-2	**
ROXY9SCLC #9-3 vs ROXY9SCLC #37-5	ns
ROXY9SCLC #9-3 vs ROXY9CSLC #6-1	**
ROXY9SCLC #9-3 vs ROXY9CSLC #15-3	***
ROXY9SCLC #12-2 vs ROXY9SCLC #37-5	ns
ROXY9SCLC #12-2 vs ROXY9CSLC #6-1	ns
ROXY9SCLC #12-2 vs ROXY9CSLC #15-3	ns
ROXY9SCLC #37-5 vs ROXY9CSLC #6-1	ns
ROXY9SCLC #37-5 vs ROXY9CSLC #15-3	ns
ROXY9CSLC #6-1 vs ROXY9CSLC #15-3	ns

Supplementary Table S3: Statistical analysis of leaf-to-petiole data obtained from stably transformed *roxy6789* with HA-L-ROXY9 active site variants. Plants were grown for 4 weeks in 12/12 h light regime. Leave and petiole length was measured of all leaves from 4 plant per line. Statistical analysis was performed by using one-way ANOVA and Tukey's post-test. *p*-value: * < 0.05, ** < 0.001, *** < 0.0001 ns: not significant; *p*-value > 0.05

Comparison	Significant difference
Col-0 vs roxy6789	**
Col-0 vs HA #4-8	ns
Col-0 vs HA #101-8	ns
Col-0 vs HA #102-8	ns
Col-0 vs ROXY9CCLC #2-1	ns
Col-0 vs ROXY9CCLC #27-4	ns
Col-0 vs ROXY9SCLC #9-3	ns
Col-0 vs ROXY9SCLC #12-2	ns
Col-0 vs ROXY9SCLC #37-5	ns
Col-0 vs ROXY9CSLC #6-1	ns
Col-0 vs ROXY9CSLC #15-3	ns
roxy6789 vs HA #4-8	ns
roxy6789 vs HA #101-8	ns
roxy6789 vs HA #102-8	ns
roxy6789 vs ROXY9CCLC #2-1	**
roxy6789 vs ROXY9CCLC #27-4	***
roxy6789 vs ROXY9SCLC #9-3	***
roxy6789 vs ROXY9SCLC #12-2	ns
roxy6789 vs ROXY9SCLC #37-5	***
roxy6789 vs ROXY9CSLC #6-1	**
roxy6789 vs ROXY9CSLC #15-3	*
HA #4-8 vs HA #101-8	ns
HA #4-8 vs HA #102-8	ns
HA #4-8 vs ROXY9CCLC #2-1	ns
HA #4-8 vs ROXY9CCLC #27-4	***
HA #4-8 vs ROXY9SCLC #9-3	ns
HA #4-8 vs ROXY9SCLC #12-2	ns
HA #4-8 vs ROXY9SCLC #37-5	ns
HA #4-8 vs ROXY9CSLC #6-1	ns
HA #4-8 vs ROXY9CSLC #15-3	ns
HA #101-8 vs HA #102-8	ns
HA #101-8 vs ROXY9CCLC #2-1	ns
HA #101-8 vs ROXY9CCLC #27-4	***
HA #101-8 vs ROXY9SCLC #9-3	**
HA #101-8 vs ROXY9SCLC #12-2	ns
HA #101-8 vs ROXY9SCLC #37-5	**
HA #101-8 vs ROXY9CSLC #6-1	ns
HA #101-8 vs ROXY9CSLC #15-3	ns
HA #102-8 vs ROXY9CCLC #2-1	ns
HA #102-8 vs ROXY9CCLC #27-4	***
HA #102-8 vs ROXY9SCLC #9-3	*
HA #102-8 vs ROXY9SCLC #12-2	ns

Comparison	Significant difference
HA #102-8 vs ROXY9SCLC #37-5	*
HA #102-8 vs ROXY9CSLC #6-1	ns
HA #102-8 vs ROXY9CSLC #15-3	ns
ROXY9CCLC #2-1 vs ROXY9CCLC #27-4	ns
ROXY9CCLC #2-1 vs ROXY9SCLC #9-3	ns
ROXY9CCLC #2-1 vs ROXY9SCLC #12-2	ns
ROXY9CCLC #2-1 vs ROXY9SCLC #37-5	ns
ROXY9CCLC #2-1 vs ROXY9CSLC #6-1	ns
ROXY9CCLC #2-1 vs ROXY9CSLC #15-3	ns
ROXY9CCLC #27-4 vs ROXY9SCLC #9-3	ns
ROXY9CCLC #27-4 vs ROXY9SCLC #12-2	**
ROXY9CCLC #27-4 vs ROXY9SCLC #37-5	ns
ROXY9CCLC #27-4 vs ROXY9CSLC #6-1	ns
ROXY9CCLC #27-4 vs ROXY9CSLC #15-3	ns
ROXY9SCLC #9-3 vs ROXY9SCLC #12-2	ns
ROXY9SCLC #9-3 vs ROXY9SCLC #37-5	ns
ROXY9SCLC #9-3 vs ROXY9CSLC #6-1	ns
ROXY9SCLC #9-3 vs ROXY9CSLC #15-3	ns
ROXY9SCLC #12-2 vs ROXY9SCLC #37-5	ns
ROXY9SCLC #12-2 vs ROXY9CSLC #6-1	ns
ROXY9SCLC #12-2 vs ROXY9CSLC #15-3	ns
ROXY9SCLC #37-5 vs ROXY9CSLC #6-1	ns
ROXY9SCLC #37-5 vs ROXY9CSLC #15-3	ns
ROXY9CSLC #6-1 vs ROXY9CSLC #15-3	ns

Supplementary Table S4: TGA factor binding sites are enriched in the 4184 SAR-induced genes. Motif mapper analysis was performed with the 4184 SAR inducible genes (log_2 FC > 1, *p*.adj < 0.05) according to transcriptome data. The number of motifs within the data set are represented before the slash, the number after the slash represents the number of motifs from randomly chosen promoters of the whole *A. thaliana* genome. Green indicates significant enrichment whereas grey indicates no significant difference (*p*-value < 0.05).

	TGACGTCA	TGACG	TACGTA	GAATTT	TTGAC	GACTTTTC
SAR-induced (4184)	62 / 54.9	4013 / 3547	897 / 741.3	2600 / 2193.7	11420 / 9357.6	297 / 217.8
not activated by TGA1, 4 or TGA2, 5, 6 (1719)	26 / 22.8	1615 / 1460	366 / 306.6	923 / 906	4254 / 3857.8	99 / 89.8
activated by TGA1, 4 (676)	13 / 8.9	669 / 574.5	101 / 119.5	430 / 355	2004 / 1514	76 / 35.1
activated by TGA2, 5, 6 (598)	8 / 7.9	602 / 509.1	160 / 107	363 / 315.9	1602 / 1342.7	41 / 31.1
activated by TGA1, 4 and TGA2, 5, 6 (1191)	15 / 15.7	1127 / 1003.3	270 / 210.3	844 / 621.2	3560 / 2650.5	181 / 61.3

Datasets

Dataset 1: ROXY6, 7, 8, 9 activate 350 genes and repress 212 genes upon nitrogen starvation. 7-day old seedlings grown on full nutrition (FN) plates under constant light conditions (70 µmol photons s^{-1} m^{-2}) were transferred to either low nitrogen (LN) plates. Two days later, roots were collected, RNA was isolated. Per treatment, RNA of 5 replicates was pooled and sent for RNA sequencing. 350 genes are lower expressed in the *roxy6789* mutant compared to Col-0 and 212 genes are higher expressed (logarithmic fold change to the base 2 (log_2 FC) > 1, adjusted *p*-value (*p*.adj) < 0.05). TPM: transcript per million.

Dataset 2: Identification of distinctly regulated genes by clade I and II TGA factors in SAR conditions. Lower leaves of 4.5-week-old *A. thaliana* plants were infiltrated with *Psm* (OD_{600} = 0.005) or left untreated. After 48 h, upper leaves were infiltrated with *Psm* or left untreated (untr). The upper leaves were collected after 8 hours, RNA was isolated. Per treatment, RNA of five plants was pooled and sent for RNA sequencing. 4184 genes are induced in the *sid2* plants after *Psm*/*Psm* treatment compared to the untr/untr control (logarithmic fold change to the base 2 (log_2 FC) > 1, adjusted *p*-value (*p*.adj) < 0.05). TPM: transcript per million.

Sequences

Sequence 1: Coding region for HA-L-ROXY9 on the plasmid pB2HA-L-ROXY9. The nucleobases marked in red encode for the CCLCY motif of ROXY9 and are altered in the active site variants as indicated below.

ATGGCATACCCATACGACGTTCCGGACTACGCTTCTTTGGGTGGTTCTAGCCCAAGCTCAGAGCTCCACCGCGG
TGGCGGCCGCATCTTTTACCCATACGATGTTCCTGACTATGCGGGCTATCCCTATGACGTCCCGGACTATGCAG
ATATCTCTAGGCAGATCACAAGTTTGTACAAAAAAGCAGGCTCCGGAGGAGGAGGTTCAGGTGGTGGTGGAT
CCGGAGGAGGTGGTTCAAATGCAATGGACAAAGTGATGAGAATGTCTTCAGAGAAAGGAGTGGTGATCTTCA
CGAAGAGCTCATGTTGTCTCTGCTACGCCGTTCAAATCCTGTTCCGTGACCTTAGGGTTCAACCAACCATCCAC
GAGATCGACAACGACCCGGACTGCCGTGAGATCGAGAAGGCTCTTCTCCGGCTCGGCTGTTCCACGGCGGTTC
CAGCTGTCTTTGTCGGAGGCAAGCTTGTTGGCTCCACCAATGAAGTCATGTCCCTTCACCTTAGTGGCTCTCTTG
TCCCATTGATCAAACCCTATCAGTCCATCCTTTACTAG

CCLC: TGTTGTCTCTGCTAC
SCLC: TCTTGTCTCTGCTAC
CSLC: TGTTCTCTCTGCTAC
CPYC: TGTCCATATTGCTAC
CCLCA: TGTTGTCTCTGCGCC

Sequence 2: Coding region for 2HA-Turbo-ROXY9 on the plasmid pUBQ10-2HA-Turbo-ROXY9.

ATGTACCCATACGATGTTCCTGACTATGCGGGCTATCCCTATGACGTCCCAGACTACGCAGCTAGCAAAGACAA
TACTGTGCCTCTGAAGCTGATCGCTCTCCTGGCTAATGGCGAGTTCCATAGTGGCGAACAGCTGGGAGAAACC
CTGGGCATGTCCAGGGCCGCTATCAACAAGCACATTCAGACTCTGCGCGACTGGGGCGTGGACGTGTTCACCG
TGCCCGGAAAGGGCTACTCTCTGCCCGAGCCTATCCCGCTGCTGAACGCTAAACAGATTCTGGGACAGCTGGA
CGGCGGGAGCGTGGCAGTCCTGCCTGTGGTCGACTCCACCAATCAGTACCTGCTGGATCGAATCGGCGAGCT
GAAGAGTGGGGATGCTTGCATTGCAGAATATCAGCAGGCAGGGAGAGGAAGCAGAGGGAGGAAATGGTTCT
CTCCTTTTGGAGCTAACCTGTACCTGAGTATGTTTTGGCGCCTGAAGCGGGGACCAGCAGCAATCGGCCTGGG
CCCGGTCATCGGAATTGTCATGGCAGAAGCGCTGCGAAAGCTGGGAGCAGACAAGGTGCGAGTCAAATGGCC
CAATGACCTGTATCTGCAGGATAGAAAGCTGGCAGGCATCCTGGTGGAGCTGGCCGGAATAACAGGCGATGC
TGCACAGATCGTCATTGGCGCCGGGATTAACGTGGCTATGAGGCGCGTGGAGGAAAGCGTGGTCAATCAGGG
CTGGATCACACTGCAGGAAGCAGGGATTAACCTGGACAGGAATACTCTGGCCGCTACGCTGATCCGAGAGCT
GCGGGCAGCCCTGGAACTGTTCGAGCAGGAAGGCCTGGCTCCATATCTGCCACGGTGGGAGAAGCTGGATAA
CTTCATCAATAGACCCGTGAAGCTGATCATTGGGGACAAAGAGATTTTCGGGATTAGCCGGGGGATTGATAAA
CAGGGAGCCCTGCTGCTGGAACAGGACGGAGTTATCAAACCCTGGATGGGCGGAGAAATCAGTCTGCGGTCT
GCCGAAAAGGGTACCATGGACAAAGTGATGAGAATGTCTTCAGAGAAAGGAGTGGTGATCTTCACGAAGAGC
TCATGTTGTCTCTGCTACGCCGTTCAAATCCTGTTCCGTGACCTTAGGGTTCAACCAACCATCCACGAGATCGAC
AACGACCCGGACTGCCGTGAGATCGAGAAGGCTCTTCTCCGGCTCGGCTGTTCCACGGCGGTTCCAGCTGTCT
TTGTCGGAGGCAAGCTTGTTGGCTCCACCAATGAAGTCATGTCCCTTCACCTTAGTGGCTCTCTTGTCCCATTGA
TCAAACCCTATCAGTCCATCCTTTACTAG

Acknowledgements

I would like to thank everyone who supported me during this thesis.

First of all, I would like to thank Prof. Dr. Christiane Gatz for giving me the opportunity to do the PhD in her department. Thanks for your helpful discussions, excellent explanations and support throughout the project as well as for all the assistance in preparing posters, presentations or this thesis. I am grateful that your door was always open for any kind of concerns and that you encouraged me to be a better researcher. I am also thankful for all the assistance during my Master Thesis, so that I could join the IRTG program. Moreover, I would like to thank you for enabling me to assist in the SARS-CoV2 diagnostics during the covid first lock down.

Many thanks to Prof. Dr. Marcel Wiermer for agreeing to be my second reviewer and member of my thesis committee. Your input and the discussions during the TAC meetings were always valuable. I would also like to thank Prof. Dr. Yuelin Zhang for also being in my thesis committee and for hosting me in his department for the research stay.

Thanks to Prof. Dr. Andrea Polle, Prof. Dr. Ivo Feußner and Prof. Dr. Kai Heimel for being part of my examination board.

During this project, Corinna constantly encouraged me, celebrated every little result and found something interesting in every experiment. Thank you very much for the supervision of my project, your support and your input. I am grateful that you always had the time to discuss weird data or new ideas when I was lost.

Many thanks to Guido, for his help with programing percivals and in any kind of IT-related questions.

Thanks also to Irene for her insights, knowledge and the conversations during lunch breaks.

I would like to thank my current and former lab mates Pascal, Ben, Isha and Louisa for all scientific discussions as well as for the time together outside the lab. Meeting you after a stressful week was always great and I enjoyed that we played so many different board games. Thanks to all of you for letting me complain so much about the more or less important things! Thanks to Pascal for knowing almost everything about glutaredoxins and biochemistry and thanks for all the explanations you gave me. Also many thanks for your calm nature which helped me to relieve my stress. Thanks to Ben for all the conversations about A Galaxy Far, Far Away, Middle-earth and other slightly nerdy topics. Thanks to Isha for her contribution to the *WRKY51* project and her insights on the plant immune system. Thanks to Louisa for our talks about veganism and sustainability. I became more self-aware because of you.

I would also like to thank my bachelor students Lena and Hannah for the work during their thesis as well as afterwards during their HiWis. You contributed a lot to the analysis of gene expression upon nitrogen starvation and I am very grateful for your help.

Ein ganz großer Dank geht an unsere fabelhaften TAs, nicht nur für die Hilfe bei allen Laborthemen, sondern auch für ihre moralische Unterstützung. Danke an Anna, dafür, dass du die beste Laborparterin bist, die ich mir wünschen kann, für die ganzen Methoden, die du mir beigebracht hast, für deine Geduld bei all den technischen Fragen, auf die du fast immer eine Antwort hattest und für die tollen Gespräche, die wir im Labor hatten. Danke an Ronny, für das Genotypisieren von hunderten von Pflanzen, bei denen du immer den Überblick behalten hast, für die Aufmunterungen während der Pausen mit komischen Witzen, die ich nicht immer verstanden habe, und dafür, dass du für frischen Kaffee gesorgt hast. Danke an Kathi für die unzähligen Basta Platten und Real Times, die du für mich

gemacht hast, für die wunderschönen Westerns, die Pflanzen-und-Puzzle-Tausch-Börse und für die Spaziergänge mit Kira zum runterkommen, wenn mir alles zu viel wurde.

Vielen Dank an die Gärtnerinnen Feli and Susanne für das Vorbereiten der Töpfe und das Ernten der Pflanzen. Vor allem vielen Dank an Feli, die meine Sonderwünsche erfüllt hat und extra für mich Töpfe mit Erdhügeln gemacht hat.

Many thanks to the whole department for their cakes and the friendly and pleasant work atmosphere. I enjoyed working with you a lot! Thanks also to Piccolino and Kira for enlightening the mood.

I would like to thank the other members of the IRTG. It was nice to know that I am not the only one with silly problems and self-doubt. I especially enjoyed the time in Vancouver with you guys and the social meetings, but also the scientific meetings were valuable.

My friends Biggi, Kelly and all MonsterMoBis&Co, thank you for being at my side in all these years. Biggi, I am so grateful for your friendship since we were teenagers. I know that I can always count on you and that you are only one phone call away. Kelly, thank you for believing in me, all your visits, the hiking trips and the sheep pictures you sent to cheer me up. Dear MonsterMoBis&Co, even though we are spread all over Germany, you were there for me during this stressful time. I want to thank all of you for having an open ear and the great time we have together.

Huge thanks to my family! Mama, Papa and Inga, thank you for always believing in me and all the encouraging conversations. Thanks to Mama for her dealing with my emotions and thanks to Papa for his optimism and rational point of view. This thesis would not have been possible without your education, love, support and also financial assistance. I know that you are always there for me and I am deeply grateful for that. Ich möchte auch meiner Oma und meiner Großmutter danken. Danke für eure Unterstützung bis zum Ende, ich wünschte ihr könntet diese Leistung mit mir zusammen feiern.

Finally, I want to express my deepest gratitude to Philipp for providing me with unfailing support, continuous encouragement and unconditional love. Thank you so much for proofreading my emails, dealing with all my emotions and being at my side through the process of researching and writing this thesis. I love you so much!

This accomplishment would not have been possible without all of you. Thank you!